THE RESPONSE OF SEA-SURFACE TEMPERATURE TO ATMOSPHERIC FORCING PROCESSES

Thesis

submitted by

ANTHONY WILLIAM DALY

for the degree of

DOCTOR OF PHILOSOPHY

University of Edinburgh

1975

CONTENTS

ABSTRACT

The present investigation is devoted entirely to an analysis of the response of the sea-surface temperature to atmospheric forcing processes over various time and space scales.

After an introductory chapter where the author has endeavoured to outline what he considers to be some of the more physical concepts involved, the simple but effective technique of 'superposed epochs' is used in an attempt to study the short-period variation of sea-surface temperature at Ocean Weather Stations 'M' and 'I' as a function of various meteorological parameters. Periods of enhanced turbulence associated with windy conditions are observed to produce a significant lowering of the sea-surface temperature when subsurface thermal stratification prevails (summer season), at both stations. Sudden increases or decreases of the sea-surface temperature at station 'I' are observed to accompany changes in the wind direction, more especially during the winter season. Failure of the sea-surface temperature at Ocean Weather Station 'I' to respond to periods of greatly increased evaporative and sensible heat cooling is attributed to a near-compensating effect of warmer water advection.

A simple algebraic method is developed in chapter 3 with the intention of relating both the magnitude and direction of induced drift currents to the corresponding geostrophic wind vector, during periods of assumed predominantly advective sea-surface temperature change; the poor quality of the sea-surface temperature data used is invoked as being largely responsible for the relative lack of success of the method in the periods studied.

Finally, following formulation in chapter 4, and description of acquiring model input data in the first part of chapter 5, an amended depth-integrated enthalpy continuity equation is used with input data from three case studies of dissimilar meteorological forcing, to provide values for the month-to-month change of mean monthly anomalous sea-surface temperature, evaluation of the model being effected through comparison of predicted anomaly changes with those observed. The individual contributions of anomalous surface cooling and anomalous advection to sea temperature anomaly change give agreement of varying closeness but on all occasions the best results are achieved from a comination of these two processes; inclusion of a horizontal eddy conductivity term produces deteriorations over 'heat and advection'-predicted values in all case studies. In regions of significant anomalous wind stress curl, neither sea temperature anomaly changes produced in part by advection due to alternative meridional Sverdrup-type flow, nor changes otherwise consequent to vertical motion (and associated effects, as mentioned in the introduction), necessarily induced as a baroclinic compensation in the absence of Sverdrup type transport, are observed to be consistent with actual changes.

PART I

Short and intermediate period variations of sea-surface temperature in selected localities.

CHAPTER 1

Introduction and General Discussion.

There has developed over the last decade or so an increasing interest in the study of the interaction between the atmosphere and the ocean. It is now well recognised that the interplay between the atmosphere and the ocean contributes very significantly to both the smaller- and larger-scale circulations of both these media. An excellent example of this interaction on a local scale is that of the appreciable lowering of the sea-surface temperature along the trajectory of a tropical cyclone and the consequent effect of this abnormally cold water on the path and development (or non-development) of subsequent cyclonic storms in the same locality (Ramage 1972). At the opposite end of the time spectrum Bjerknes has investigated the behaviour of Atlantic sea-surface temperatures parallel with climatic trends varying over periods from years to decades; a cooling and warming of the Atlantic was always observed during periods of increased and decreased zonal index respectively.

Perhaps one of the more practical and important uses of the sea-surface temperature, or more exactly of the anomalous sea-surface temperature field, has been in connexion with long-range weather forecasting; 'anomaly' here and henceforth signifies the departure of an element from the corresponding long-period average at the same position.

Irregularities in the atmospheric circulation can arise from

the existence of abnormal extensive and persistent heat sources and sinks. Large pools of anomalously cold or warm water which partly govern the amounts of heat exchange between the ocean and the atmosphere readily provide such sources and sinks. In a similar way it may be argued that an anomalous gradient of sea-surface temperature will be rapidly transmitted to air masses, thereby establishing a field of increased baroclinicity which undeveloped depressions arriving in the area may tap as an additional energy source. Sawyer (1964) in a survey of possible causes of long-term weather anomalies provided some quantitative estimation of the effect of anomalous heat supplies on the atmospheric circulation and concluded that the effect of anomalies in the release of latent heat, arising primarily from anomalies of sea-surface temperature, will have an effect appreciably greater than those arising from other causes. Although the physical mechanism of the origin and maintenance (or reversal) of thermal anomalies in the ocean and the relation to the atmospheric circulation have by no means been firmly established it has been suggested by Namias (1969) that, more often than not, sea-surface temperature anomalies assist in restoring the same type of synoptic activity which may have been responsible for their formation in the first place. The same author has demonstrated with the aid of circumstantial evidence not only relations between seasonal weather patterns and anomalous macroscopic sea-surface temperature patterns over the North Pacific Ocean but even the joint behaviour of semi-permanent sea temperatures and

an almost decadal climatological change over North America. It would appear reasonable at this stage therefore that further studies of both the production and control of sea-surface temperature anomalies be made. A major part of the present study will be concerned with the thermal response of the ocean boundary layer to the prevailing meteorological regime on a synoptic monthly scale. At this point some of the more important methods of investigating variations of the anomalous sea-surface temperature field in relation to the corresponding overlying atmospheric circulation are described. Furthermore some time is allotted to a brief digression on some of the more fundamental physical processes involved; while it is hardly the intention that this discussion should be in any way comprehensive, it is nevertheless hoped that it will serve to illustrate the complex nature of the problem.

The broad features of long-term average oceanic circulation, usually depicted in the form of mass transport or of integrated velocity stream functions, have been investigated and satisfactorily reproduced, with varying degrees of refinement, by means of models. The common ingredient of such models has been the solution of the steady-state hydrodynamical and continuity equations when subjected to surface forcing, usually in the form of mean wind stress curl, the other boundary conditions being related to motion at inter-level depths and/or the sea bottom, and at the model west or east boundary walls. Although useful in elucidating the wind-driven ocean circulation on a long-term

global scale, these models are of little practical value in the context of the present problem in that they fail to contribute to the understanding of fluctuations in currents (and the associated fluctuations in temperature) in relation to the transient meteorological stimuli. On the other hand, time-dependent studies of the type developed by Veronis and Stommel, (1956) in which ocean current response to transient wind stress forcing of variable wavelength and frequency has been examined in terms of baroclinic- and barotropic-type responses, now exist The former of these relates to tilting of the density surfaces and the latter to full flow at all depths as a function of surface slope; both components are formed as a superposition of the various normal modes of the system. These studies have provided insight into the qualitative and also certain quantitative aspects of time-dependent current response. Most models, however, operate with simple input stress forcing e.g. $\tau = \tau_o \sin(kx-wt)$ where w is the angular frequency and k the wave number; any real stress field would therefore require to be Fourier-analysed before being of use as input data to a model of this type. Furthermore, adjustment of the method to incorporate sea-surface temperature dependence is not at all an obvious extension, even though the temperature response is expected to be sensitive to the current response. These are but a very few remarks in relation to time-dependent models, but it is perhaps because of reasoning of this nature, apart from the questionable practicality of using refined models with what are often inaccurate

and inadequate input and output marine data, that the use of time-dependent models in association with sea-surface temperatures and their anomalies has not yet superceded the more direct, less rigorous approach.

The work of Namias (1959) was the first of its kind in attempting to relate sea-surface temperature anomalies to the overlying wind systems on a synoptic scale. The essence of Namias's preliminary method was to superimpose on the mean monthly or seasonal sea-surface isotherms an additional surface current drift component, v, derived directly from the corresponding anomalous pressure distribution, by means of classical Ekman theory, viz., the normal isotherms were vectorially displaced by a distance derived from $\frac{v}{W} = \frac{.0127}{(\sin\lambda)^{\frac{1}{2}}}$, where λ is the geographic latitude, W is the magnitude of the computed anomalous geostrophic wind and is in a direction at an angle of 45 degrees cum sole to the wind. An improvement to this method later resulted in the inclusion of the initial state of the system, i.e. the assumption that the temperature distribution was initially everywhere normal was removed by incorporating into the scheme the initial monthly mean sea-surface temperature anomalies. Provided that each actual mean variable can be written as a long-term mean part (denoted by a bar) plus a departure therefrom or anomaly (denoted by a prime), e.g. $\bar{T} = T + T'$, then subtraction of two simple advection equations, one of which contains long-term mean values and the other actual values, yields a convenient summary of the basic method, as follows:

$$T'(t_2) = T'(t_1) - \int_{t_1}^{t_2} (\bar{\underline{V}} + \underline{V}').\nabla T' dt - \int_{t_1}^{t_2} \underline{V}'.\nabla \bar{T}\, dt + \frac{dT'}{dt}$$

(a) (b) (c) (d)

where T denotes sea-surface temperature, $\underline{V}$ the total surface current.

In the amended Namias version, for example, only terms (a) and (c) are included. In spite of many simplifications the above technique has yielded significant positive correlations between the calculated and observed anomalous sea-surface temperatures; in the remaining cases (or areas) of poor agreement much of the failure has been attributed to the total neglect of upwelling and downwelling phenomena which are prevalent in many coastal regions and should also be detectable beneath convergent and divergent wind systems, respectively. It would appear more likely however that the neglect of term (d) in relation (1), which comprises the contribution of all non-advective processes, not least the anomalous heating/cooling term (due to anomalous evaporative, sensible and radiative heat exchange), may be responsible for the discrepancies. In a single case study which additionally included evaporative and sensible heat exchange, Jacobs (1967) found considerable improvement of his prognostic model over the purely advective methods, especially in predicting actual centres of positive and negative change in sea-surface temperature anomaly. The overall superiority of winter predictions over summer case studies may well originate from the obvious expectation that the relative effect of advection on the sea-surface temperature

should be closely dependent on the season and may therefore, for example, be subordinate to other processes during the late spring/early summer period. During summer months the processes of radiative absorption and entrainment (dependent on surface cooling, wind-produced turbulence and the strength of the seasonal thermocline) with the alternate erosion and reformation of transitory near-surface mini thermoclines, and, in cases of intense turbulence, even partial decay of the seasonal thermocline are worthy of mention in this respect; the entrainment process is analagous to the increased warming of the atmospheric surface boundary layer due to the entrainment of potentially warmer air at the inversion during anticyclonic conditions. An excellent example of the dominant influence of factors other than advection is provided by the sudden appearance of extensive areas of abnormally cold water (2-3^{o}C below normal) over the North Atlantic from the American seaboard to the British Isles, during the period late May - early June 1972. It is believed that a greater-than-usual surface cooling, but above all extra windiness and cloudiness associated with unusual cyclogenesis, drastically inhibited the rapid radiative warming of the superficial oceanic layers which normally occur at this time of the year.

With regard to upwelling and downwelling processes, it is often stated that these cause a lowering and raising respectively of the sea-surface temperature. In the presence of a vertical temperature gradient existing to the sea surface itself, then it

appears reasonable that an upward vertical velocity, induced as a result of Ekman divergence under a cyclonic wind system, will produce a systematic lowering of the sea-surface temperature. With the more normal state of an upper well-mixed isothermal layer and thermocline below it is obvious that until such time as the upper layer has been depleted (i.e. until upwelling has advected the thermocline to the surface) there can be no reduction in the sea-surface temperature. In the presence of a shallow mixed layer during the summer months, and at all times in the vicinity of oceanic fronts, it is probable that intense upwelling would eventually result in a lowering of the sea-surface temperature through vertical advection alone. The abrupt fall in sea-surface temperature following the passage of a hurricane, mentioned before, is probably due to pure upwelling as is evident from an inspection of the subsequent temperature-depth traces. If, however, as is likely, upwelling is accompanied by enhanced wind-induced turbulence and surface heat loss to the atmosphere, then it appears reasonable that with the tendency of increasing shallowness of the mixed layer, entrainment processes should become more effective. During the winter period when isothermal conditions often prevail to depths exceeding 250 metres and with only weak stratification below it is doubtful if upwelling will result in any appreciable reduction of the sea-surface temperature even after a month or so of intense cyclonic conditions. It is therefore hypothesised that an enhanced entrainment process could well

be the more effective agent in lowering the sea-surface temperature in many upwelling situations; in mixed layer conditions this mechanism will manifest itself in the form of a fall of surface temperature long before any purely vertical advective effect.

In a numerical prediction model of the month-to-month change in anomalous sea-surface temperature, Adem (1970) included both linear and bulk expressions for the latent and sensible heat fluxes as well as empirical radiative exchange formulae in attempting to assess the effect of these non-advective processes on the sea-surface temperature field; also included were terms for heat transfer to the thermocline and for turbulent horizontal diffusion, the latter parameterised in the usual manner with the aid of a turbulent eddy coefficient, K_H, by direct analogy with the molecular case. It was claimed by Adem that skill in predicting the change in temperature anomalies is achieved with the diffusion term alone. A depth-integrated thermodynamic equation essentially identical to relation (1) was used in finite-difference form, the lower limit of integration being the bottom of the mixed-layer depth, h.

Two alternative methods for determining h were adopted: in the first case a uniform depth of 100m was assumed, and in the second, the empirical wind-dependent relationships of Thorade (1914), which were really intended for use with the 10m wind speed, were utilised, with the aid of calculated geostrophic wind speeds. It is believed that neither of these alternatives

is particularly appropriate. The first which implies uniformity on a hemispheric scale is not in agreement with observed mean mixed-layer depths which in winter may vary from approximately 50m in the subtropics to over 300m in high northern latitudes and sometimes to over 1000m in polar regions. The second approximation for h caters for constancy of temperature produced by wind mixing along (purely mechanical turbulence) thereby excluding effects of convective turbulence (due to surface cooling) or the more efficient Langmuir circulation which will be mentioned later. Although turbulence induced by wind stress may well, in the short term, predominate in destroying near-surface stable stratification and thus produce isothermal conditions down to a depth which can be shown theoretically to have a maximum value dependent on the magnitude of the wind stress, on the initial stratification in the water and on the Coriolis parameter (i.e. short-term response), the overriding influence of surface cooling is readily observed on longer time scales (vid. e.g. Pollard, Rhines and Thomson 1973). There have emerged since the preliminary studies of S.A. Kitaigorodsky (1960) several detailed investigations, again mainly by Russian authors, in which attempts have been made to relate mean mixed-layer depths to total heat exchange at the surface, for example by multiple regression analysis, and by the introduction of other parameters, normally based on dimensional arguments (Kitaigorodsky and Miropol'skiy, B.N. Filyushkin, B.N. Filyushkin et al). Unfortunately these investigations

have been restricted to fixed locations and to the summer period only. Berson (1962), in a study of sea temperature anomaly changes related to anomalous atmospheric forcing, incorporated into his model a logarithmic regression of the mixed-layer depth on sea-surface temperature; this ultimately had the effect of introducing exponential terms into his temperature prediction equation. The procedure in this case is perhaps more justifiable, as the entire investigation was confined to a limited latitude-longitude band in the central Pacific.

In the absence of actual monthly mean mixed-layer depth data, it is suggested that the long-period average distribution of mixed-layer depth should be used in preference to any of the afore-mentioned alternatives.

Finally, by way of illustrating the difference in assigned numerical values, it is worth while comparing, for example, the magnitudes of horizontal eddy conductivity, K_H, of Adem (1970) with those quoted by Bathen (1970). The latter, in a climatological analysis of advection and heat storage in the upper 250m layer of the North Pacific, found best agreement with observation for values of K_H varying linearly from $10^6 cm^2 sec^{-1}$ at 7^oN to $1.1 \times 10^7 cm^2 sec^{-1}$ at 70^oN - values range between one and two orders of magnitude smaller than Adem's constant assigned value of $3 \times 10^8 cm^2 sec^{-1}$!

Fundamental to the Ekman-type advective processes invoked as major contributary agents to changes in sea-surface

temperature has been the assumption that the downward flux of horizontal momentum in the constant-flux layer of the atmosphere is communicated across the air-sea interface in a continuous and organised manner, immediately to appear as a sheared current system in the water medium. Before any reference to the oceanographic aspects of the simplified advective method is made, a résumé is given of possible momentum transfer mechanisms.

Turbulent and molecular momentum transfers at the air-sea interface are effected respectively through a combination of bluff-body drag of the wind on the wave surface itself and molecular skin friction on the aerodynamically smooth part of the water surface through a hypothesised laminar sub-layer where all motion is molecular in nature. Only the latter of these can give rise to the classical Ekman solution directly; the former is associated with wave production. With regard to mean water currents produced from the momentum transfer it is important to know the respective fractions of the momentum flux used in these two processes. As well as acting as a momentum carrier, sheared current motion is rotational ($\nabla \times \underline{V} \neq 0$) and as such is influenced by the Coriolis force; pure wave motion which is irrotational in character can carry horizontal momentum but is unaffected by the Coriolis force. The eventual energy loss of a wave through, for example, initial wave breaking and subsequent viscous dissipation, is accompanied by a conversion of the wave momentum into a mean water movement, i.e. the drift current. During the process however, momentum may well have been transported far

from the source.

The shearing stress of the wind on the underlying water surface, whether it be aerodynamically rough or smooth, is quantified in the normal way by means of a drag coefficient $C_D(z)$ or roughness length z_o; the drag coefficient, measured at a specific height z above the surface is a physical measure of the effectiveness of the surface as a momentum absorber and is related to the stress, τ, by the simplified so-called 'bulk' relationship:

$$\tau = \rho C_D(z) |u(z)|^2$$

where ρ is the air density and u(z) is the wind speed at the height z. In a similar way the coefficients C_H, C_V, often referred to as the Stanton number and Dalton number, respectively, permit a parameterisation of the sensible and latent heat fluxes at the sea surface. Unlike momentum transfer over a land surface, one is confronted in the air-sea interfacial zone by the additional obstacle that the roughness elements are the waves themselves, whose form and velocity are a function of fetch, wind speed and wind duration. It would therefore appear at first sight that, owing to the temporal and spatial variability of the topography of a sea surface which is subjected to a transient wind régime, the roughness length and hence also the related drag coefficient might assume values dependent on these wave-controlling factors. From a comprehensive survey of drag coefficient measurements (Roll 1965), it is apparent that values quoted by different investigators vary by as much as an order of magnitude. These discrepancies have almost invariably been

attributed to inherent inaccuracies in the various indirect methods used to determine C_D. Notwithstanding large scatter in measured values, an approximately constant value, or in some cases a weak dependence of drag coefficient on mean wind speed, over a wide wind speed range has been claimed.

In attempting to reconcile these observations with the wind speed-dependent aspect of wave growth, it has been suggested that wind-wave interaction operates primarily with short gravity and capillary waves; these belong to the high frequency end of the wave spectrum which is quickly saturated and has the same power over a wide range of wind velocities (Kraus 1972). Additionally, the apparent measured independence of the drag coefficient on fetch and on wind duration has similarly been explained in terms of a wind-shortwave interaction. Some doubt of the validity of this explanation has however recently arisen from the JONSWAP experiments during which it was unexpectedly discovered that the amplitude of the short waves tends to decrease as fetch increases and does not therefore remain constant. This and other recent evidence, e.g. the calculations of Dobson 1971, lend support to the conclusion that input by wind to waves is mostly in the central region of the wave spectrum. In spite of this wealth of seemingly incompatible information and moreover, in the absence of any oceanwide network of routine micrometeorological/marine environmental observations, there can be little doubt that use of momentum drag coefficients and the

heat and vapour flux equivalents in the respective bulk formulae, provides the best estimate of momentum, heat and vapour transfers between the atmosphere and the ocean which can be achieved on a synoptic scale at the present time. Particularly encouraging in this respect have been the comparisons between the fluxes calculated from profile and eddy correlation tehniques and the corresponding bulk parameter products $|u(10)|^2$, $u(10)\Delta\theta_{10}$ and $u(10)\Delta e_{10}$ (vide e.g. M. Dunckel et al.1973), where linear regressions have been obtained with relatively small scatter. In addition, if need be, all bulk parameters can of course be adjusted by the inclusion of stability factors which are dependent on Richardson number.

It is common practice in climatological studies to asume similarity for momentum, heat and vapour transfers, viz. $C_D = C_H = C_V$. However, the action of pressure forces on the individual roughness elements themselves (the waves) may considerably augment the momentum transfer, whereas the analogous effect does not arise with heat and vapour transfer, each of which relies on molecular diffusion at the surface proper. This physical reasoning suggests that C_V and C_H should, for aerodynamically rough surfaces at least, be systematically smaller than C_D. This point of view will be adhered to in later numerical calculations involving the use of bulk coefficients.

From a purely oceanographic point of view the treatment of the advective drift current as a solely surface effect (45^o to

right of wind for Ekman solution) is incompatible with the normally observed well-mixed isothermal surface layer, especially in winter-time conditions. In the absence of vertical convective mixing, the exponential attenuation and shearing nature of the classical Ekman solution would, in the presence of horizontal temperature gradients, even with initial vertical homogeneity, result in the formation of a vertical temperature gradient with stable or unstable stratification according as warm water was advected over colder or vice versa. If, however, the time scale of turbulent mixing through the column of initial mixed-layer depth, h, (where $h > d$, the depth of frictional influence) is comparable with the time scale of horizontal advective temperature changes, as instantaneous isothermal observations would tend to imply, then it is more pertinent to use a drift current vertically integrated over the depth of the mixed layer, h, and not a surface current vector in forming the scalar product with the sea temperature gradient. This procedure is consistent with the alternative treatment of the wind stress as a body force distributed uniformly through the mixed layer, as for example, the inertial current observations of Pollard and Millard (1970) seemed to indicate. In this latter respect, with the usual assumption that below the mixed layer the shearing stress is negligible compared with that at the surface, then the steady-state solution (time scale of mean motion >> inertial period) of the integrated mean drift current, $\underline{\bar{V}}$, independent of pressure gradient terms, is simply

$$\underline{\bar{V}} = -\frac{1}{f\rho h}\,\underline{\hat{k}} \times \underline{\bar{\tau}}$$

where $\underline{\hat{k}}$ is a unit vector in the vertical direction. The solution is of course invalid as long as the motion remains irrotational. If (monthly) mean drift components are to be calculated in this manner, then any computation of mean surface wind stress from mean winds which have been derived through the geostrophic relation from the gradient of the mean pressure distribution, should be treated with caution, as any such calculation will tend to underestimate the true means stress, unless the variance of the pressure gradient terms has been accounted for.

Still on the subject of advective currents, it would appear feasible at first sight that the Lagrangian or Stokes drift, V_{ST}, of surface gravity waves (Kenyon 1969) which cannot be detected with a fixed constant flow meter, should nevertheless behave as an advective agent, open to influence by the Coriolis force; it has been suggested, for example by Hasselman (vid. Kraus 1970), that the Coriolis force acting on V_{ST} causes a small departure from the strictly two-dimensional wave particle motion in a vertical plane. In an exact mathematical solution, however, Pollard (1970), and also private communication (1974), has shown that in the presence of Coriolis forces a true Lagrangian or Stokes drift cannot be maintained. The Stokes drift has consequently been dismissed as unimportant in the advective sense.

Until relatively recently there has been little direct observational evidence of the existence of Ekman spirals, or

indeed of any other mechanism of transporting momentum downwards through the mixed layer in the open ocean. However, as a result of a set of experiments in the Bermuda area (over the period 1968-1970), based on aerial photographs of a variety of dye injections and floating cards in the surface layer under different conditions of wind and sea state, Assaf, Gerard and Gordon (1971) have estimated circulation rates within the ocean mixed layer through various observed Ekman/Langmuir cell mechanisms. Only under slight-moderate wind conditions (<10 knots) was the Ekman Spiral observed but even then in coexistence with small surface Langmuir cells. Under moderate to strong wind conditions (10-30 knots) small and medium size Langmuir cells were accompanied by a hierarchy of large cells whose maximum spacing was approximately equal to the mixed layer depth. During the period of existence of the large Langmuir cells no Ekman spiral was observed. It was estimated that the onset of instability in Ekman flow, with subsequent transition to large organised Langmuir circulation, occurred at a turbulent Reynolds number ($Re = \frac{V_o}{(Kf/2)^{\frac{1}{2}}}$ where V_o is taken as 0.02 x wind speed, and K is the eddy viscosity of the Ekman flow before transformation) of approximately 100. In the Langmuir cell circulation the more rapid advancement of the water in the convergence zone relative to the water in the divergence zone, coupled with the sinking at the convergence and upwelling at the divergence zone, demonstrates that these cells are so structured as to transport horizontal momentum

downwards. Estimates of an equivalent 'eddy diffusivity' for the large Langmuir cells yielded values of K = 5,300 $cm^2 sec^{-1}$ for cells of 280m spacing (mixed-layer depth at this time was between 200 and 300m). This figure alone provides evidence for an approximate fifty-fold increase in efficiency of mixing or downward distribution of horizontal momentum through the mixed layer in comparison with mixing due to Ekman eddy viscosity; this circulation mechanism leaves no conceptual difficulty in treating the stress as a body force distributed uniformly through the mixed layer.

Implicit in the framework of all computations of advective sea-surface temperature variation has been the treatment of all anomalous current components as purely drift systems. While this interpretation is consistent with the useful and reasonably accurate representation of the total surface current as a vector sum of the drift and gradient currents, it nevertheless precludes temperature variations consequent to possible anomalies in the latter. Gradient currents which are related to the surface slope and horizontal density gradient are normally fairly swift, deep-reaching systems (to the 'layer of no motion' if such a concept is still meaningful) and as such have great inertia. This fact alone has often been used as sufficient reason for emphasising the semi-permanence of these well-established currents (vid. e.g. Stommel, Bjerknes). Surge-like movements of water which may for example result from the cummunication of sudden changes in the atmospheric pressure gradient to the sub-surface

layers without sufficient time for level compensation, or perhaps from the effects of water piling (windstau) more especially in land-locked waters, may well be important as short-period local phenomena in individual storms, but are viewed as insignificant in mean large-scale bulk water movements. Yet another reason for the neglect of variations in the gradient current probably arises from the common result of most numerical and analytical time-dependent ocean models where the response of the baroclinic component which is associated with non-uniform horizontal density distributions is shown to be characteristically sluggish in comparison with drift current response or barotropic response. This is however a point which must not be overemphasised; in particular the low value of the Coriolis factor has been cited by Lighthill (1969) in explaining, through Rossby wave propagation, the very rapid response of the highly baroclinic Somali current to the onset of the S.W. Monsoon. Much of the above reasoning is however speculative; without extensive and continuous current measurements to supplement the few existing detailed measurements concerning inertial motion in areas largely devoid of gradient systems, the theory must be regarded as incomplete. It is nevertheless anticipated that with a systematic approach, not necessarily bound by mathematical rigour, but based on intuitive physical insight, at least the broad aspects of the response of the sea-surface temperature to atmospheric forcing should largely unravel. The endeavour of the present investigation is to test (and where necessary modify) in the simplest and most direct way possible, some of the already discussed physical concepts.

CHAPTER 2

The short period fluctuations of meteorological variables and associated changes in sea-surface temperature at Ocean Weather Stations 'M' and 'I'.

2.1 Introduction.

The distribution and temporal fluctuation of sea-surface temperatures are greatly affected by atmospheric processes. It might therefore appear reasonable that a synoptic analysis of the sea-surface temperature should be made on the same time scale as that of the 'weather'. Unfortunately, inadequate and poor quality data over large areas of the ocean have rendered an analysis on this time scale quite unrealistic. It is nevertheless anticipated that with the further development of infra red techniques as employed on orbiting satellites, this problem will be considerably alleviated.

With regard to the irregular short period variations of sea-surface temperature and the possible inter-relationship with the corresponding meteorological parameters, it would appear from the absence of this and related topics in the literature, that the problem has been little investigated. A relevant publication was however produced by Hay (1956) who, having compiled five day block means of sea-surface temperature for Ocean Weather Stations 'I' and 'J' for the years 1948-1951 inclusive, related them to corresponding means of air temperature and wind data, by way of serial correlation.

The present study serves to investigate in a different manner,

changes of sea-surface temperature over periods of from one to five days, at Ocean Weather Stations 'M' and 'I', in relation to the meteorological stimuli producing them.

Occasional reference to the above-mentioned publication will be made in the course of the ensuing study.

2.2 Method.

The method, known formally as the 'n method' or method of 'superposed epochs', is an extension of one which has been employed in various geophysical time series. As the method has not previously been employed in oceanographic problems of the type here in question, it is considered appropriate to describe it in some detail.

Firstly, a meteorological variable which, from a physical point of view is considered may contribute significantly to changes in the sea-surface temperature, is chosen. Secondly, a decision of probable 'shape' of time variation of the meteorological variable selected as a forcing function (e.g. plateau-trough-plateau, plateau-step decrease-plateau) is made. From a continuous time series of this variable as many instances as possible of the selected configuration are collected with the exclusion, however, of all overlapping and immediately consecutive cases. These restrictions ensure independence of the cases (epochs), a condition which is important in the final analysis. Each case takes the form of a value of the meteorological variable on one 'key' or 'zero' day, together with values of the same variable on four or five days, both before (- days), and after (+ days) the chosen key day. The latter may denote for example a day of abrupt change,

or perhaps coincide with the crest or trough of the trend in the variable. For each case the instantaneous departures of the daily sea-surface temperature from thirty one-day running means, previously calculated for all days of the period under investigation, are noted for the characteristic days (i.e. key day, + and - days) and an arithmetic mean is formed over all selected cases. Treatment of the sea-surface temperature in this way removes the seasonal trend from the time series.

Any systematic variation of the sea-surface temperature associated with the variation of the chosen meteorological variable should now be apparent, statistical significance being estimated in relation to the standard error of the mean concerned.

For the purpose of ascertaining whether or not any other meteorological variable is simultaneously exerting any influence on the sea-surface temperature, similar arithmetic means are calculated for all characteristic days for each variable in turn: the resultant curves are then examined for variations around the key day.

The mechanism of this method becomes readily apparent when actual examples are considered.

2.3 The data.

For Ocean Weather Station 'M' all meteorological data and sea-surface temperature data were obtained from the Daily Weather Report of the British Meteorological Office. Each value of daily sea-surface temperature was taken as the mean of the three observations at 06h, 12h and 18h whereas the meteorological terms were

noted at 06h and 18h only. Comparison of the sea-surface temperatures calculated in this way with those compiled by Håkon Mosby directly from the ship's bathythermograph log sheets often revealed large discrepancies. (There can be little doubt that the latter publication contains the more accurate values; large gaps in the data, however, prohibited the use of this data source.) Meteorological data comprising surface pressure, air temperature, dew point temperature, wind speed and direction were obtained for all days of the four years 1961, 1962, 1965 and 1967; the mean sea-surface temperature was extracted for the same days and expressed for each day as the departure from the thirty one-day running mean centred on that day.

For Ocean Weather Station 'I', in order to minimise the amount of noise inherently associated with the sea-surface temperature data obtained from the Daily Weather Report, it was decided to extract all sea-surface temperature data directly from the bathythermograph log (Met.01 Form H19). All meteorological variables were also obtained from this source. Each daily value of sea-surface temperature, meteorological parameter, and additionally sea-surface salinity, was computed as the mean of the 010h and 021h observations. Data were obtained for the five-year period 1967-1971. Owing to numerous periods of missing data in the original collection other sources had to be contacted; in all no fewer than five sources were required to provide a complete data set.

In view of the more reliable sea-surface temperatures and additional salinity data obtained for Ocean Weather Station 'I', a

more thorough analysis was performed for this station.

At both stations the marine and meteorological data were grouped according to season. The subsequent choice of examples of meteorological types thought likely to affect the sea-surface temperature was confined to one season at a time. In this way any additional purely seasonal-dependent constraint, imposed for example by the presence or absence of thermal stratification in the superficial oceanic layer, should be detectable.

2.4 Results for Ocean Weather Station 'M'.

The meteorological variables chosen for examination were air pressure, air temperature T_a, dew-point temperature T_d, and scalar wind speed $|W|$. Variations in the air and dew-point temperatures were assumed to represent simultaneously corresponding variations in sensible and latent heat fluxes respectively. Strictly speaking, of course, the compound expressions $(T_s - T_a)|W|$ and $(e_s - e_a)|W|$ should have been employed to determine the flux variations but as fluctuations in both T_a and T_d are in general much greater than those in T_s, maxima and minima in the trends of the single variables T_a and T_d are assumed to coincide with corresponding maxima and minima in the sensible and latent heat fluxes. The accumulated scalar wind speed for chosen T_a and T_d days also supported this assumption. The scalar wind speed was chosen as a measure of the sea-surface temperature change due to wind-produced turbulent mixing in the water medium; this is in agreement with theoretical considerations which point to a square root of wind stress dependence (vid. appendix (i)).

2.4.1 Spring Period.

In figure 2.4.1a the key day was chosen to coincide with a maximum in the scalar wind speed. The mean accumulated air temperature, dew-point temperature and surface pressure for the same key day and other characteristic days are also shown. The corresponding sea-surface temperature variation shows a drop occurring simultaneously with increase in scalar wind speed of approximately four times the standard error of the sea-surface temperature mean. A minimum in the scalar wind was chosen in figure 2.4.1b and the trend in other variables determined as before. A peak in the sea temperature coincident with the wind speed minimum is detectable but this is barely significant in terms of the relevant standard error. Troughs in air temperature and dew-point temperature which together are taken to represent a maximum in the total surface heat flux, in accordance with the previous reasoning, are seen in figure 2.4.1c to occur in parallel with a significant drop in the sea-surface temperature. Organised pressure variations do not appear to be associated with any systematic variation in the sea-surface temperature as figure 2.4.1d will verify.

2.4.2 Summer Period.

Variations in air- and dew-point temperatures were considered to be generally too small to warrant any investigation during this period. Key days based on abrupt changes in scalar wind speed were, however, selected. Figures 2.4.2a and 2.4.2b illustrate curves of rapid increase and decrease, respectively,

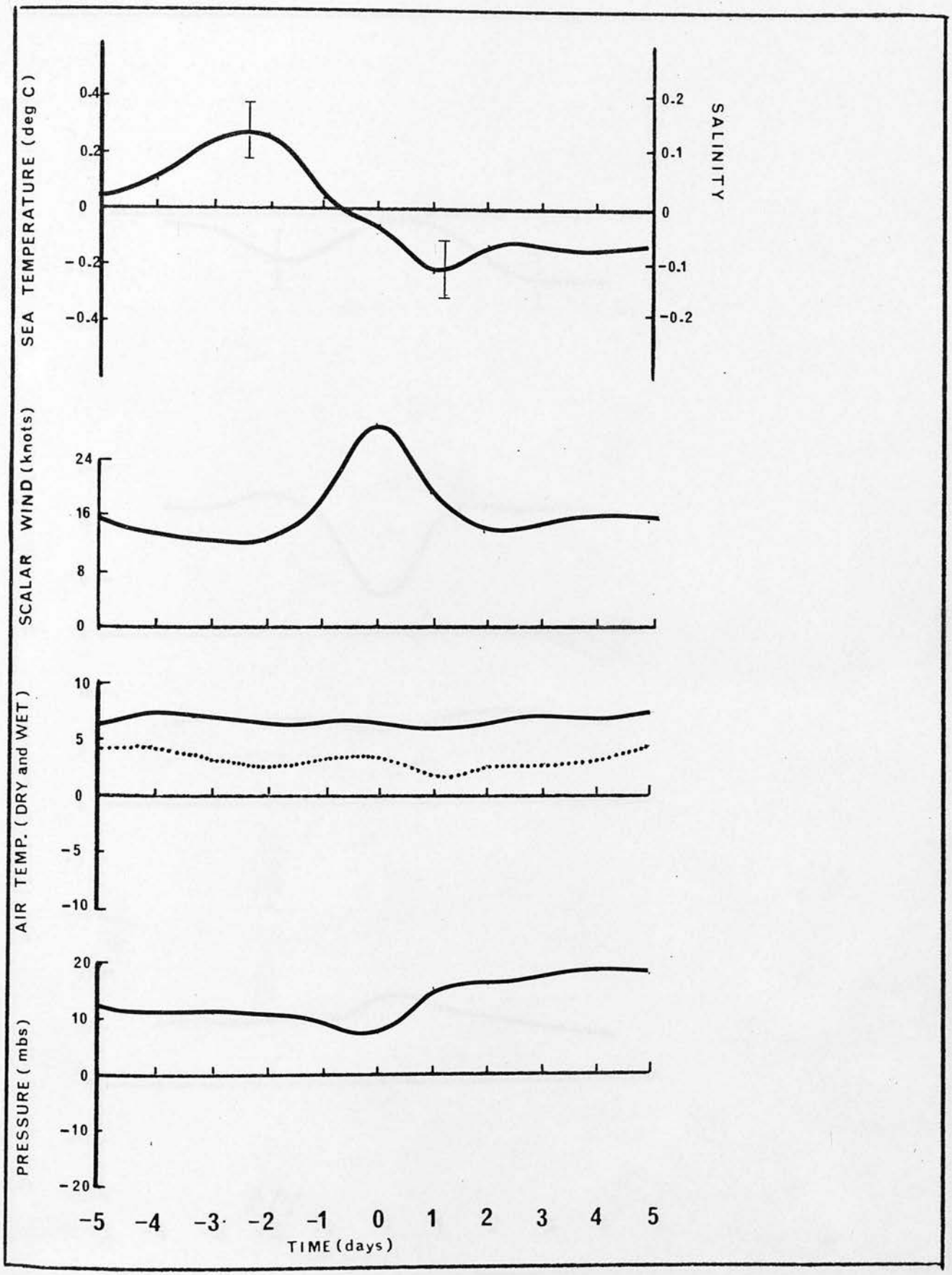

FIGURE 2.4.1a OWS 'M', SPRING; KEY DAY COINCIDENT WITH SCALAR WIND SPEED CREST.

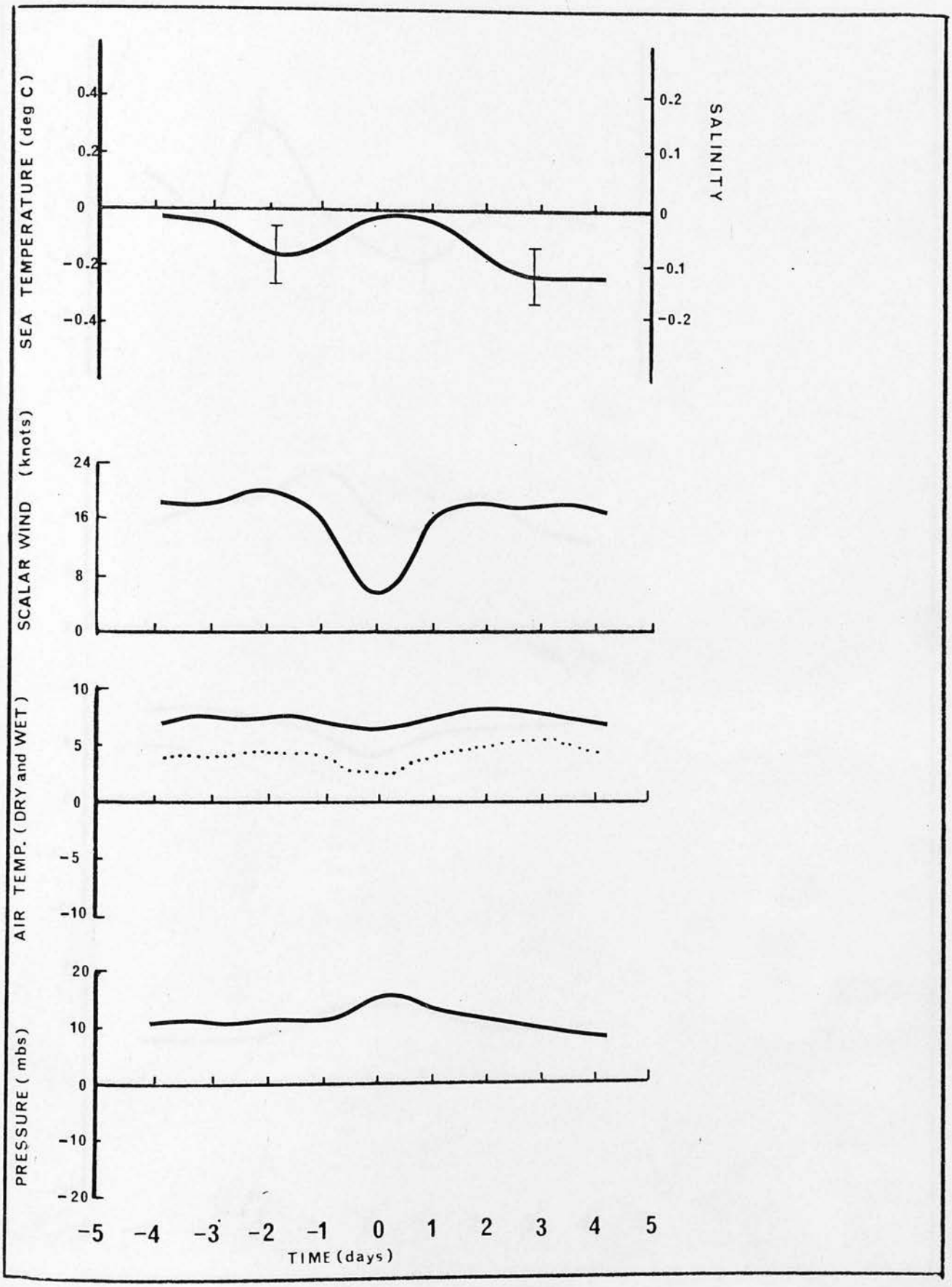

FIGURE 2.4.1b OWS 'M', SPRING; KEY DAY COINCIDENT WITH SCALAR WIND SPEED TROUGH.

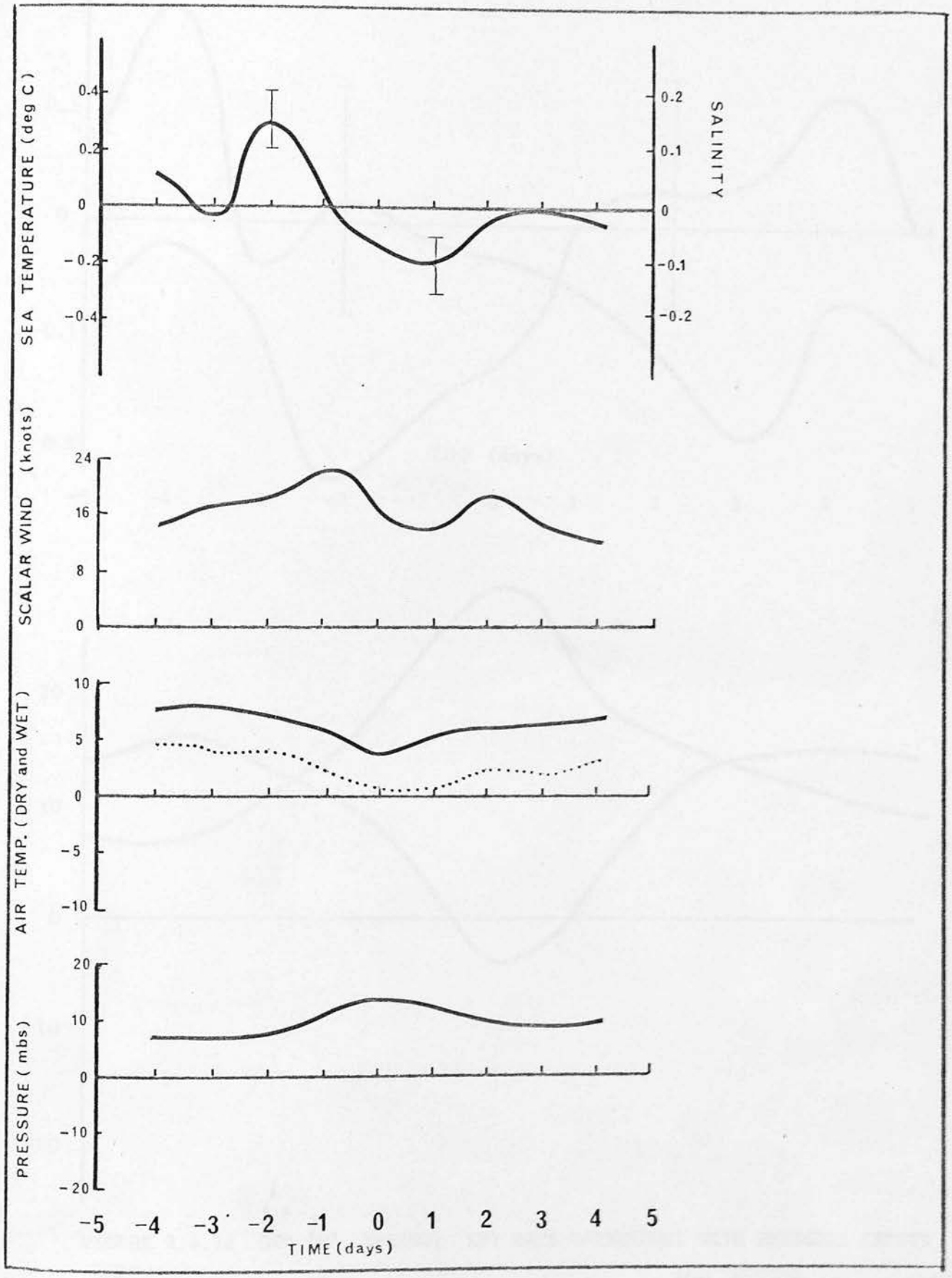

FIGURE 2.4.1c OWS 'M', SPRING; KEY DAY COINCIDENT WITH AIR TEMPERATURE TROUGH.

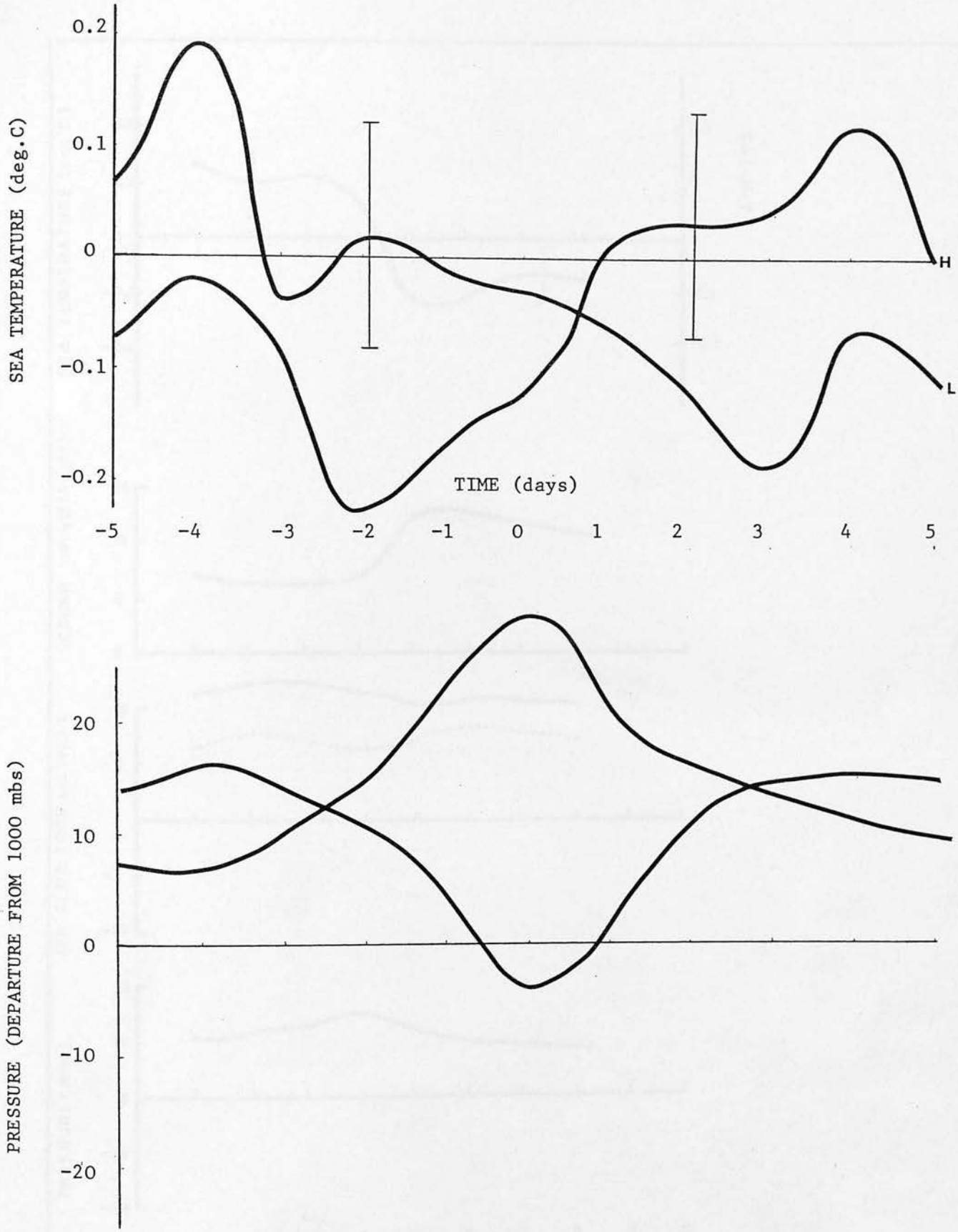

FIGURE 2.4.1d OWS 'M', SPRING; KEY DAYS COINCIDENT WITH PRESSURE CRESTS AND TROUGHS

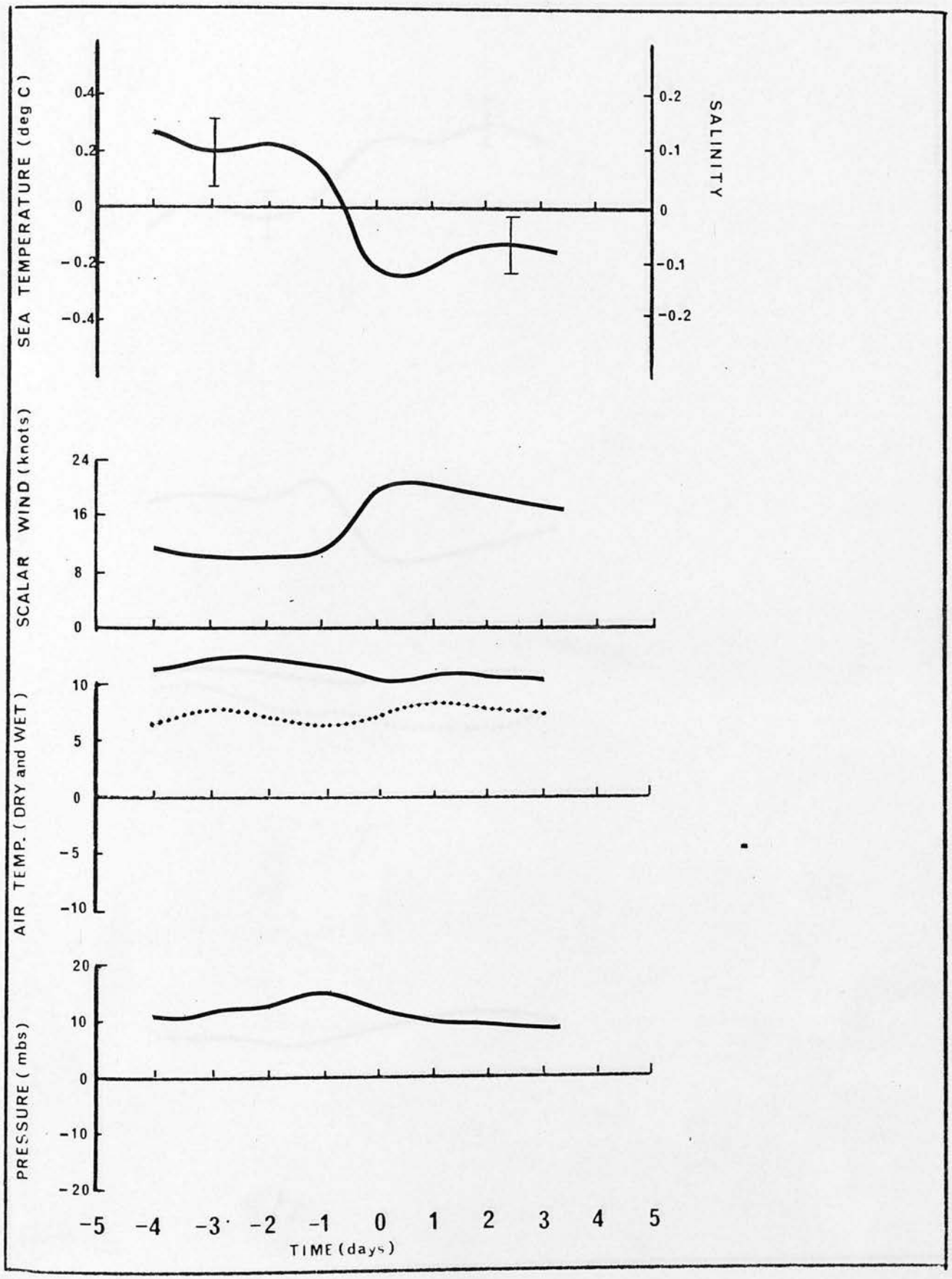

FIGURE 2.4.2a OWS 'M', SUMMER; KEY DAY BASED ON SCALAR WIND SPEED INCREASE.

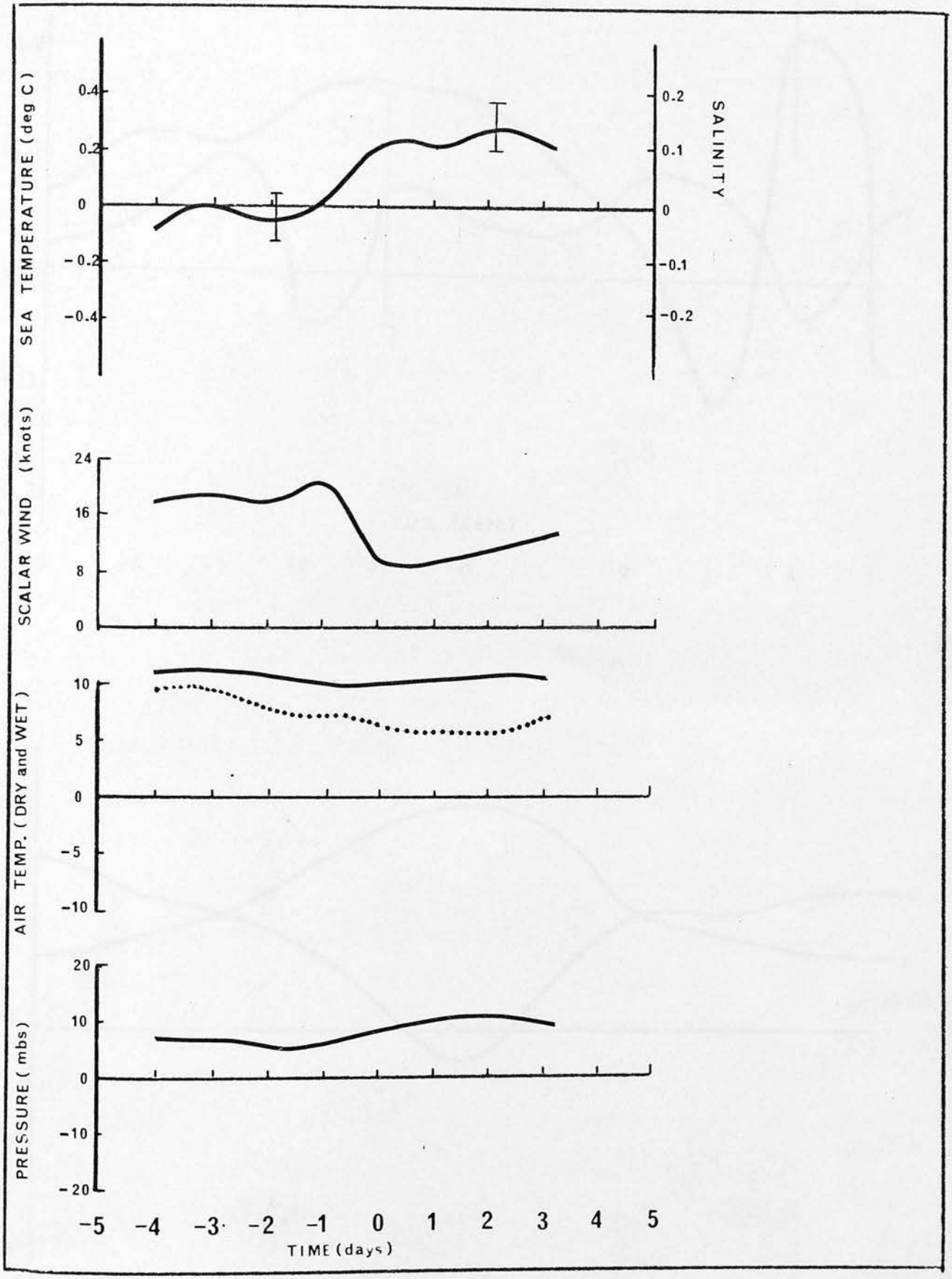

FIGURE 2.4.2b OWS 'M', SUMMER; KEY DAY BASED ON SCALAR WIND SPEED DECREASE.

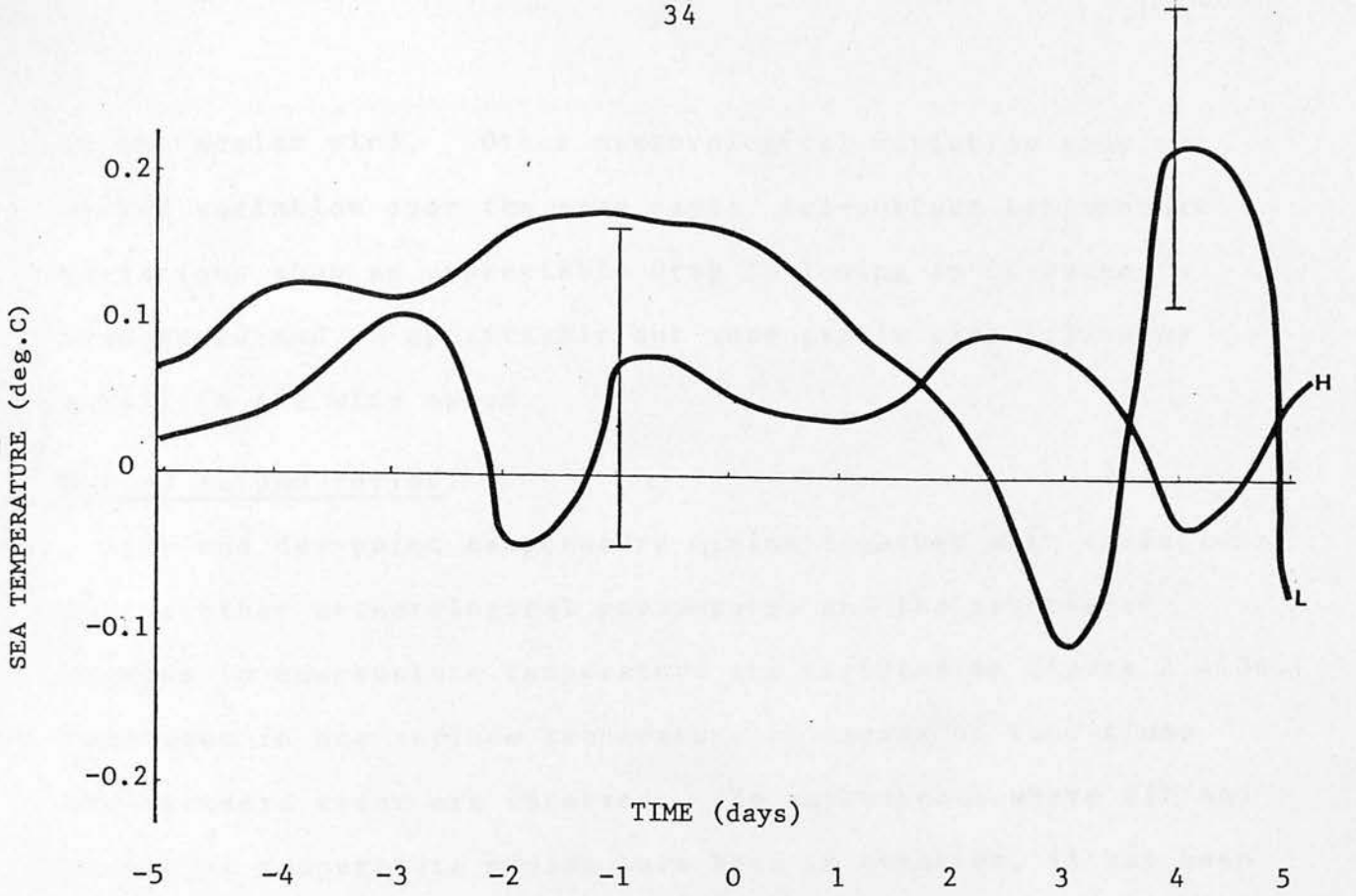

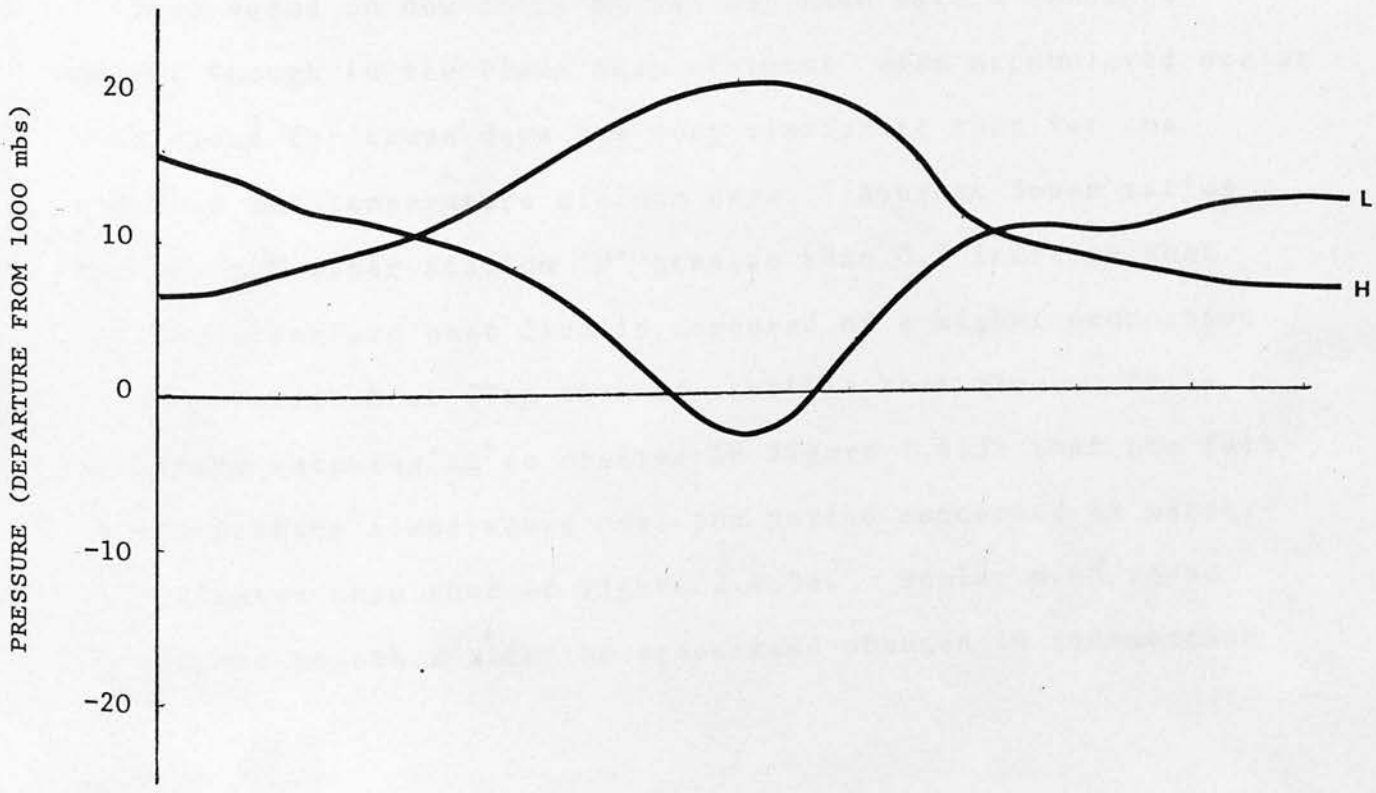

FIGURE 2.4.2c OWS 'M', SUMMER; KEY DAYS COINCIDENT WITH PRESSURE CRESTS AND TROUGHS

in the scalar wind. Other meteorological variables show no marked variation over the same days; sea-surface temperature variations show an appreciable drop following an increase in wind speed and an appreciable but more gentle rise following a fall in the wind speed.

2.4.3 Autumn Period.

Air- and dew-point temperature minima together with variations in the other meteorological parameters, and the associated changes in sea-surface temperature are depicted in figure 2.4.3a. Decreases in sea-surface temperature in excess of four times the standard error are observed. In experiments where air and dew-point temperature minima have been in question, it has been practice to base the selection of days on air temperature only; on average the dew-point temperature mean follows the same trend as the air temperature. As a further experiment a selection of days based on dew-point minima was made with a somewhat deeper trough in the final mean minimum; mean accumulated scalar wind speed for these days was very similar to that for the previous air temperature minimum days. Average Bowen ratios for Ocean Weather Station 'M' greater than 0.5 indicate that the total surface heat flux is composed of a higher proportion of evaporative heat flux than of sensible heat flux. It is therefore encouraging to observe in figure 2.4.3b that the fall in sea-surface temperature over the period concerned is measurably greater than that of figure 2.4.3a. Scalar wind speed variations together with the associated changes in sea-surface

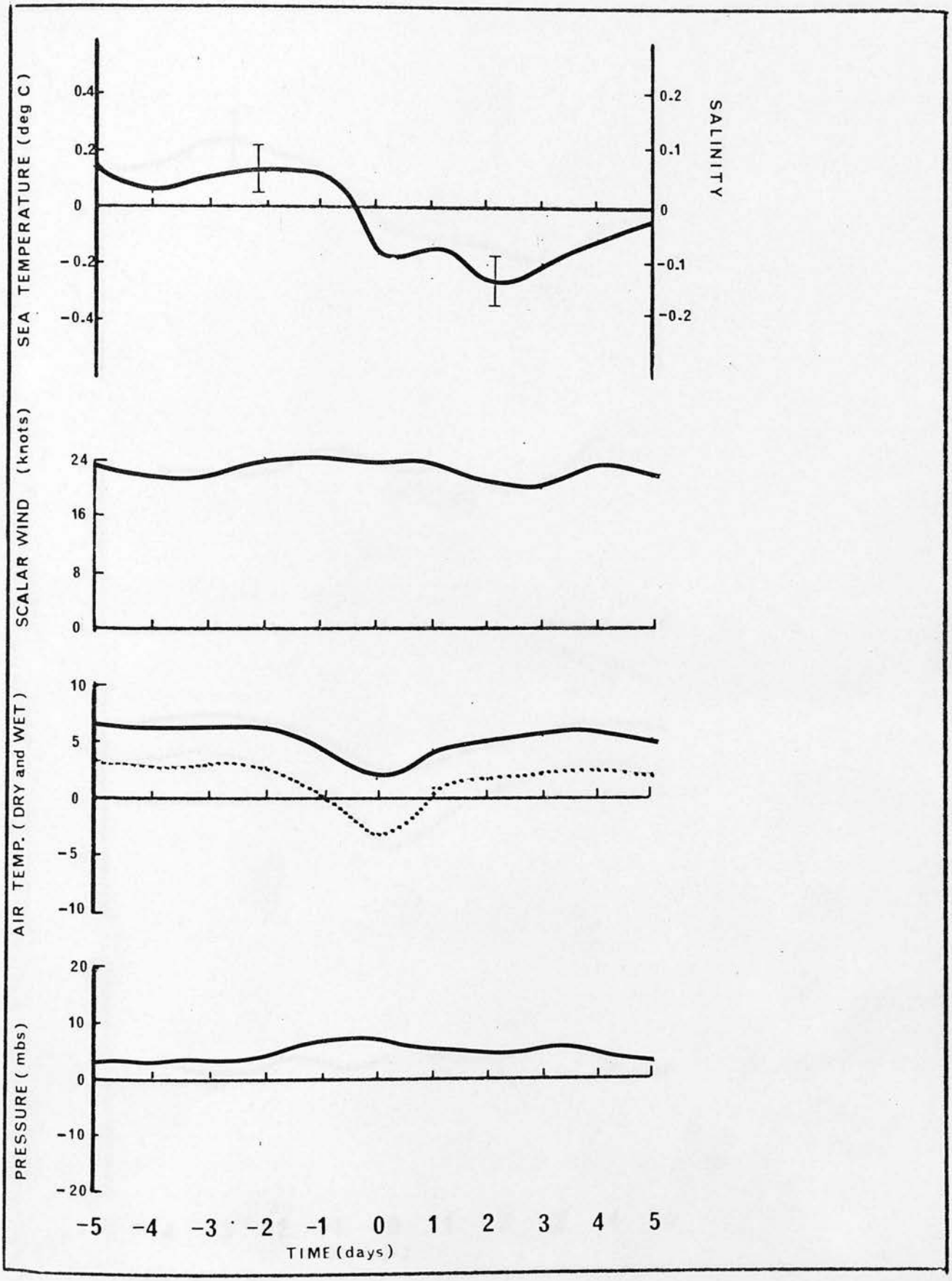

FIGURE 2.4.3a OWS 'M', AUTUMN; KEY DAY COINCIDENT WITH AIR TEMPERATURE TROUGH.

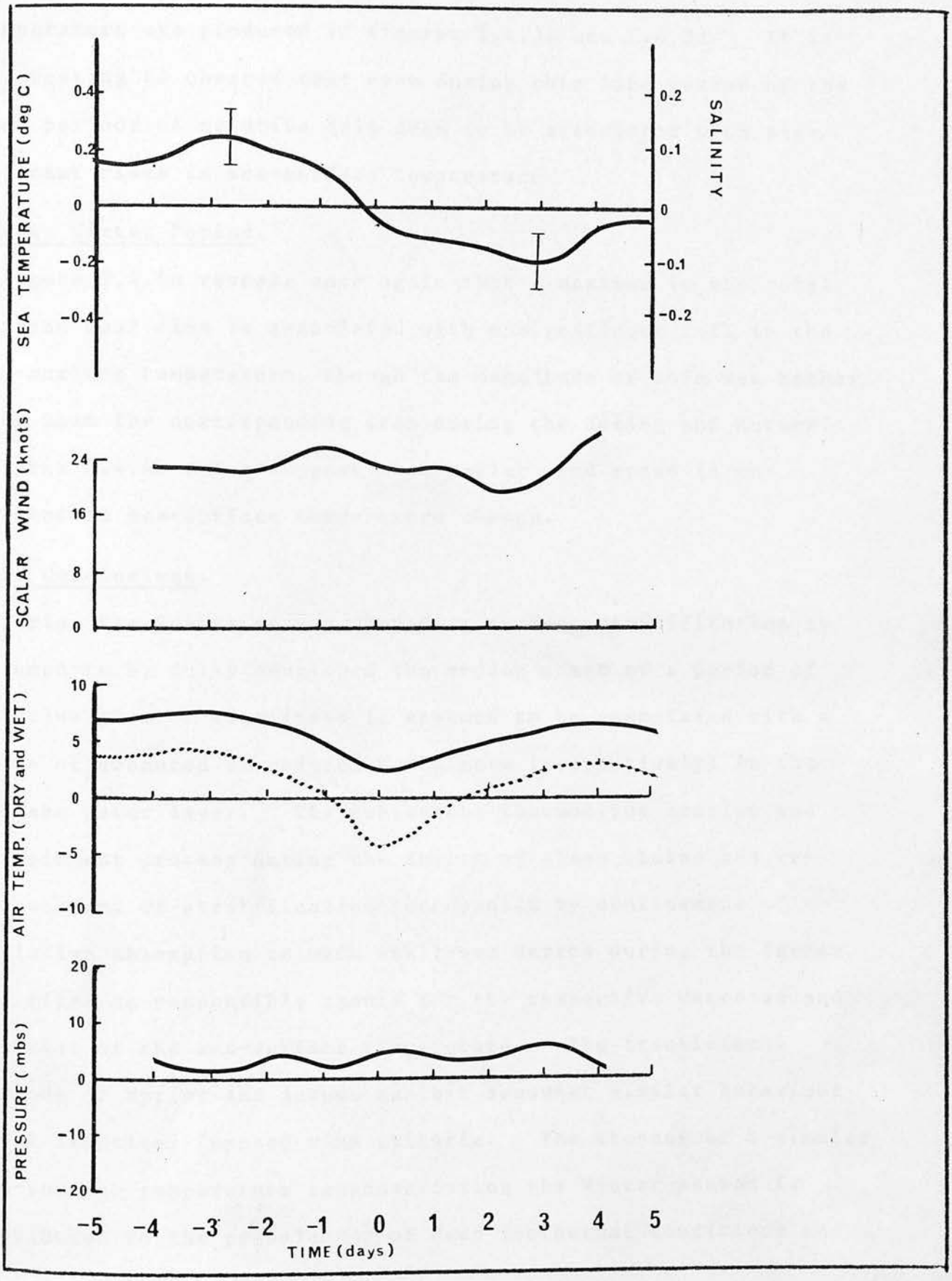

FIGURE 2.4.3b OWS 'M', AUTUMN; KEY DAY COINCIDENT WITH DEW-POINT TEMPERATURE TROUGH.

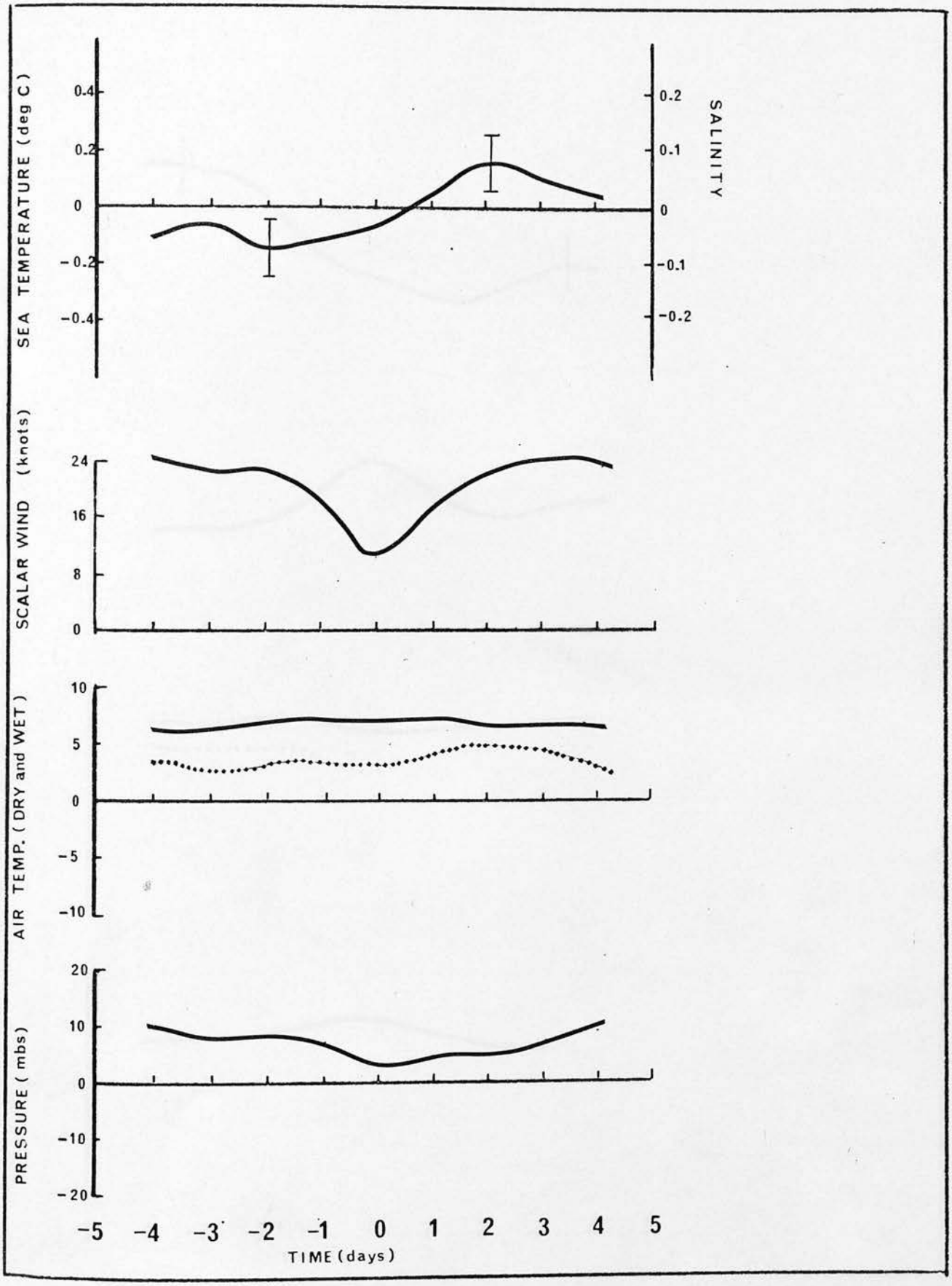

FIGURE 2.4.3c OWS 'M', AUTUMN; KEY DAY COINCIDENT WITH SCALAR WIND SPEED TROUGH.

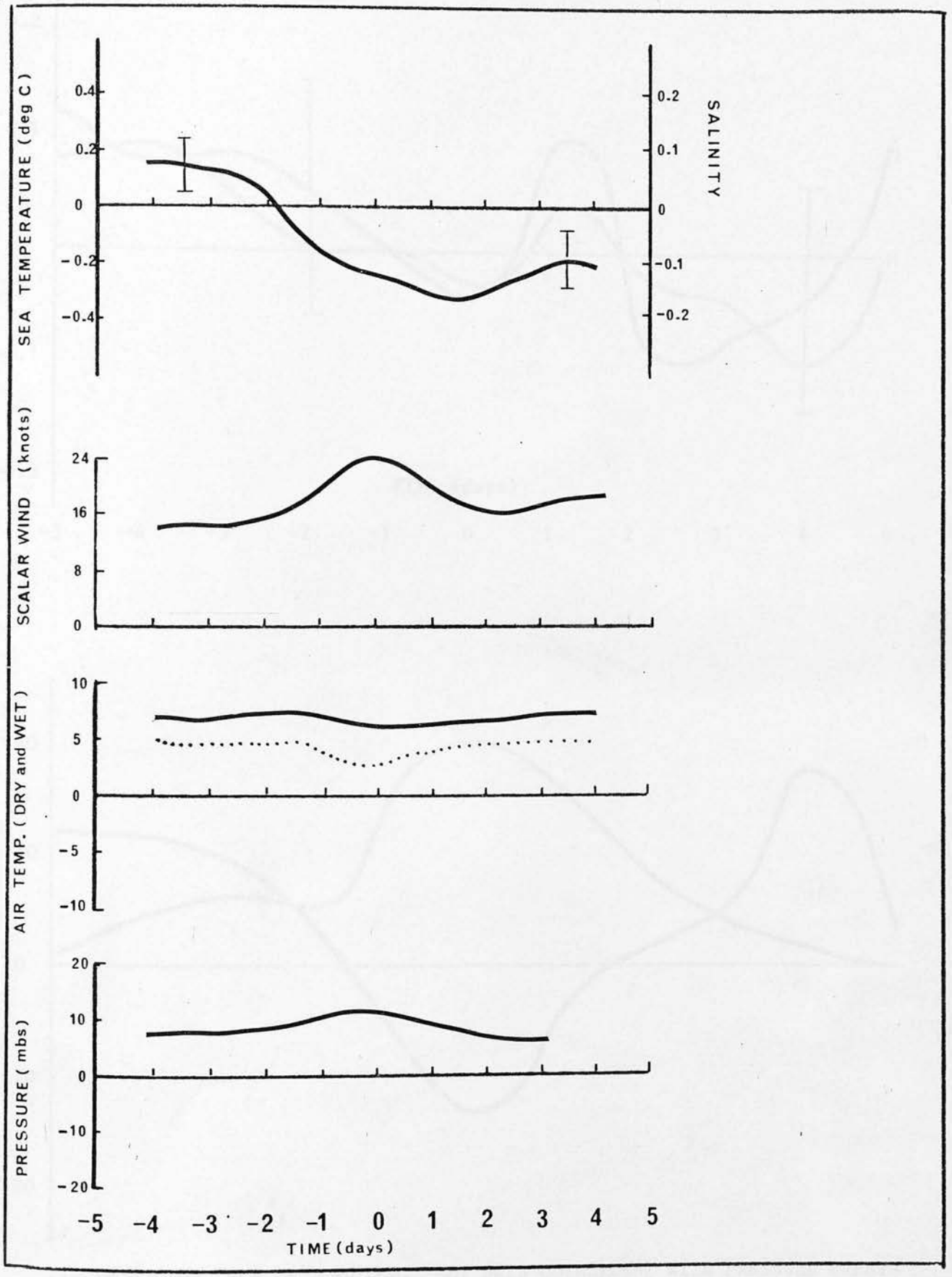

FIGURE 2.4.3d OWS 'M', AUTUMN; KEY DAY COINCIDENT WITH SCALAR WIND SPEED CREST.

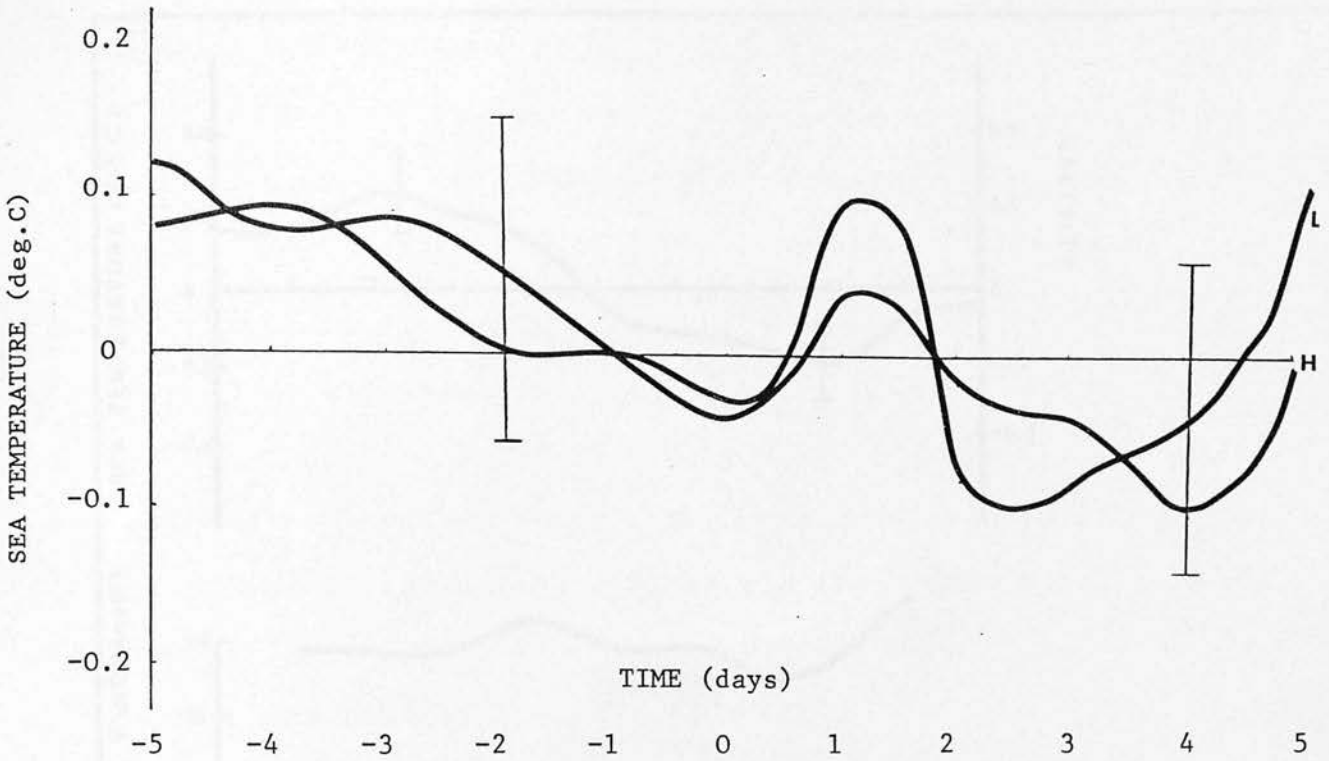

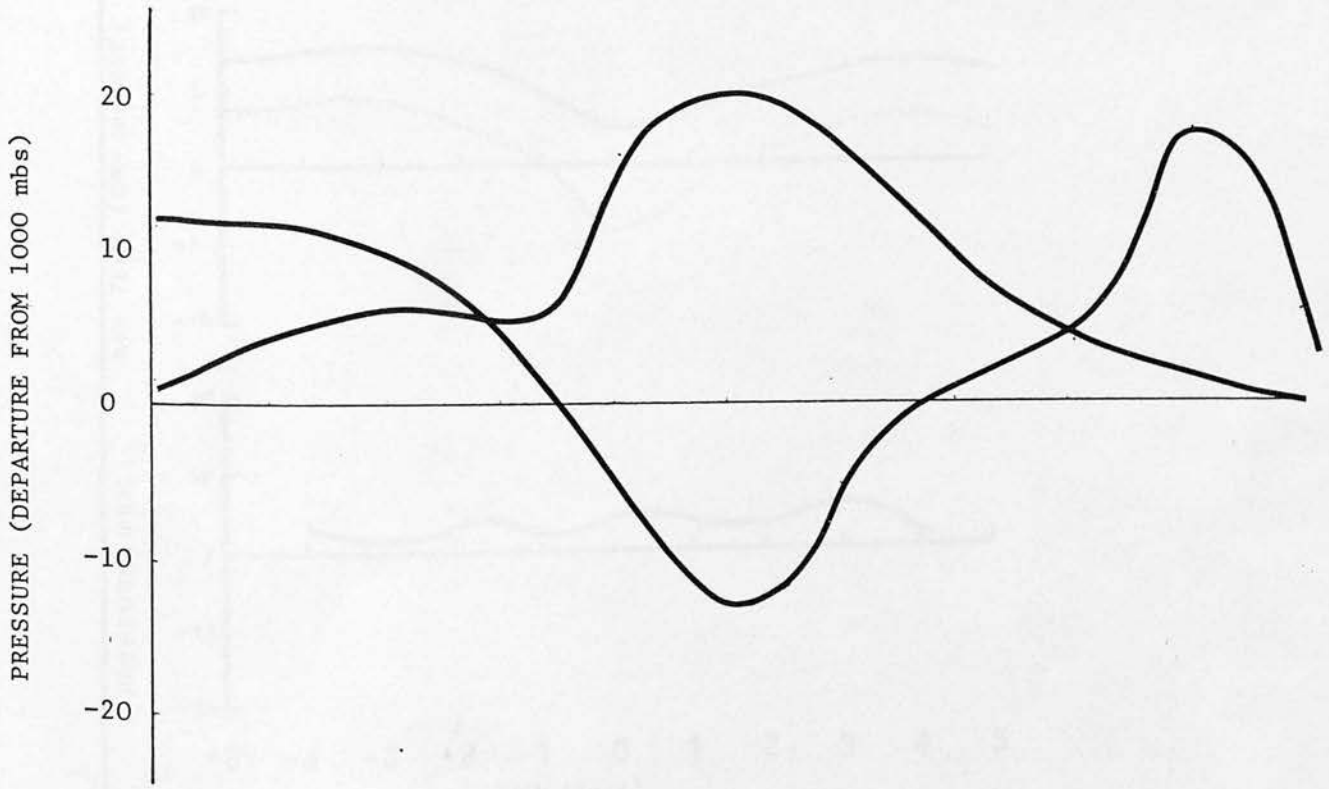

FIGURE 2.4.3e OWS 'M', AUTUMN; KEY DAYS COINCIDENT WITH PRESSURE CRESTS AND TROUGHS

temperature are produced in figures 2.4.3c and 2.4.3d. It is interesting to observe that even during this late period of the year periods of relative calm seem to be associated with significant rises in sea-surface temperature

2.4.4 Winter Period.

Figure 2.4.4a reveals once again that a maximum in the total surface heat flux is associated with a significant fall in the sea-surface temperature, though the magnitude of this was rather less than the corresponding drop during the Spring and Autumn. Figures 2.4.4b and c suggest that scalar wind speed is unrelated to sea-surface temperature change.

2.5 Conclusions.

During the Summer season when near-surface stratification is assumed to be fully developed the sudden onset of a period of relative clam or storminess is assumed to be associated with a state of enhanced or reduced turbulence (respectively) in the surface water layer. The subsequent thermocline erosion and entrainment process during the former of these states and reinforcement of stratification accompanied by confinement of radiative absorption to much shallower depths during the latter, are cited as responsible agents for the respective decrease and increase of the sea-surface temperature. The transitional periods of Spring and Autumn exhibit somewhat similar behaviour under identical imposed wind criteria. The absence of a similar sea-surface temperature response during the Winter season is attributed to the prevalence of deep isothermal conditions and

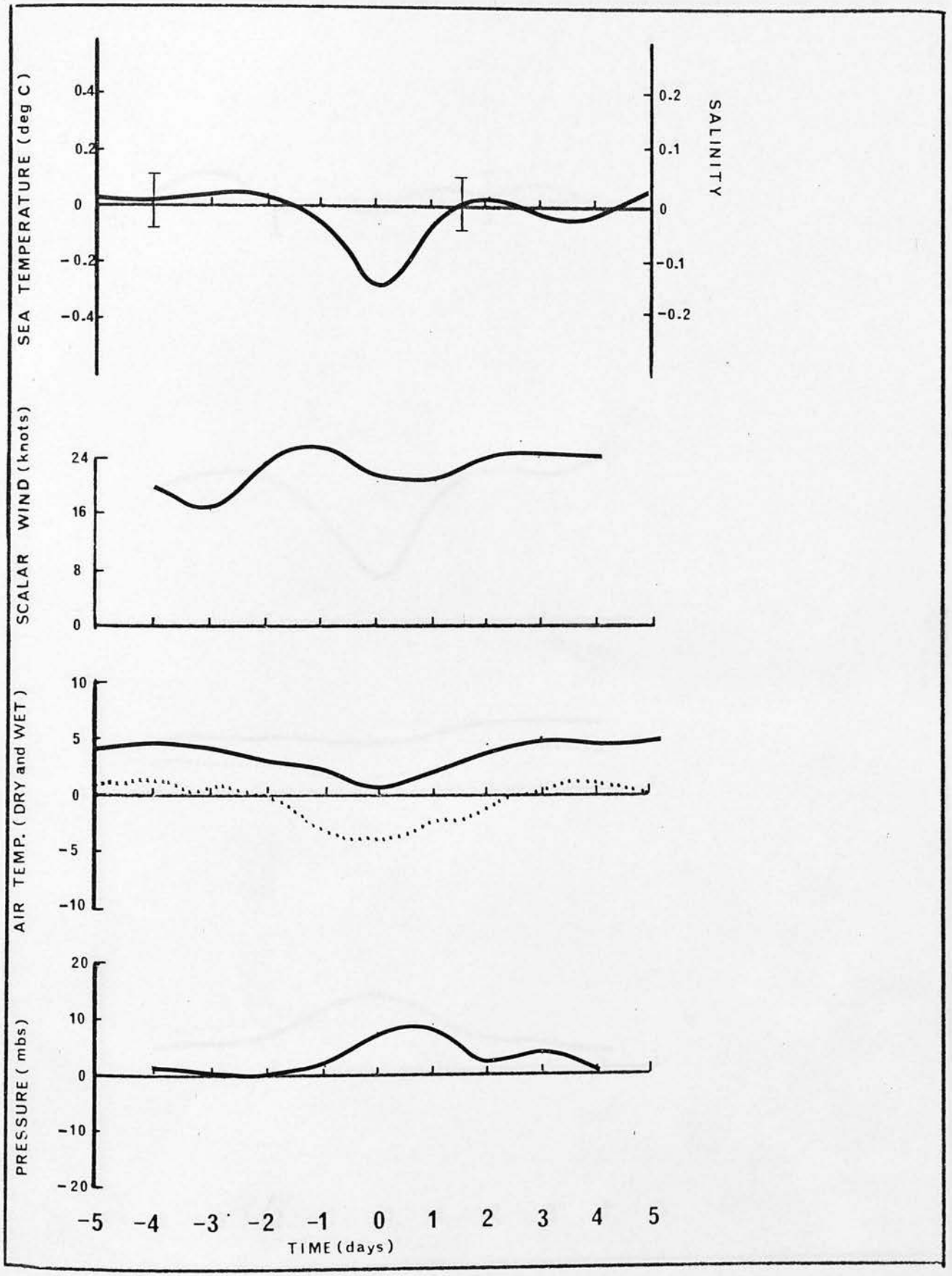

FIGURE 2.4.4a OWS 'M', WINTER; KEY DAY COINCIDENT WITH AIR TEMPERATURE TROUGH.

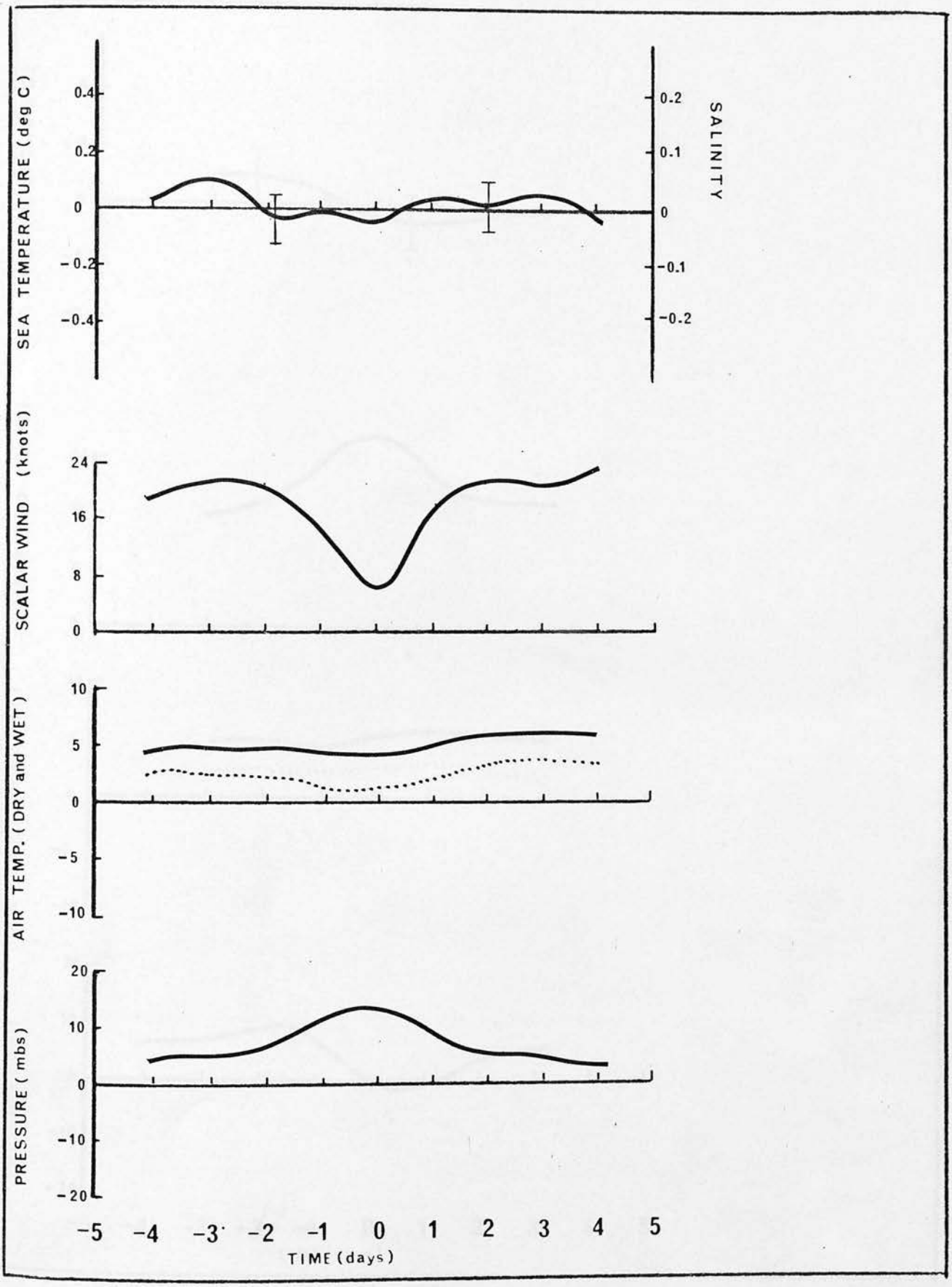

FIGURE 2.4.4b OWS 'M', WINTER; KEY DAY COINCIDENT WITH SCALAR WIND SPEED TROUGH

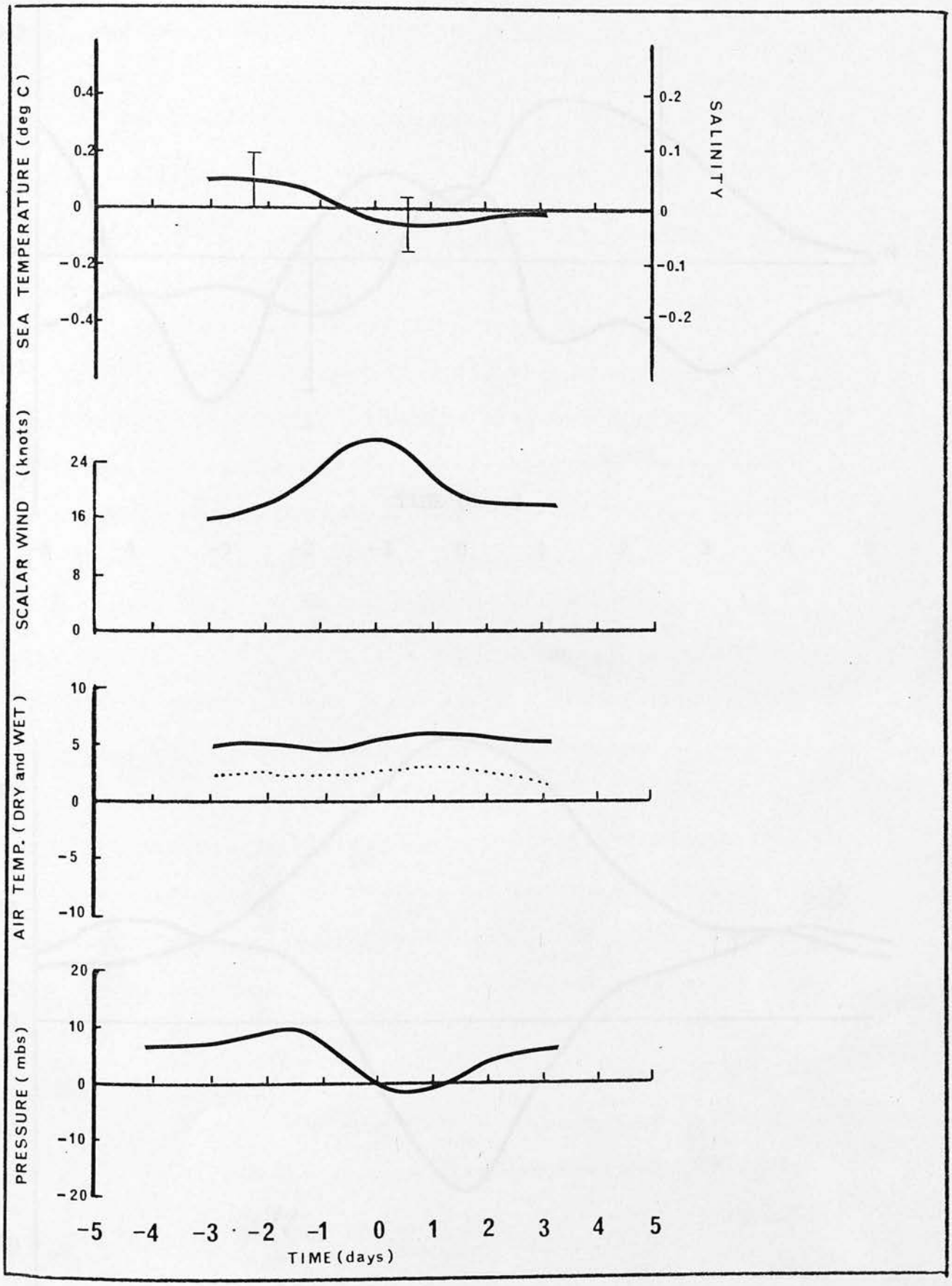

FIGURE 2.4.4c OWS 'M', WINTER; KEY DAY COINCIDENT WITH SCALAR WIND SPEED CREST.

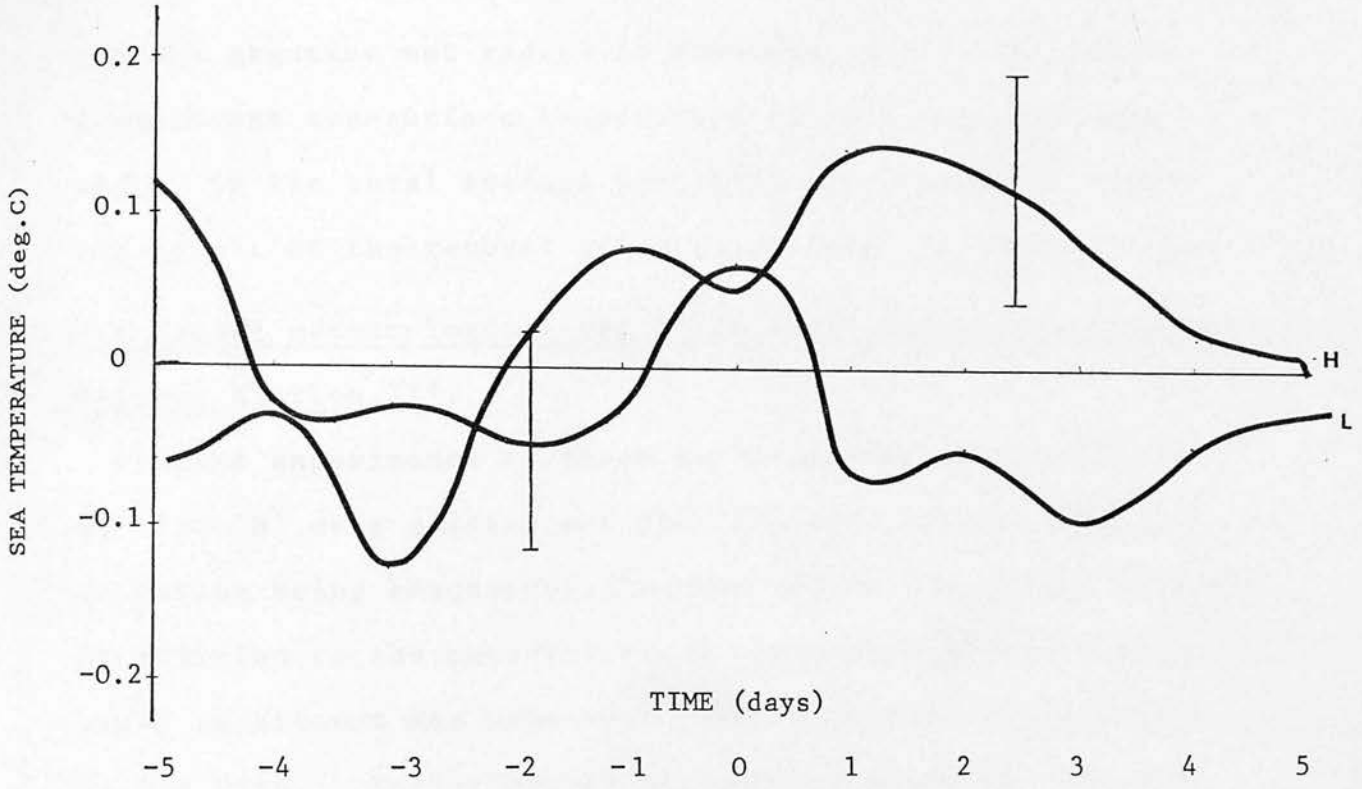

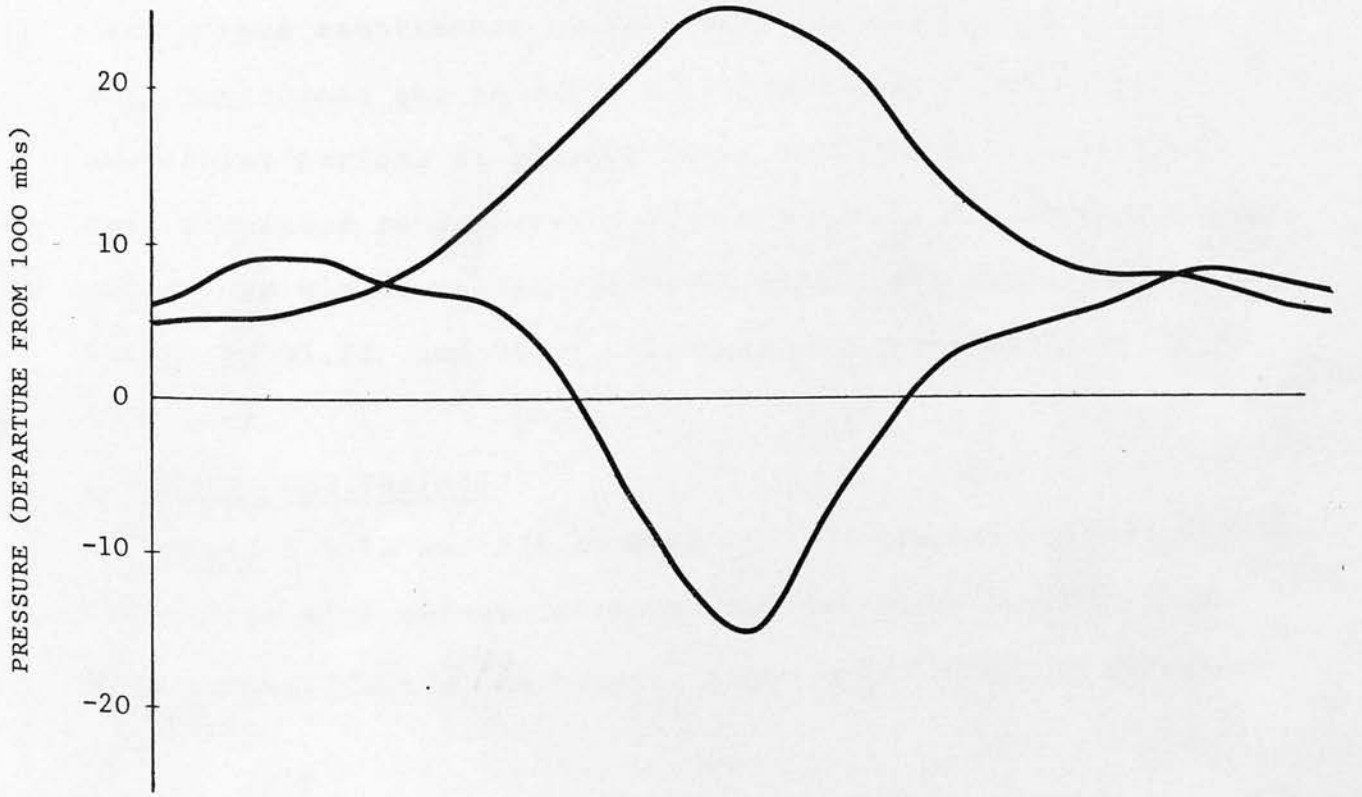

FIGURE 2.4.4d OWS 'M', WINTER; KEY DAYS COINCIDENT WITH PRESSURE CRESTS AND TROUGHS

overall negative net radiative exchange during that season. Significant sea-surface temperature falls associated with maxima in the total surface heat flux are considered simply the result of the removal of enthalpy from the surface layer.

2.6 Joint meteorological-sea temperature variations at Ocean Weather Station 'I'.

Similar experiments to those performed for Ocean Weather Station 'M' were carried out for 'I', with however most attention being concentrated on the winter and summer seasons. In addition to the meteorological parameters already investigated an attempt was made to include the directional aspect of the wind. Variations of sea-surface salinity have also been included where it was thought likely that these would assist the physical argument. Changes in the sea-surface salinity are shown as broken curves on the same graph as the sea-surface temperature variations; the right-hand vertical axis represents the relevant salinity scale. Owing to occasional periods of missing data, salinity values have not been presented as departures from thirty-one day running means; summer and winter values represent departures from constant values of 35.2‰ and 35.3‰ respectively, multiplied by 10 in each case.

2.6.1 Summer Period.

Figures 2.6.1a and 2.6.1b show sea-surface temperature trends associated with abrupt increases and decreases in the scalar wind respectively. As before, other meteorological variables

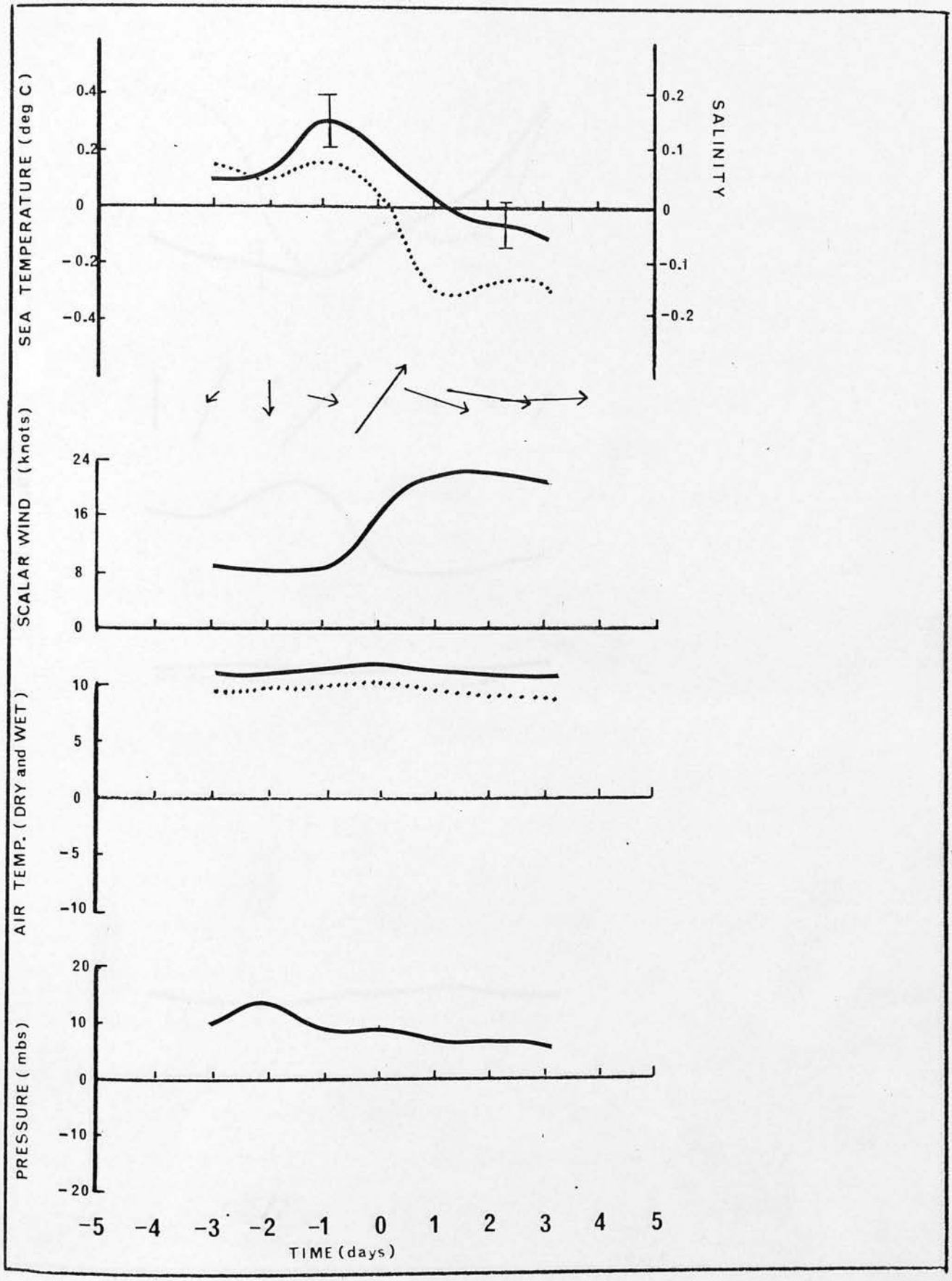

FIGURE 2.6.1a OWS 'I', SUMMER; KEY DAY BASED ON SCALAR WIND SPEED INCREASE.

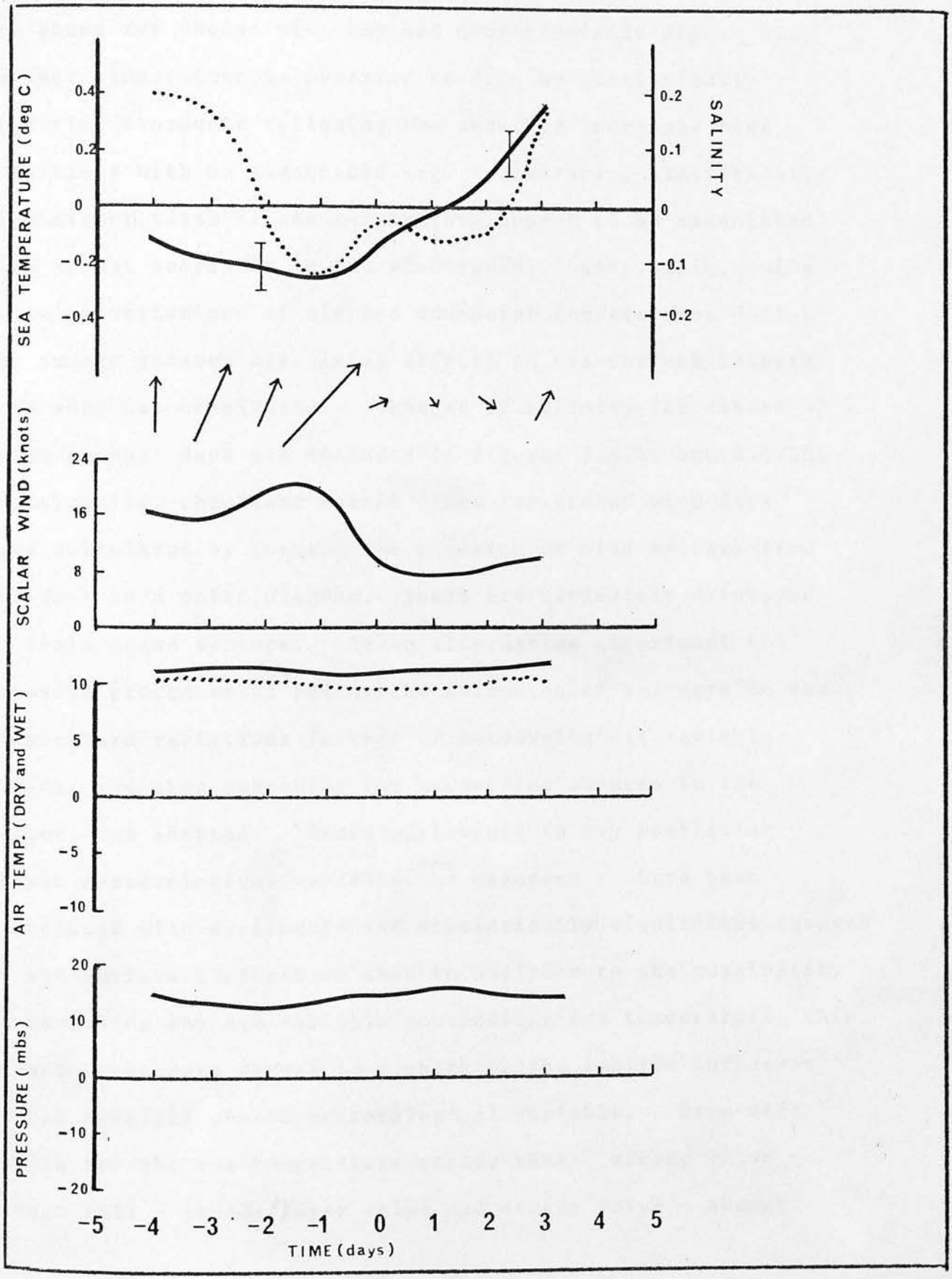

FIGURE 2.6.1b OWS 'I', SUMMER; KEY DAY BASED ON SCALAR WIND SPEED DECREASE.

are shown for chosen wind key and characteristic days. Sea-surface temperature is observed to drop by statistically significant amounts following the onset of increased wind conditions with no measurable lag. Similarly, statistically significant rises of sea temperature appear to be associated with abrupt decreases in the wind speed. Once again, owing to small variations of air and dew-point temperatures during the summer season, associated effects on sea-surface temperature were not considered. Changes of salinity for chosen 'wind change' days are included in figures 2.6.1a and 2.6.1b. Additionally, resultant vector winds for chosen wind days were calculated by forming the addition of wind vectors (two per day) on a polar diagram. These are ultimately displayed as scale drawn vectors. As an alternative experiment the opposite procedure of basing the selection of key days on sea temperature variations instead of meteorological variable trends, and then searching for associated changes in the latter, was adopted. Where variations in any particular chosen meteorological variable were observed to have been associated with systematic and statistically significant changes in sea-surface temperature then in addition to the possibility of revealing any new variable controlling sea temperature, this reverse procedure served as a check on the implied influence of the original chosen meteorological variable. Days were chosen for the sea temperature trends thus: steady value - abrupt fall - steady lower value and steady value - abrupt

rise - steady higher value. The mean magnitudes of sea temperature rise and fall over the key days were 0.46°C and 0.47°C respectively, i.e. 5.1 and 5.6 times the relevant summer standard errors. Salinity variations were also included as were also vector winds and other meteorological variables. The results are displayed in figures 2.6.1c and 2.6.1d. Particular attention should be devoted to the trend of scalar wind speed and corresponding vector wind variations in association with the sea temperature and salinity changes; discussion follows in the conclusion section. The necessary return of bathythermograph data to lending sources, before further extraction, prohibited a more quantitative comparison of sea temperature fall due to mixing which could have been estimated with the aid of expression * of appendix (i) and mean sea temperature profiles for the day prior to onset of windy (increased stress) conditions.

2.6.2 Winter Period.

Figures 2.6.2a and 2.6.2b show sea temperature trends associated with scalar wind variations similar to those investigated during the summer season. The overall apparent fall of sea temperature following the onset of windy conditions, being barely three times the standard error concerned can only be regarded as marginally statistically significant. Generally higher values of sea temperature were associated with periods of low wind speed than were observed in the immediately preceding windy conditions. Key days based on periods of relatively

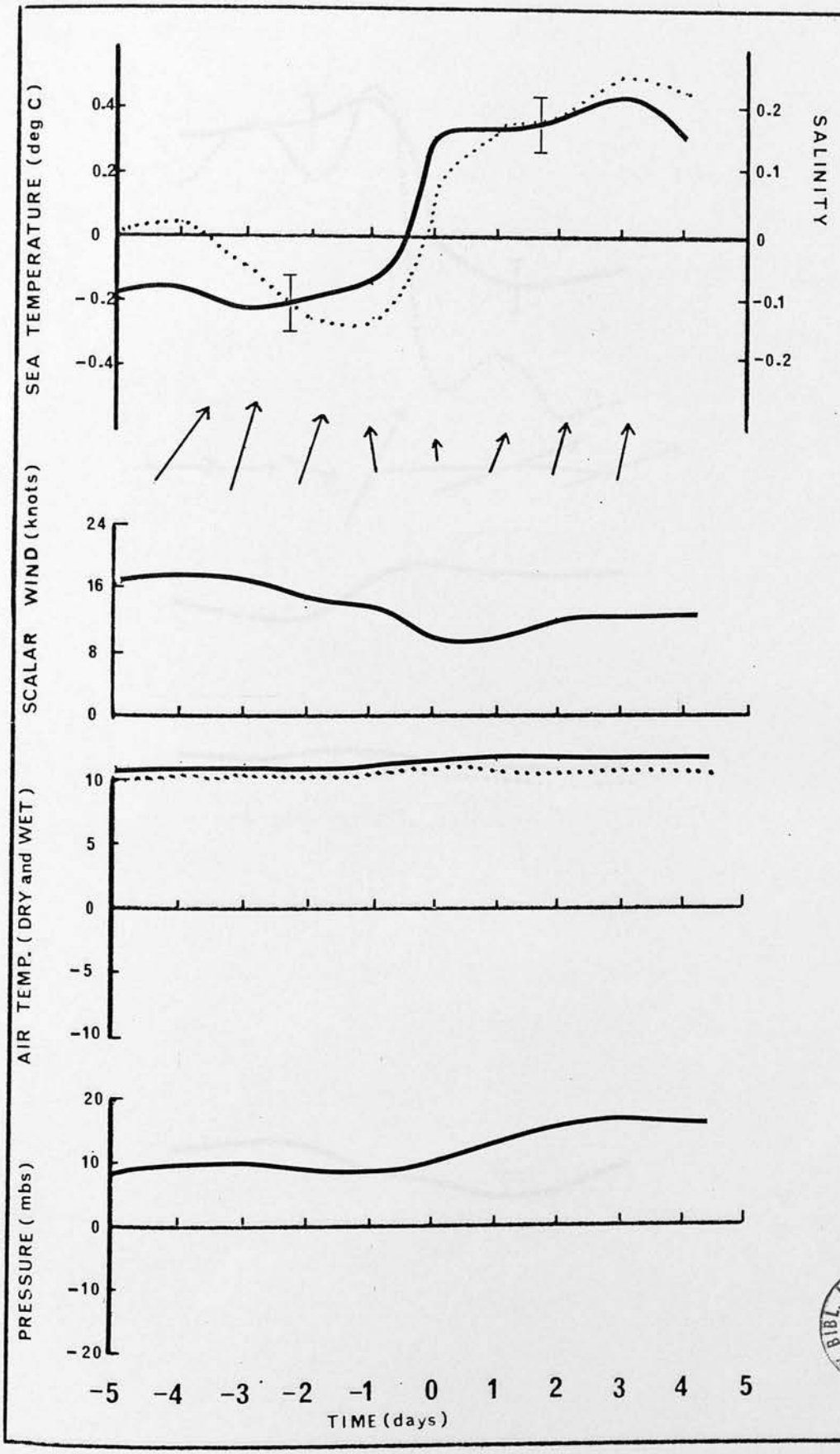

FIGURE 2.6.1c OWS 'I', SUMMER; KEY DAY BASED ON SEA TEMPERATURE INCREASE.

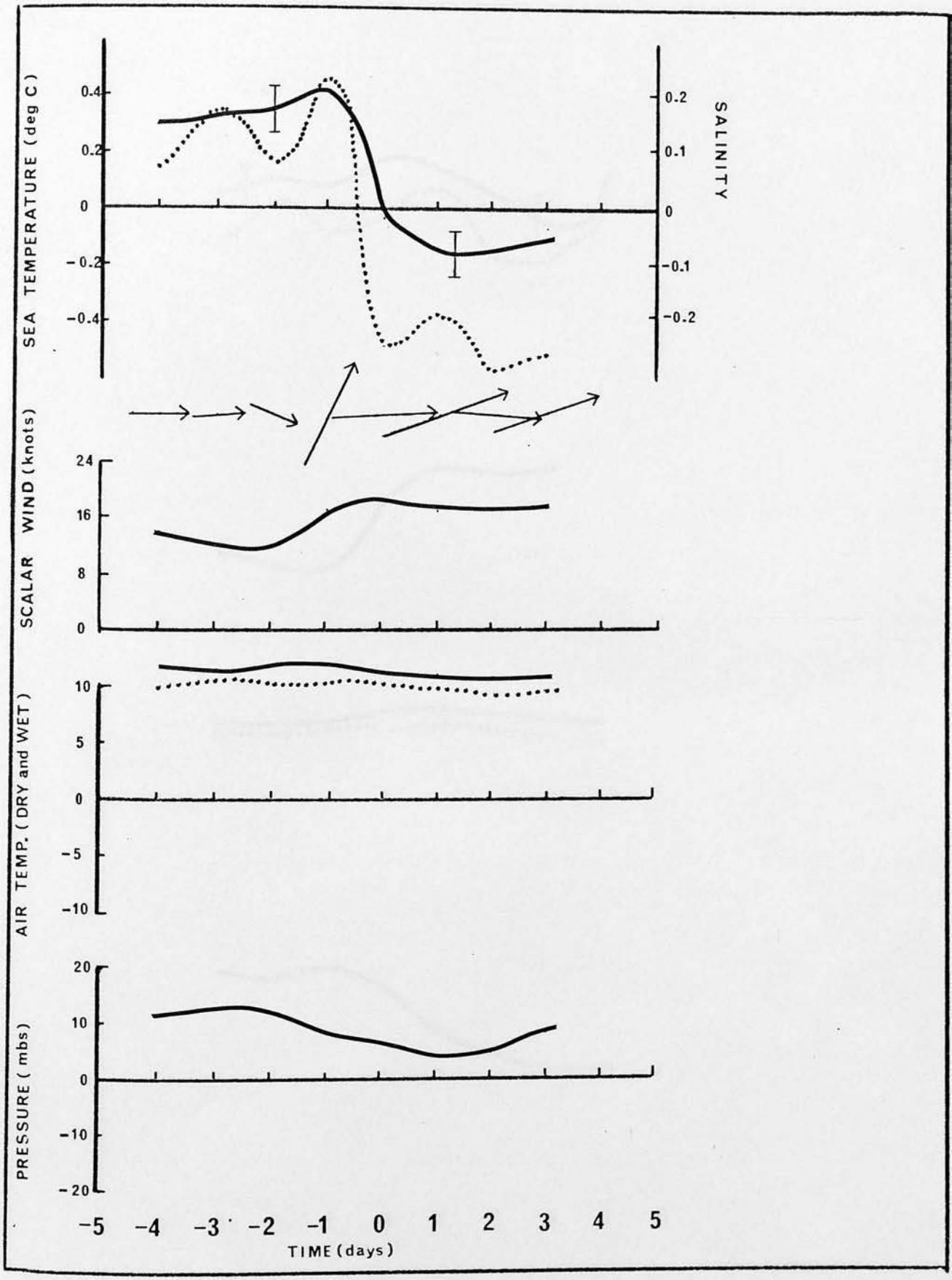

FIGURE 2.6.1d OWS 'I' SUMMER; KEY DAY BASED ON SEA TEMPERATURE DECREASE.

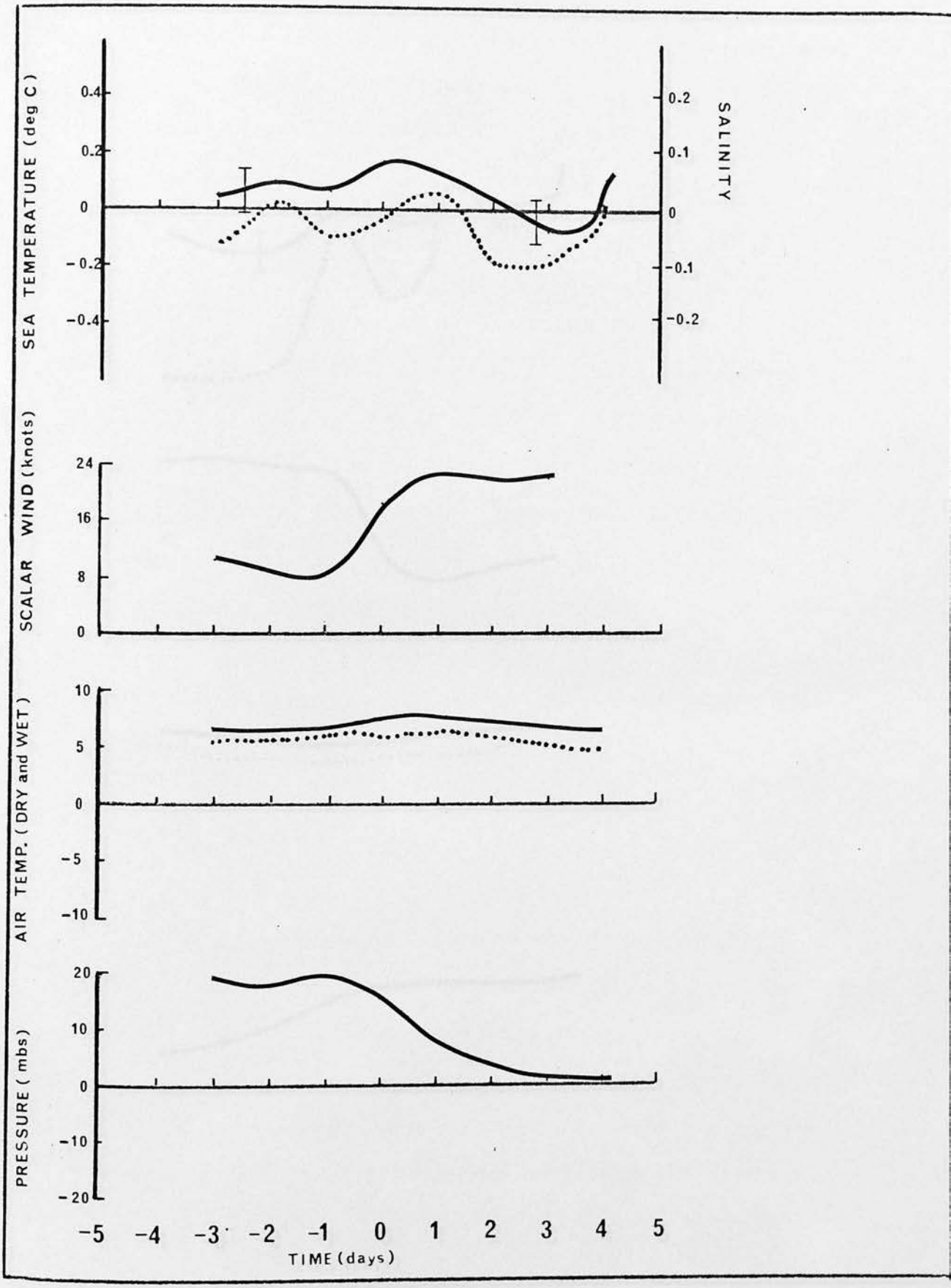

FIGURE 2.6.2a OWS 'I', WINTER; KEY DAY BASED ON SCALAR WIND SPEED INCREASE.

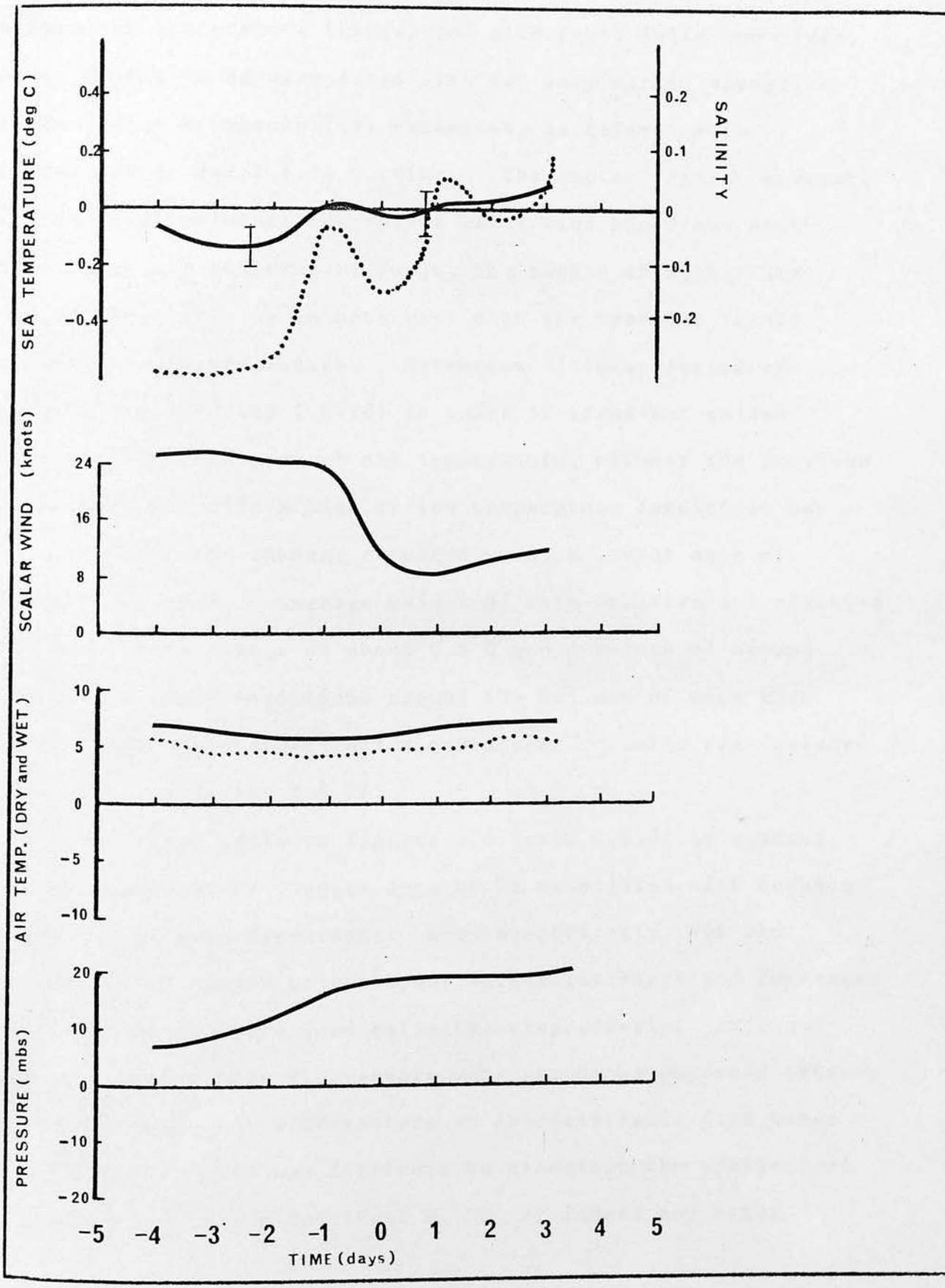

FIGURE 2.6.2b OWS 'I', WINTER; KEY DAY BASED ON SCALAR WIND SPEED DECREASE.

uniform sea temperature interspaced with rapid falls and rises, do not appear to be associated with any very marked variation of the scalar meteorological variables, as reference to figures 2.6.2c and 2.6.2d verfies. The latter figure, however, provides some evidence for rather lower wind speed and somewhat higher air temperature during the period of higher sea temperature; this is in agreement with the previous result indicated in figure 2.6.2b. Extension of these latter experiments (2.6.2c and 2.6.2d) to cases of transient sudden increases and decreases of sea temperature, without the previous restriction of uniform high or low temperature conditions before and after the change, resulted in much larger sets of accumulated cases. Average values of both positive and negative sea temperature change of about $0.5^{o}C$ and n values of around 50 together imply variations around the key day of more than twelve times the standard error concerned; results are depicted in figures 2.6.2e and 2.6.2f.

With reference again to figures 2.6.2c to 2.6.2f it appears that sea temperature changes seem to be associated with changes to particular wind directions: more specifically, SSE and W or WSW winds appear to accompany marked increases and decreases of the sea temperature (and salinity) respectively. Since, however, considerable wind shears were sometimes observed between successive resultant wind vectors on characteristic days other than the key day, it was difficult to ascertain the statistical significance of say a resultant W, SE, or indeed any other

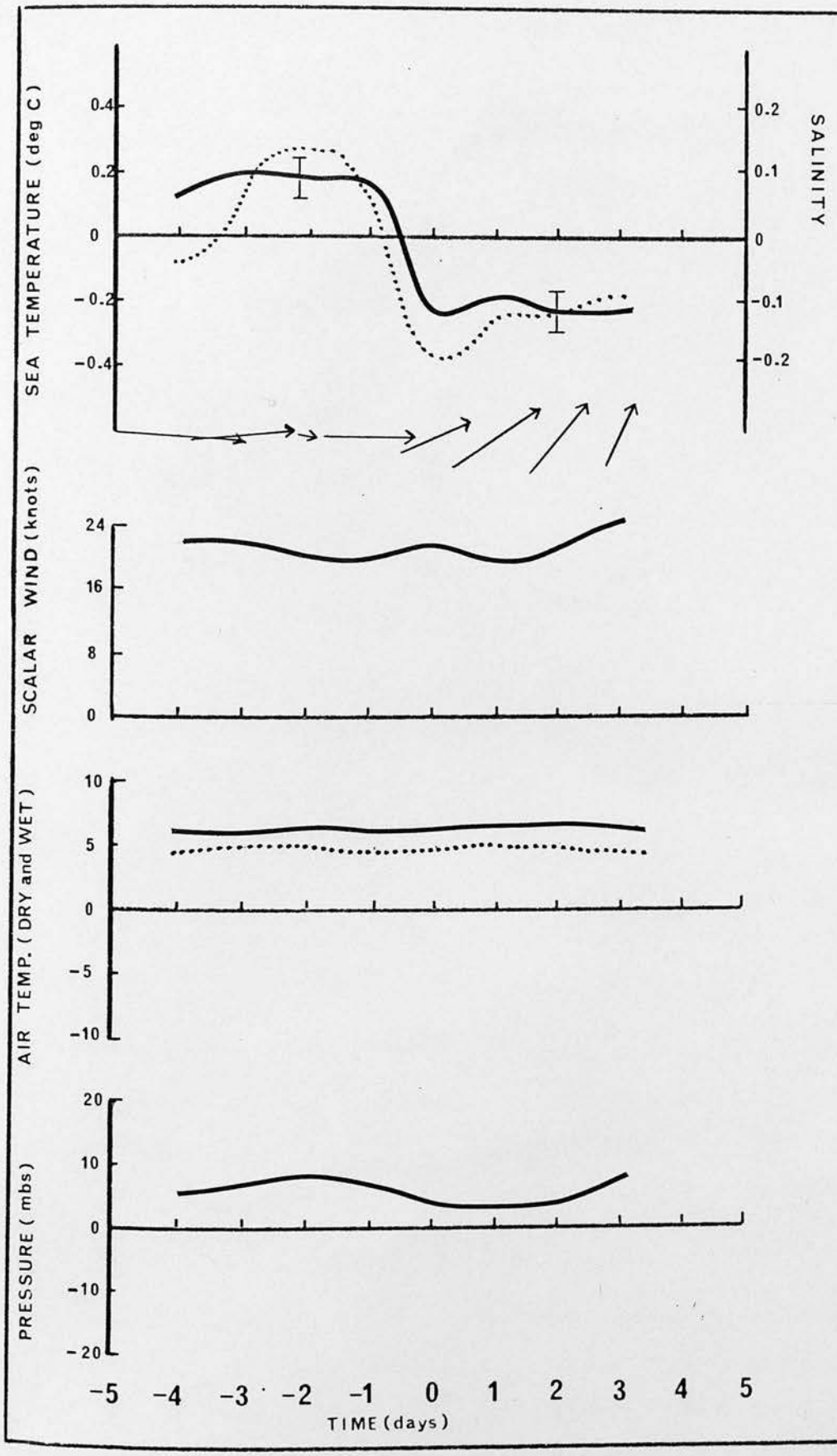

FIGURE 2.6.2c OWS 'I', WINTER; KEY DAY BASED ON SEA TEMPERATURE DECREASE.

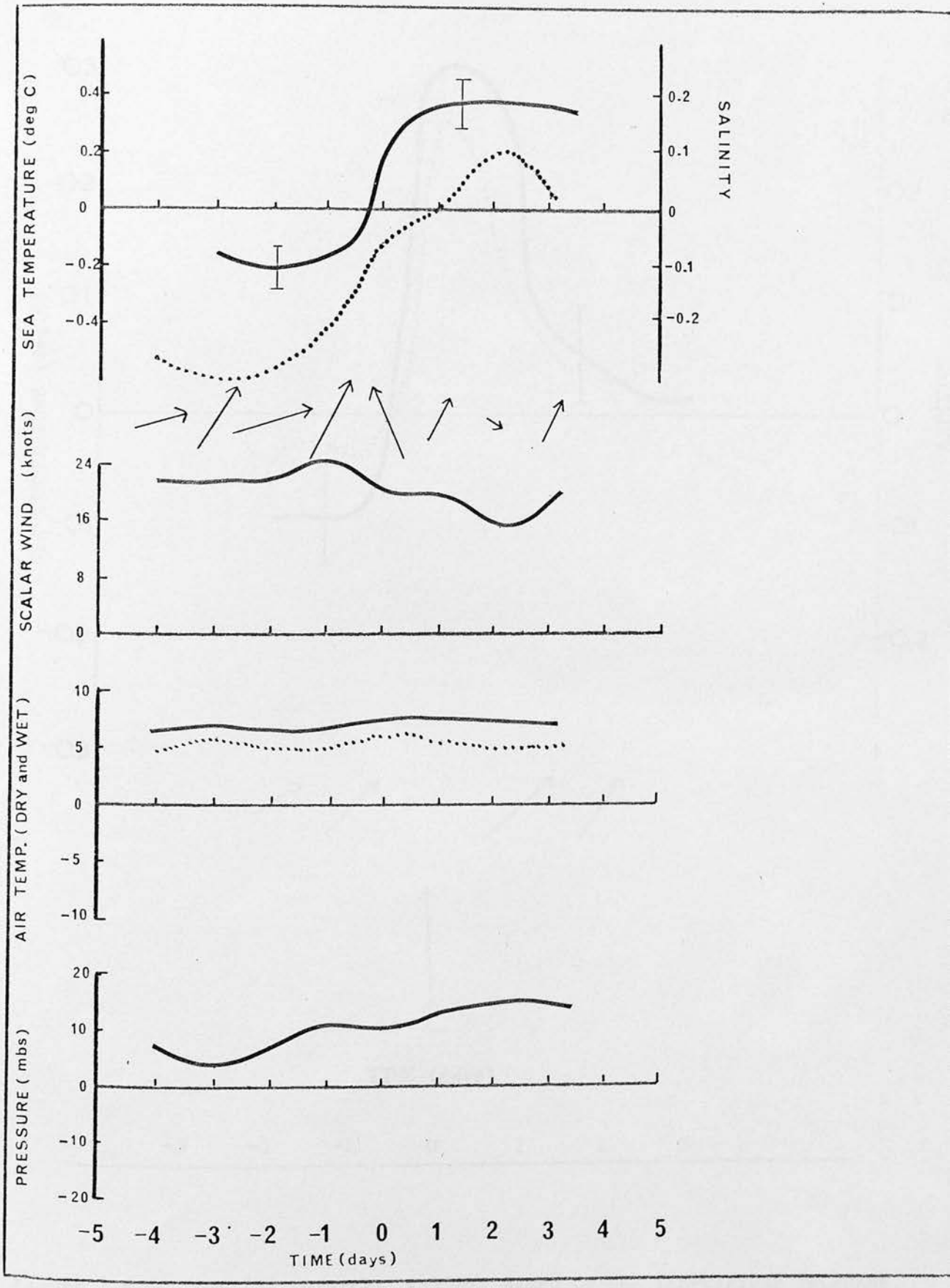

FIGURE 2.6.2d OWS 'I', WINTER; KEY DAY BASED ON SEA TEMPERATURE INCREASE.

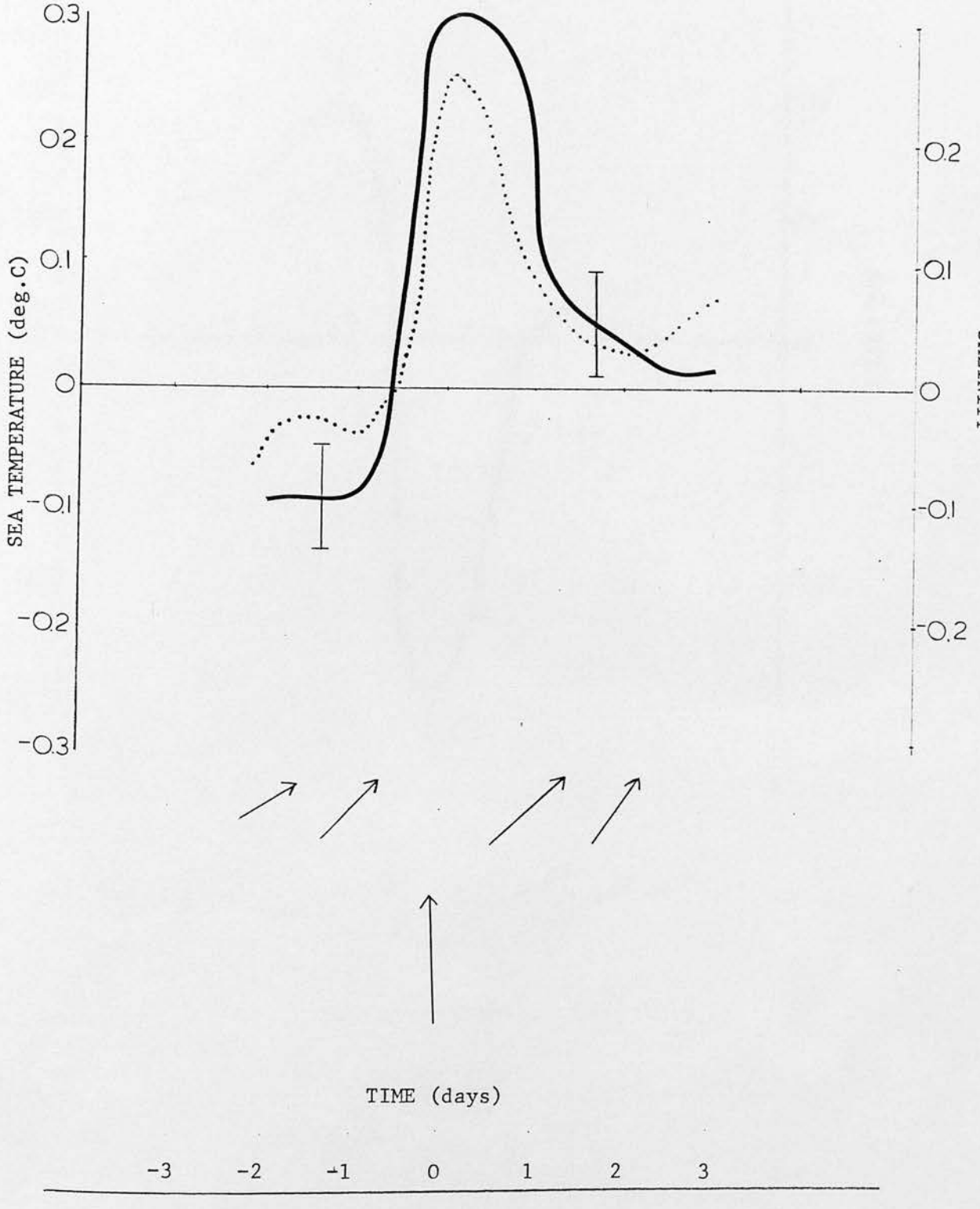

FIGURE 2.6.2e OWS 'I', WINTER; KEY DAY BASED ON SEA TEMPERATURE INCREASE.

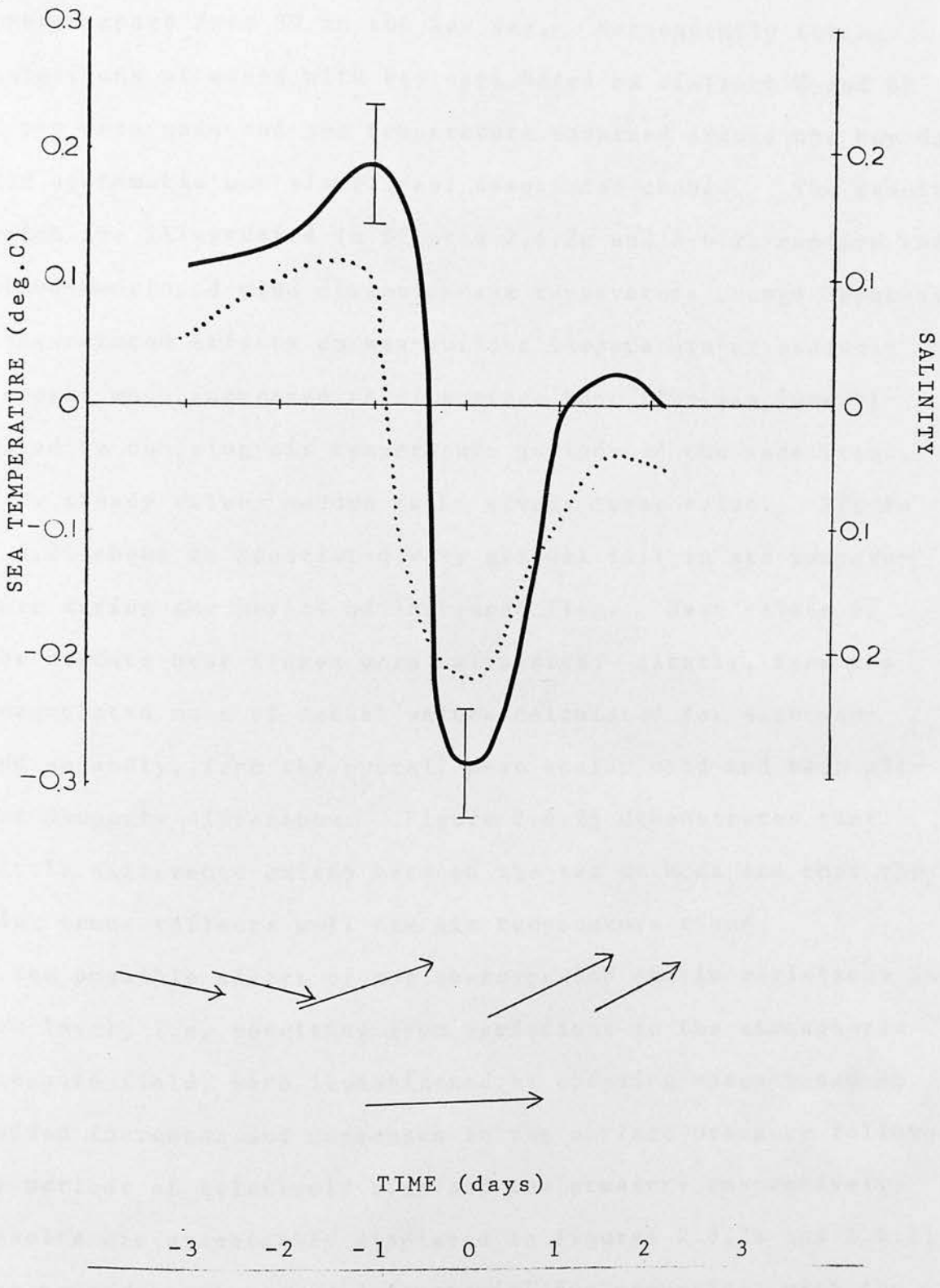

FIGURE 2.6.2f OWS 'I', WINTER; KEY DAY BASED ON SEA TEMPERATURE DECREASE.

vector apart from SW on the key day. Consequently further selections of cases with key days based on distinct W and SE types were made and sea temperature examined around the key day for systematic and significant associated change. The results which are illustrated in figures 2.6.2g and 2.6.2h confirm the above-mentioned wind direction-sea temperature change hypothesis.

Associated effects on sea-surface temperature of suddenly imposed much increased total surface heat flux was investigated by choosing air temperature periods of the same trend, i.e. steady value - sudden fall - steady lower value. Figure 2.6.2i shows an associated very gradual fall in sea temperature during the period of increased flux. Mean values of the surface heat fluxes were calculated: firstly, from the accumulated mean of actual values calculated for each day- and secondly, from the overall mean scalar wind and mean air-sea property difference. Figure 2.6.2j demonstrates that little difference exists between the two methods and that the flux trend reflects well the air temperature trend.

The possible effect of any short-period steric variations in sea level, i.e. resulting from variations in the atmospheric pressure field, were investigated by choosing cases based on sudden increases and decreases in the surface pressure followed by periods of relatively high and low pressure respectively; results are graphically displayed in figures 2.6.2k and 2.6.2l. The procedure also provided material for comparison with the results of Hay who found that during winter anticyclonic

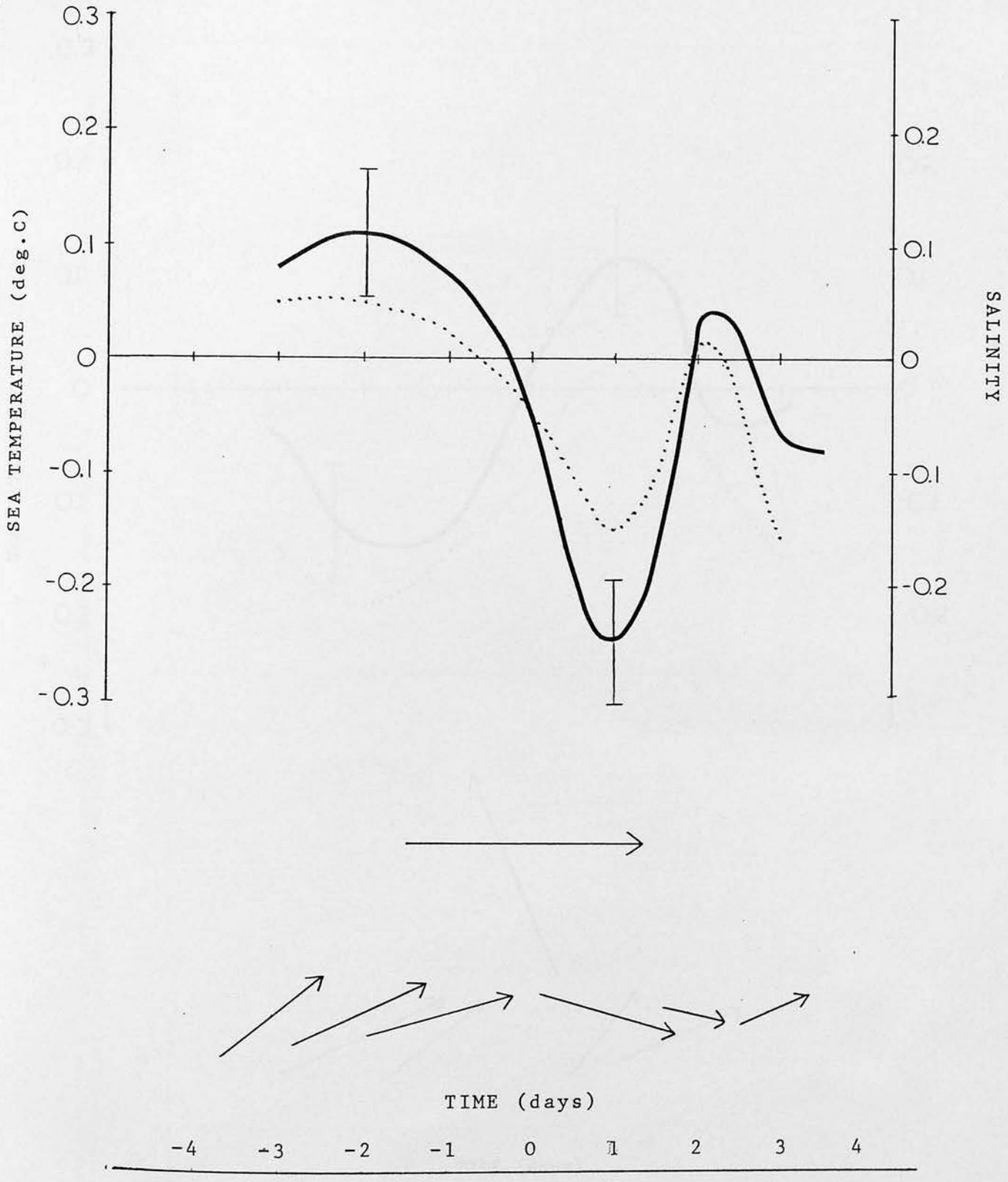

FIGURE 2.6.2g OWS 'I', WINTER; KEY DAY BASED ON LARGE WESTERLY COMPONENT

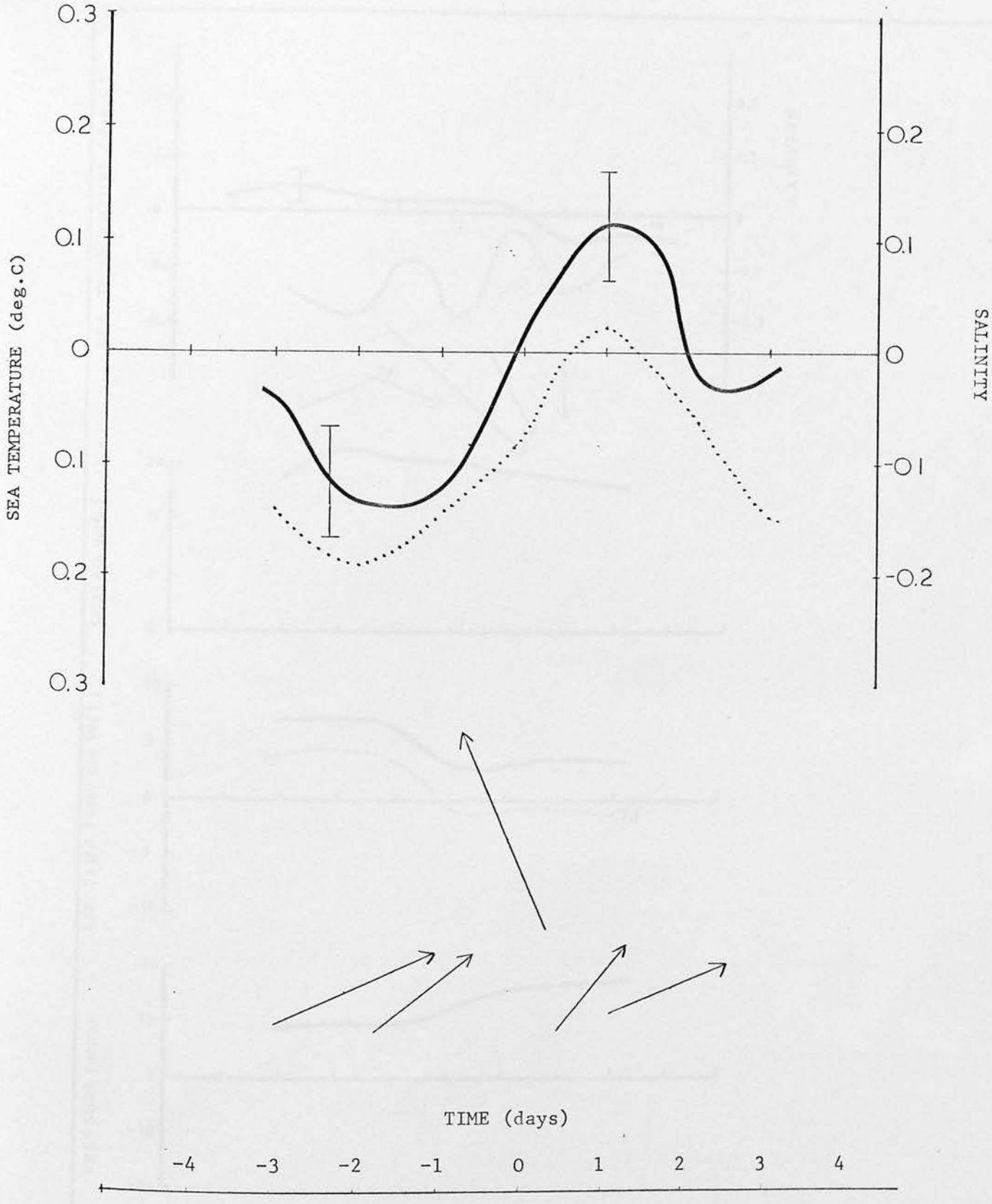

FIGURE 2.6.2h OWS 'I', WINTER; KEY DAY BASED ON LARGE SOUTH-EASTERLY COMPONENT

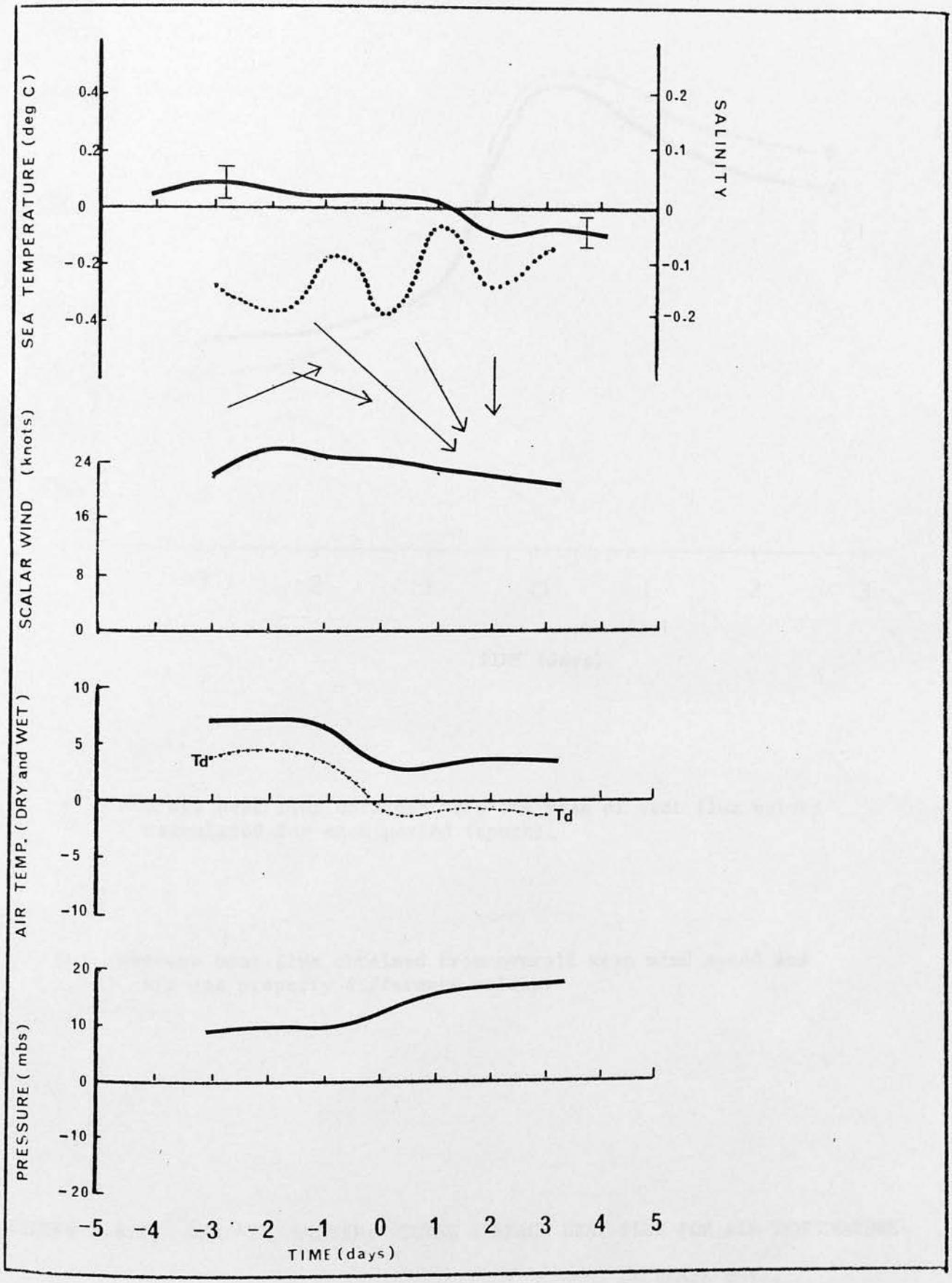

FIGURE 2.6.2i OWS 'I', WINTER; KEY DAY BASED ON AIR TEMPERATURE DECREASE.

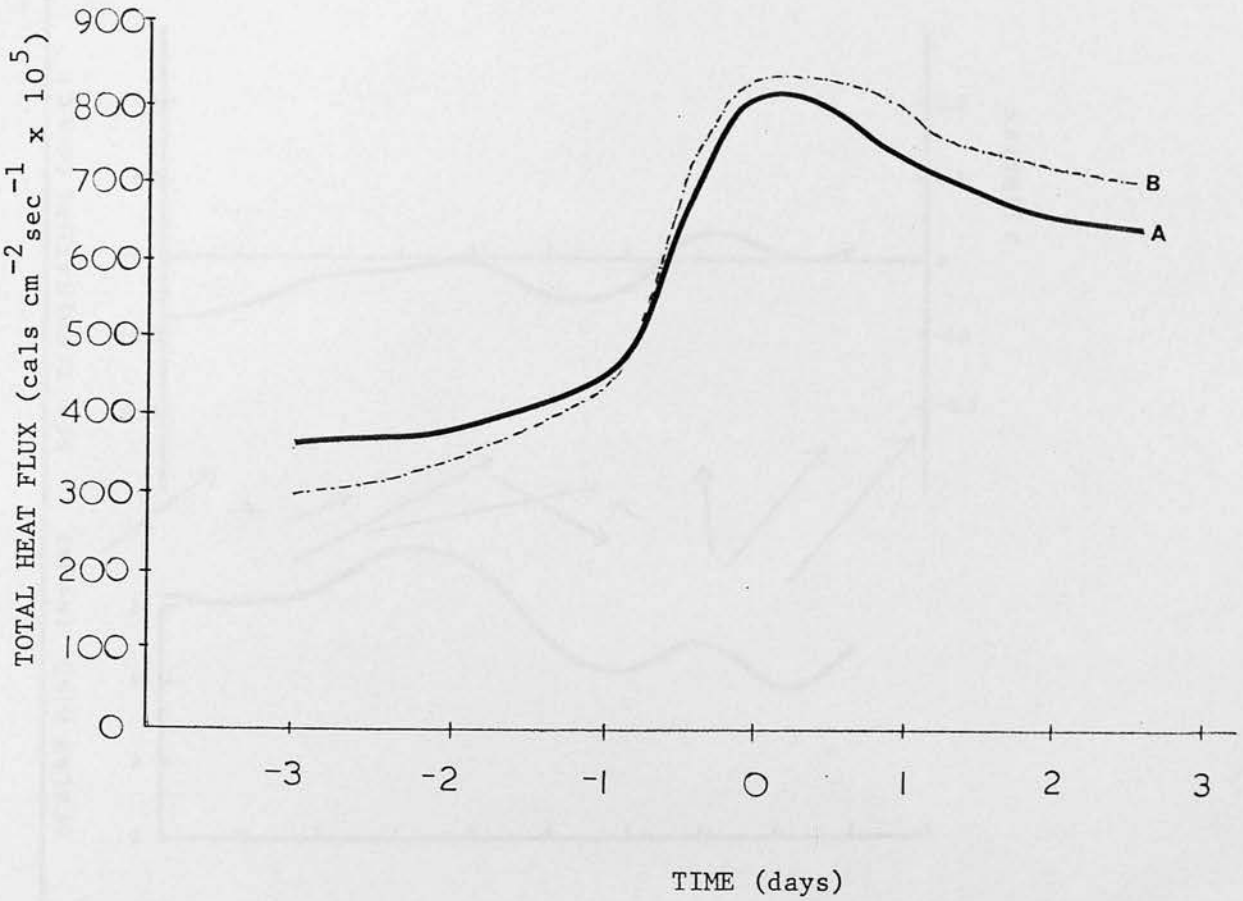

A Average heat flux obtained from the mean of heat flux values calculated for each period (epoch).

B Average heat flux obtained from overall mean wind speed and air-sea property difference values.

FIGURE 2.6.2j OWS 'I', WINTER; TOTAL SURFACE HEAT FLUX FOR AIR TEMPERATURE DECREASE DAYS.

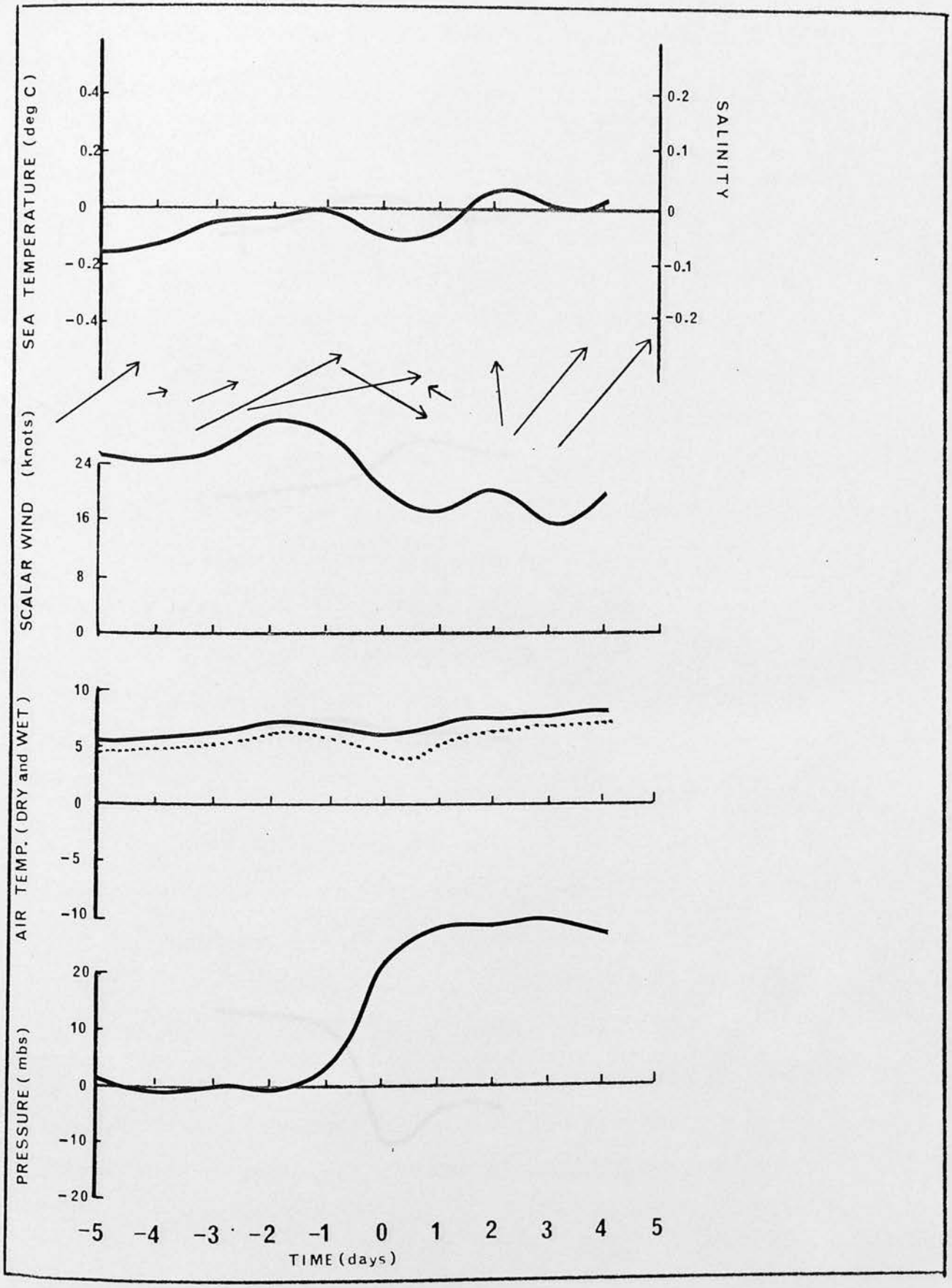

FIGURE 2.6.2k OWS 'I', WINTER; KEY DAY BASED ON PRESSURE INCREASE.

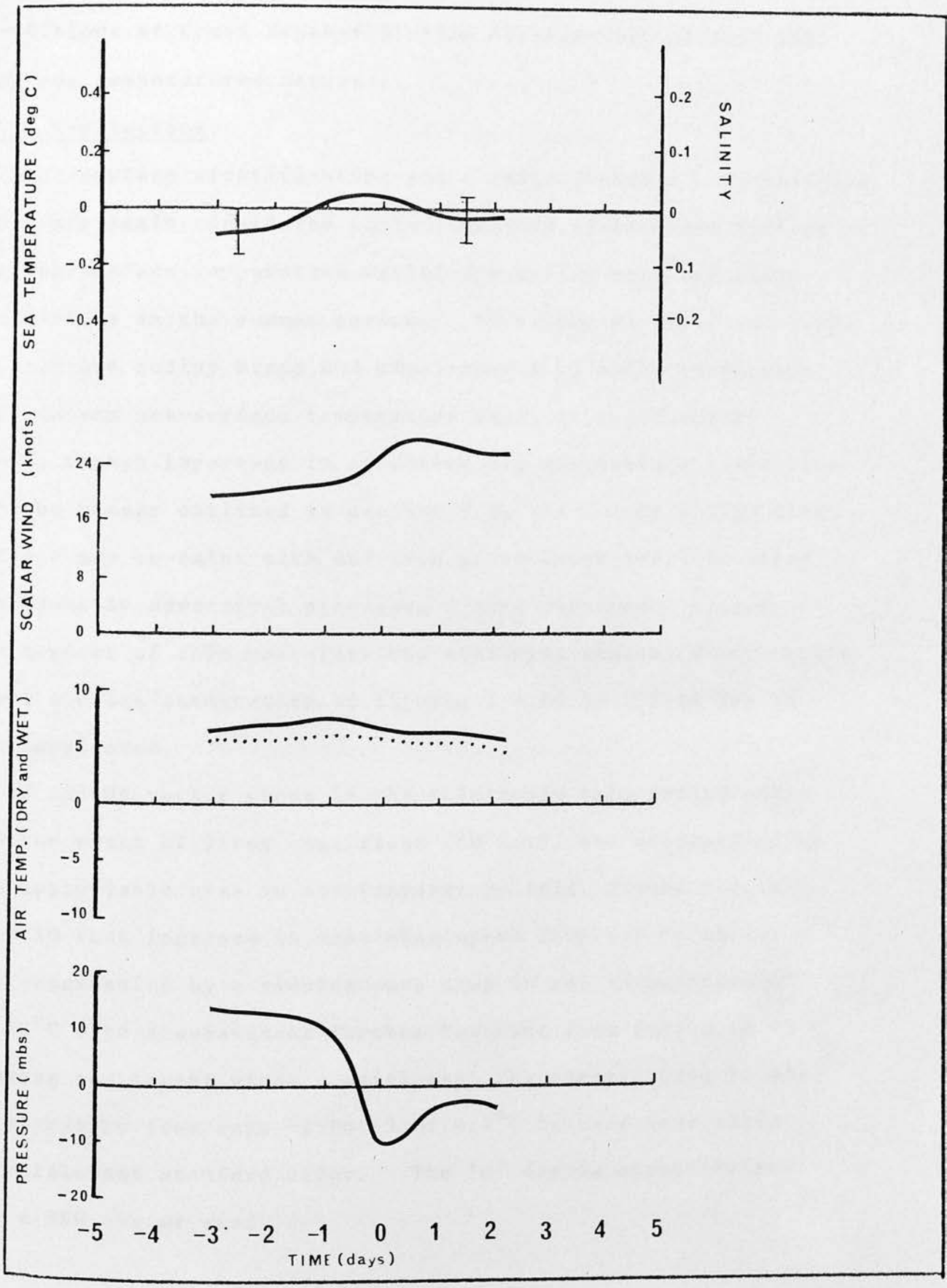

FIGURE 2.6.21 OWS 'I', WINTER; KEY DAY BASED ON PRESSURE DECREASE.

conditions at Ocean Weather Station 'J' warmings of both air and sea temperatures occurred.

2.7 Conclusions.

Near-surface stratification and a large positive net radiative flux are again considered to be important controlling factors in sea-surface temperature variations during calm and windy conditions in the summer period. By virtue of observing both vector and scalar winds and simultaneous salinity variations for chosen sea-surface temperature days, it would appear that, though important in effecting sea temperature variations in the manner outlined in section 2.5, the purely scalar wind effect may co-exist with and even prove subordinate to other (presumably advective) processes during the summer season. In support of this postulate the following remarks which result from a close examination of figures 2.6.1a to 2.6.1d are to be considered.

NW and NE vector winds in the relatively calm period prior to the onset of windy conditions ('0'day), are accompanied by an appreciable rise in sea temperature (vid. figure 2.6.1a). The 10 knot increase in mean wind speed from day -1 to day 0 is accompanied by a simultaneous drop in sea temperature of $0.12^{o}C$ with a subsequent further lowering from days 0 to +3 during continuing windy conditions; the overall drop in sea temperature from days -1 to +3 of $0.4^{o}C$ is over four times the relevant standard error. The '0' day is characterised by a SSW vector wind.

Although figure 2.6.1d demonstrates again that the period of lower sea temperatures is associated with a corresponding period of higher wind speed values, a closer examination reveals a fall in sea temperature of 0.47°C from day -1 to day 0, associated with a rise in wind speed of only 1.5 knots. The smaller increase of wind speed (relative to figure 2.6.1a) of about 5 knots from days -2 to -1 is not associated with a simultaneous fall in sea temperature. The vector wind for '0' day in this case is almost pure westerly. Again, salinity variations follow sea temperature with almost perfect parallelism.

Similarly, comparison of figure 2.6.1c with 2.6.1b demonstrates that in the case of the former a drop in wind speed of 10.7 knots from days -1 to 0 is associated with a rise in sea temperature of 0.12°C. Vector winds over days -1 and 0 remain SW. Sea temperatures continue to rise over the remaining days of relatively calm conditions but salinity values tend to fall slightly over days 0 to +2. The increased air temperature and wet-bulb temperatures together with the much reduced wind speeds over days 0 to +3 imply a considerably reduced evaporative flux,E; mean values of precipitation, P, for the same days did not provide evidence for any noticeable change over the days concerned. The observed variation of salinity over days 0 to +2 is therefore consistent with the usual assumption of taking salinity as a function of E - P. Wind vectors varying from NNW to SSW accompany a further

appreciable rise in sea temperature of 0.24°C from days +2 to +5 with a parallel rise in salinity. The latter figure 2.6.1b shows a rise in sea temperature from day -1 to day 0 of 0.46°C together with simultaneous large rise in salinity; the corresponding fall in wind speed is however only 4.3 knots. Vector winds on days -1 and 0 are observed to be SSE.

Notwithstanding the lack of relevant observations or of evidence of any threshold of wind speed increase in effecting erosion of the near-surface stratified layer (analagous for example to claimed critical wind speeds in wave production) such a threshold cannot be dismissed as an unreasonable possibility. Furthermore, the relative amounts of erosion and re-inforcement of near-surface stratification, to which respective decreases and increases of sea temperature are related, must naturally reflect the initial strength of the stratified layer which is to be subjected to increased wind conditions, or, conversely, in the case of the latter process, the degree of perturbation prior to the onset of calmer conditions.

These points are readily exemplified by comparing the relative wind conditions of figures 2.6.1a to 2.6.1d, e.g. the considerably lower initial wind speed values and subsequent larger step increase in wind speed of figure 2.6.1a in comparison with the corresponding values of figure 2.6.1d might well explain the lack of immediate sea temperature response in the latter case; the statistically significant much greater fall in sea temperature for a much smaller increase in wind speed (c.f. figures 2.6.1a and 2.6.1d) and equally significant much greater

sea temperature rise for a much smaller decrease in wind speed (c.f. figures 2.6.1c and 2.6.1b) cannot however be explained in terms of the above concepts. It is instead postulated that advection of colder water induced by a W. wind type and of warmer water induced by both S.E. and winds with N. components (see also later) are largely responsible; this is also substantiated by parallel trends in the salinity.

Although not illustrated here, the mean total cloud amount present was obtained from the ship's log sheets and the means calculated for chosen days of all four summer studies; no marked variation was observed over the chosen days on any occasion. It should however be noted that according to the results of F.E. Lumb (1964) the normal climatological formulae which determine amounts of radiation incident on the sea surface in terms of mean total cloud amount, do not prove satisfactory for short-period calculations; they have instead developed regression equations for Ocean Weather Stations 'A', 'J', in which the intensity of incident radiation is related to different types of low, medium and high level cloud. The absence of a similar analysis here renders indeterminable any associated effect on the sea-surface temperature.

From his results Hay suggested that in short periods of a day or a few days in summer, sea temperatures followed air temperatures fairly closely with a lag of a day or two, but in winter the relationship was much less close. Although the changes in question are small, these observations are to

a large extent supported here. A close relationship between air temperature and sea temperature is apparent from figures 2.6.1a to 2.6.1b; little or no lag is however detectable. On the other hand, in spite of the oscillatory nature of the air temperature trend, it is apparent from figures 2.6.2c and 2.6.2b that somewhat higher values of air temperature prevail during periods of both higher and lower sea-surface temperature. It is considered significant and noteworthy that all figures, summer and winter combined, indicate increases of sea-surface temperature and salinity not only for S.E. days but also for days with a N. wind component; a corresponding decrease of sea-surface temperature and salinity for westerly days (without large components of north or south) was similarly observed. Corresponding lags in sea temperature response vary from zero to at most one day in so far as these can be determined from the figures with such accuracy. A quasi-compensatory advective warming effect due to the NW and NNW vector winds of increased flux days is suggested as a likely reason for the very gradual negative gradient and small decrease of sea temperature over these days; it is easily estimated that even with enthalpy loss distributed uniformly over the top 100 metres, the increased fluxes observed would otherwise necessitate an overall temperature fall over the post '0' days in excess of $0.3^{o}C$.

It must finally be mentioned that although no lack of consistency exists between the sign of sea temperature change

attributed to W. and S.E. wind types and the configuration of mean winter isotherms at Ocean Weather Station 'I', 'cum sole' drift current deflections fail to account for the magnitudes of the changes involved when taken in the scalar product of the mean sea-surface temperature gradient. Furthermore, neither the sign nor the magnitude of change can be explained in the case of suggested 'warming' by wind types with appreciable northerly component. In the absence, therefore, of some fine structure of sea temperature (observations have confirmed such structure for Ocean Weather Station 'J') not revealed in the usual mean isotherm distributions, the advective mechanism invoked cannot be regarded as of a purely 'drift' nature.

Since the prime purpose of this chapter has been to provide evidence of an association of sea-surface temperature change with parallel change in the meteorological variables, little has been said of any inter-relationship of the meteorological variables themselves. Any such relation is, however, apparent from a visual inspection of any of the sea temperature-meteorological variable diagrams, e.g., figures 2.6.2a, 2.6.2b and 2.6.2k suggest, for the winter period, relatively higher pressure for quiet periods than for stormy periods, and vice-versa.

CHAPTER 3

A synoptic approach to detect wind-induced drift currents by means of observing intermediate period changes in sea-surface temperature.

3.1 Introduction

It has already been suggested that seasonal or monthly variations in the anomalous sea-surface temperature field owe much of their existence to anomalous current systems which are related to the corresponding mean anomalous surface (or geostrophic) wind field. On the much shorter time scale of a few days, the results of chapter 2 would tend to imply, for Ocean Weather Station 'I' at least, that sudden and appreciable changes in sea-surface temperature accompany certain changes in the wind direction, while at the same time other sea temperature controlling factors remain relatively invariable. The present chapter is designed to examine this wind-current relationship, on an intermediate time-scale of about a week by means of specially selected periods of investigation during which other non-advective processes were considered to have a negligible effect.

3.2 Method

The procedure is visualised as an extension of the single station investigation of chapter 2, to a more numerical and synoptically-based approach of establishing current-wind relationships with temperature as a tracer of the motion.

The basic method follows from a simplification and trans-

formation of the turbulent equivalent of the molecular heat diffusion equation. As a modified form of this equation will be used in the next chapter in connection with longer-period sea-temperature anomaly changes, a more detailed analysis is postponed until then; for the sake of brevity, only the main steps in the argument are outlined here.

The enthalpy continuity equation is reduced to the simple advective equation

$$\frac{\partial \bar{T}}{\partial t} = - \underline{\bar{V}}.\nabla \bar{T} + \bar{D} \qquad \ldots\ldots \quad 3.2(1)$$

where $\underline{\bar{V}}$ is the average total advective current and $\bar{D}$ is the sum of all non-advective processes which may contribute to the temperature change, namely surface sensible and latent heat exchanges, net radiation and horizontal and vertical mixing; bars indicate time averages, where the period of averaging is here taken to be five days. Also $\underline{\bar{V}} = \underline{\bar{V}}_G + \underline{\bar{V}}_D$ where the subscripts G and D denote geostrophic and drift components respectively. If now the drift component $\underline{\bar{V}}_D$ is taken as a linear function of the geostrophic wind and directed at some angle, α, to the right of the wind, i.e.

$$\begin{bmatrix} u_d \\ v_d \end{bmatrix} = k \begin{bmatrix} \cos\alpha & \sin\alpha \\ -\sin\alpha & \cos\alpha \end{bmatrix} \begin{bmatrix} W_{gx} \\ W_{gy} \end{bmatrix} \qquad \ldots\ldots \quad 3.2(2)$$

where u_d and v_d are the drift current components and likewise u_g and v_g and k is a constant, then with substitution of the usual relation for the geostrophic wind components W_{gx}, W_{gy} in

terms of the atmospheric pressure gradient, i.e.

$$W_{gx} = -\frac{1}{f\rho}\frac{\partial p}{\partial y}$$

and

$$W_{gy} = \frac{1}{f\rho}\frac{\partial p}{\partial x} \qquad \ldots\ldots \quad 3.2(3)$$

the following equation is obtained after some manipulation and rearrangement:

$$\sum_{i=1,5} D_i - \sum_{i=1,5} C\sin\alpha \nabla\bar{T}_i . \nabla\bar{p}_i - \sum_{i=1,5} C\cos\alpha \frac{\partial(\bar{T},\bar{p})}{\partial(x,y)} = (\bar{T}_6 - \bar{T}_1)/t$$

where t = 1 day. $\ldots\ldots$ 3.2(4)

$\sum_{i=1,5}$ denotes summation of five-day running means from the first to the fifth in sequence. C is another constant which includes the previous constant k. ∇_H represents the horizontal gradient operator and $\frac{\partial(\bar{T},\bar{p})}{\partial(x,y)}$ is the Jacobian of sea-surface temperature and atmospheric pressure with respect to the Cartesian coordinates x and y. It is immediately apparent that equation 3.2(4) is of the form

$$a\theta + b\phi + d = c \quad \text{where}$$

$a = C\sin\alpha$, $b = C\cos\alpha$, $d = \sum_{i=1,5} D_i$ and θ, ϕ, c are all calculable quantities.

By solving the set of simultaneous equations

$$\begin{bmatrix} \theta_1 & \phi_1 & 1 \\ \theta_2 & \phi_2 & 1 \\ \theta_3 & \phi_3 & 1 \end{bmatrix} \begin{bmatrix} a \\ b \\ c \end{bmatrix} = \begin{bmatrix} c_1 \\ c_2 \\ c_3 \end{bmatrix} \qquad \ldots\ldots \quad 3.2(5)$$

at adjacent grid points, values of a, b and d may be obtained whence

$$\alpha = \tan^{-1}\frac{a}{b} \quad \text{and} \quad k = \frac{f\rho}{\frac{a}{\sin(\tan^{-1}\frac{a}{b})}} \qquad \ldots\ldots \quad 3.2(6)$$

Sea-surface temperatures were interpolated from six consecutive running mean charts at each of twenty-five grid points positioned at one degree latitude-, one degree longitude-intersections, within the area under study. Similarly atmospheric pressure values, two per day, were interpolated at the same grid points and were then averaged to give five day running means contemporaneous with the isotherm charts.

3.3 Assumptions of the method.

In deriving equation 3.2(4) from 3.2(1) and applying in the form 3.2(5) it has been necessary to make certain assumptions. These are now outlined below.

(i) The variation of the Coriolis parameter with latitude is ignored over the small variations in latitude concerned.

(ii) The drift current, integrated or otherwise has been taken as a linear function of the geostrophic wind speed. Implicit in this is the assumption that the angular departure and reduced magnitude of the surface wind speed from the geostrophic value are uniformly equal over the area of investigation. With approximately uniform stability conditions and the absence of isobar curvature over the area during the chosen periods of study, this is considered a reasonable assumption; it does not, however, allow for any higher power functional dependence of the drift current on the surface wind, e.g. simple theoretical considerations suggest an integrated drift current-wind stress (proportional to wind speed squared) relation.

(iii) No explicit account of variations in the temperature resulting from gradient current advection has been made (except perhaps implicit inclusion in the d term if such variations could be regarded as everywhere equal over the area). This matter has very briefly been mentioned already in the introductory chapter; however, with the distinct lack of direct observational data, it can only be attempted to support this assumption with hypothetical reasoning. It is supposed that the superimposed wind field does not give rise to irregular sea-surface slope and that any adjustment of the gradient current as a result of an organised non-erratic redistribution of mass as effected by a quasi-steady drift current, should proceed in such a manner as to maintain a quasi-stationary geostrophic state, i.e. any re-orientation of the streamlines of the gradient current is expected to follow the density redistribution, thereby preserving a state of parallelism between the isotherms (neglecting salinity dependence of density) and the geostrophic streamlines. This latter adjustment of the gradient current is similar to that cited by Federov (1960) in his study of the seasonal variation of ocean currents.

(iv) With relatively uniform atmospheric conditions over the region it is asserted that sensible and latent heat losses which comprise the greatest portion of the d term vary little from one grid point to the next, more especially in directions normal to the wind direction.

3.4 Data Source.

The data used in the present study were of two main types: firstly, the five-day running mean sea-surface isotherm chart produced daily by the British Meteorological Office and, secondly, the Daily Weather Report from the same source.

3.5 Area of investigation.

For the purpose of the present study, attention was focussed on that region of the N.E. Atlantic and southern Norwegian Sea lying between 62°N and 66°N and between 7°W and 1°E. Before applying the technique and attempting to analyse any results a brief survey of the hydrography of the area is relevant.

Characteristic of the region during the winter period is a moderate horizontal gradient of sea-surface temperature and average constant density depth (isothermal layer) of about 100 metres although this extends to greater and more variable depths in the extreme N.W. and S.E. of the area in association with the frontal zones of the East Iceland and North Atlantic current respectively; these boundary current systems coincide with the regions of crowding and steepening of isotherms and isopycnals on the right and left of figures 3.5a and 3.5b which show vertical distributions of temperature and density in a N.E.-S.W. section across the area of study.

3.6 Case Studies.

In order to facilitate later comparison of results, three synoptically similar meteorological situations were selected within the same season: 8-16 January 1972, 28 January-5 Feb-

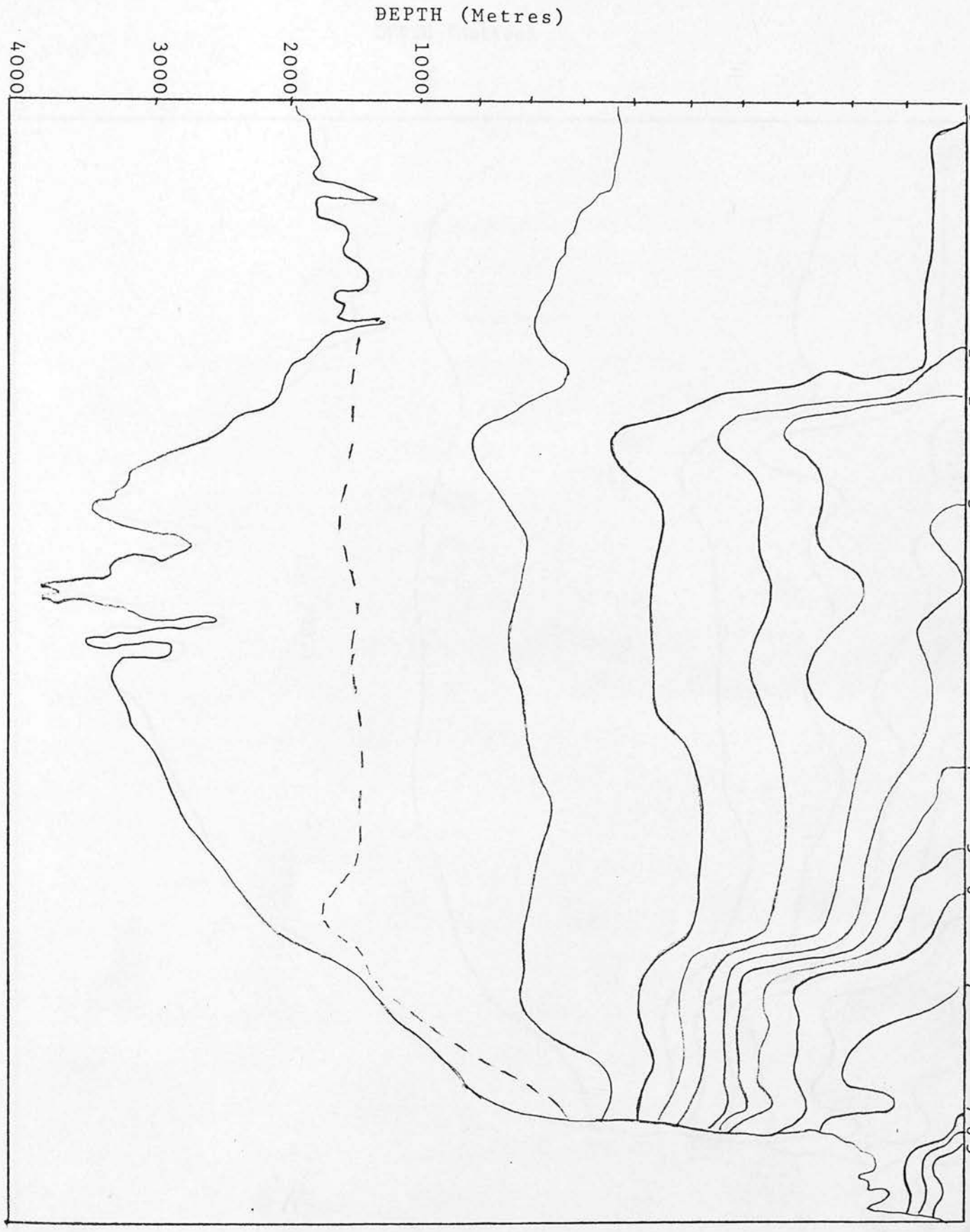

FIGURE 3.5a TEMPERATURE CROSS SECTION, SOUTHERN NORWEGIAN SEA.

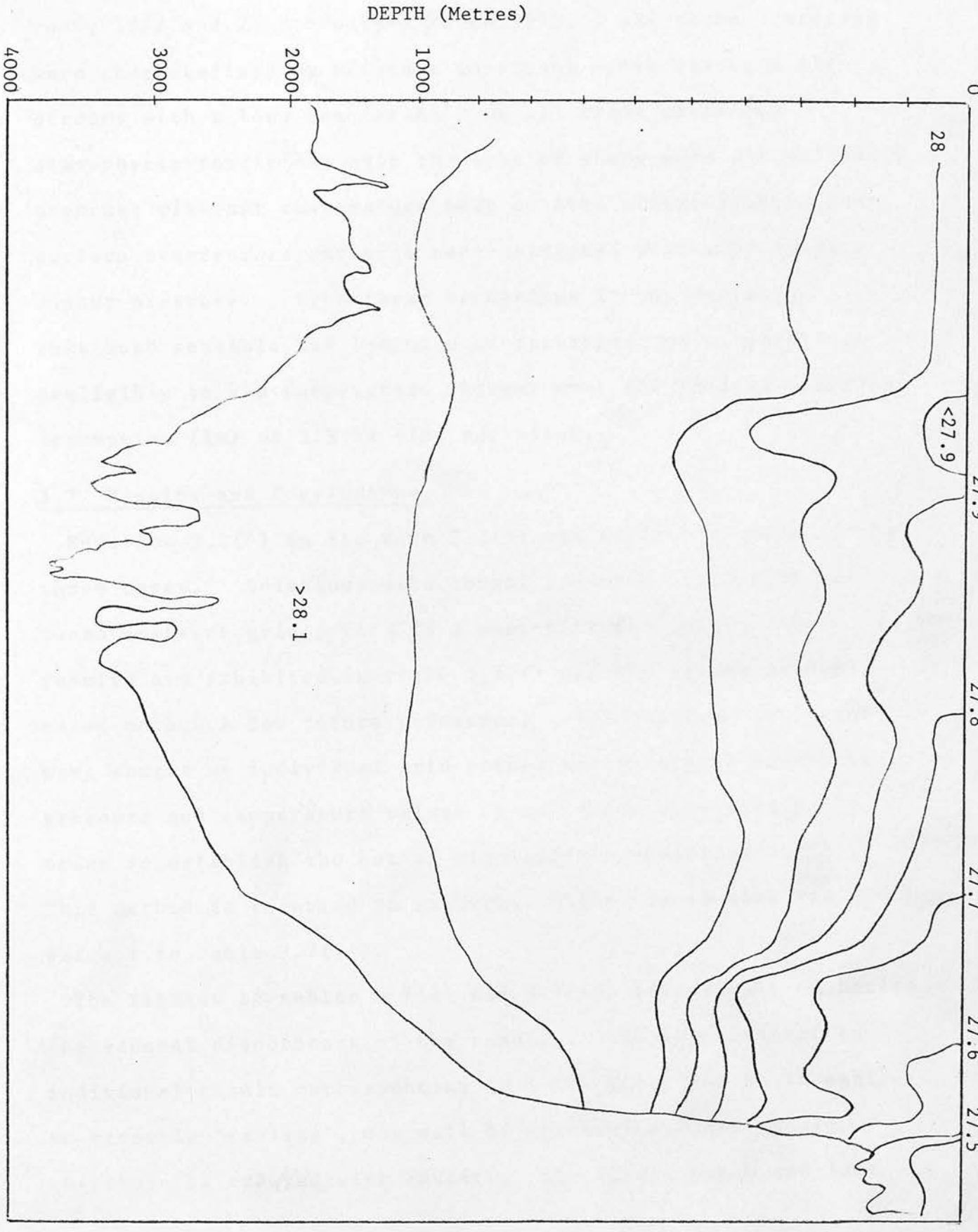

FIGURE 3.5b DENSITY CROSS SECTION, SOUTHERN NORWEGIAN SEA.

ruary 1972 and 25 February-4 March 1972. All three occasions were characterised by moderate to strong south-easterly air-streams with a long sea fetch. On all three occasions atmospheric conditions over the area of study were predominantly overcast with air temperature near or even slightly above sea-surface temperature and with near-saturated values of surface vapour pressure. With these conditions it was envisaged that both sensible and latent heat exchanges would contribute negligibly to sea temperature changes over the periods concerned; assumption (iv) of 3.3 is also satisfied.

3.7 Results and Conclusions.

Equation 3.2(4) in the form 3.2(5) was applied to each of the three cases. Solutions were sought assuming similarity between adjacent grid points in a west-east direction; the results are exhibited in table 3.7(i) and the method is designated method A for future reference. Alternatively solutions were sought at individual grid points using at each point the pressure and temperature values of all three case studies in order to establish the set of simultaneous equations 3.2(5). This method is referred to as Method B and the results are set out in table 3.7(ii).

The figures of tables 3.7(i) and 3.7(ii) immediately emphasise the general discordance of the results. In this respect an individual result corresponding in a way which may be thought to resemble 'reality', may well be fortituitous and should therefore be treated with caution; the first, sixth and last

d	Deflection α	Wind factor k
-1.28	59.8	0.025
1.61	134.1	0.025
4.45	133.8	0.109
-0.09	153.0	0.005
-1.23	289.1	0.014
-0.04	15.9	0.014
-4.59	61.9	0.085
1.66	184.0	0.04
0.05	90.0	0.017

TABLE 3.7(i) DRIFT CURRENT RESULTS, METHOD A.

d	Deflection α	Wind factor k
23.20	158.8	0.861
3.03	138.7	0.096
21.34	150.1	0.682
0.62	166.6	0.020
-6.27	2.0	0.150
-3.14	359.0	0.082
5.50	203.7	0.071
0.15	83.5	0.010
0.55	233.0	0.014

TABLE 3.7(ii) DRIFT CURRENT RESULTS, METHOD B.

results of table 3.7(i), together with the penultimate result of table 3.7(ii), all of which show wind factors of at most a few per cent, cum sole deflections from wind vector between 0 and 90^{o} and low values for d, may fall into this category. As a totally negative inference is however considered to be over-pessimistic some conjecture for the lack of consistency in the results is appropriate. The following remarks may provide a possible explanation.

(a) The inconsistencies of table 3.7(i), more especially the scatter of the d values, suggest a lack of similarity in non-advective contributions between adjacent grid points. From the point of view of sensible and latent heat loss this seems unlikely. As far as other effects are concerned the disagreement could feasibly arise from an encroachment on either of the frontal zones cited earlier. With the assumption, however, that these frontal zones are relatively permanent in nature and not susceptible to sudden horizontal shifts, this difficulty should have been largely removed in method B; these results are unfortunately also observed to be inconsistent.

(b) The method as applied in either A or B is sensitive to term c in equation 3.2(5), i.e. the change at grid points of consecutive block five-day means of sea-surface temperature. Furthermore, the formulation of equation 3.2(4) was based on a strict definition of a five-day mean (i.e. a continuous set of observations over the period). For these reasons it is important that the sea-surface temperature data attain a reasonable standard of accuracy.

Since this investigation was performed, the author has had occasion to observe the manner of preparation and production of the five-day mean charts utilised in this study. Without going into detail it suffices to say that there exists considerable spatial and temporal incoherence of data over the area in question. As a result it is the author's firm belief that data effect (b) above could well have played a very significant rôle in affecting the outcome of the analysis. It is therefore suggested that the results of this section be regarded as inconclusive rather than totally negative. Furthermore, it is believed that the method deserves further investigation in different marine areas and under different meteorological conditions; with the employment of more consistent infra red sea-surface temperature data (where available) and extension of the method to perhaps longer periods a more conclusive result should emerge.

PART II

An investigation of the month-to-month change of anomalous sea-surface temperature over a large area of the North Atlantic Ocean in relation to the corresponding anomalous meteorological regime.

CHAPTER 4

Formulation and discussion of computational method.

4.1 Introduction

The methods of the previous two chapters were devised to examine the dependence of sea-surface temperature variations on simultaneous atmospheric forcing processes. Whereas the first of these methods provided satisfactory qualitative evidence of a localised sea-surface temperature meteorological input response on the time scale of a few days, an attempt to confirm, on larger space and time scales, the presence of wind-induced drift currents by observing what were expected to be purely advective temperature changes during specially selected periods, has, whether for data reasons or otherwise, not met with the same success. It is now proposed to describe what is fundamentally the same type of investigation on still larger time and space scales. The procedure - in a sense the converse of that adopted in chapter 3 - is to apply a predetermined driving force based on physical reasoning and compare the predicted changes in the temperature field with real data.

4.2 The enthalpy continuity equation.

The three-dimensional heat energy conservation equation is written in the basic form

$$\frac{\partial}{\partial t}(\rho C_p \bar{T})_{x,y,z} = -\nabla.(\rho C_p \bar{T}\underline{\bar{V}} + C_p \rho \overline{\underline{V}'T'}) + \Sigma Q(z) \quad \ldots\ldots \quad 4.2(1)$$

with $$\Sigma Q(z) = \alpha R_n e^{-\alpha z} + 2F\delta(z) \quad \ldots\ldots \quad 4.2(2)$$

where α is a linear absorption coefficient for the incoming radiation; R_n = Total incoming radiation incident on the sea surface; F = B + H + LE, i.e. sum of infrared back radiation plus surface sensible heat loss plus surface latent heat loss. The Dirac delta function, $\delta(z)$, conveniently represents the concentration at the sea surface of the processes included in F, and is such that $\int_o^h \delta(z)dz = \frac{1}{2}$ for all h > 0. The lower limit of integration, o, is taken to be the sea surface (temporal and spatial variability is neglected) and the upper limit, h, is assumed to mark the bottom of the mixed layer (or turbulent boundary layer). Consistent with previous notation bars represent time-averaging of quantities and primes instantaneous departures therefrom. It should also be noted that the molecular conductivity term, $\kappa\frac{\partial T}{\partial z}$, which should normally have appeared within the brackets of the first right-hand term of equation 4.2(1), in its instantaneous form, has been neglected. From a comparison of the relative orders of magnitude of the terms in 4.2(1), this is most certainly permissible within the region of turbulent flow. However, from a strictly mathematical point of view integration of equation 4.2(1) from the sea surface to some small distance, δ , just below the mixed-layer depth, necessitates evaluations within a purely molecular sublayer, where by definition terms such as $\overline{\omega'T'}$ are identically zero, and where, molecular conductivity terms such as $\kappa\frac{\partial T}{\partial z}$ must therefore be introduced to preserve the required heat flow continuity. Here, however, because H is contained in the definition of $\Sigma Q(z)$, inclusion of the molecular con-

ductivity term is not required at the surface proper. Integration of equation 4.2(1) from the surface to some small distance, δ, just beneath the mixed-layer depth, h, yields after some manipulation and re-arrangement of terms the following:

$$h\frac{\partial \bar{T}}{\partial t} + \Gamma(\bar{T} - \bar{T}(h + \delta))(\frac{\partial h}{\partial t} - \omega_f) = \underline{\bar{V}}h.\nabla\bar{T} + \bar{T}h\nabla.\underline{\bar{V}} + (\Delta\underline{\bar{V}}\bar{T}).\nabla_H h$$
$$\text{(a)} \qquad \text{(b)} \qquad\qquad\qquad \text{(c)} \qquad \text{(d)} \qquad\qquad \text{(e)}$$

$$+ h\nabla_H\underline{\overline{V'T'}} + \frac{(F + R_n)}{C_p\rho} \quad \ldots\ldots \quad 4.2(3)$$
$$\text{(f)} \qquad\quad \text{(g)}$$

where Δ denotes property difference between mixed-layer and beneath. $\frac{\partial h}{\partial t}$ corresponds to the observed total rate of change of mixed-layer depth and ω_f is the frictionally induced vertical velocity. In this way the difference between these terms yields the deepening of the mixed layer due to entrainment alone, ω_e; further $\Gamma = 0$ for $\omega_e < 0$ and $\Gamma = 1$ for $\omega_e > 0$ (deepening). The temperature at the sea surface is identified with that of the mixed layer; this neglects the temperature difference of perhaps a few tenths of a degree between the surface film of water (depth of the order of a few millimetres) and the mixed layer below. It is to be expected, for example, that infrared methods would give the former 'sea-surface' temperature and the bucket or engine intake methods, the latter. Term (b) is identifiable with changes in heat content of the column brought about by entrainment of colder water from beneath the mixed layer. Term (c) is the mean flow advection term. Term (d) which includes the three-dimensional divergence is assumed to be zero; this is equivalent to assumption of

constant density following the motion (i.e. $\frac{d\rho}{dt} = -\nabla.\underline{V} = 0$). Term (e) would probably contribute to changes in the enthalpy of the column in regions of appreciable mixed layer depth gradient, e.g., in the vicinity of oceanic fronts. Term (f) represents the effect of turbulent horizontal eddy heat transport. Term (g) gives the combined effect of net radiation and sensible and latent heat loss on the column. A more thorough discussion and analysis of variations of equation 4.2(3) is to be found in Appendix (ii). With parameterisation of the horizontal turbulent transfer term, $\overline{\underline{V}'T'}$, in the usual manner and with the above simplifications, equation 4.2(3) assumes the simplified form:

$$h\frac{\partial \bar{T}}{\partial t} + \Delta\bar{T}\frac{\partial h}{\partial t} = -\bar{\underline{V}}h.\nabla\bar{T} + hK_H\nabla_H^2\bar{T} + \frac{(R_n + F)}{\rho C_p} \quad \ldots\ldots \quad 4.2(4)$$

where $\nabla_H^2 \equiv \frac{\partial^2}{\partial x^2} + \frac{\partial^2}{\partial y^2}$, and $\bar{\underline{V}} = \bar{\underline{V}}_G + \bar{\underline{V}}_D$,

$\bar{\underline{V}}_D$ and $\bar{\underline{V}}_G$ being the mean integrated drift and geostrophic current components respectively.

4.3 The Model Equations.

The imposed wind stress is considered to act as a body force distributed uniformly throughout the mixed layer. The mean integrated drift current component is related to the surface wind stress τ (see later), by the relation

$$h\bar{\underline{V}}_D = \int_0^h \bar{\underline{V}}_D(z)\, dz = \frac{\underline{\tau} \times \hat{\underline{k}}}{f\rho} \quad \ldots\ldots \quad 4.3(1)$$

where f is the Coriolis parameter, $\underline{\bar{\tau}}$, the mean vector wind stress and $\hat{\underline{k}}$ is a unit vector in a positive upward direction.

As the sea-surface temperature is being taken equal to that of the well-mixed layer, the terms 'sea-surface temperature' and 'sea temperature' where the latter refers to the mixed layer depth, are considered synonymous and interchangeable in all that follows. The effect of persistence is removed from the initial sea temperature field by considering, not the month-to-month change of actual sea-surface temperature, but the change of the mean monthly anomaly. Additionally, as all the case studies are winter occasions then, for reasons outlined in the introduction, the entrainment term is omitted from the analysis. Substitution of 4.3(1) in 4.2(4) and replacement of all actual mean quantities by long term average quantities (denoted by double bars) and departures therefrom (denoted by primes), in equation 4.2(4) and subtraction of a similar equation with long-term mean values gives the equation

$$\frac{\partial T'}{\partial t} = \underbrace{\frac{-(\underline{\tau}' \times \hat{\underline{k}})}{f\rho\bar{h}} \cdot \nabla\bar{\bar{T}}}_{(a)} - \underbrace{(\bar{\bar{\underline{V}}}_G + \frac{(\bar{\bar{\underline{\tau}}} \times \hat{\underline{k}})}{f\rho\bar{h}}}_{(b)} + \underbrace{\frac{(\underline{\tau}' \times \hat{\underline{k}})}{f\rho\bar{h}}}_{(c)} + \underbrace{\frac{(\underline{\tau}' \times \hat{\underline{k}})}{f\rho\bar{h}}}_{(d)}) \cdot \nabla T'$$

$$+ \underbrace{K_H \nabla_H^2 T'}_{(e)} + \underbrace{\frac{(F' + R_n')}{\rho C_p \bar{h}}}_{(f)} + \text{Terms containing factor } \frac{h'}{\bar{h}} \quad \ldots\ldots \quad 4.3(2)$$

Term (a) is the advection of normal isotherms by the anomalous drift current. Terms (b) and (c) are together taken to be the total normal ocean current; terms (b), (c) and (d) in combination

are therefore interpreted as the advection of the anomalous isotherms by the actual total ocean current. Term (e) is the large-scale anomalous horizontal diffusion coefficient, and term (f) represents temperature changes of the column resulting from anomalous heat sources and sinks. In the final simplification of 4.3(2), terms in $\frac{h'}{\bar{h}}$ are neglected as also is the anomalous net radiation term. The former are estimated small in comparison with other terms and the latter is negligible during the winter season. With these final adjustments 4.3(2) assumes the final form

$$\frac{\partial T'}{\partial t} = \frac{-(\underline{\tau}' \times \hat{\underline{k}})}{f\rho\bar{h}} \cdot \nabla\bar{\bar{T}} - (\bar{\underline{V}}_{TOT} + \frac{(\underline{\tau}' \times \hat{\underline{k}})}{f\rho\bar{h}}) \cdot \nabla T' + K_H \nabla^2 T' + \frac{(H' + LE')}{\rho C_p \bar{h}} \quad \ldots\ldots 4.3(3)$$

Equation 4.3(3) represents the final model equation. In 4.3(3), C_p and ρ were assumed constant and f was allowed to vary with latitude. All other quantities are monthly mean values, the computation of which is described in detail in the next chapter.

As an alternative to using the integrated drift current in forming the anomalous advection of the normal sea-surface isotherms (term (a) of 4.3(2)), changes of sea temperature anomaly resulting from anomalous Sverdrup-type meridional advection of the normal zonal sea isotherms were calculated and produced as computer printout. From the simplified steady-state hydrodynamic equations and continuity equations which

are written as

$$-f\rho v + \frac{\partial p}{\partial x} = \frac{\partial \tau}{\partial z}x, \quad f\rho u + \frac{\partial p}{\partial y} = \frac{\partial \tau}{\partial z}y \qquad \ldots\ldots \quad 4.3(4)$$

and

$$\frac{\partial u}{\partial x} + \frac{\partial v}{\partial y} + \frac{\partial w}{\partial z} = 0 \qquad \ldots\ldots \quad 4.3(5)$$

the following integrated equation is easily obtained:

$$\omega(h) - \omega(\zeta) = \frac{1}{f\rho}(\underline{\nabla} \times \underline{\tau}) - \frac{\beta}{f\rho}\int_{\zeta}^{h} v\,dz + \text{terms in } \nabla\rho,\ \nabla p,\ \nabla\zeta \text{ and } \nabla h \quad \ldots \quad 4.3(6)$$

where ω is the vertical velocity component, β is the rate of change of the Coriolis parameter with latitude $= \frac{\partial f}{\partial y}$, and ζ denotes the instantaneous free surface. The gradient terms of 4.3(6) are estimated small in comparison with the other terms. The ultimate form of 4.3(6) in anomalous component form is

$$\omega'(h) = \frac{1}{f\rho}\,\underline{\nabla} \times \underline{\tau}' - \frac{\beta}{f}\int_{\zeta}^{h} v'\,dz \qquad \ldots\ldots \quad 4.3(7)$$

4.4 Method of Solution.

Equation 4.3(3) was arranged in finite-difference form and a computer programme written to provide values of the change in the monthly sea temperature anomalies at grid points. In addition the programme was arranged to supply printout of mean monthly integrated drift current components and Sverdrup meridional flow. Advective temperature anomaly changes due to the latter were also computed. All details will be found in the case study sections.

If all terms on the right-hand side of 4.3(3) are calculated at month i in an attempt to predict T' at month i + 1, then

4.3(3) can be regarded as a prognostic equation; in the absence, however, of a lag in sea-surface temperature response to changes in the anomalous forcing processes, this is essentially equivalent to assuming near steady-state atmospheric conditions over the two months concerned. A time integration of all the right-hand side terms of 4.3(3) from month i to month i + 1 is mathematically what is required; approximation of this ideal condition was obtained by forming the average of the right-hand side of 4.3(3) for months i and i + 1, after which this average value was used in determining values of the change in T'. Values of change in T' were produced in computer printout form both for this latter 'diagnostic' and for the former 'prognostic' approaches. Since the prime purpose of this section is to establish the mechanism of regulating sea temperature anomalies rather than to produce a predictive method, it is appropriate to judge the model on the basis of diagnostic evaluations.

4.5 Area of Study.

The region of the North Atlantic between 30°N and 65°N and between 10°W and 50°W was covered in the present analysis. Solutions for the change in mean monthly anomalies of sea-surface temperature were obtained at grid points located at two and a half degree latitude, five degree longitude intersections contained within the above area, i.e. excluding points on the outer periphery.

CHAPTER 5

Distributions of the anomalous meteorological and oceanographic parameters and evaluation of case studies.

5.1 Method of Construction.

In accordance with the previous definition of anomaly, distributions of the anomalous mean monthly meteorological and oceanographic variables were obtained. With the exception of the mean monthly sea-surface temperature and surface air and dew point temperature which were obtained from data sources to be mentioned later, fields of the long-term averages of all other variables had to be independently constructed. Relevant details are given separately in the subsections devoted to specific variables.

In spite of the opportunity of using objective analysis techniques which would have considerably reduced the effort involved in the construction of distribution maps, it was considered more reliable to draw all fields by hand, in some cases with the additional assistance of maps of related variables, e.g. use of anomalous monthly surface pressure as a guideline in constructing the anomalous monthly wind stress distribution.

Although the distributions of long-term and actual monthly means were initially derived from values computed at different data source locations, a set pattern was followed in obtaining fields of all variables, not only those for use as final input data to the model, but also those intermediate in construction.

The following section is intended as a concise description of the basic procedures involved.

From the data supplied at ocean weather stations and representative areas, calculated values of the variable whose distribution was required, were plotted at each observation and corresponding isopleths were drawn. Extraction of data from these maps, for use in combination with other data in computing model parameters, was effected by interpolating values at the centre of five degree sub-Marsden squares on the original hand-drawn maps. Maps showing isopleths of the new parameter formed in this way were now drawn, only this time using values at the centres of the five-degree squares as initial data points. All input data to the model were ultimately extracted from maps formed in the above-described manner by interpolating values at grid points located at two and a half degree latitude, five-degree longitude intersections.

Since only one large time step, of duration one month, is used in the present model, it is not expected that computational instability problems of the type so often encountered with multi-time step numerical methods, should arise. Notwithstanding this fact, the grid scheme chosen, although containing variable grid lengths in the latitudinal sense, was such as to preserve the condition $\frac{c\Delta t}{\Delta x} < 1$ which is the usual computational stability criterion for centre difference time steps in simple advective type equations; here, Δx is the grid length, Δt the duration of a time step and c the speed of the fastest 'wave'. Further-

more grid lengths were at least several times smaller than the smallest wavelength of an advected parameter, the most important parameter in this respect being that of the initial anomalous sea-surface temperature field.

In view of the relatively small grid lengths used it was not considered that errors due to curvature effects were of a magnitude large enough to warrant the use of a polar coordinate system instead of the cartesian system used.

5.2 Data.

Anomalous monthly sea-surface temperature data were supplied by the Climatological Division of the Meteorological Office in the form of computer output containing pseudo monthly values for all five degree squares over the North Atlantic.

Data for use in the computation of all long term fields were obtained from the Climatological Atlas for Mariners, Washington Weather Bureau. Air temperature, dew point temperature and wind data summarised in wind rose form are included in this category. Long term mean monthly sea-surface temperature was obtained from the Oceanographic Atlas of the North Atlantic Ocean, Pub. No.700. The H.M.S.O. publication 'Climatological Summaries for the North Atlantic East of 50°W and North of 20°N' provided air temperature, dew-point temperature, sea-surface temperature and tabulated wind data all on a monthly basis. All other oceanographic data were produced as computer output and were obtained directly from the National Oceanographic Data Centre, Washington.

Figures 5.2a and 5.2b show ocean weather station and representative

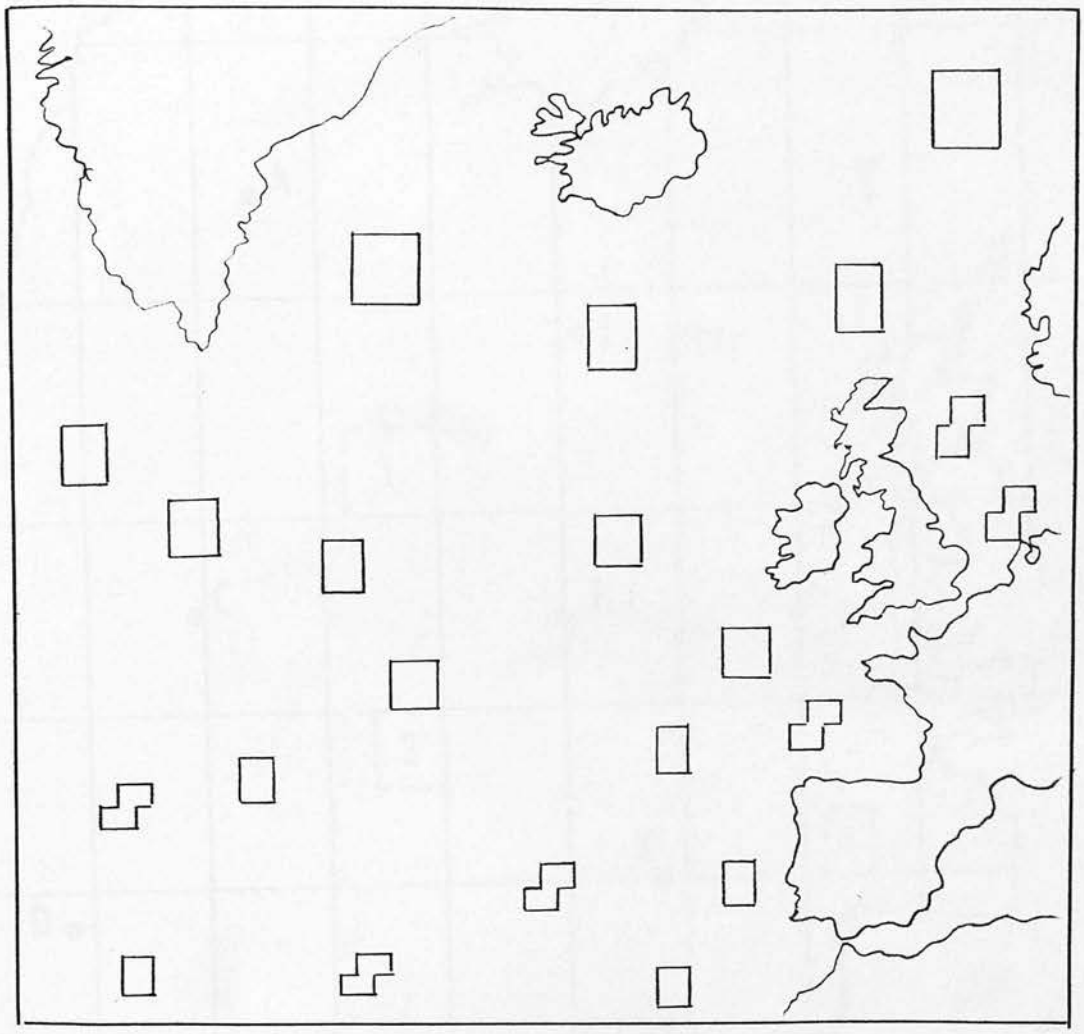

FIGURE 5.2a OCEAN WEATHER STATIONS AND REPRESENTATIVE AREA LOCATIONS; LONG TERM COMPUTATIONS.

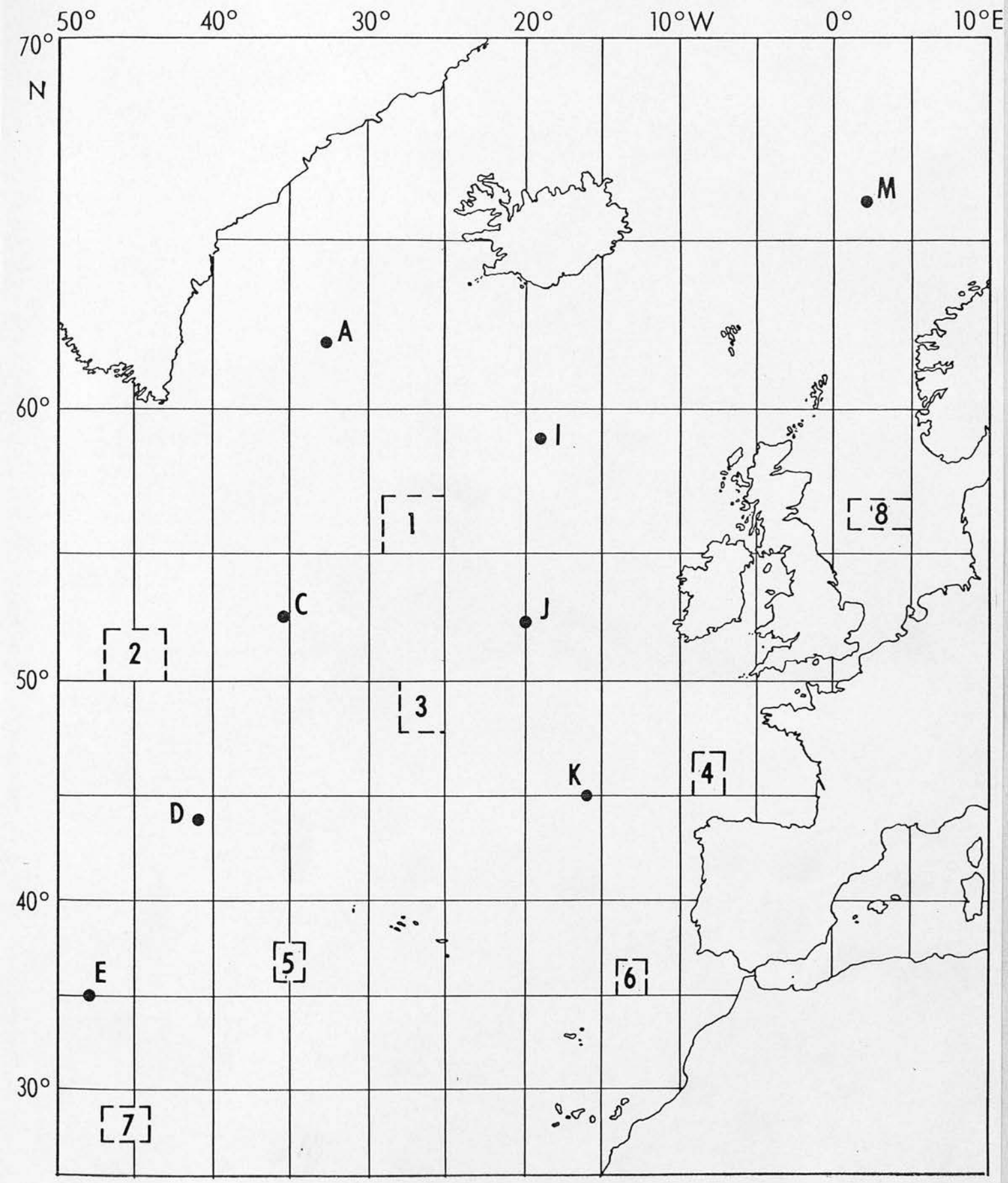

FIGURE 5.2b OCEAN WEATHER STATIONS AND REPRESENTATIVE AREA LOCATIONS; ACTUAL MONTHLY MEAN COMPUTATIONS.

area locations which provided data for the construction of long term mean and actual monthly mean maps respectively.

All maps produced are traced copies of the original hand drawn versions and as such do not retain the actual numerical values on the basis of which the isopleths were drawn. Actual numerical values at the data location points have however been additionally included in a few of the initial maps which are thus intended to serve as typical examples.

5.3 The computation of the meteorological terms.

5.3.1 The actual mean monthly scalar wind.

Figure 5.3.1 illustrates the layout of tabulated wind data for ocean weather stations and representative areas respectively. The mean monthly scalar wind, $\bar{W}$, for each location and for any particular month is simply obtained from the expression

$$\overline{|W|} = \frac{\sum_{i,j} W(j)F(i,j)}{\sum_{i,j} F(i,j)} \quad \ldots\ldots \quad (a)$$

where $\sum_{i,j}$ denotes summation over all windspeed (j), and F(i,j) represents the frequency of any observation and wind direction (i) class intervals.

As the mean monthly wind data were computed at the same points for which air temperature, dew-point temperature and sea-surface temperature were available, they were combined directly with these elements in forming other parameters, thus avoiding the need of initial interpolation from separately drawn scalar wind distributions.

5.3.2 The long term mean monthly scalar wind distribution.

All wind rose data from the Climatological Atlas for Mariners

STATION A 1963

TABLE 8 WIND - Percentage frequency of speed and direction

Month	Speed (knots)	Direction in 30 degree sectors (centre value given)													
		Calm	Var.	360	030	060	090	120	150	180	210	240	270	300	330	Total
	0-4	2.4	..	0.1	0.3	..	..	..	0.4	..	0.1	0.3	0.5	..	..	4.2
	5-9	..	..	0.8	2.2	2.4	0.8	0.1	0.5	0.3	0.4	2.8	2.3	1.4	1.1	15.1
	10-14	..	..	2.7	2.8	1.8	2.0	1.2	1.4	0.3	0.7	0.9	2.4	1.8	0.5	18.4
Jan.	15-19	..	..	1.2	2.2	3.0	0.7	1.8	2.0	0.5	0.7	1.6	1.1	0.4	0.1	15.2
	20-24	..	..	..	1.9	1.9	5.0	2.7	2.7	0.3	1.1	2.3	2.8	..	..	20.6
	25-29	..	..	..	0.1	0.1	1.1	1.6	2.6	0.5	2.0	0.9	1.2	..	..	10.2
	30-39	..	..	..	0.4	..	..	0.8	2.3	3.9	4.2	1.1	0.4	..	..	13.1
	40-49	..	..	..	..	..	..	0.4	0.1	0.4	0.3	0.8	1.2	..	..	3.2
	50-59	..	..	..	..	..	..	..	..	..	..	..	..	..	..	..
	≥60	..	..	..	..	..	..	..	5.	..	..	..	..	..	..	..
	Total	2.4	..	4.9	9.8	9.2	9.6	8.6	12.0	6.2	9.4	10.8	12.0	3.5	1.8	100.0
	Number of obs.	18	0	36	73	68	71	64	89	46	70	80	89	26	13	743

AREA 3 1963

TABLE 9 WIND - Monthly frequency of direction and force

Number of observations for each direction and force

Month	Direction (degrees)	Beaufort force													Total
		0	1	2	3	4	5	6	7	8	9	10	11	12	
	variable	..	1	2	..	..	..	..	..	..	..	..	..	..	3
	350-010	..	1	1	..	2	..	1	1	..	1	..	..	..	7
	020-040	..	..	1	..	3	1	..	1	..	..	..	..	..	6
Jan.	050-070	..	..	2	6	7	4	1	1	1	..	..	..	..	22
	080-100	..	..	2	3	5	2	3	1	3	..	..	..	..	19
	110-130	..	..	..	1	1	4	1	3	..	..	..	..	..	10
	140-160	..	..	..	1	..	3	..	..	..	..	..	..	..	4
	170-190	..	..	2	..	1	1	..	..	..	..	..	..	..	4
	200-220	..	..	..	3	1	..	..	..	..	..	..	..	..	4
	230-250	..	..	..	..	..	1	..	..	..	..	..	..	..	1
	260-280	..	..	..	..	..	..	..	..	..	..	..	..	..	..
	290-310	..	..	..	..	..	..	1	..	..	..	..	..	..	1
	320-340	..	..	..	..	..	..	1	1	..	..	..	..	..	2
	Total	..	2	10	14	20	16	8	8	4	1	..	..	..	83

FIGURE 5.3.1 LAYOUT OF TABULATED WIND DATA FOR OCEAN WEATHER STATIONS AND REPRESENTATIVE AREAS.

were re-arranged into a tabulated form identical to that of figure 5.3.1 (low part). This greatly facilitated the direct application of methods already used for actual monthly wind-dependent data to similar long-term data. In this case, application of method (a) to the data re-arranged in this fashion yielded values of the long-term monthly mean scalar wind.

The results for January and February are reproduced in figures 5.3.2a and 5.3.2b respectively where numerical values indicate mean scalar wind speed in knots.

5.3.3 The actual mean monthly wind stress field.

With the basic assumption that the surface wind stress vector, $\underline{\tau}$, and the vector wind have the same direction, the former can then be represented as having zonal and meridional components both of which are proportional to the same respective components u, v, of the surface vector wind, i.e.

$$\underline{\tau} = \tau_x(u)\hat{\underline{x}} + \tau_y(v)\hat{\underline{y}}$$

where τ_x and τ_y are the stress components in the positive zonal, (W-E) and positive meridional, (S-N) directions respectively. $\underline{x}$ is a unit vector in the positive zonal direction and similarly $\underline{y}$ in the positive meridional direction.

Fields of the actual monthly mean wind stress are expressed as separate distributions of zonal and meridional components. This equally applies to both the long-term and anomalous monthly mean wind stress fields, not yet mentioned.

With the previous notation for i and j, the mean monthly zonal component, $\bar{\tau}_x$, and meridional component, $\bar{\tau}_y$, are obtained from the tabulated wind data by means of the relationships

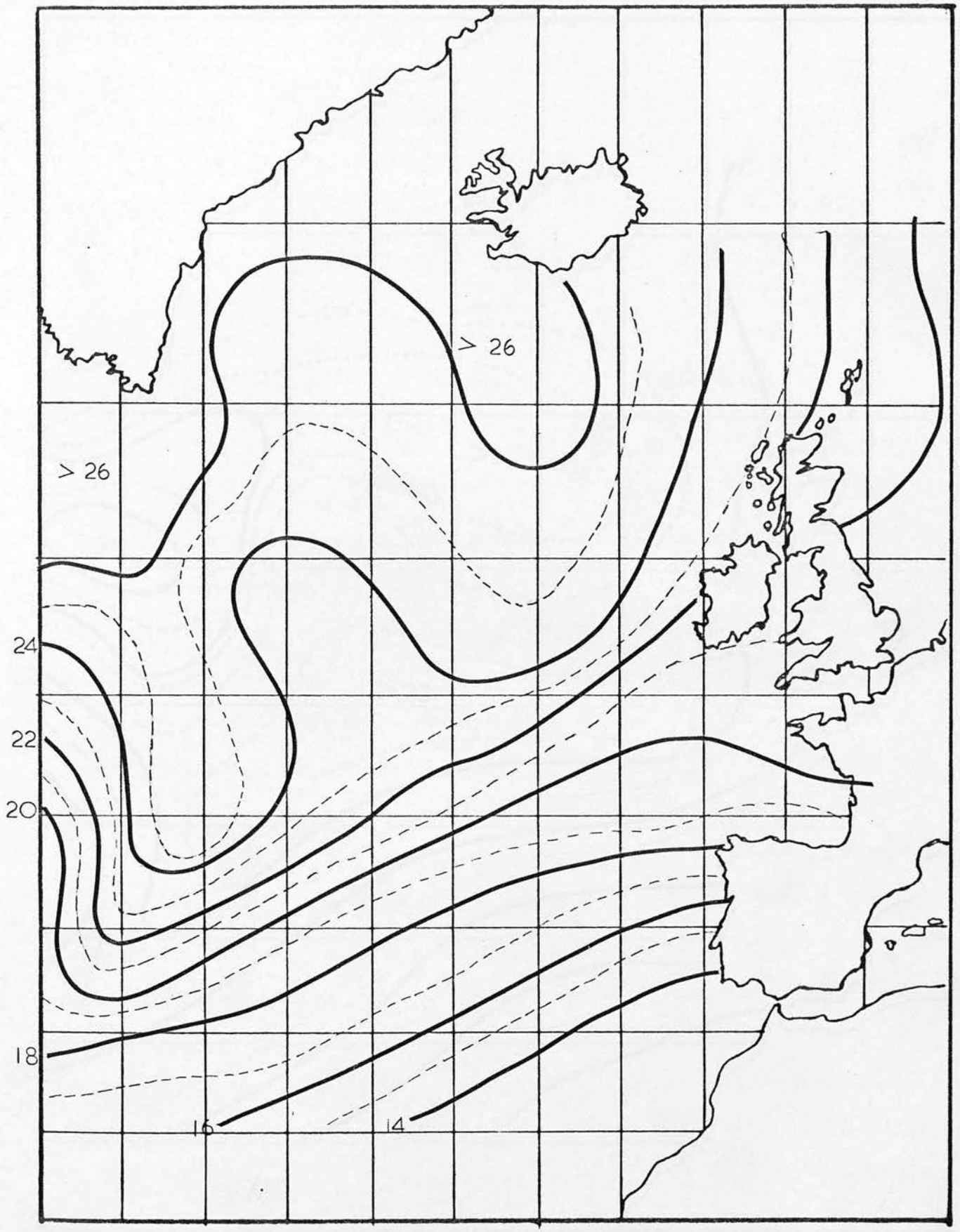

5.3.2a MEAN SCALAR WIND SPEED. JANUARY.

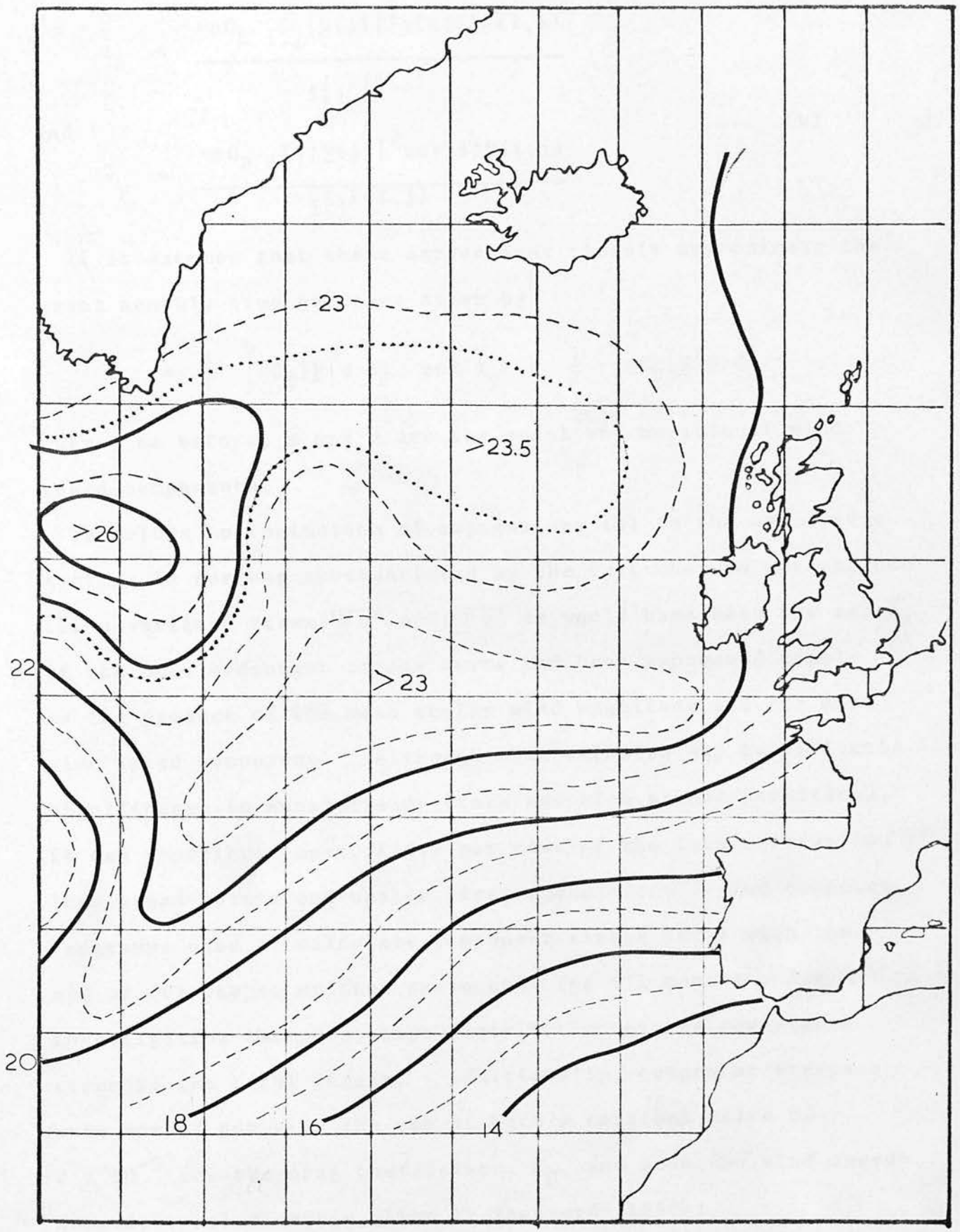

FIGURE 5.3.2b MEAN SCALAR WIND SPEED. FEBRUARY.

$$\bar{\tau}_x = \frac{-\rho C_D \sum_{i,j} |\underline{W}(j)|^2 \sin(i) F(i,j)}{\sum_{i,j} F(i,j)}$$

and

$$\bar{\tau}_y = \frac{-\rho C_D \sum_{i,j} |\underline{W}(j)|^2 \cos(i) F(i,j)}{\sum_{i,j} F(i,j)} \quad \ldots\ldots \quad (b)$$

It is assumed that these expressions closely approximate the exact monthly time averages tiven by

$$\bar{\tau}_x = \frac{1}{T} \int_0^T \rho C_D |\underline{W}| u \, dt, \text{ and } \bar{\tau}_y = \frac{1}{T} \int_0^T \rho C_D |\underline{W}| v \, dt$$

where, as before, u and v are the zonal and meridional wind speed components.

The close approximation of expressions (b) to the exact time average is further substantiated by the fact they do not exclude the covariance terms $|\overline{\underline{W}'u'}$ and $|\overline{\underline{W}'v'}$ as would have been the case if the mean component stress terms had been expressed simply as the product of the mean scalar wind magnitude and the mean wind speed component. Although this omission may be of little significance in quasi-steady state and high stress conditions, it can contribute up to fifty per cent of the total stress in less steady state and weaker stress conditions. The computer programme used to calculate component stress terms with the aid of (b) was so written as to show for all months under investigation the percentage contribution of the covariance terms to the total stress. Additionally, component stresses were worked out with the use of both a constant value of 2×10^{-3} for the drag coefficient, C_D, and also the wind speed-dependent relationship given by Sheppard (1958):

$$C_D(10) = (0.80 + 0.00114u(10))10^{-3}$$

While this proved useful by way of comparison with the constant C_D case, only the results of the former alternative were ultimately used in the model.

5.3.4 The long-term wind stress distribution.

With the wind data in re-arranged tabulated form as in section 5.3.2, the relationships (b) were directly applied to yield long-term monthly wind stress components. The resultant distributions are given in figures 5.3.4a to 5.3.4d. Numerical values of isopleths on all wind stress maps are given in dynes cm^{-2}.

It should perhaps be mentioned that with the reduced number of wind speed and wind direction class intervals in the long-term calculations, these must naturally assume a cruder form than the equivalent actual monthly fields. It is believed, nevertheless, that they represent the best possible results from data available at present.

5.3.5 The anomalous wind stress distribution.

Application of the procedure of interpolating values at the centres of five degree squares to both the actual and long term monthly mean distributions, with subsequent subtraction of the latter from the former, provided initial values for the construction of the anomalous stress distributions. These were produced for three case studies discussed later, and are reproduced with the numerical notation of the case study sections.

5.3.6 The actual mean monthly sensible heat flux.

Values of the mean monthly air-sea temperature difference, $\Delta\bar{T}$, were obtained for all data points from the Climatological Summaries

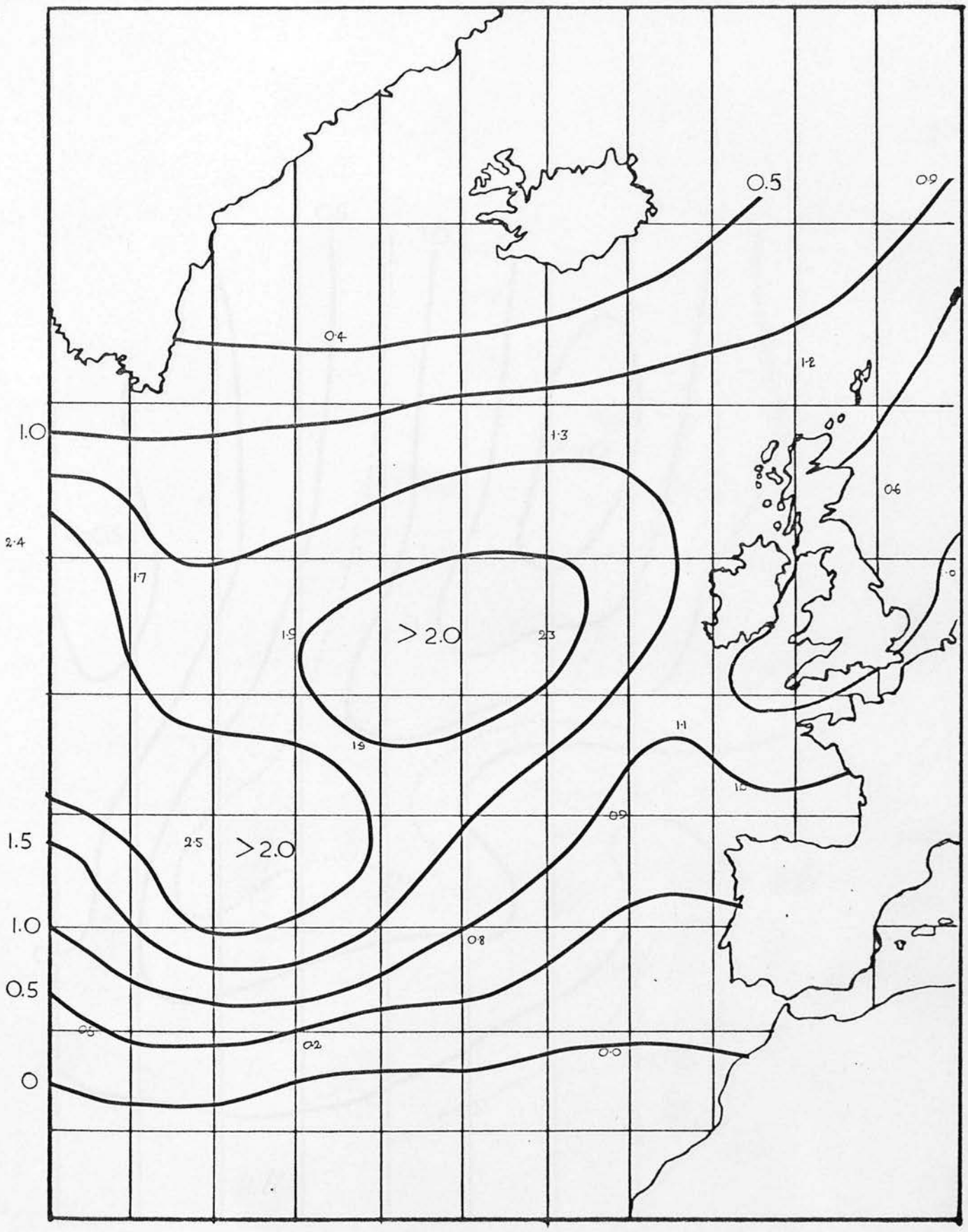

FIGURE 5.3.4a MEAN ZONAL CPT. SURFACE WIND STRESS JANUARY

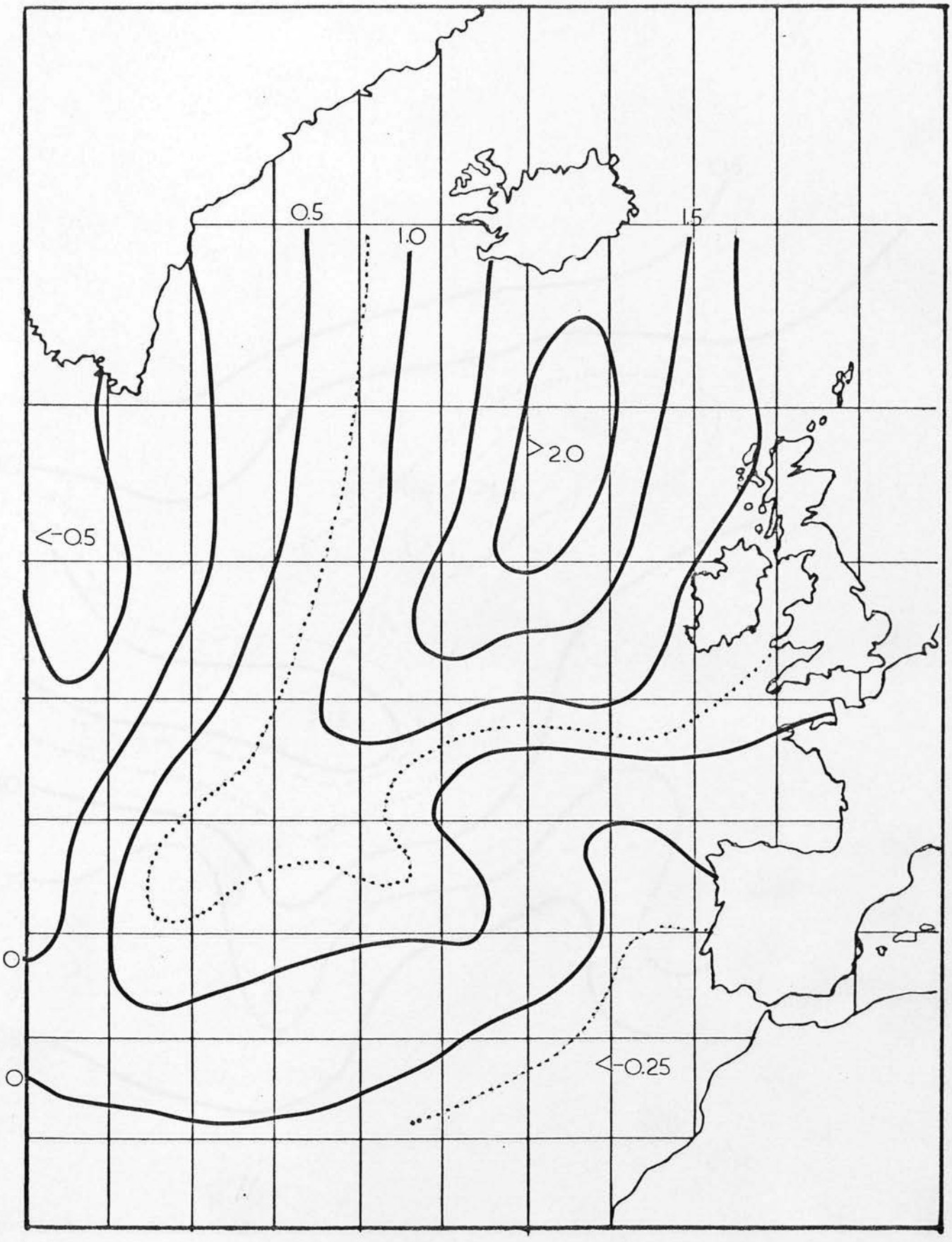

FIGURE 5.3.4b MEAN MERIDIONAL CPT. SURFACE WIND STRESS . JANUARY

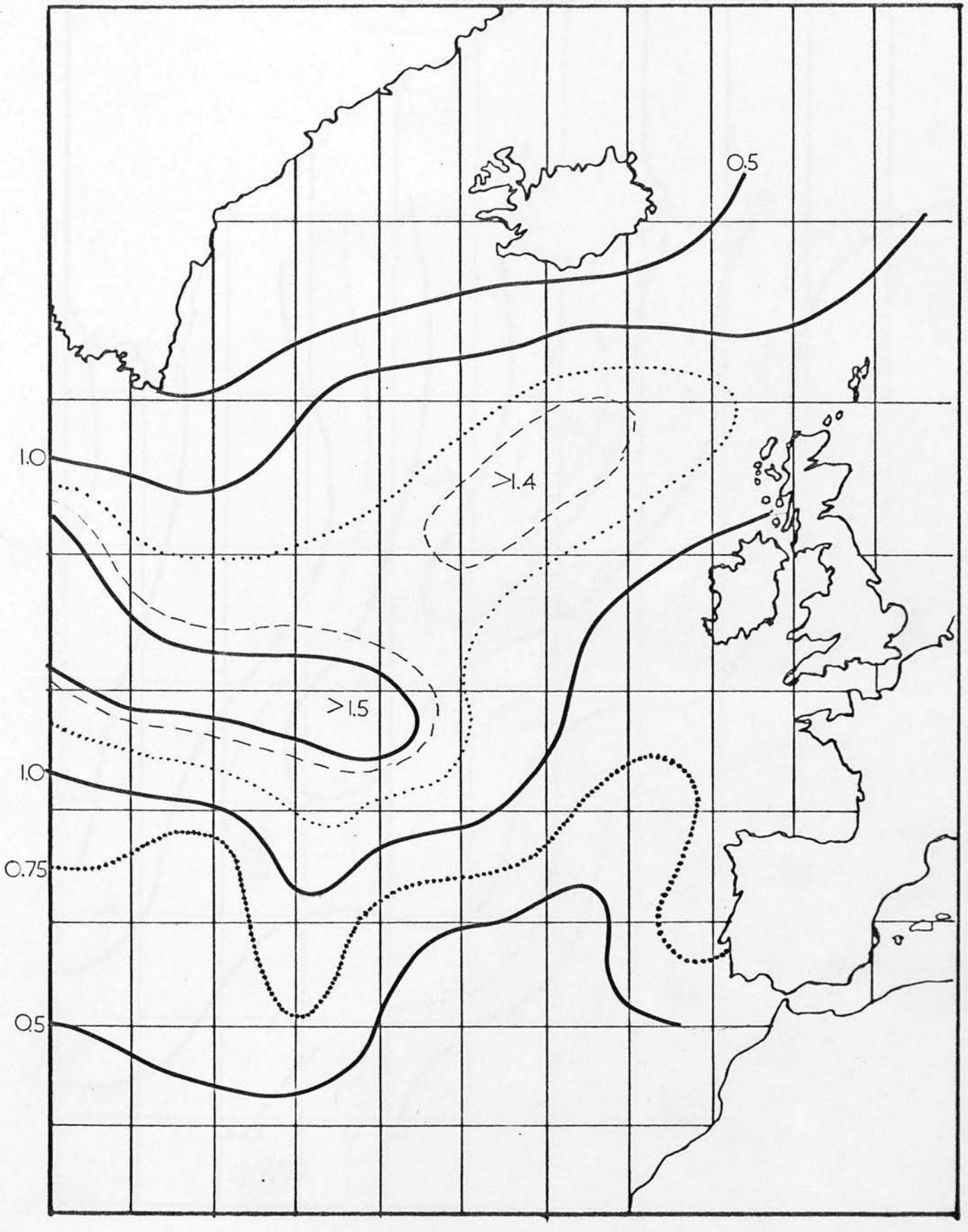

FIGURE 5.3.4c MEAN ZONAL CPT. SURFACE WIND STRESS. FEBRUARY

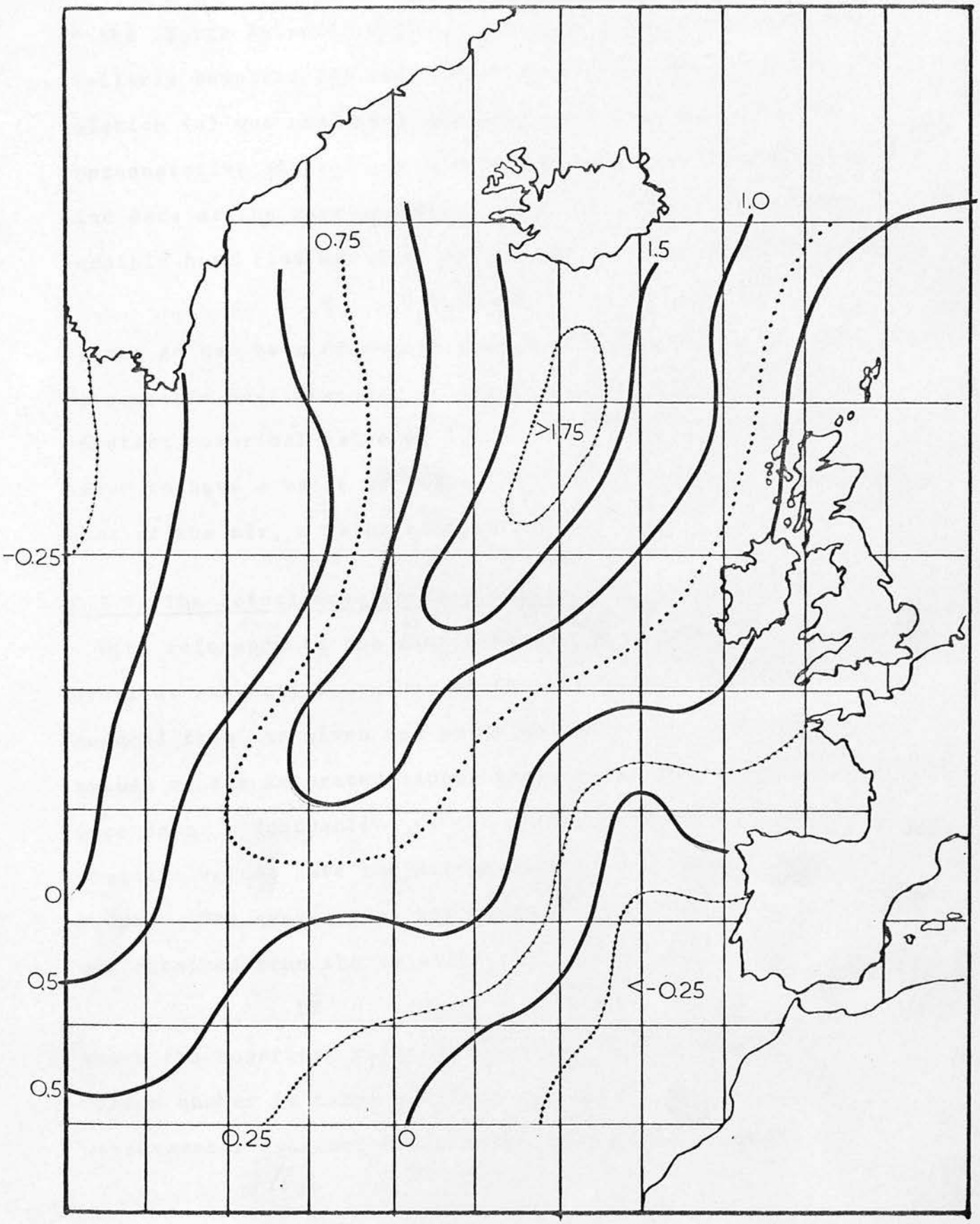

FIGURE 5.3.4d MEAN MERIDIONAL CPT. SURFACE WIND STRESS. FEBRUARY.

of the North Atlantic Ocean. As mean scalar wind data were similarly supplied for ocean weather station points only, relation (a) was used with the tabulated wind data for the representative areas in obtaining equivalent mean monthly scalar wind data at the representative area locations. The mean monthly sensible heat flux was then calculated from the bulk formula

$$\bar{H} = \rho C_p C_H \overline{|\underline{W}|} \Delta\bar{T} \quad \ldots\ldots\ldots \quad (c)$$

where, as has been discussed previously, C_H, the drag coefficient for sensible heat transfer or Stanton number has been assigned a constant numerical value of 1.5×10^{-3}. The air density, ρ, is taken to have a value of 1.2×10^{-3} gm cm^{-3} and C_p, the specific heat of the air, a value of 0.24 cal gm^{-1} deg^{-1}.

5.3.7 The actual mean monthly evaporative heat flux.

With reference to the same data source as that used in the previous subsection, values of the air vapour pressure were deduced from the given dew point monthly means and likewise, values of the saturated vapour pressure at the sea-surface temperature data. Subtraction of the former from the latter vapour pressure values gave the air-sea vapour pressure difference, $\Delta\bar{e}$, in mb. The evaporative heat flux, $L\bar{E}$, by direct analogy with $\bar{H}$, was obtained from the relation

$$L\bar{E} = \rho C_p C_v \cdot \frac{1}{\gamma} \cdot \overline{|\underline{W}|} \Delta\bar{e} \quad \ldots\ldots\ldots \quad (d)$$

where the numerical value of C_v, the vapour drag coefficient or Dalton number is taken equal to C_H, and γ, the thermodynamic psychrometer constant has a constant value of 0.66 mb deg^{-1}.

5.3.8 The actual mean monthly total surface heat flux.

The total surface heat flux, defined to be the sum of the sensible and evaporative heat fluxes was obtained simply by addition of $\bar{H}$ and $L\bar{E}$, i.e

$$\text{Total Heat Flux, } F = \bar{H} + L\bar{E}.$$

Distributions of this quantity are to be found under the case study sections. Isopleth magnitudes are in units of cals $cm^{-2} sec^{-1} \times 10^{5}$.

5.3.9 The long-term mean monthly total heat flux.

Values of both long-term mean monthly air temperature and dew point temperature were interpolated at five degree sub-Marsden square centre points, from distributions contained in the Climatological Atlas for Mariners. Mean monthly sea-surface temperatures were similarly interpolated from the Oceanographic Atlas of the North Atlantic Ocean, whereafter the values of all three parameters (given in degrees Fahrenheit) were converted to Centigrade degrees. Air-sea temperature and vapour pressure differences were then readily acquired; combination of these differences with scalar wind values interpolated from the maps described in section 5.3.2, yielded, with the aid of relations (c) and (d), magnitudes of the long-term mean monthly sensible and evaporative heat fluxes respectively. The complete distributions for January and February are displayed in figures 5.3.9a and 5.3.9b.

Unlike the wind stress calculations in section 5.3.3, the present calculation of total heat flux, both of the actual and

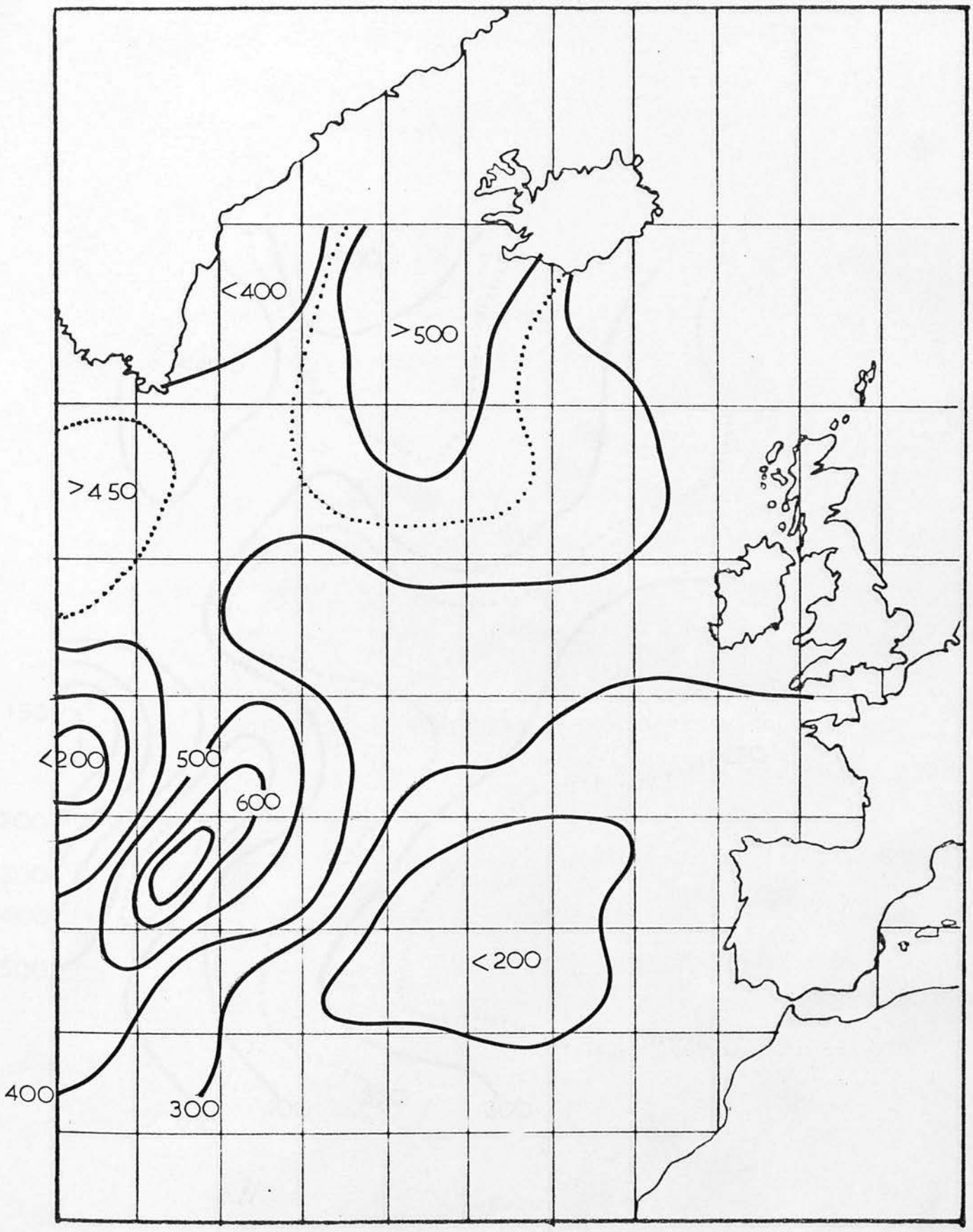

FIGURE 5.3.9a MEAN MONTHLY TOTAL SURFACE HEAT FLUX. JANUARY.

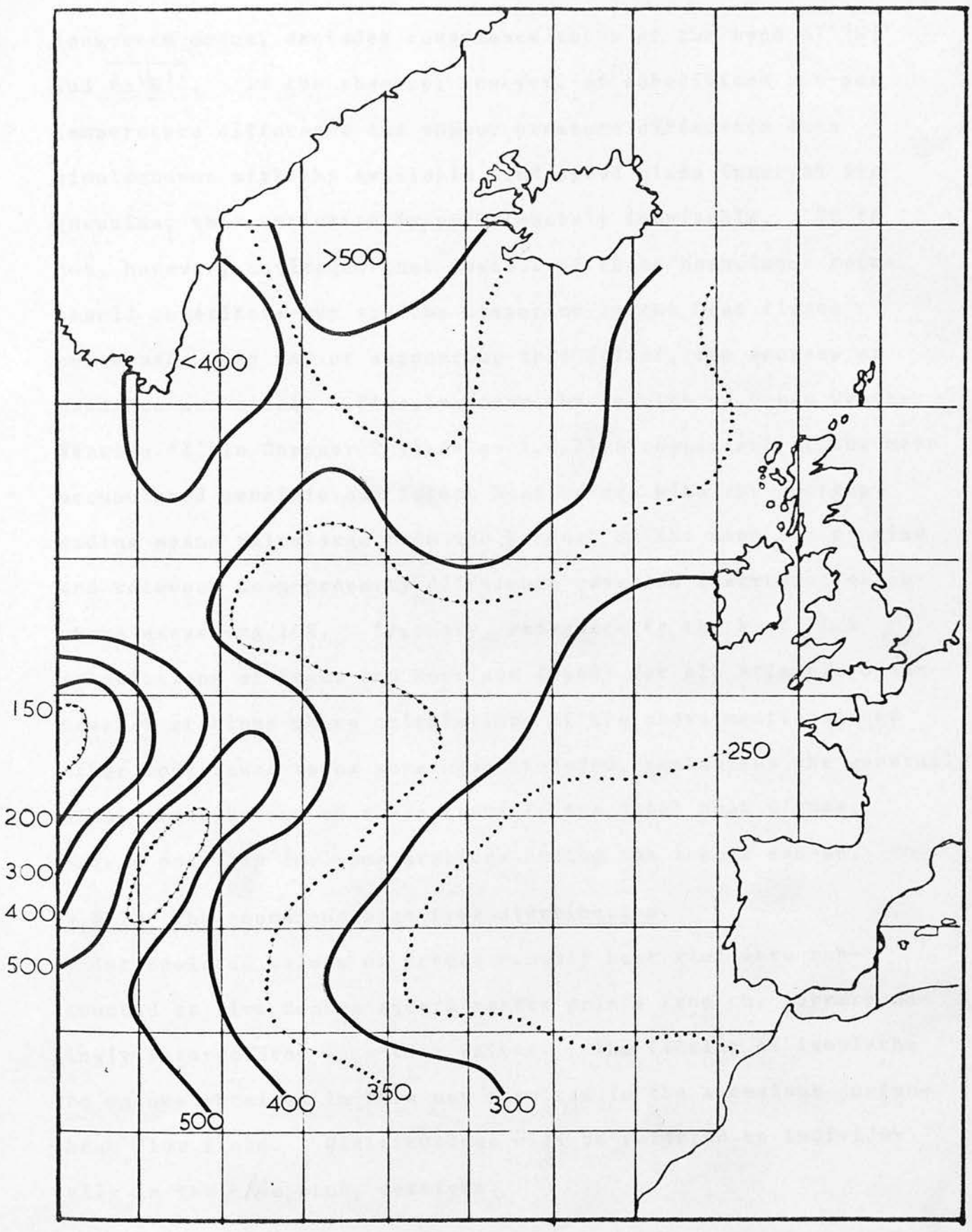

FIGURE 5.3.9b MEAN MONTHLY TOTAL SURFACE HEAT FLUX. FEBRUARY.

long-term means, excludes covariance terms of the type $\overline{\Delta T' |\underline{W}|'}$ and $\overline{\Delta e' |\underline{W}|'}$. In the absence, however, of sub-divided air-sea temperature difference and vapour pressure difference data simultaneous with the available wind speed class interval frequencies, this exclusion is unfortunately inevitable. It is not, however, envisaged that neglect of these covariance terms should constitute any serious disparity in the heat fluxes concerned. By way of supporting this belief, two sources of evidence are cited. Firstly, from the results of Ocean Weather Station 'I' in Chapter 2 (section 2.6.2) a comparison of the mean accumulated sensible and latent heat values with the corresponding means calculated from the product of the mean scalar wind and relevant mean property difference revealed discrepancies nowhere exceeding 10%. Secondly, reference to the heat flux calculations of Kraus and Morrison (1966) for all Atlantic ocean weather stations where calculations of the above-mentioned and other covariance terms were also included, emphasises the generally small contribution of these terms to the total heat fluxes, except possibly for some stations during the summer season.

5.3.10 The anomalous heat flux distribution.

Interpolated values of actual monthly heat flux were subtracted at five degree square centre points from the correspondingly interpolated long-term values. The fitting of isopleths to values obtained in this way resulted in the anomalous surface heat flux field. Distributions will be referred to individually in the case study sections.

5.4 The Oceanographic Terms.

5.4.1 The mean monthly sea-surface temperature.

As already mentioned, all long-term mean monthly sea-surface temperature data were extracted from the Oceanographic Atlas of the North Atlantic, Publication 700.

Whereas use of values interpolated at five degree square centre points was made in the computation of H and LE, outlined previously, additional arrays of interpolations at two and a half degree latitude, five degree longitude intersection points were used directly as model input data in the formation of one of two advected temperature fields.

5.4.2 The anomalous sea-surface temperature.

The transfer of the pseudo monthly means supplied by the Meteorological Office as computer printout, to five degree square centre points on blank North Atlantic maps permitted the construction of mean monthly anomalous sea-surface temperature fields which, after further interpolation yielded input data to the model for the other advected temperature field.

5.4.3 The long-term average surface current.

Surface current data for the period 1904-1945 were obtained from the National Oceanographic Data Centre, Washington, in the form of computer printout containing statistical current data summarised by five degree Marsden square and by month. Although this statistical summary included such information as current speed in fourteen class intervals of speed and direction, maximum individual current speed, resultant current direction, etc., only mean vector current data in the form of W-E and S-N

components were required in the present study. Owing to the occasionally small number of observations for any particular month and/or location, data comprising the current component magnitudes together with the number of observations for four months December to March were combined to form winter average values. In view of the lack of any appreciable variation in the monthly current values during the winter season, it is considered unlikely that use of winter average current values rather than actual monthly values should constitute any significant error. The resultant distributions for E-W and N-S components are revealed in figures 5.4.3a and 5.4.3b respectively; numerical values are in cm sec^{-1}. Certain features observed from a close inspection of these figures afford support for the general overall validity of these distributions. In particular, the area of maximum northward flow to the south-east of Iceland near $60^{o}N$ $30^{o}W$ coincides with the region of maximum wind stress curl as examination of the long-term stress fields previously referred to will verify.

5.4.4 The mixed-layer depth distribution.

Computer printout data indicating mean mixed-layer depth and thermocline depth by month and by one degree square were obtained from the National Oceanographic Data Centre, Washington. Temperature gradient criteria were specified in advance for the determination of these depths. Data for each one degree square and for the four months December-March were plotted at the relevant location within each corresponding five degree sub-Marsden square. Inspection of the final data plottings

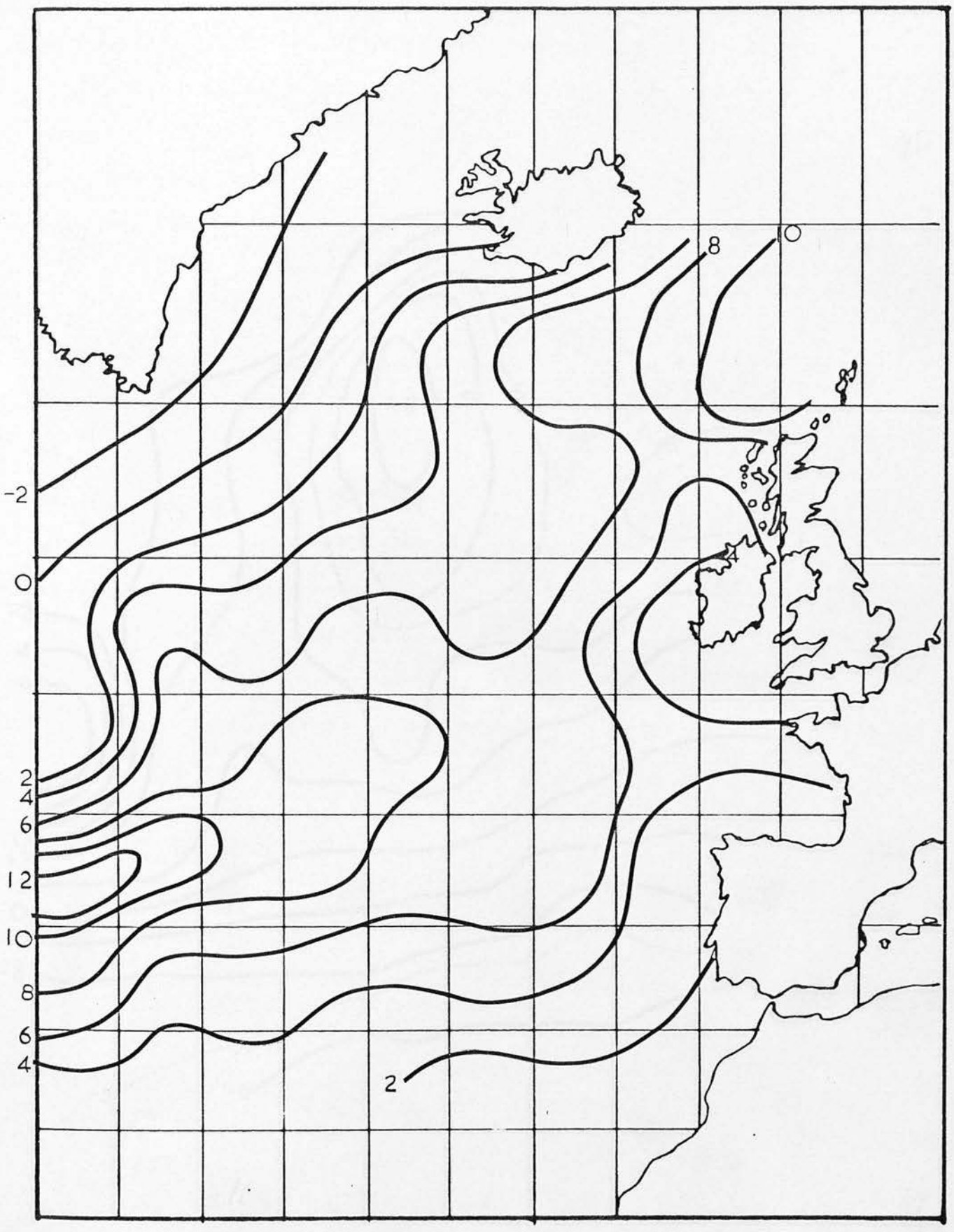

FIGURE 5.4.3a ZONAL CPT. AVERAGE SURFACE CURRENT. WINTER.

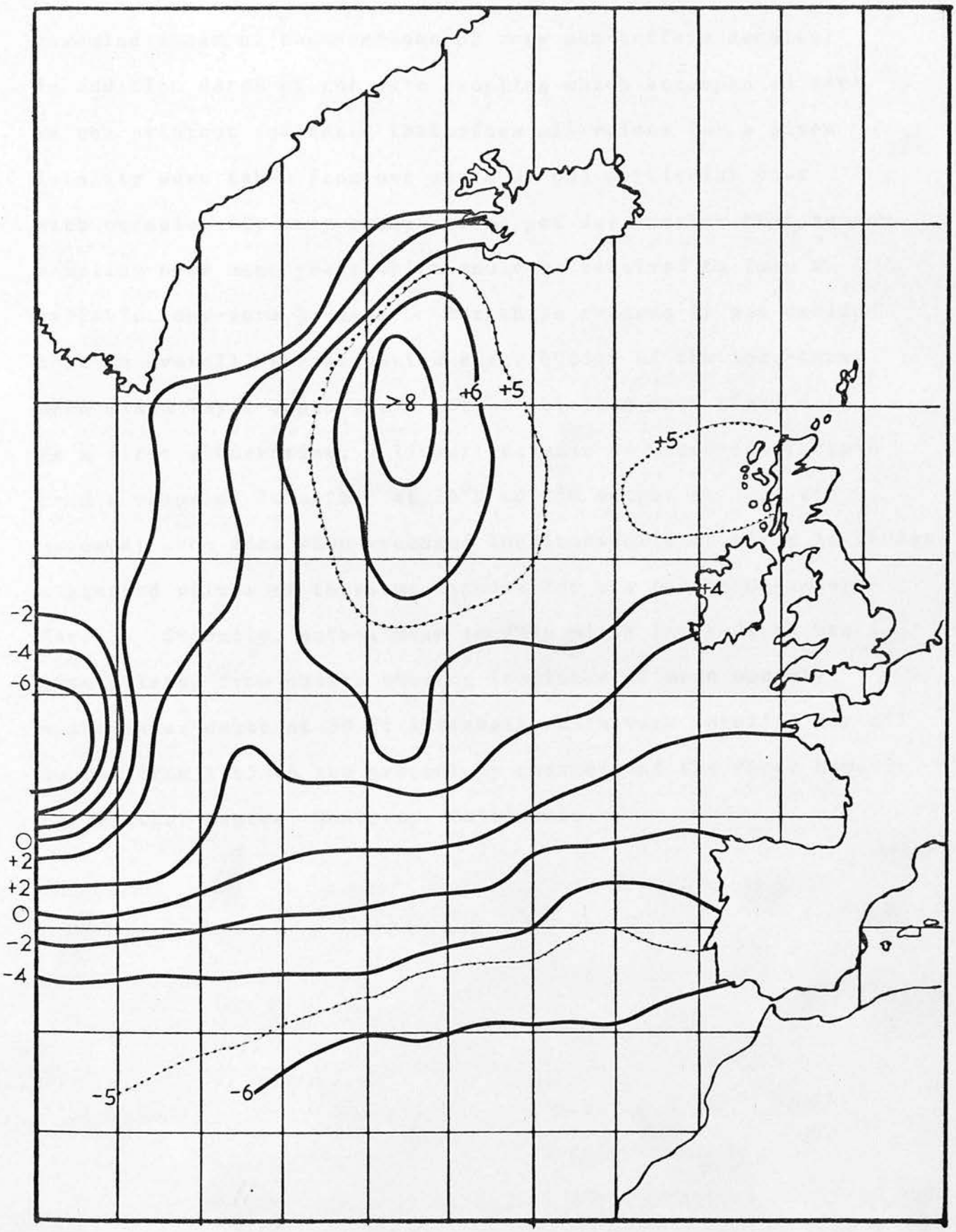

FIGURE 5.4.3b MERIDIONAL CPT. AVERAGE SURFACE CURRENT. WINTER.

revealed a set of observations of very non-uniform density; in addition dates of the data sampling which accompanied data on the printout indicated that often all values for a given locality were taken from one month of one particular year with occasionally many observations per day, rather than random sampling over many years which would be required to form a reliable long-term average. For these reasons it was decided that an overall representative distribution of the long-term mean mixed-layer depth could not be obtained from these data. As a first alternative, a linear increase of mixed-layer depth from a value of 70 metres at 30^{o}N to 250 metres at 70^{o}N was assumed; the data when averaged longitudinally at these latitudes suggested values of these magnitudes for the months December - March. Secondly, actual mean monthly mixed layer-depth was interpolated from charts showing isopleths of mean monthly mixed-layer depth at 50 ft intervals which were supplied for all months from 1965 to the present by courtesy of the Fleet Numerical Weather Centre, Monterey, California.

5.5 Case Study (1)

5.5.1 Synoptic situation; meteorological and sea temperature distributions.

The two months January and February 1966 were selected on the basis of their well-defined quasi steady state anomalous meteorological régime as particularly appropriate for the first of three case studies intended to evaluate the model by comparing predicted changes in monthly mean anomalous sea-surface temperature with those actually observed. Reference to figures 5.5a and 5.5b which show the anomalous pressure distribution for the months in question confirms the existence in January of a large anomalous low pressure area (central pressure anomaly <-16mb) centred near $45^{o}N$, $0^{o}W$ and dominating most of the North Atlantic. February is similarly characterised by the same low pressure area, only a slight north-eastward migration of the centre having occurred in the interim. Associated with this system are intense anomalous easterly winds (immediately apparent from the 'tightness' of the meridional pressure gradient) over the northern part of the region and stronger than usual westerlies in the south and south-west.

The actual wind stress component fields for January and February 1966 are produced in figures 5.5c, 5.5d and 5.5e, 5,5f, respectively, as are the corresponding anomalous component wind stress fields in figures 5.5g to 5.5j. Particularly noteworthy is again the very large easterly component anomalous wind stress, more especially in February (<-4 dynes cm^{-2})

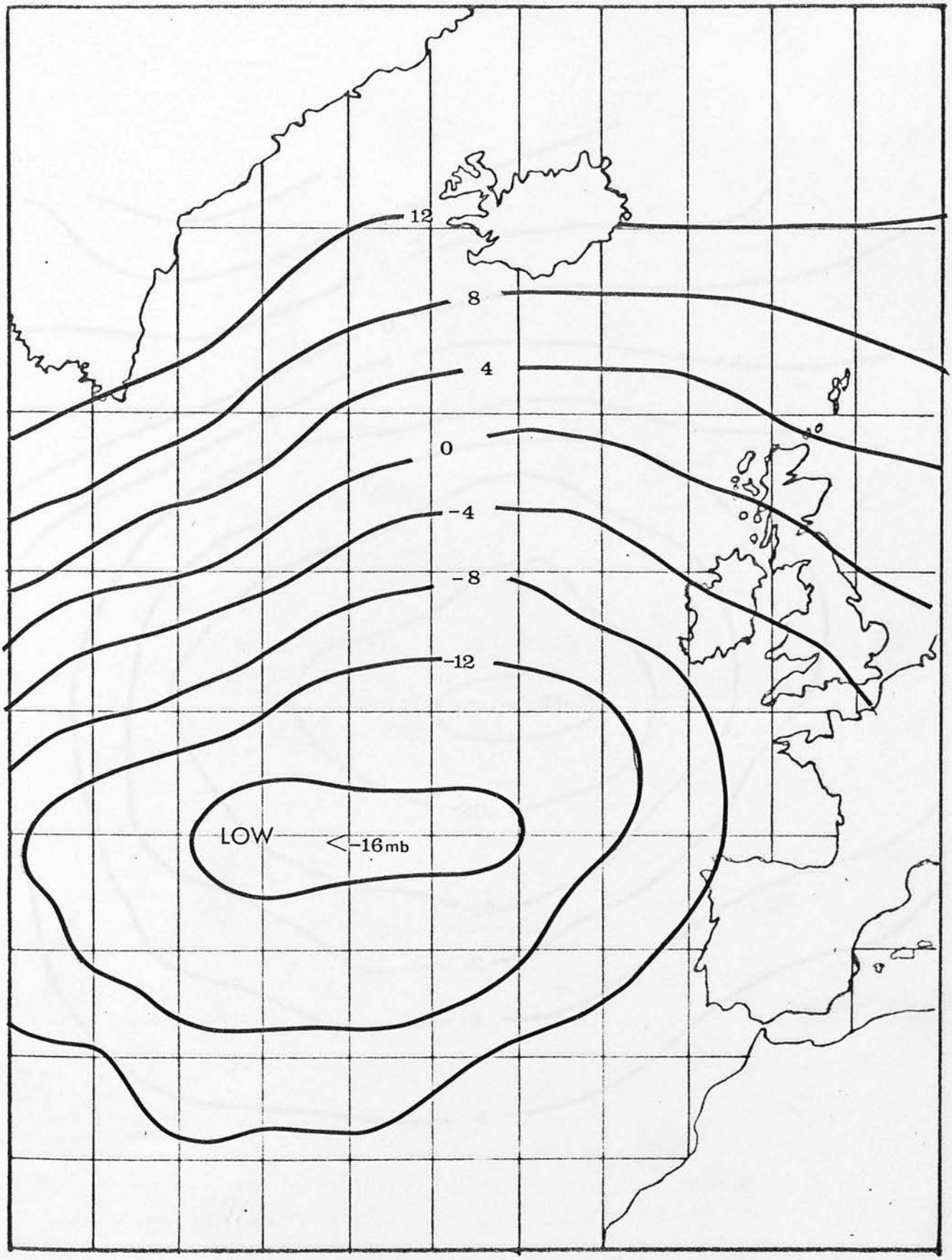

FIGURE 5.5a ANOMALOUS PRESSURE DISTRIBUTION. JANUARY 1966

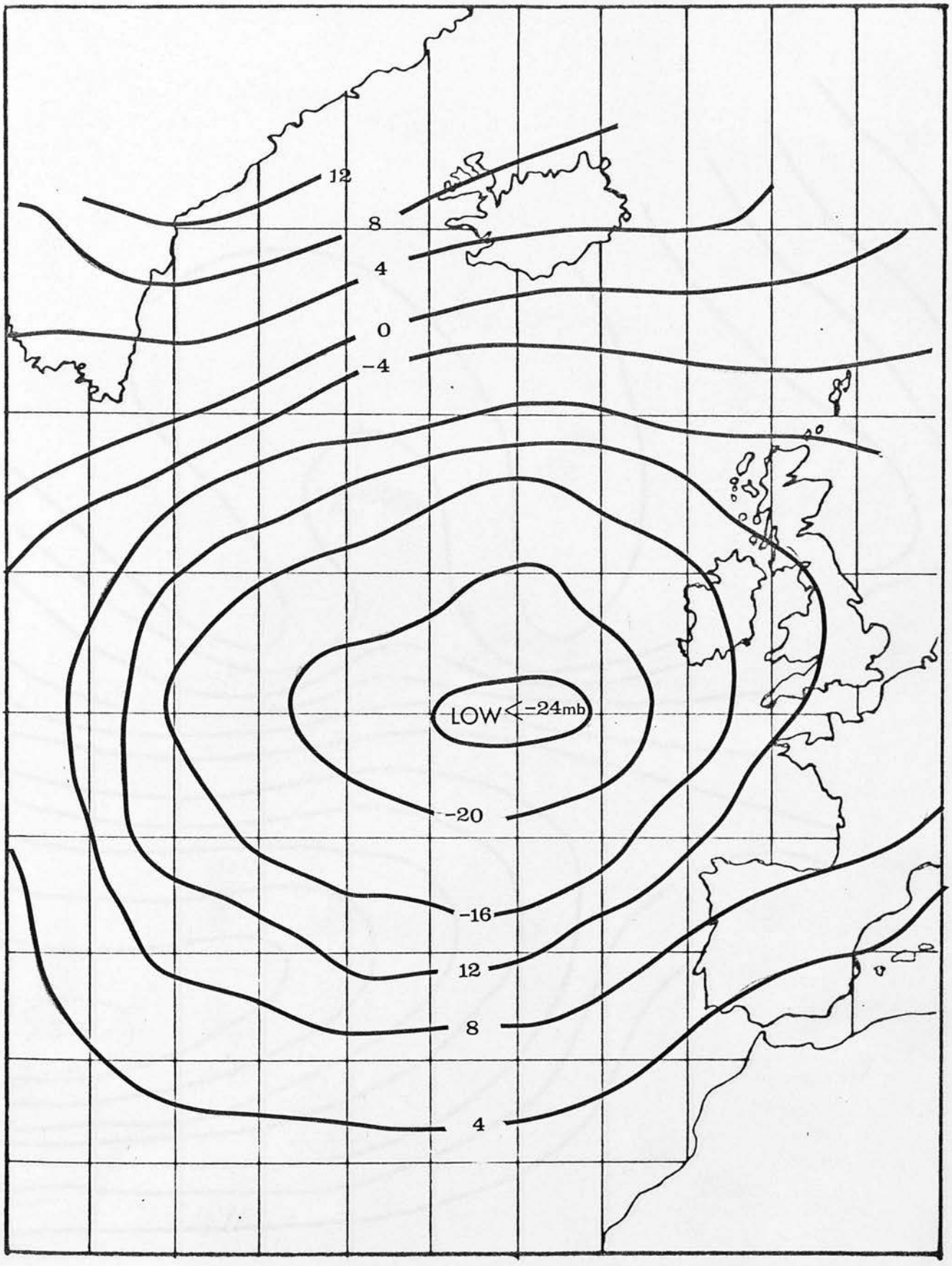

FIGURE 5.5b ANOMALOUS PRESSURE DISTRIBUTION. FEBRUARY 1966

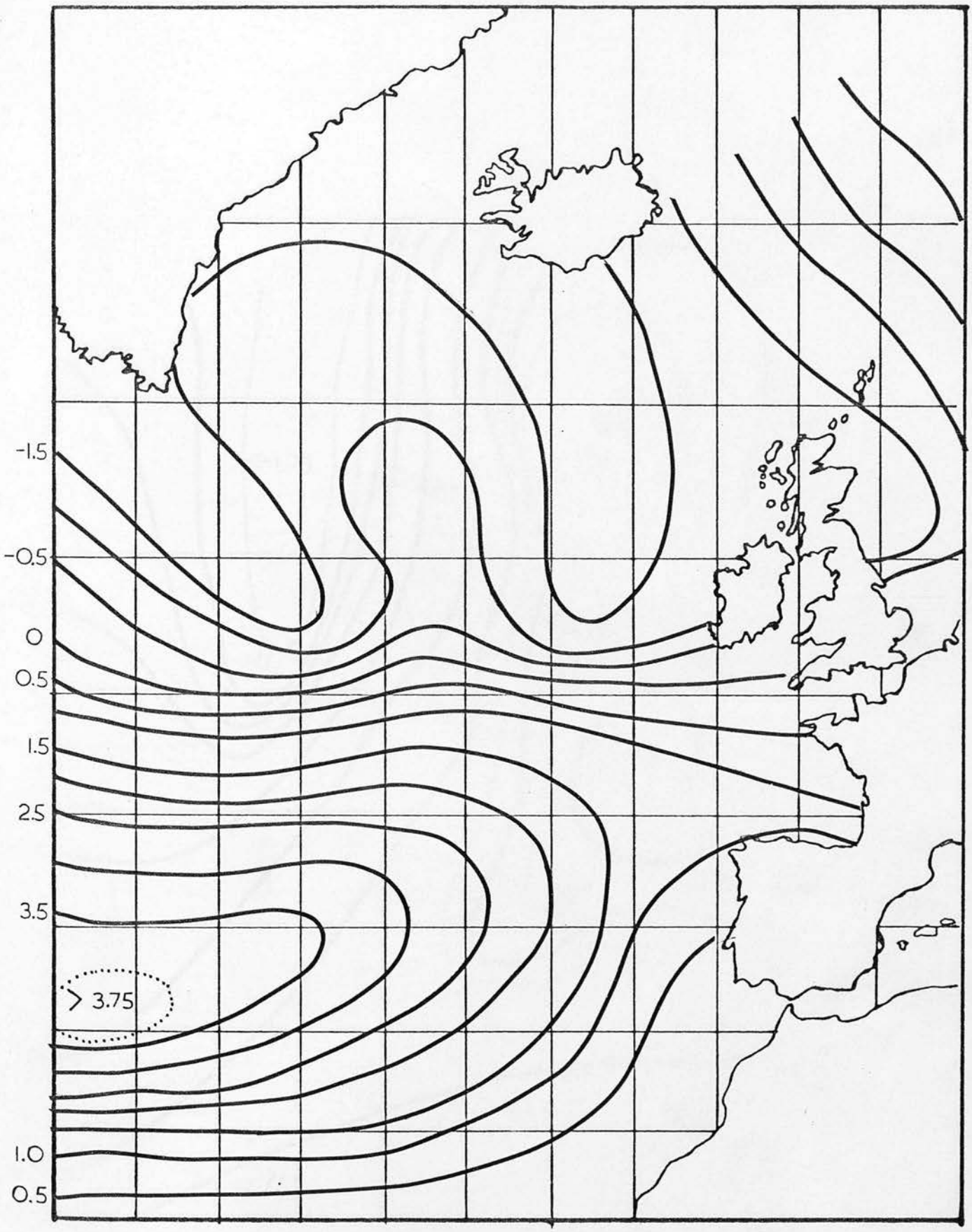

FIGURE 5.5c MEAN ZONAL CPT. SURFACE WIND STRESS. JANUARY 1966

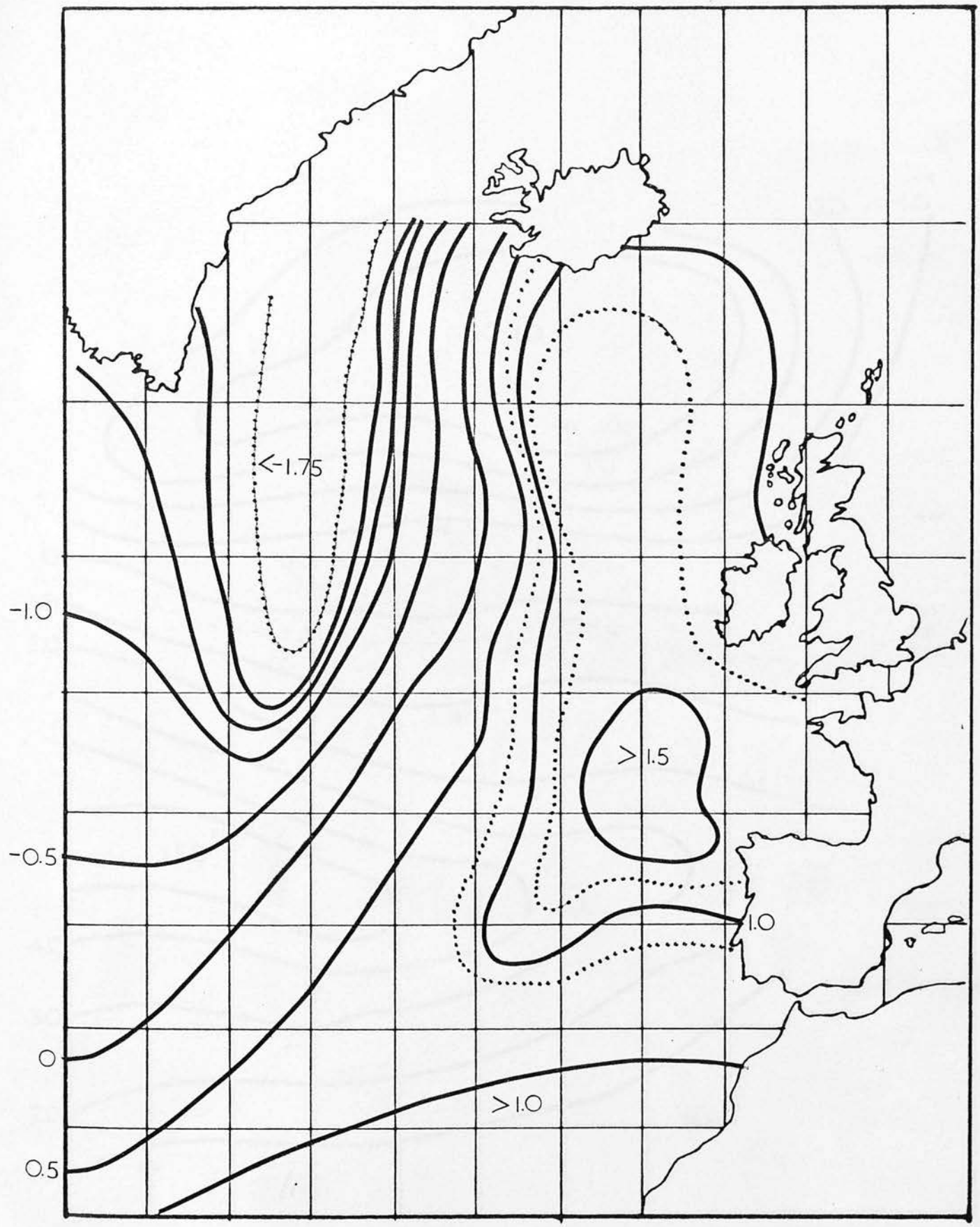

FIGURE 5.5d MEAN MERIDIONAL CPT. SURFACE WIND STRESS. JANUARY 1966

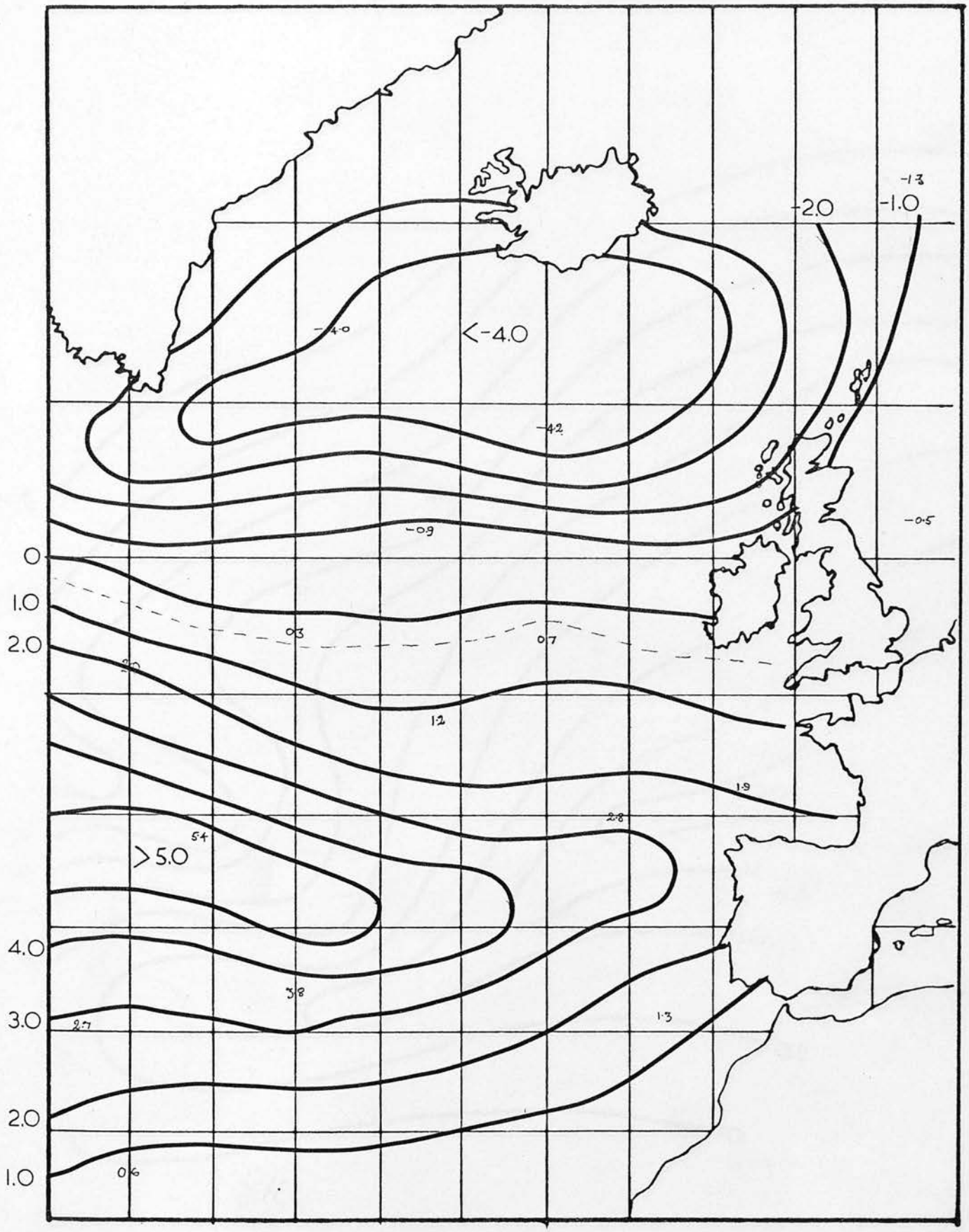

FIGURE 5.5e ZONAL CPT SURFACE WIND STRESS FEBRUARY 1966

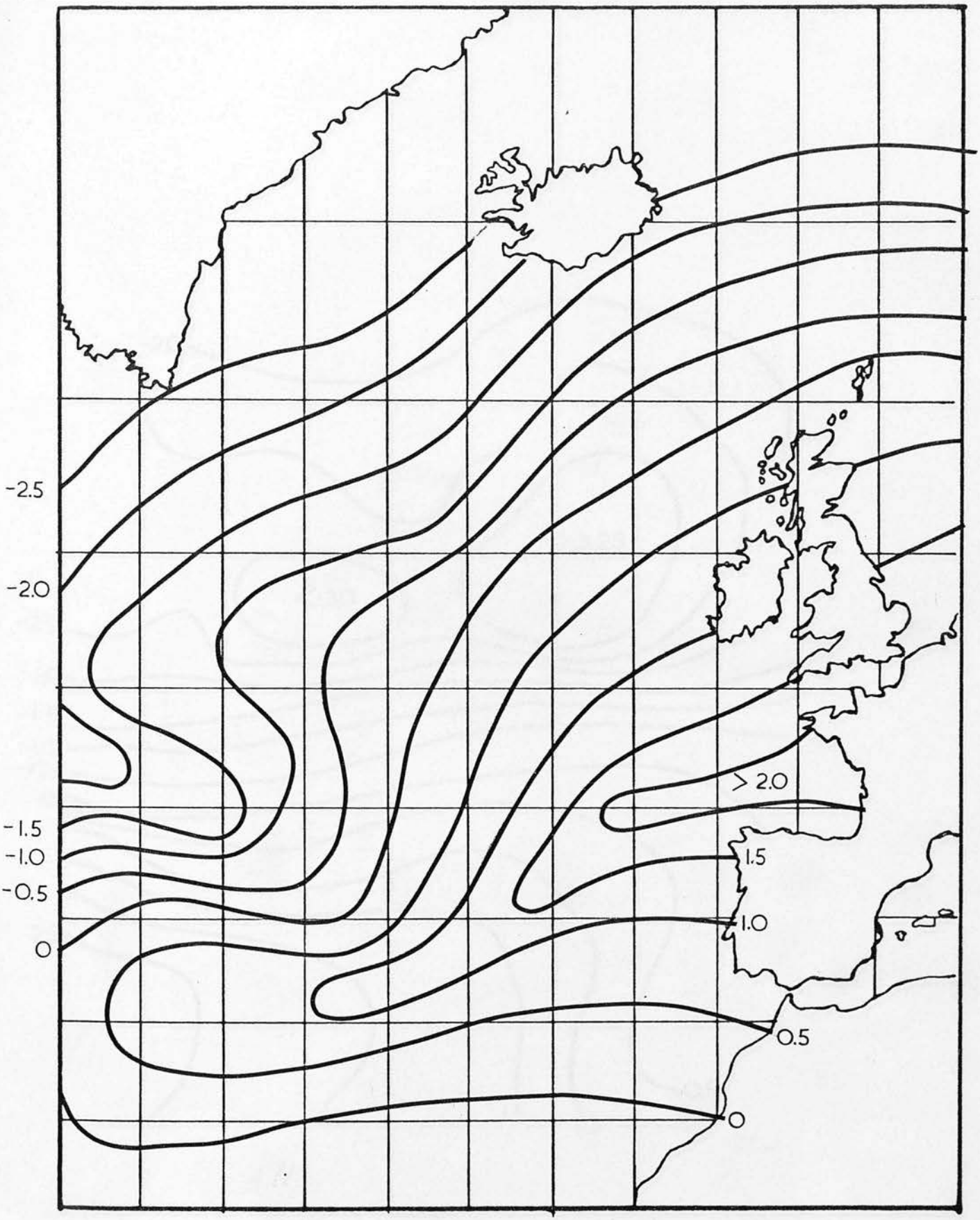

FIGURE 5.5f MERIDIONAL CPT SURFACE WIND STRESS FEBRUARY 1966

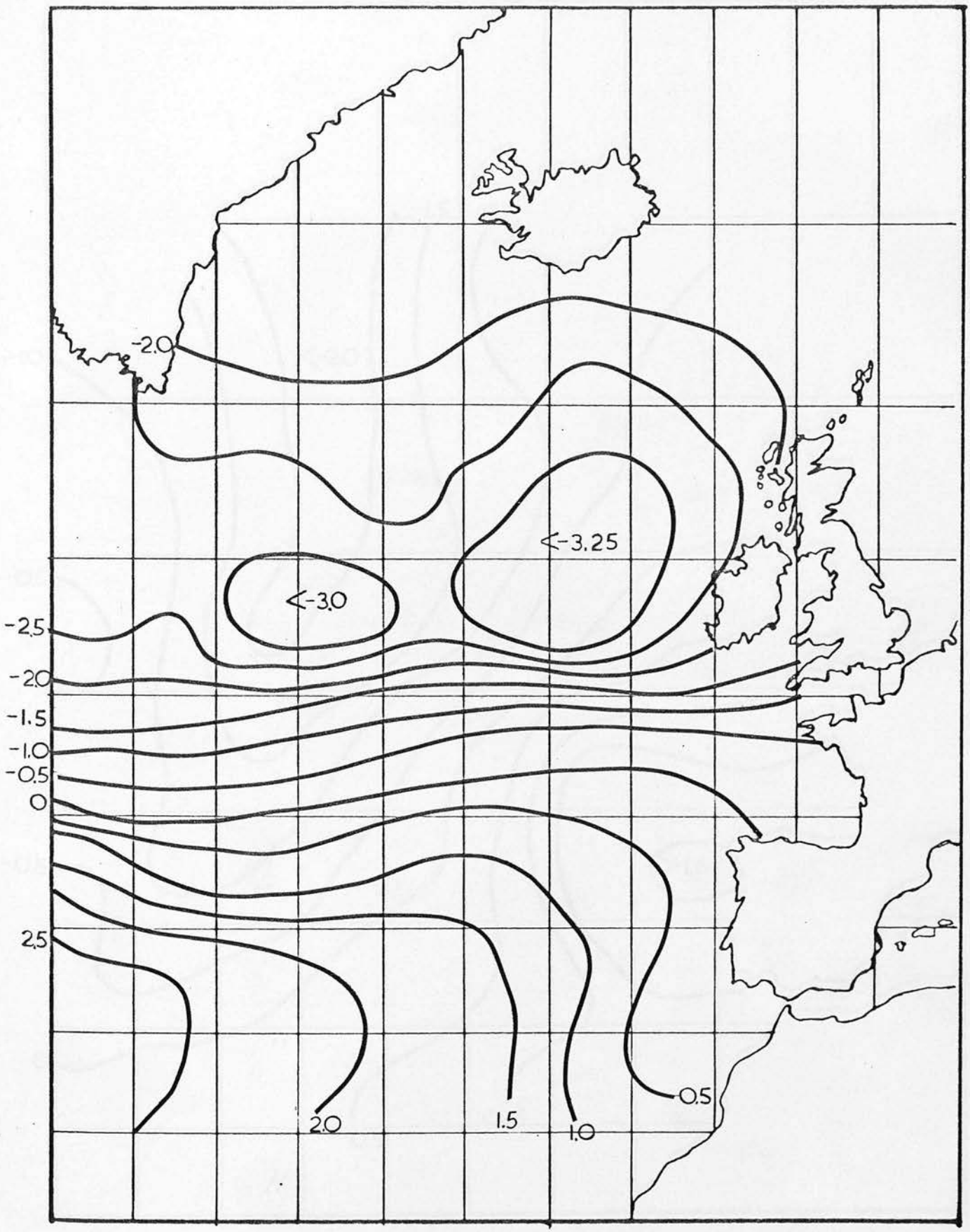

FIGURE 5.5g ZONAL CPT. ANOMALOUS SURFACE WIND STRESS. JANUARY 1966

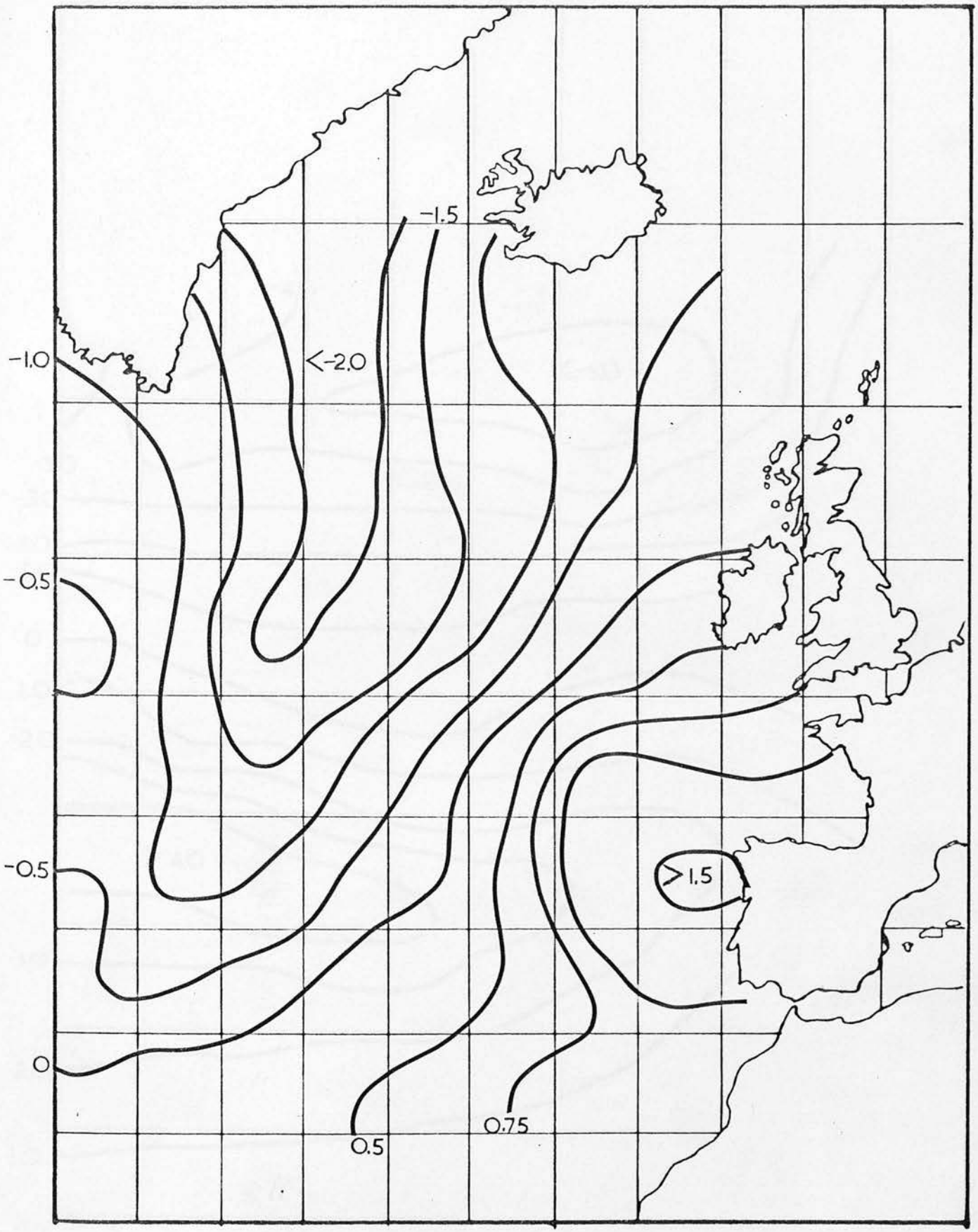

FIGURE 5.5h MERIDIONAL CPT. ANOMALOUS SURFACE WIND STRESS. JANUARY 1966

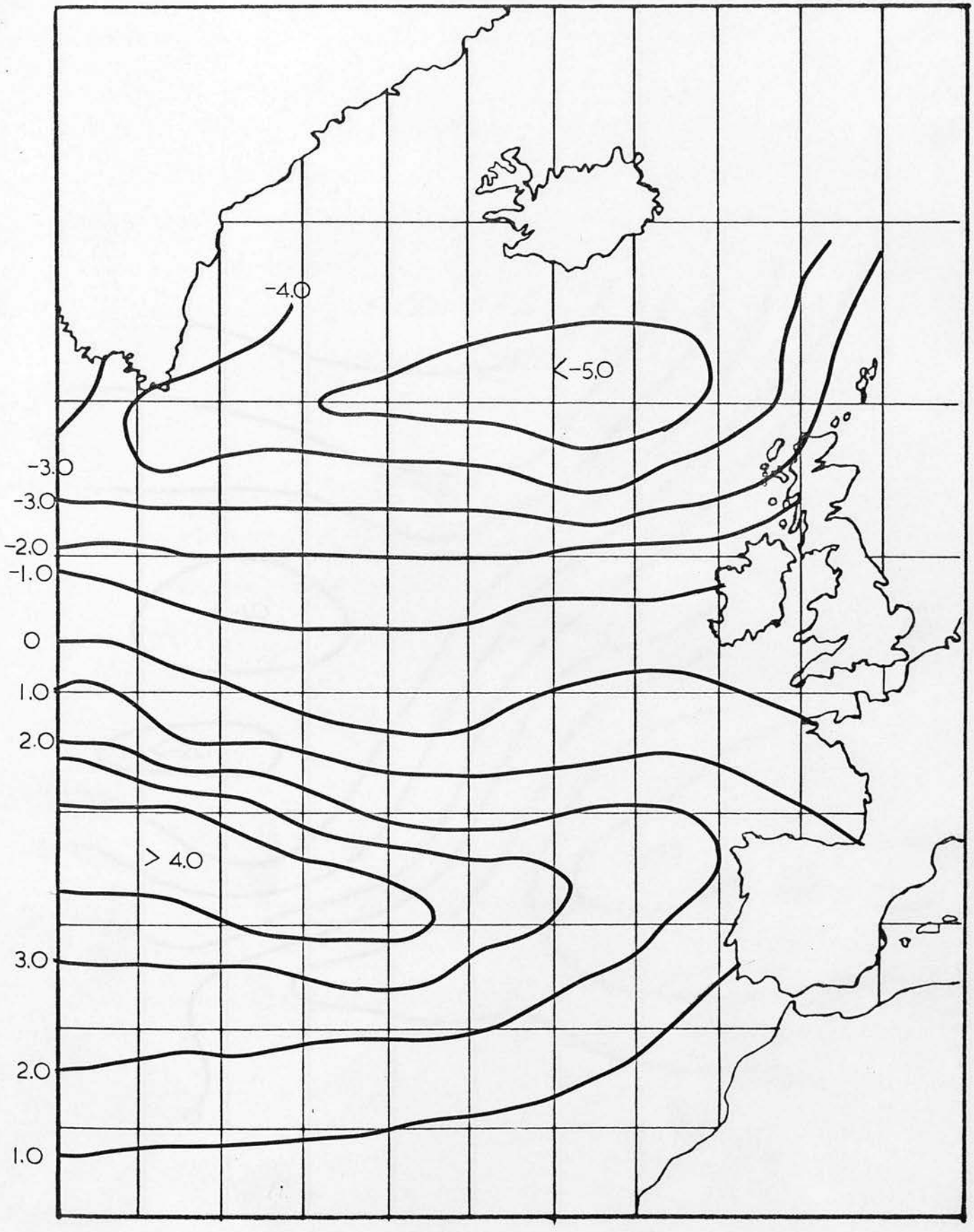

FIGURE 55i ZONAL CPT ANOMALOUS SURFACE WIND STRESS FEBRUARY 1966

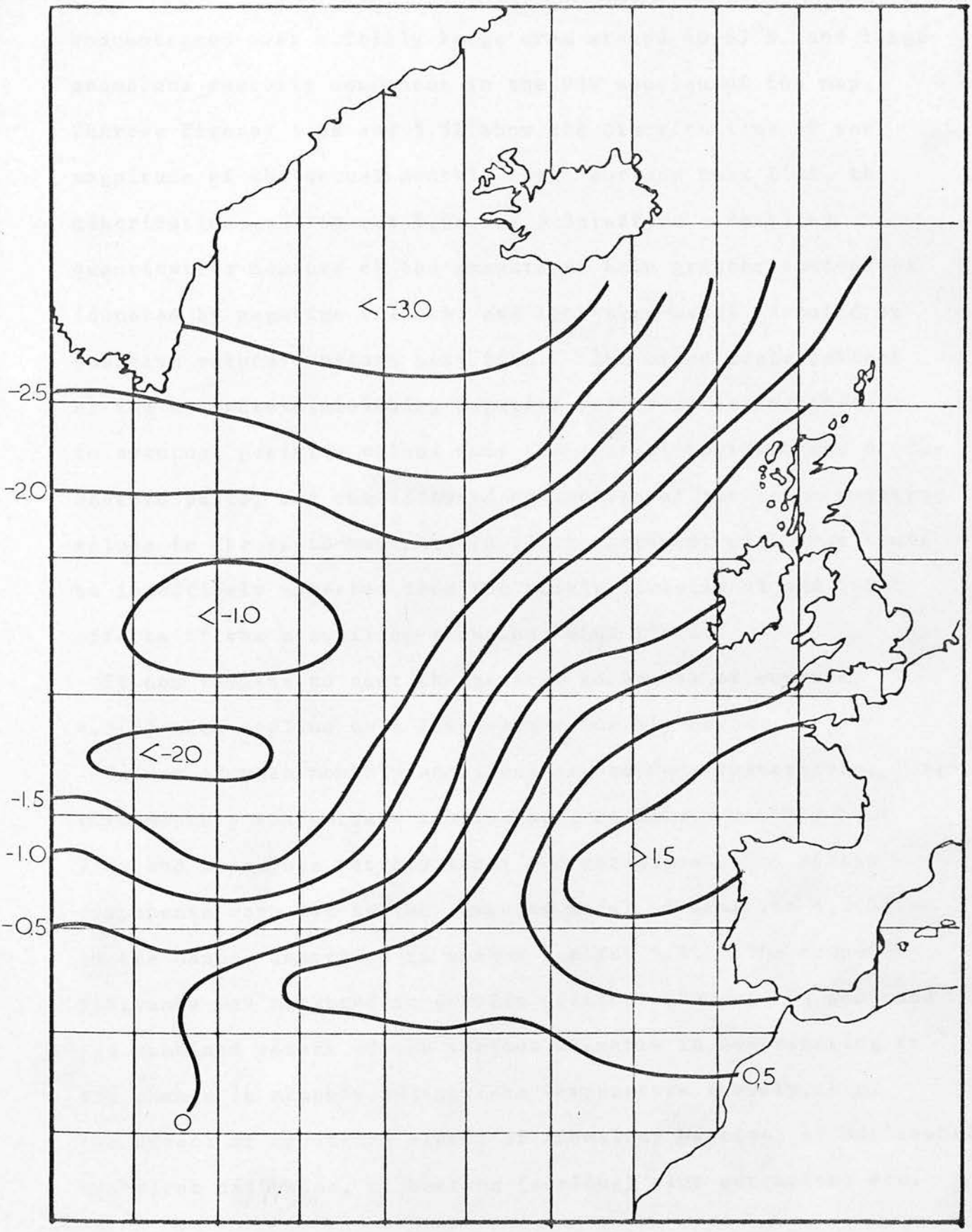

FIGURE 5.5j MERIDIONAL CPT. ANOMALOUS SURFACE WIND STRESS. FEBRUARY 1966

concentrated over a fairly large area around 60-65°N, and large anomalous westerly component in the WSW section of the map. Whereas figures 5.5k and 5.51 show the distributions of the magnitude of the actual monthly total surface heat flux, the distributions of figures 5.5m and 5.5n afford a detailed quantitative measure of the amounts of both greater-than-usual (denoted by negative values), and less-than-usual (denoted by positive values) surface heat flux. The broad scale pattern of the westward-diminishing negative values of the north-east to eventual positive values over the central-northern and north-western parts, and the eastward diminution of the large negative values in the south-west, are in close agreement with what would be intuitively expected from the purely directional and fetch effects of the prevailing anomalous wind field.

It now remains to test the general soundness of equation 4.3(3) when applied on a large-scale monthly basis.

Values of mean monthly anomalous sea-surface temperature, long-term monthly sea-surface temperature, anomalous monthly heat flux and anomalous monthly zonal and meridional wind stress components were fed to the computer model of equation 4.3(3) in the manner described in method section 5.1. The computer programme was arranged to provide printout showing the separate and combined effect of the various elements in contributing to the change in monthly sea-surface temperature anomaly, e.g. the effect of advection alone, of anomalous heating, of horizontal turbulent diffusion, of heating (cooling) plus advection, etc.

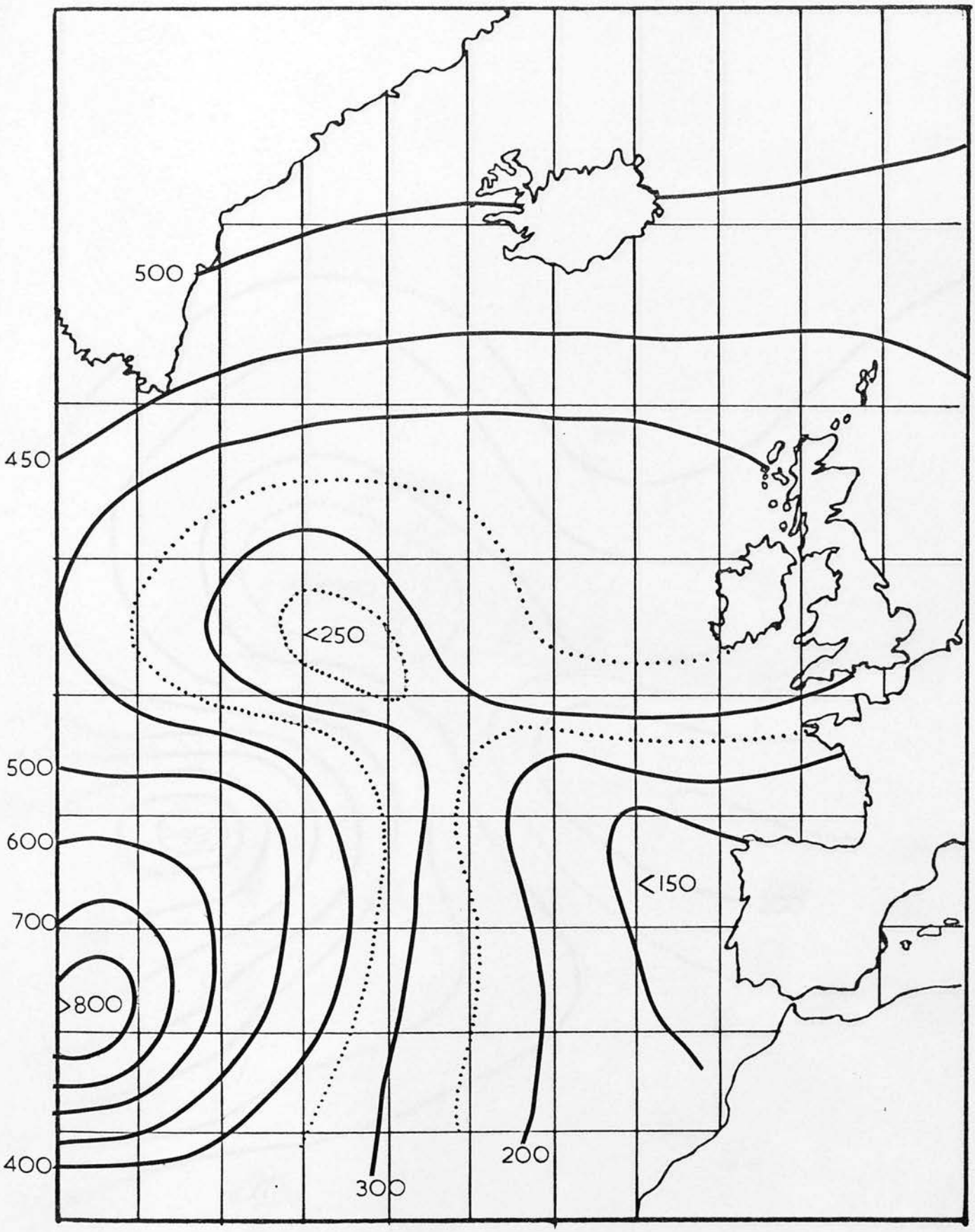

FIGURE 5.5k TOTAL SURFACE HEAT FLUX JANUARY 1966

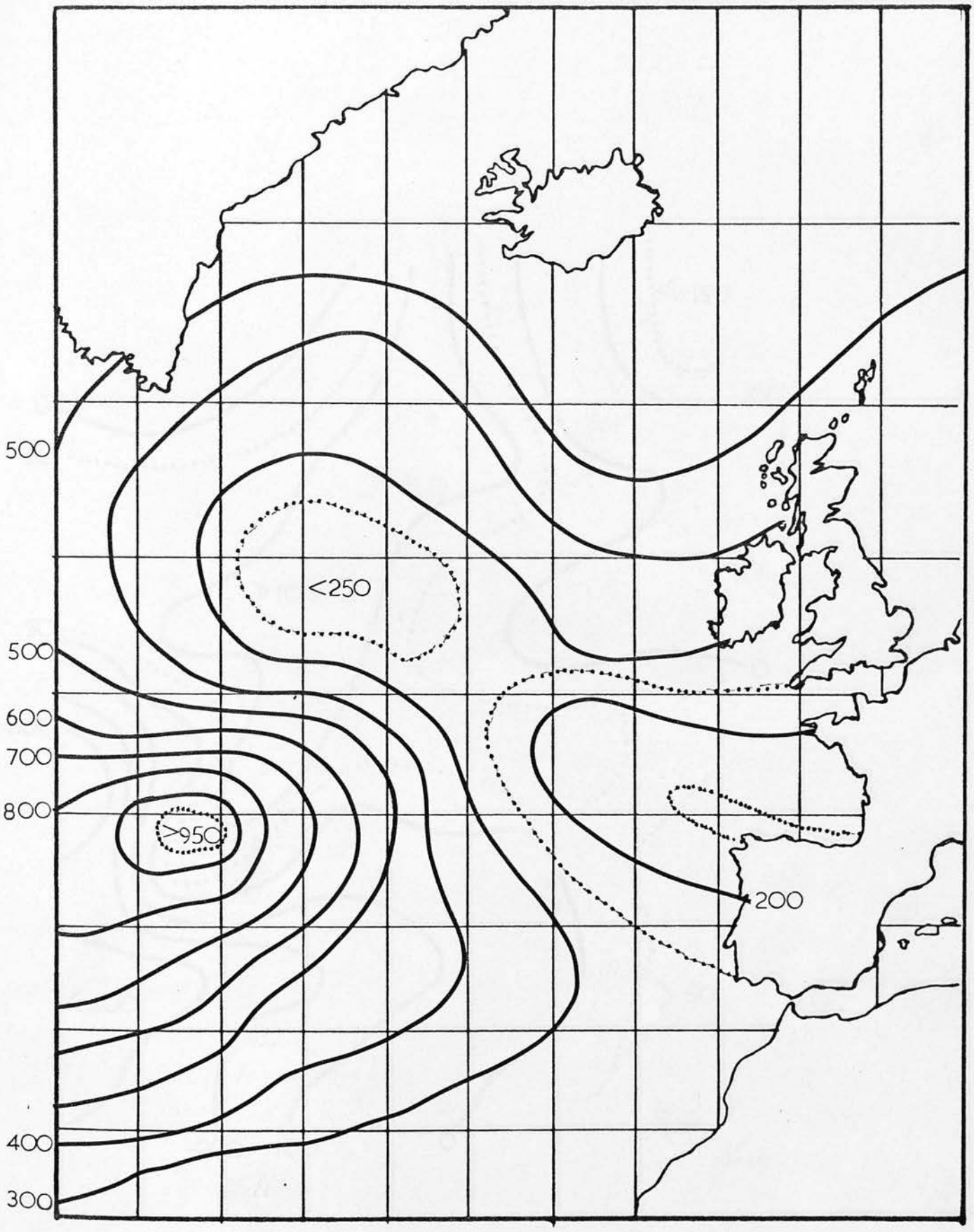

FIGURE 5.51 TOTAL SURFACE HEAT FLUX FEBRUARY 1966

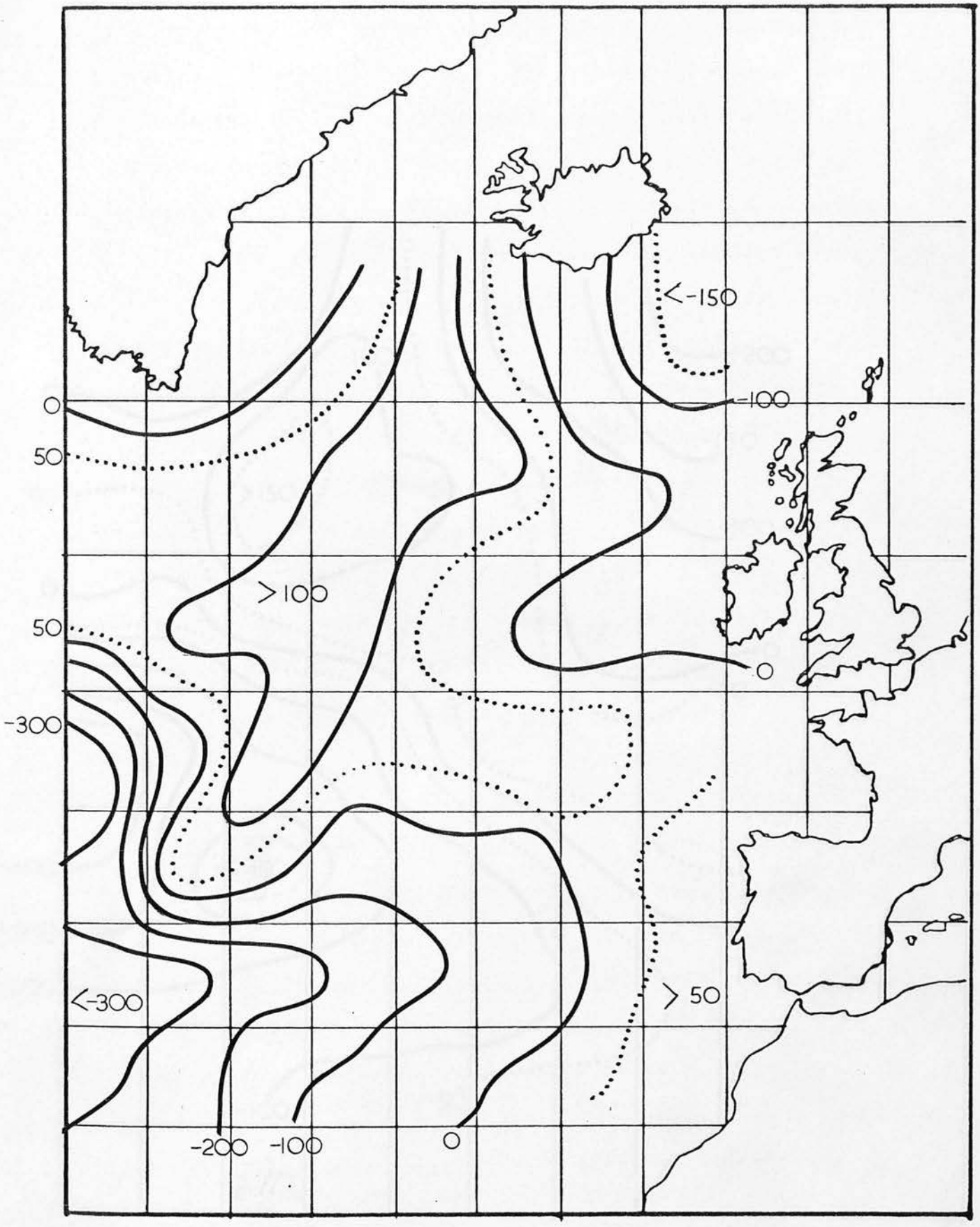

FIGURE 5.5m ANOMALOUS TOTAL SURFACE HEAT FLUX JANUARY 1966

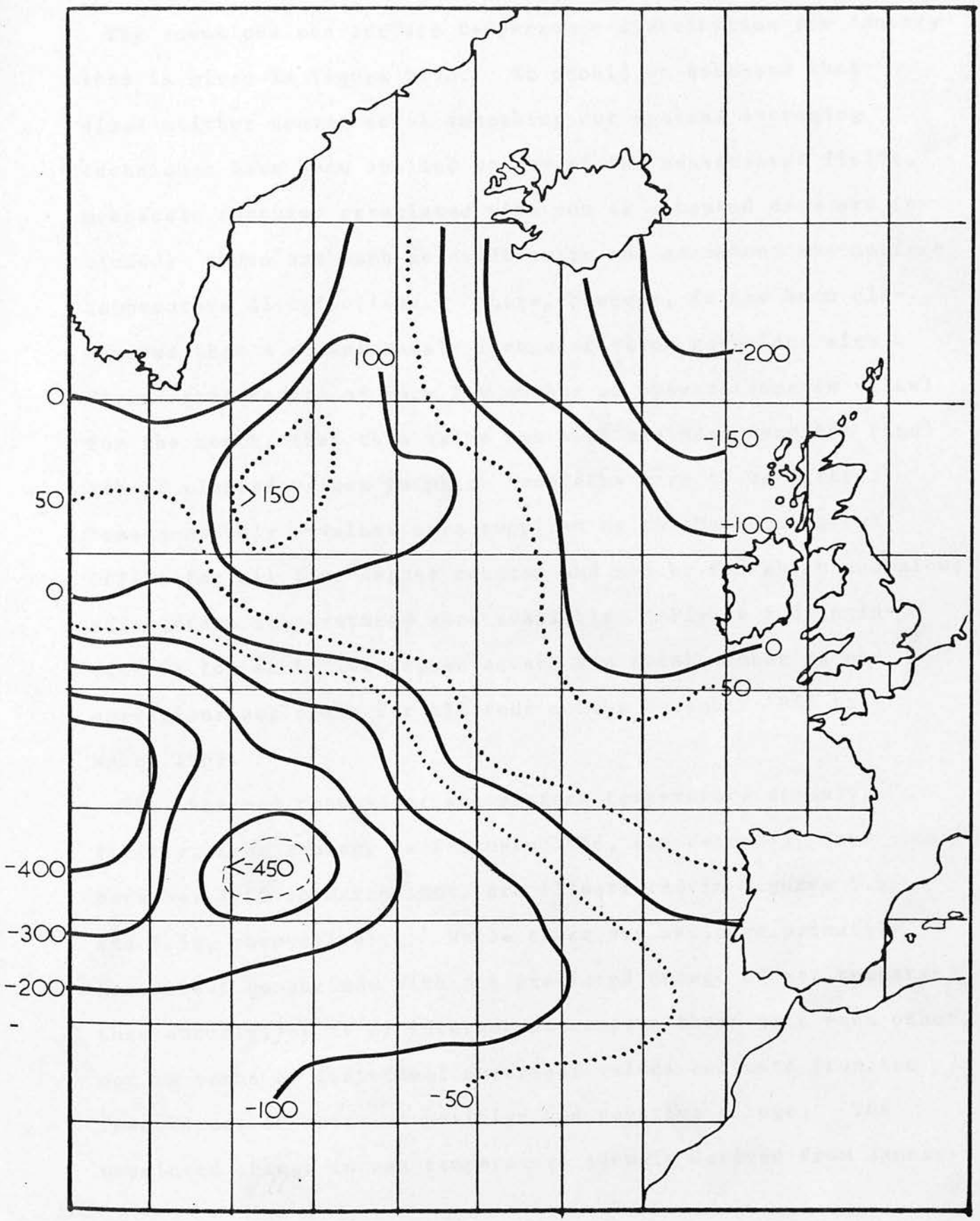

FIGURE 5.5n ANOMALOUS TOTAL SURFACE HEAT FLUX FEBRUARY 1966

The anomalous sea-surface temperature distribution for January 1966 is given in figure 5.5o. It should be stressed that since neither conventional smoothing nor spatial averaging techniques have been applied to any of the constructed fields, mesoscale features associated with raw or computed data are included; these are much in evidence in the anomalous sea-surface temperature distributions. Where, however, it has been discovered that a conspicuously irregular value coincided with a five-degree square of very low number of observations (n value) for the month, then this value has been excluded from the final set of plotted values to which isopleths were to be fitted. Pseudo-monthly n-values were supplied by the Meteorological Office for all five-degree squares and months for which anomalous sea-surface temperatures were available. Figure 5.5.1p indicates for each five-degree square the total number of observations per month for all four months December 1965 to March 1966.

The observed changes of sea-surface temperature anomaly, firstly, from January to February 1966, and secondly, from December 1965 to March 1966, are illustrated in figures 5.5p and 5.5q, respectively. While these are included primarily for direct comparison with the predicted change of sea temperature anomaly, it is of interest to compare these with each other, not in terms of individual numerical values but more from the coincidence of areas of positive and negative change. The predicted change in sea temperature anomaly derived from January

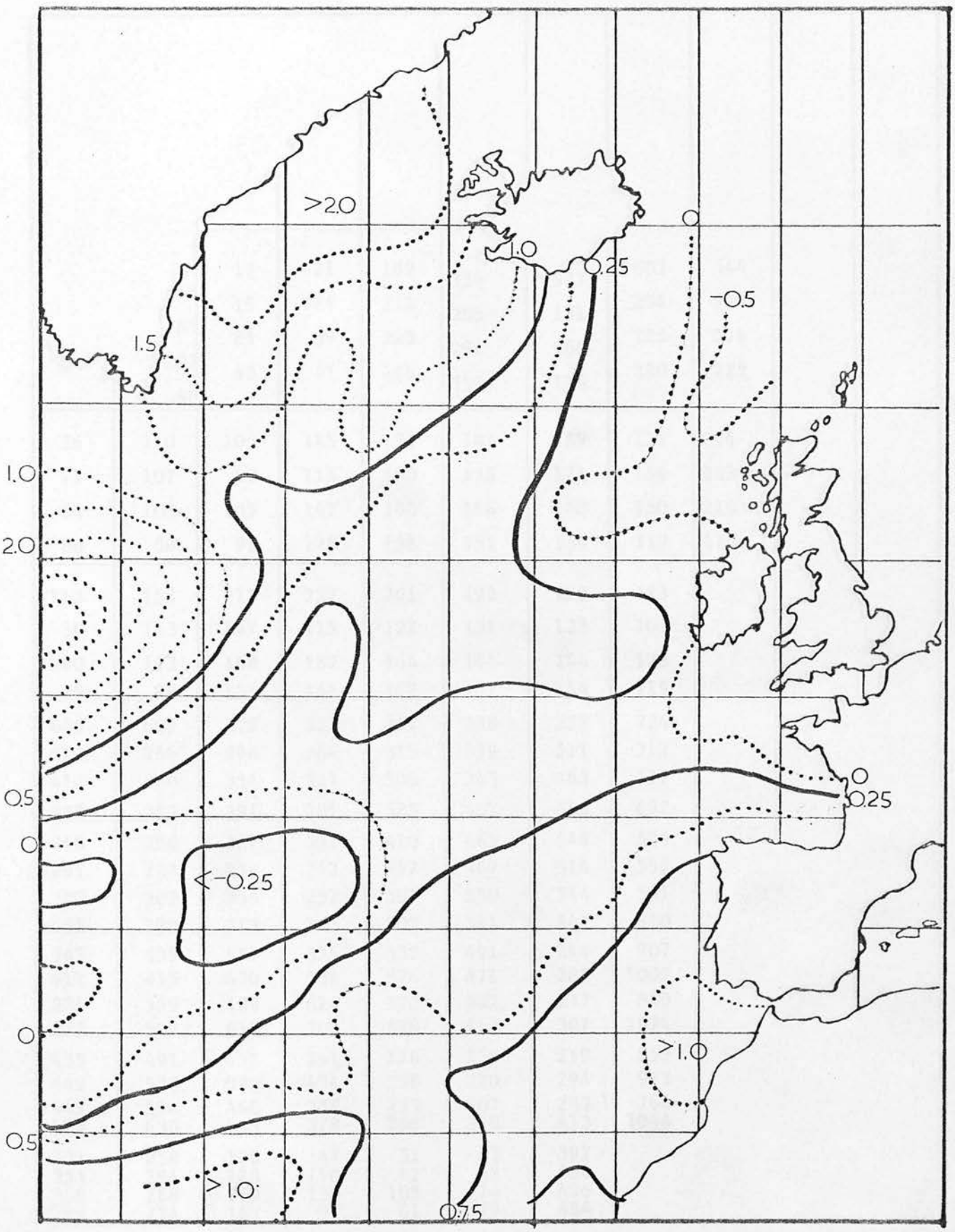

FIGURE 5.5o ANOMALOUS SEA-SURFACE TEMPERATURE DISTRIBUTION; JANUARY 1966.

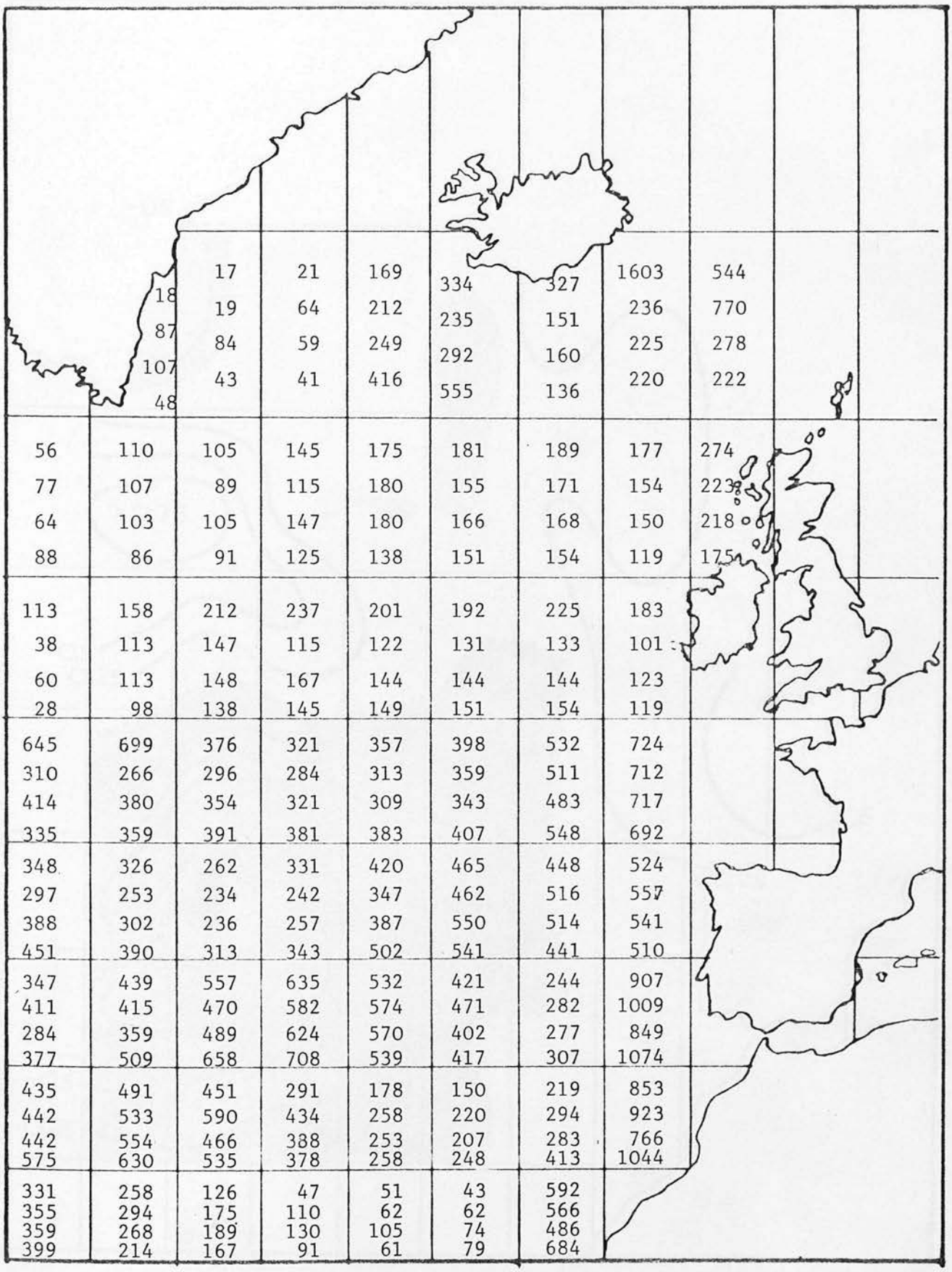

		17	21	169	334	327	1603	544
18		19	64	212	235	151	236	770
87		84	59	249	292	160	225	278
107		43	41	416	555	136	220	222
48								
56	110	105	145	175	181	189	177	274
77	107	89	115	180	155	171	154	223
64	103	105	147	180	166	168	150	218
88	86	91	125	138	151	154	119	175
113	158	212	237	201	192	225	183	
38	113	147	115	122	131	133	101	
60	113	148	167	144	144	144	123	
28	98	138	145	149	151	154	119	
645	699	376	321	357	398	532	724	
310	266	296	284	313	359	511	712	
414	380	354	321	309	343	483	717	
335	359	391	381	383	407	548	692	
348	326	262	331	420	465	448	524	
297	253	234	242	347	462	516	557	
388	302	236	257	387	550	514	541	
451	390	313	343	502	541	441	510	
347	439	557	635	532	421	244	907	
411	415	470	582	574	471	282	1009	
284	359	489	624	570	402	277	849	
377	509	658	708	539	417	307	1074	
435	491	451	291	178	150	219	853	
442	533	590	434	258	220	294	923	
442	554	466	388	253	207	283	766	
575	630	535	378	258	248	413	1044	
331	258	126	47	51	43	592		
355	294	175	110	62	62	566		
359	268	189	130	105	74	486		
399	214	167	91	61	79	684		

FIGURE 5.5.1p PSEUDO MONTHLY n-VALUES. DECEMBER 1965 - MARCH 1966.

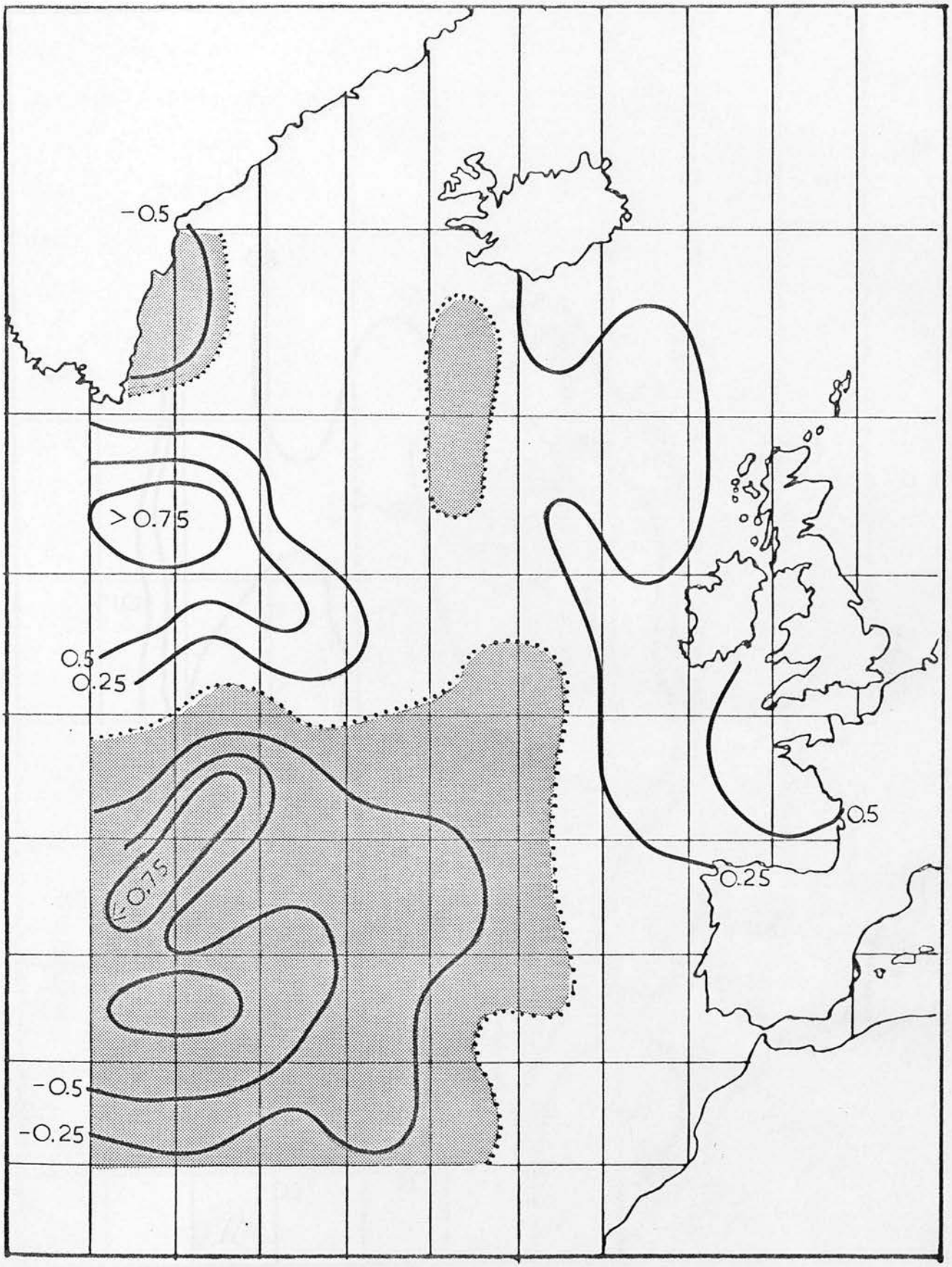

FIGURE 5.5p OBSERVED SEA-SURFACE TEMPERATURE ANOMALY CHANGE,
JANUARY-FEBRUARY 1966.

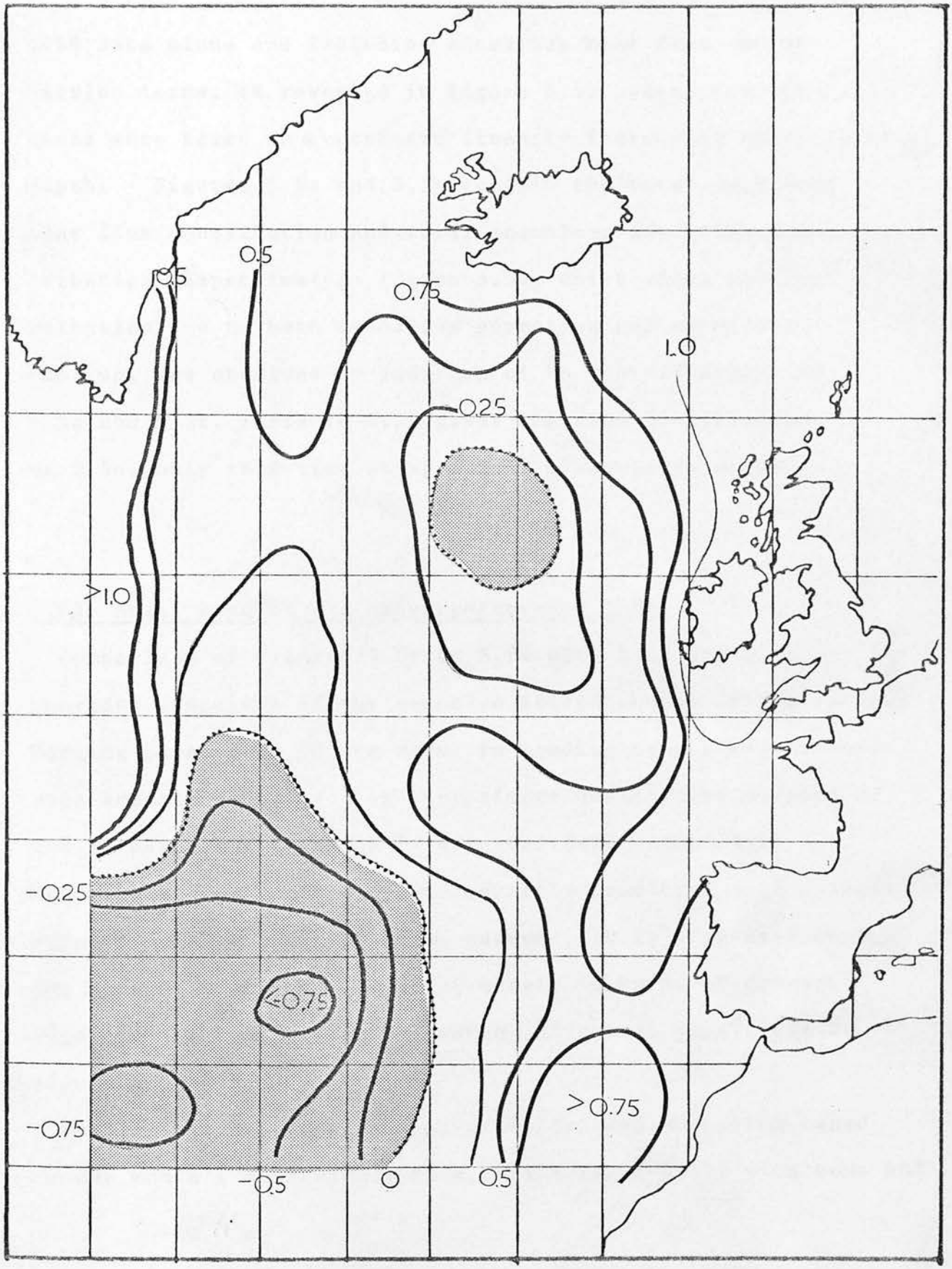

FIGURE 5.5q OBSERVED SEA-SURFACE TEMPERATURE ANOMALY CHANGE,
DECEMBER 1965 - MARCH 1966.

1966 data alone and including anomalous heat flux and advection terms, is revealed in figure 5.5r, where computations were based on a northward linearly increasing mixed-layer depth. Figures 5.5s and 5.5t exhibit the total anomalous heat flux contribution and total anomalous advection contribution respectively; figure 5.5u, which shows the contribution due to both anomalous advection and anomalous cooling, was obtained by addition of the contributions of 5.5s and 5.5t. Figure 5.5v gives the same contributions as 5.5u, only this time using actual mixed-layer depth.

5.5.2 Model Results for January-February 1966.

Comparison of figures 5.5r to 5.5v with 5.5p and 5.5q provides a measure of the relative effectiveness of the various forcing parameters of the model in predicting the sea temperature anomaly changes. An approximate qualitative measure of the success of prediction is afforded (vid. Adem 1970) by calculating the percentage of correctly predicted sign changes at grid points. Unlike Adem, however, it is suggested that the present model be judged not merely in terms of correct sign changes but also on the weight of actual magnitudes of sign changes.

Predictions due to anomalous heat loss and advection based on one month's data alone, have considerable skill with some 80%

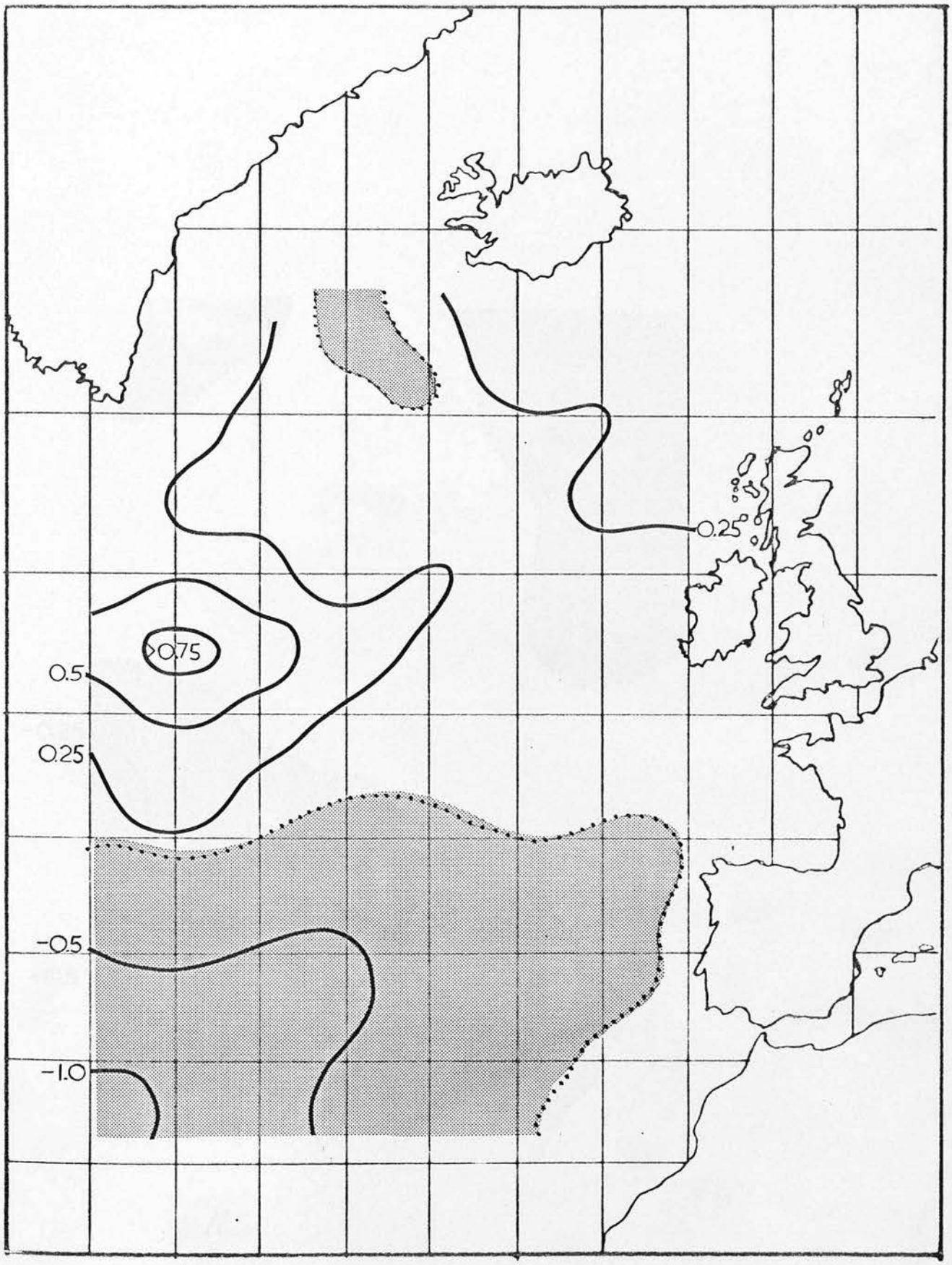

FIGURE 5.5r PREDICTED SEA TEMPERATURE ANOMALY CHANGE, JANUARY-FEBRUARY 1966; ADVECTION PLUS HEAT LOSS CONTRIBUTIONS.

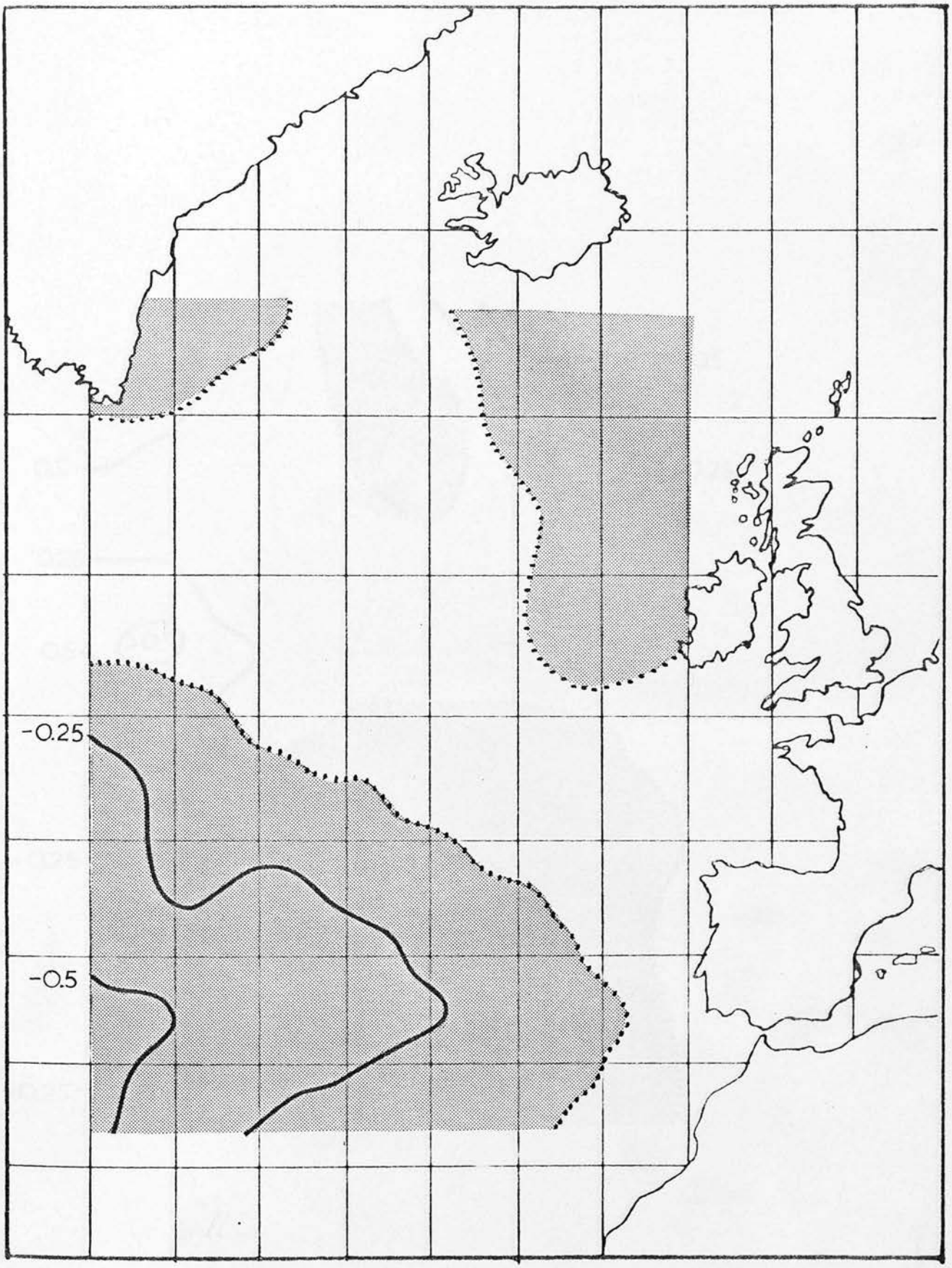

FIGURE 5.5s SEA TEMPERATURE ANOMALY CHANGE, JANUARY-FEBRUARY 1966;
HEAT LOSS CONTRIBUTION ONLY.

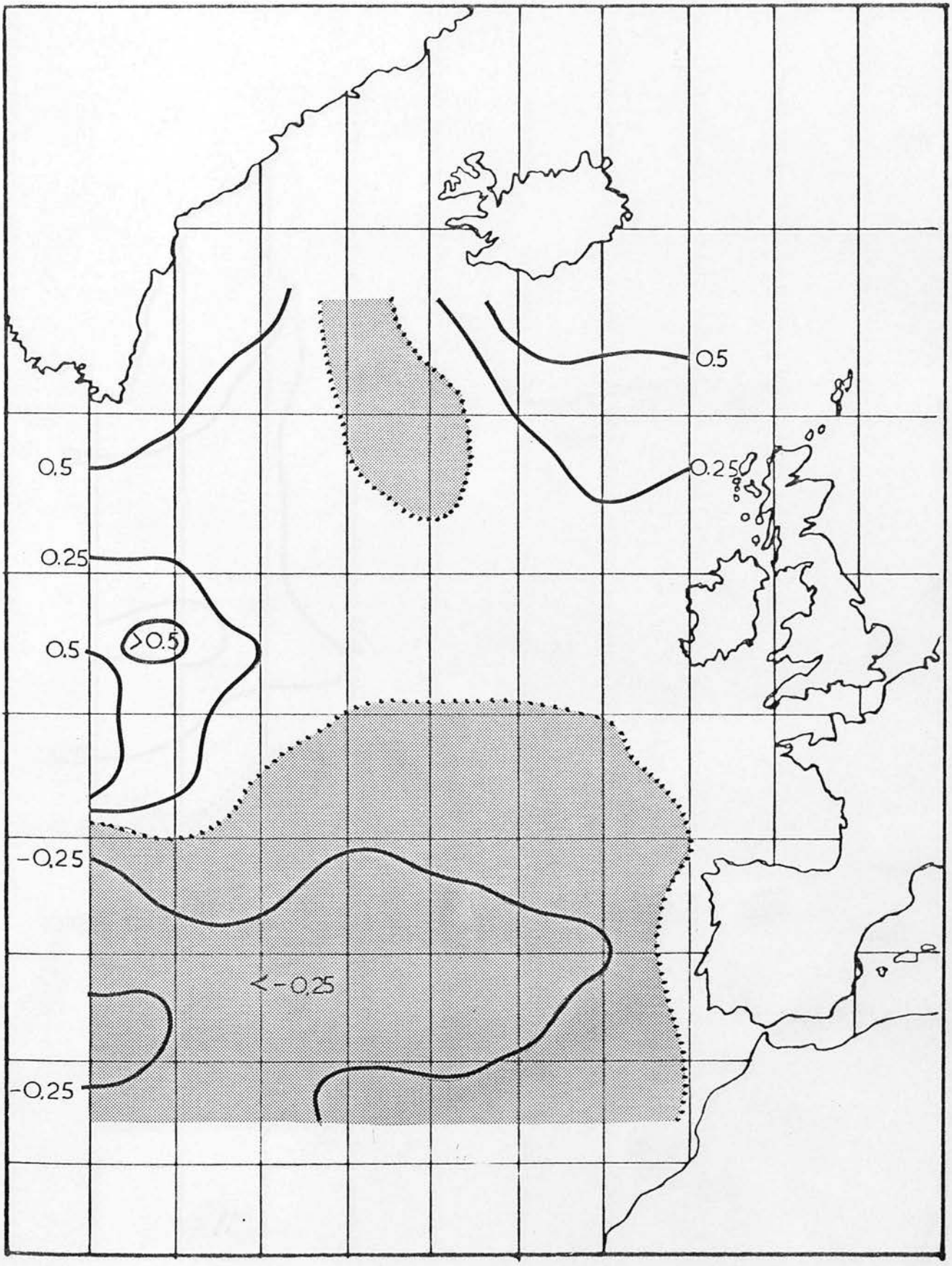

FIGURE 5.5t SEA TEMPERATURE ANOMALY CHANGE, JANUARY-FEBRUARY 1966;
ADVECTION CONTRIBUTION ONLY.

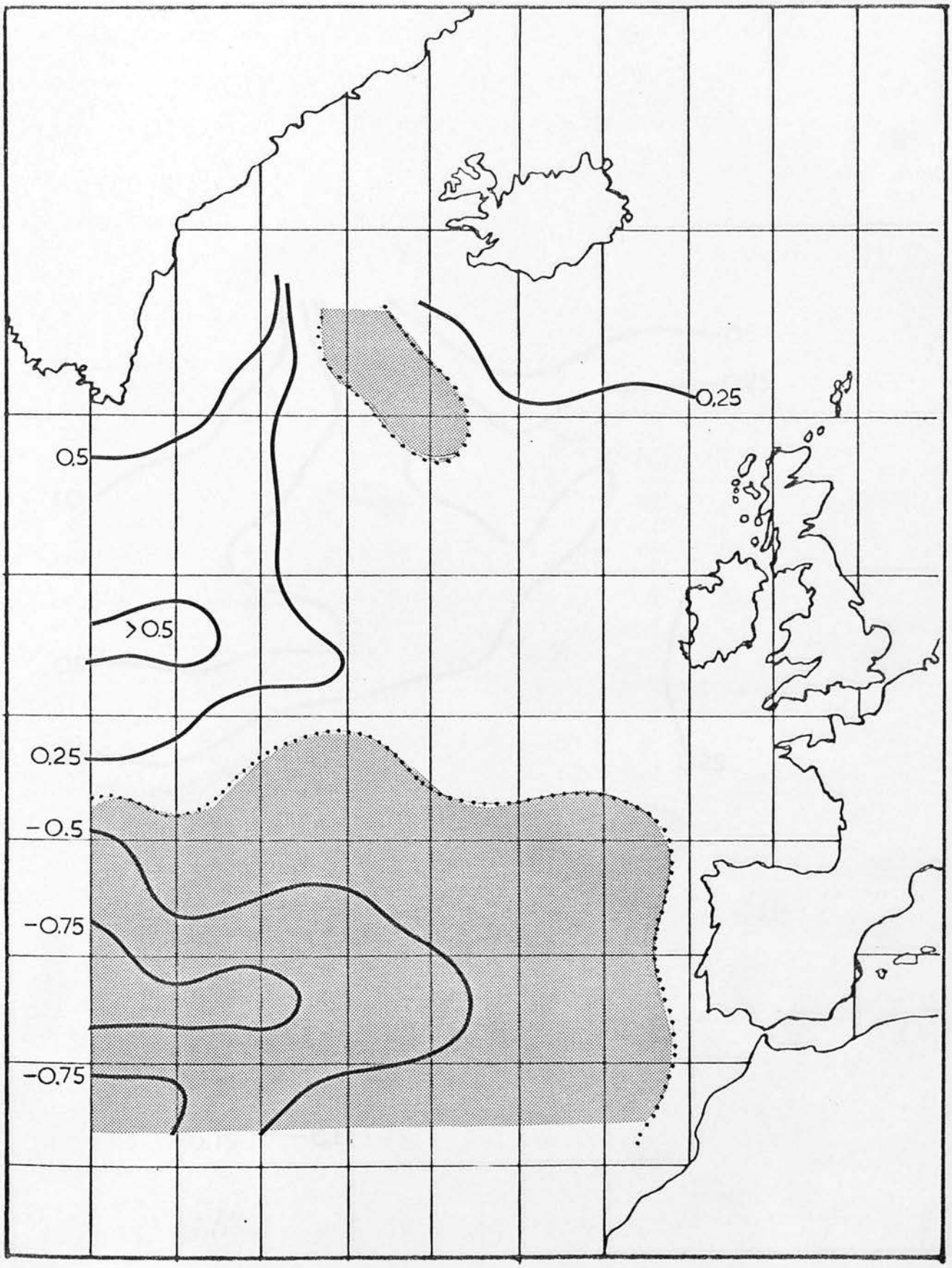

FIGURE 5.5u SEA TEMPERATURE ANOMALY CHANGE, JANUARY-FEBRUARY 1966;
ADVECTION PLUS HEAT LOSS CONTRIBUTIONS.

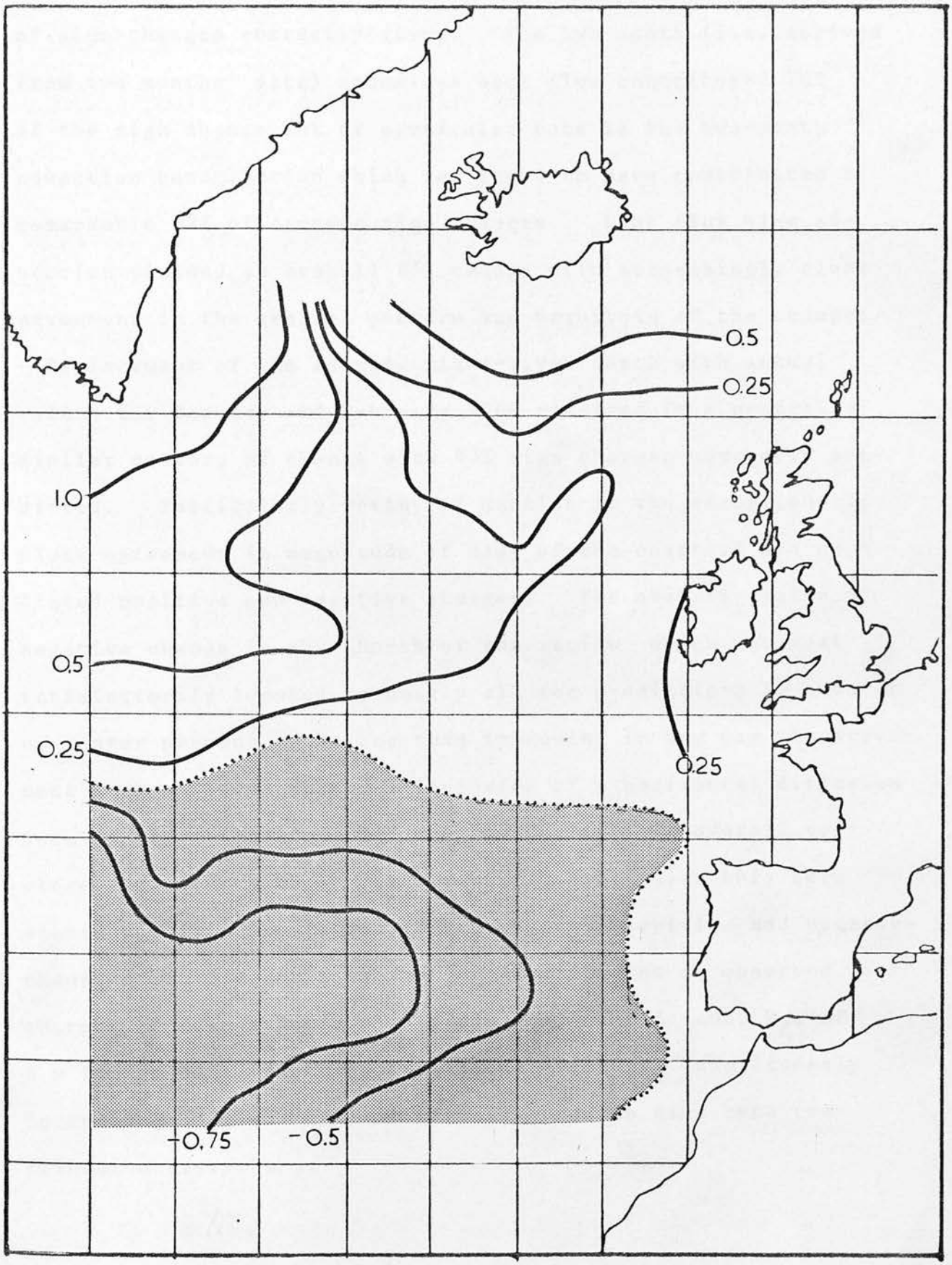

FIGURE 5.5v SEA TEMPERATURE ANOMALY CHANGE, JANUARY-FEBRUARY 1966;
ADVECTION PLUS HEAT LOSS CONTRIBUTIONS
('REAL' MIXED-LAYER DEPTH).

of sign changes correctly given. The two month (i.e. derived from two months' data) anomalous heat flux contributed 70% of the sign change but of particular note is the two-month advection contribution which was found to have contributed a remarkable 82% of correct sign changes. Heat flux plus advection yielded an overall 85% change with surprisingly close agreement in the general pattern and magnitude of the changes.

Replacement of the assumed mixed-layer depth with actual values for January and February 1966 resulted in a generally similar pattern of change with 83% sign changes correctly predicted. Particularly worthy of mention is the exceptionally close agreement in magnitude of many of the observed and predicted positive and negative changes. The overall region of negative change in the North of the region which was most satisfactorily located by nearly all the predictions is however no longer present. Rather than improving in any way the agreement with observed changes, inclusion of a horizontal diffusion term in this case study did much to destroy the overall very close agreement with the observed; in particular this term seemed to give rise to spurious centres of positive and negative change which did not exist on the distribution of observed changes. Adem's horizontal diffusion coefficient, K_H, of 3×10^8 $cm^2 sec^{-1}$ was used in all case studies; the linearly increasing 'Bathen' coefficient was found to give zero contribution everywhere.

5.6 Case Study (2)

5.6.1 Synoptic situation; meteorological and sea temperature distributions.

The months of November and December 1966 again provided a situation of well-defined anomalous atmospheric circulation. In contrast to the pressure distributions of January and February 1966, figures 5.6a and 5.6b show in November and December 1966 anomalous high pressure centres in regions which were dominated by anomalous low centres in the former two months. Generally speaking, therefore, the anomalous circulations of these pairs of months were very different; consequently their effects on the coresponding pre-existing anomalous sea-surface temperature pattern provide an interesting comparison. Once again, no really significant change in the pressure anomaly pattern is observed to have taken place over the two months of November and December 1966, except perhaps for a weakening of the central pressure anomaly and a NW-SE elongation of the anomalous anticyclonic pressure system in December 1966. Characteristic of this case study was the W/NW stress in the north and E/SE stress in the south of the area. Figures 5.6c to 5.6f inclusive exhibit the actual monthly mean wind stress components for November and December 1966 and similarly 5.6g to 5.6j contain the corresponding anomalous wind stress component distributions. Actual monthly mean total surface heat flux for both months are given in figures 5.6k and 5.61 and the equivalent anomalous total heat loss dis-

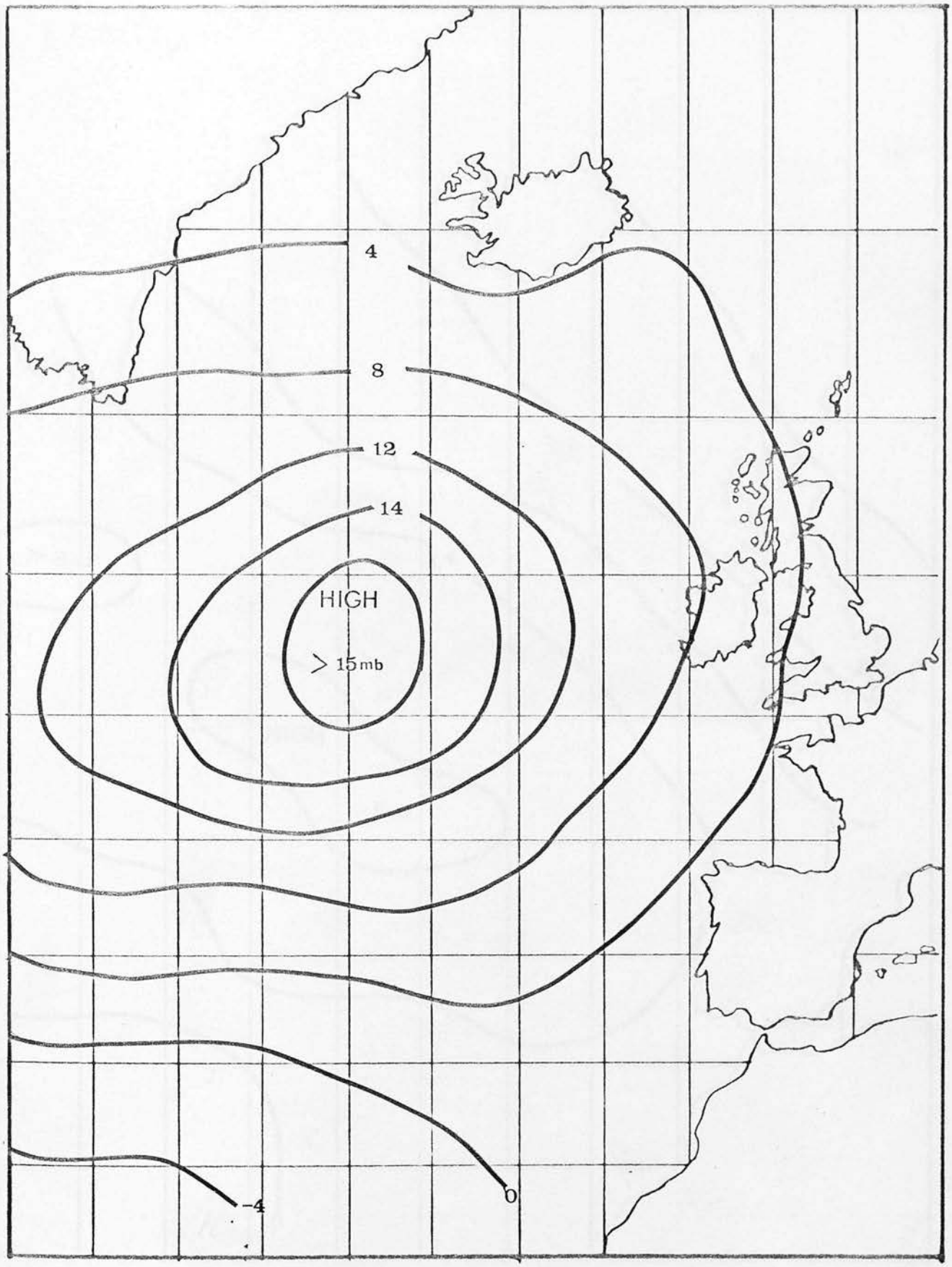

FIGURE 5.6a ANOMALOUS PRESSURE DISTRIBUTION. NOVEMBER 1966

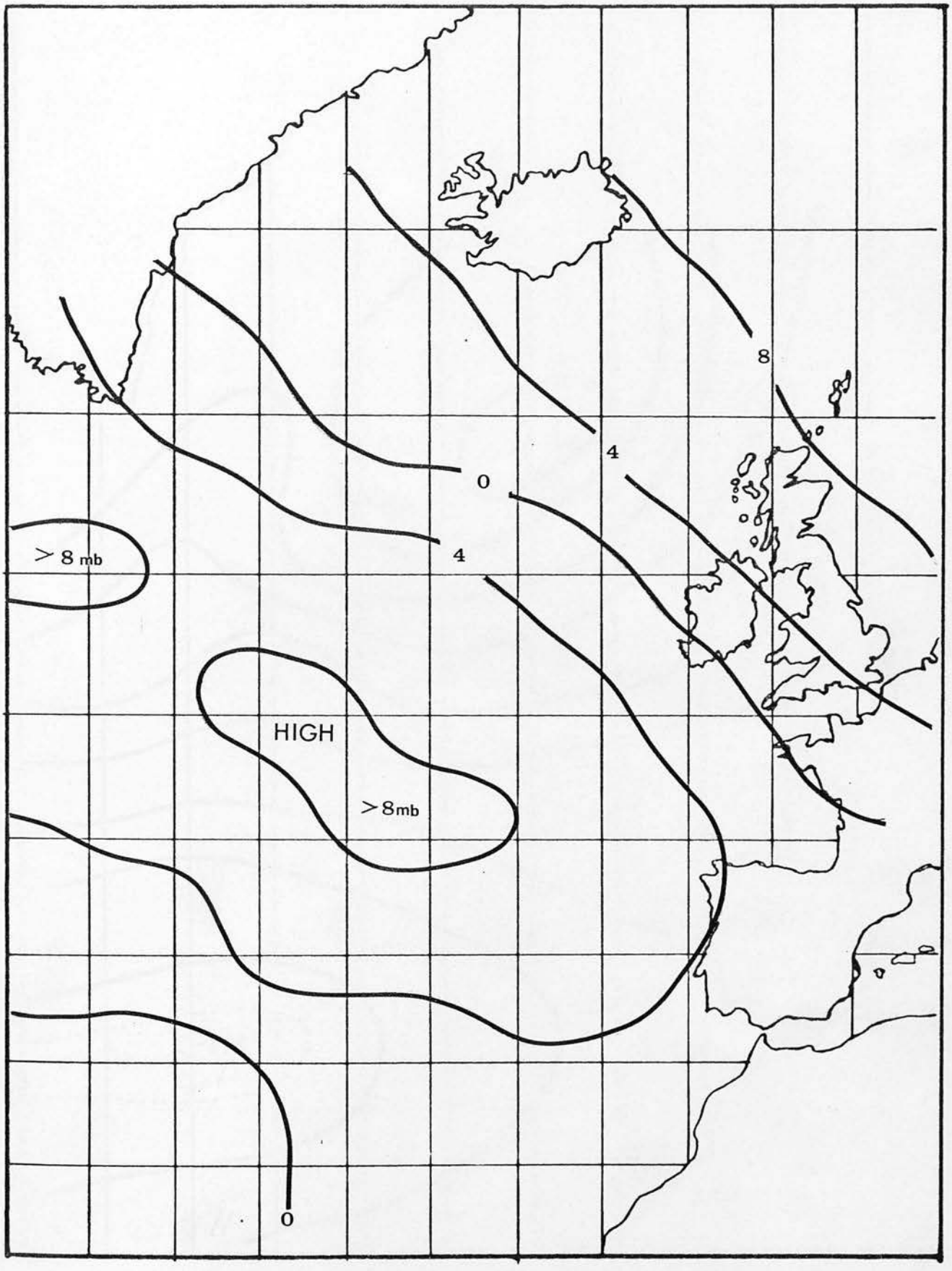

FIGURE 5.6b ANOMALOUS PRESSURE DISTRIBUTION. DECEMBER 1966

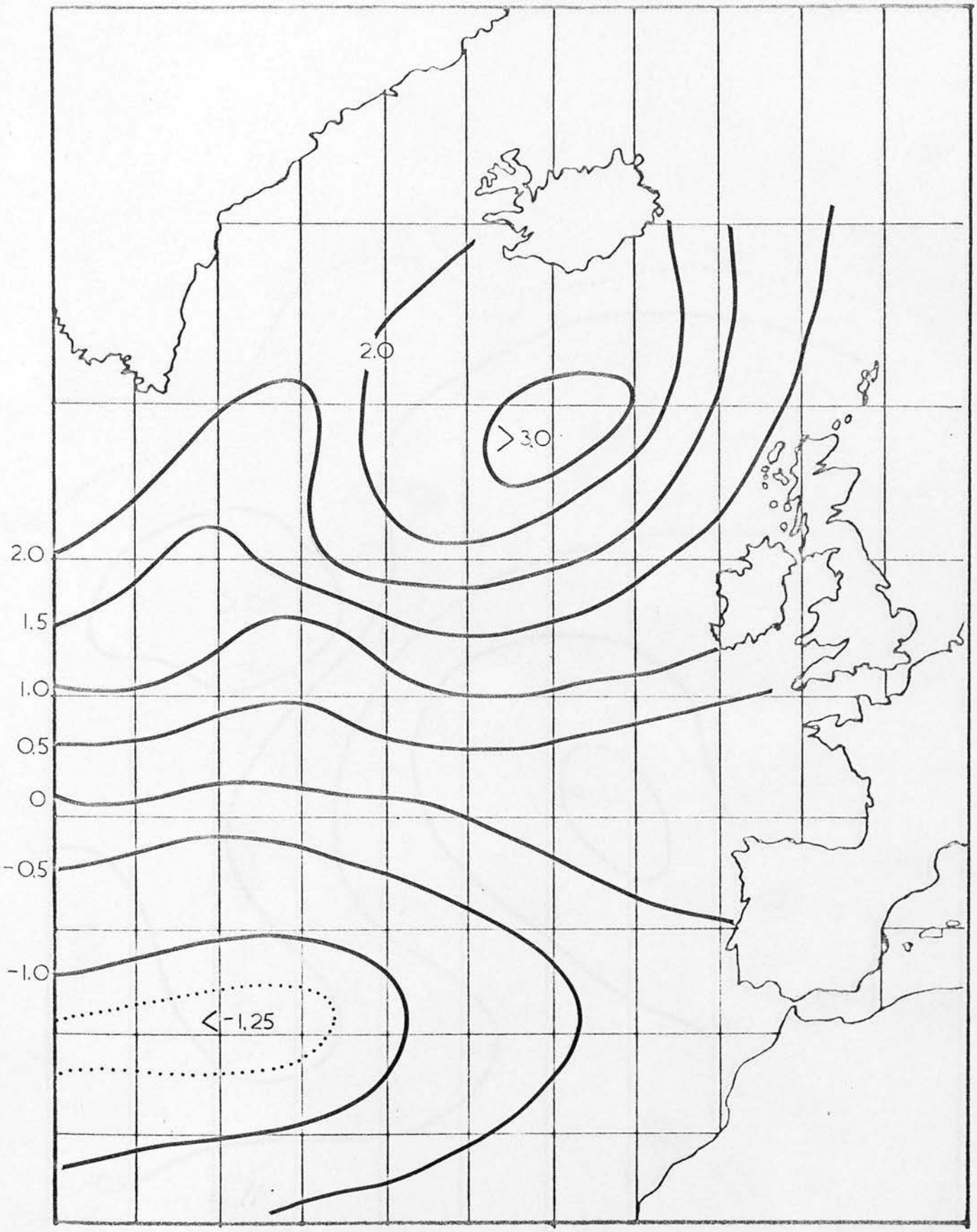

FIGURE 5.6c MEAN ZONAL CPT. WIND STRESS. NOVEMBER 1966

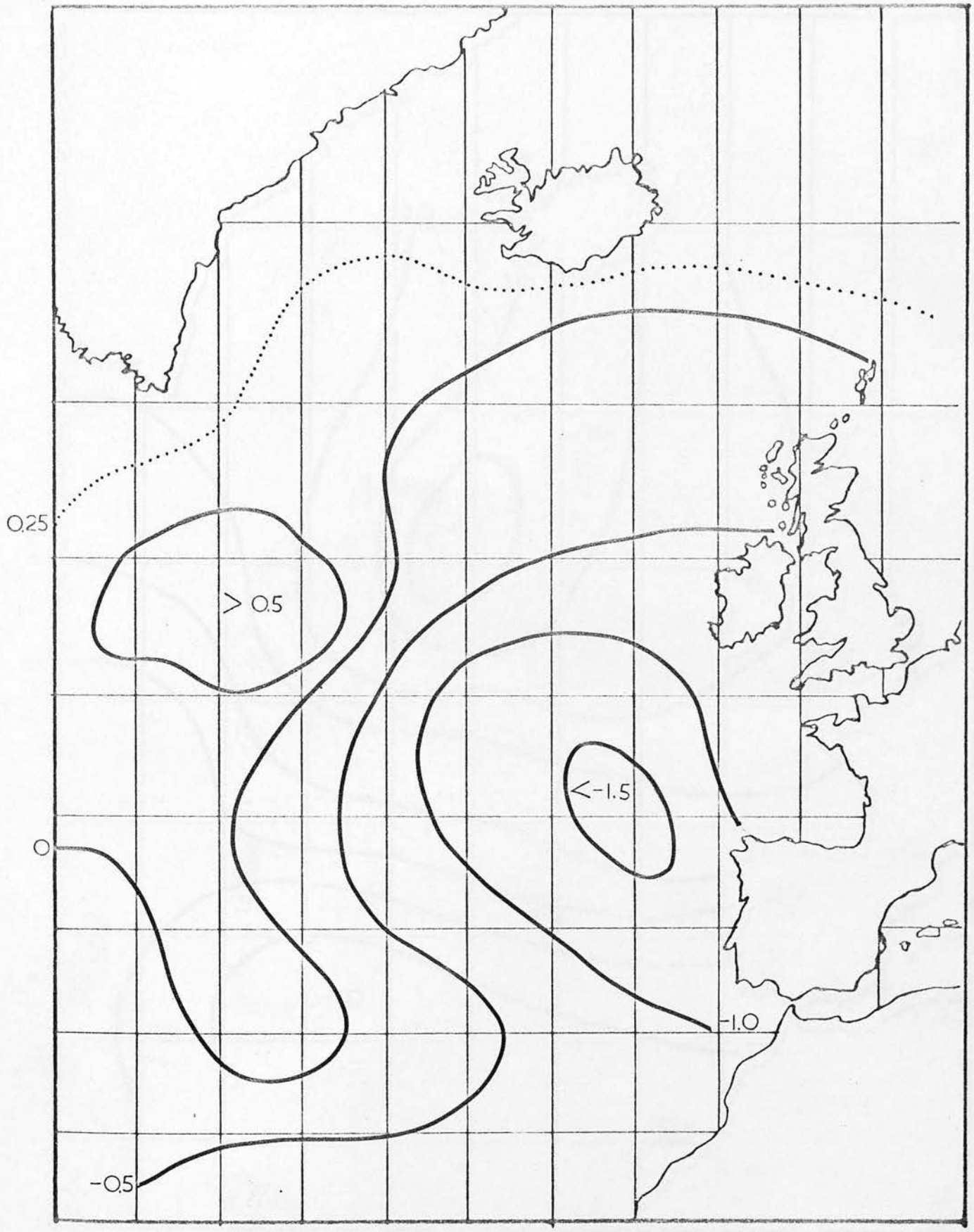

FIGURE 5.6d MEAN MERIDIONAL CPT. WIND STRESS. NOVEMBER 1966

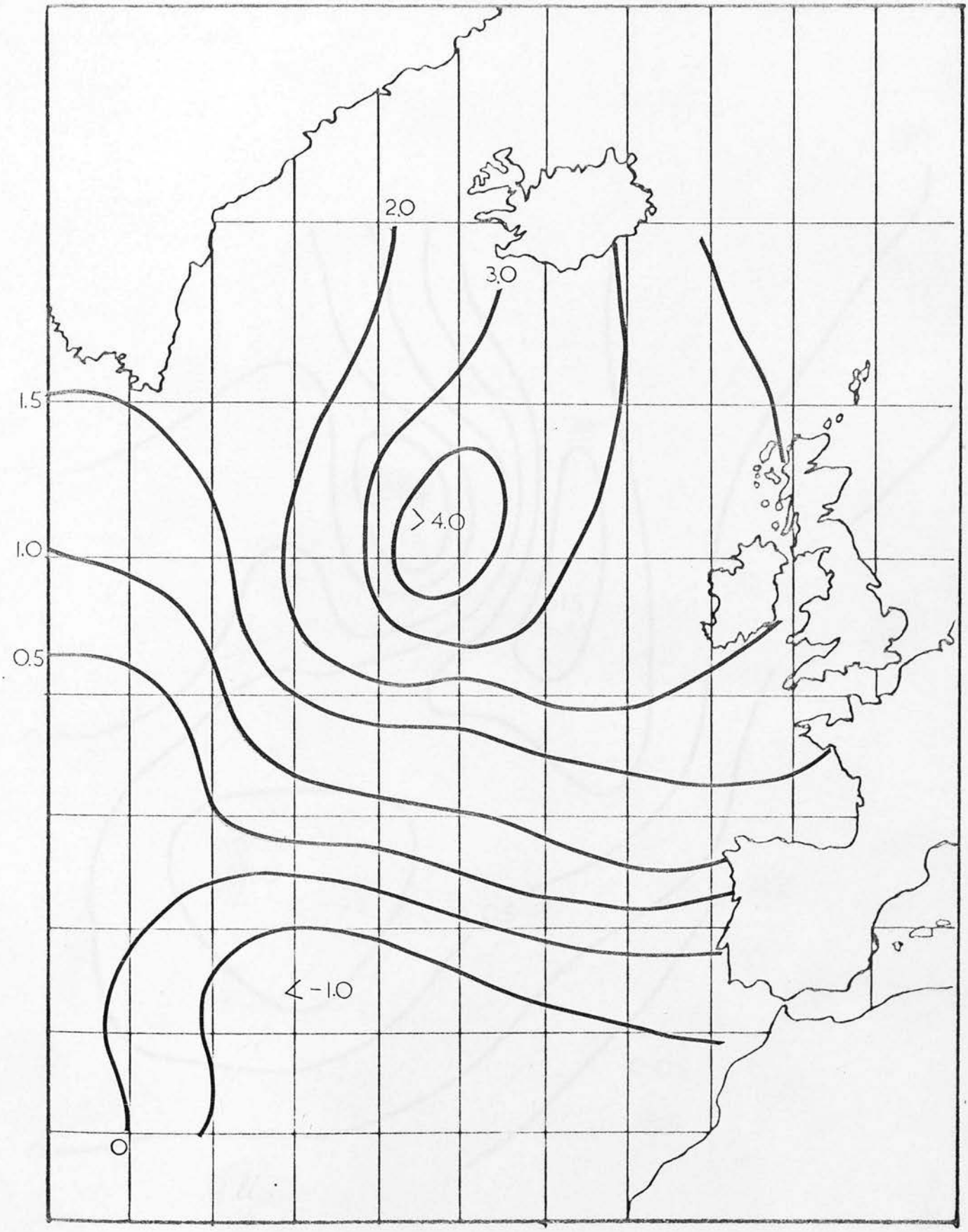

FIGURE 5.6e MEAN ZONAL CPT. WIND STRESS. DECEMBER 1966

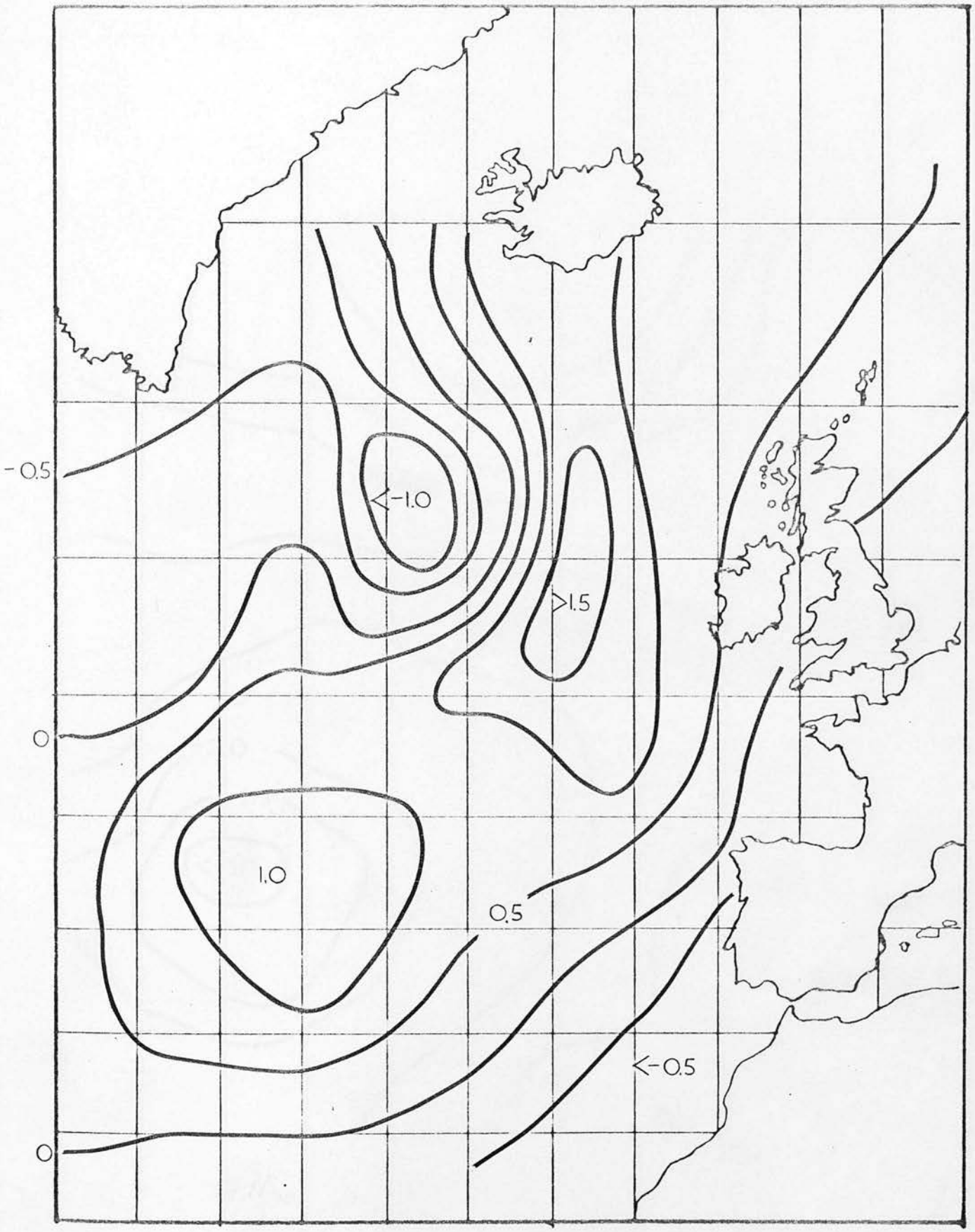

FIGURE 5.6f MEAN MERIDIONAL CPT. WIND STRESS. DECEMBER 1966

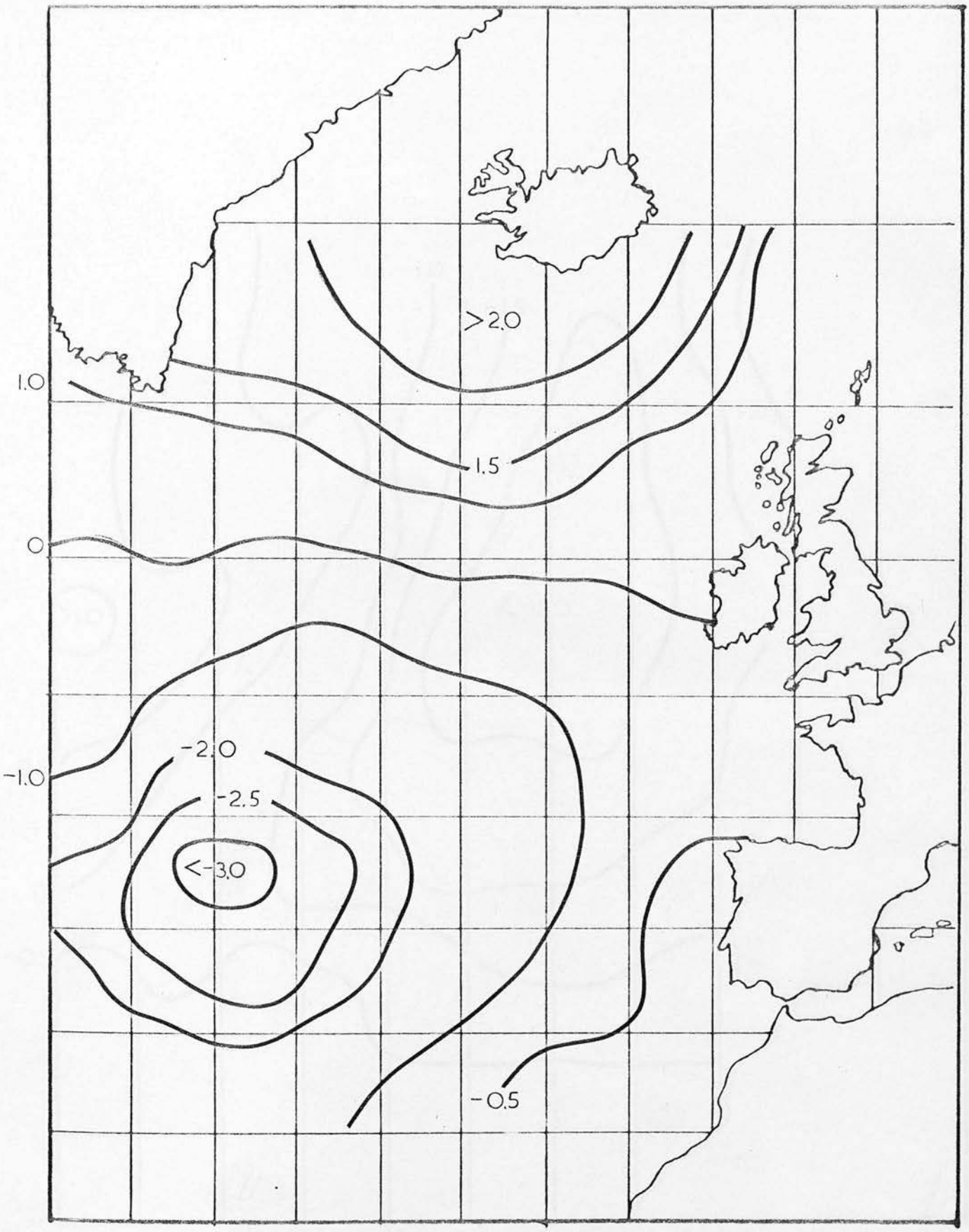

FIGURE 5.6g ZONAL CPT. ANOMALOUS WIND STRESS. NOVEMBER 1966

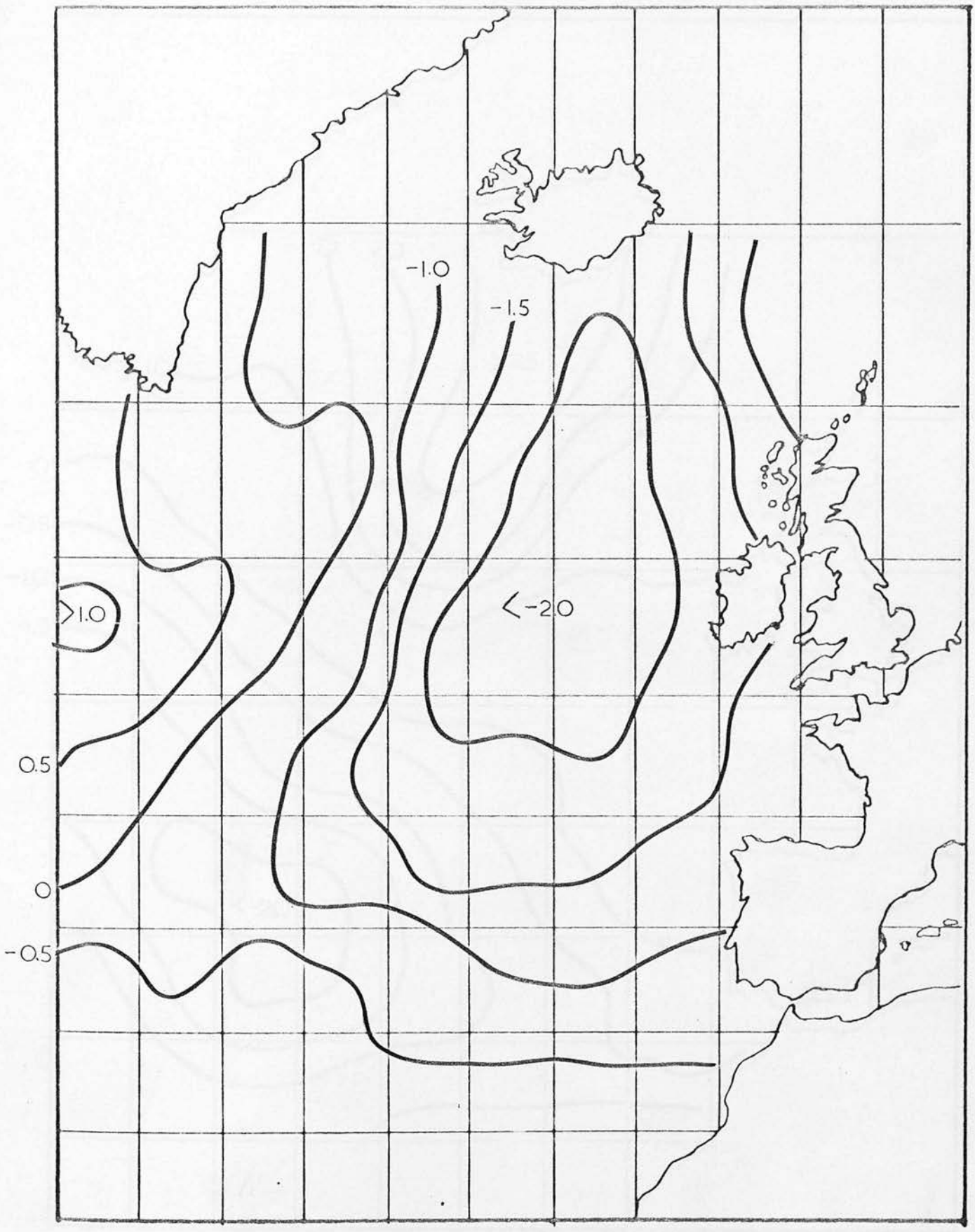

FIGURE 5.6h MERIDIONAL CPT. ANOMALOUS WIND STRESS. NOVEMBER 1966

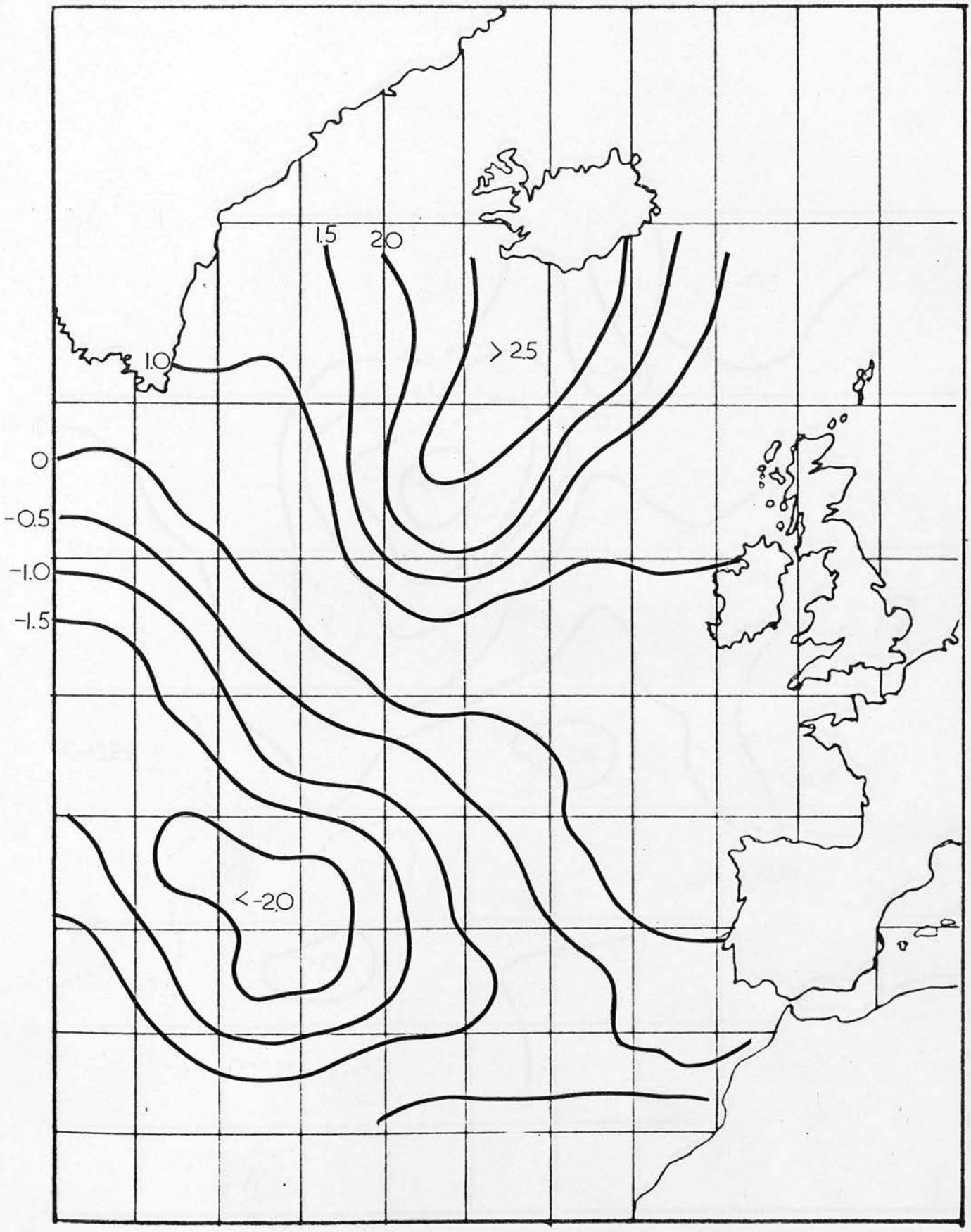

FIGURE 5.6i ZONAL CPT. ANOMALOUS WIND STRESS. DECEMBER 1966.

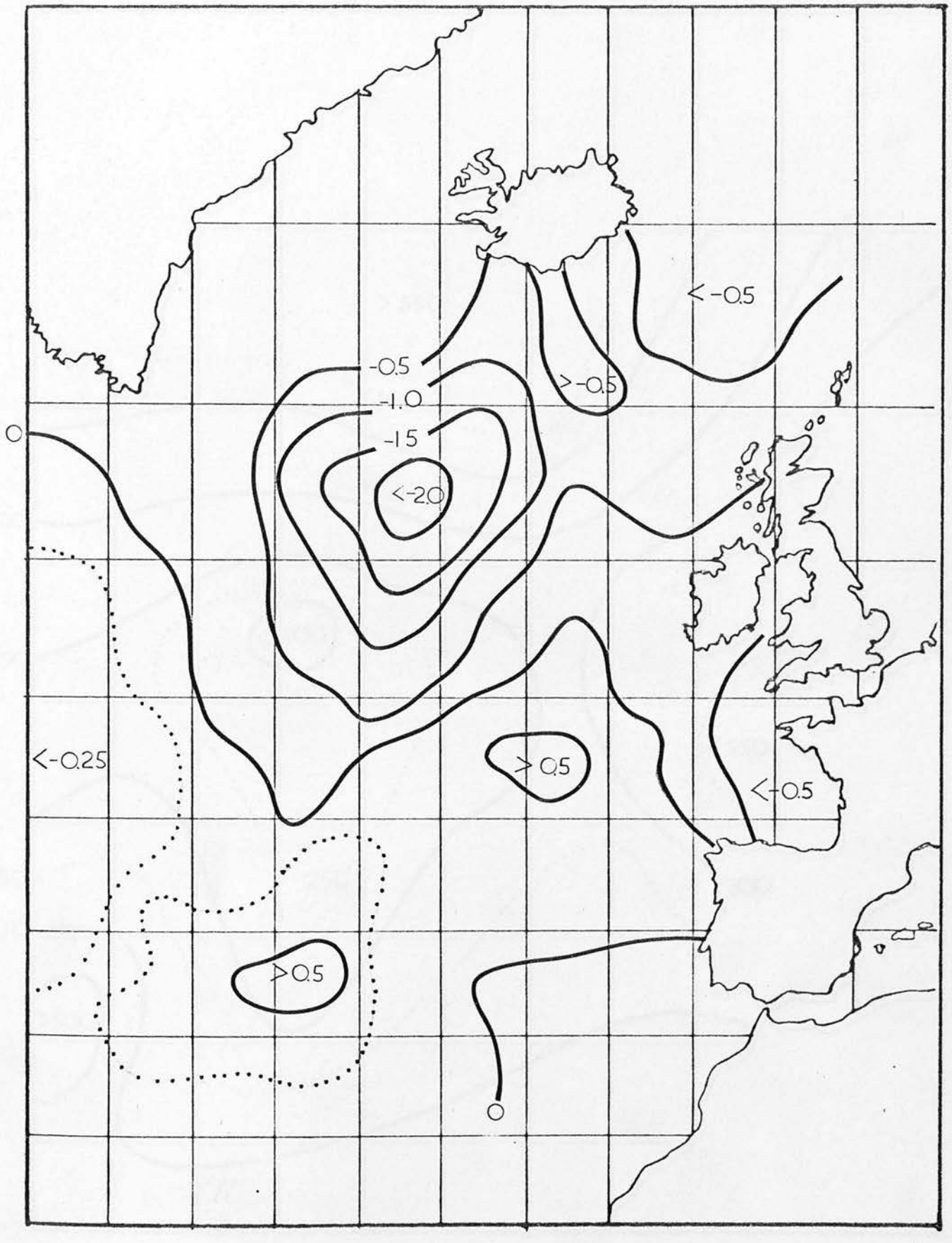

FIGURE 5.6j MERIDIONAL CPT. ANOMALOUS WIND STRESS. DECEMBER 1966.

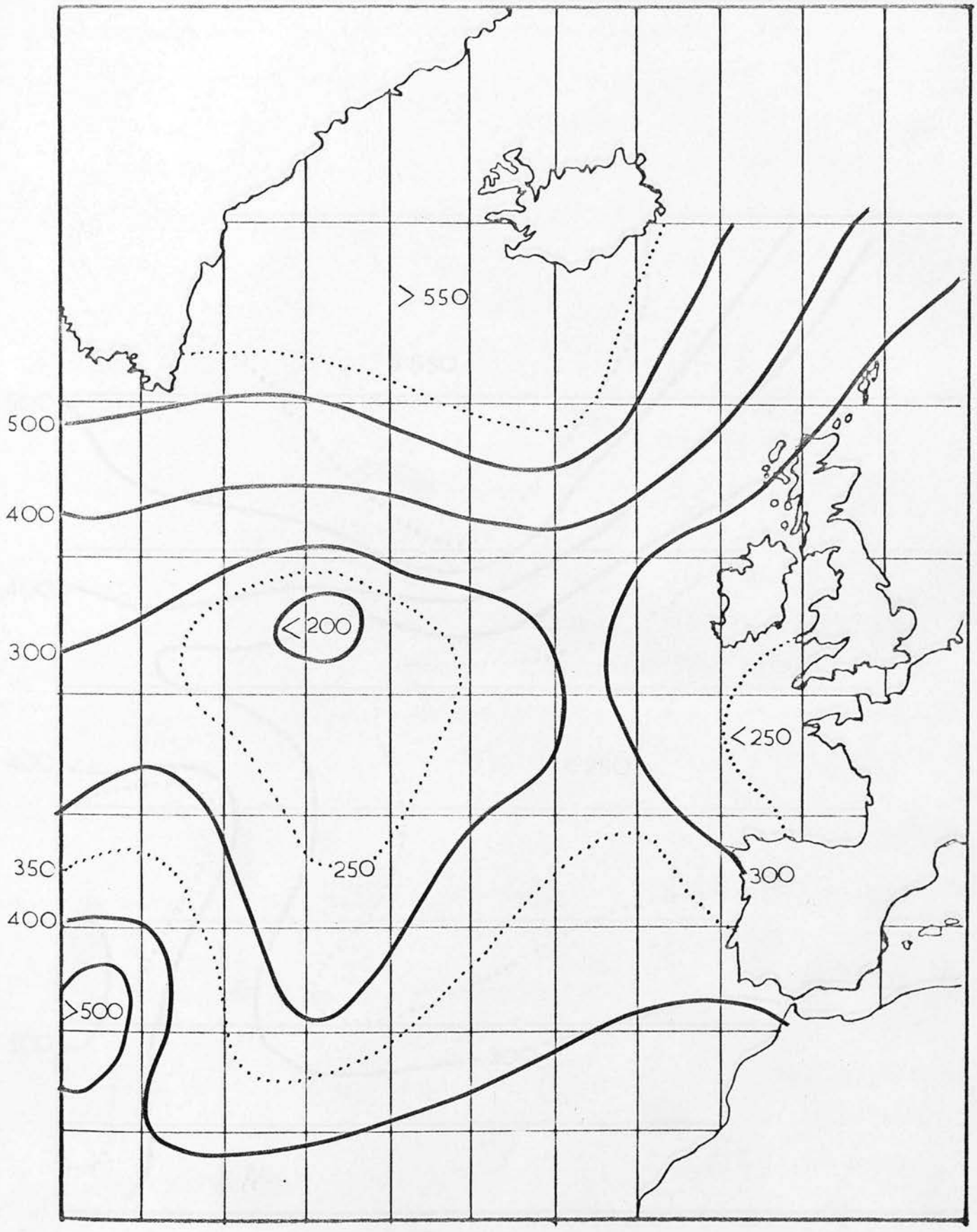

FIGURE 5.6k TOTAL SURFACE HEAT FLUX. NOVEMBER 1966

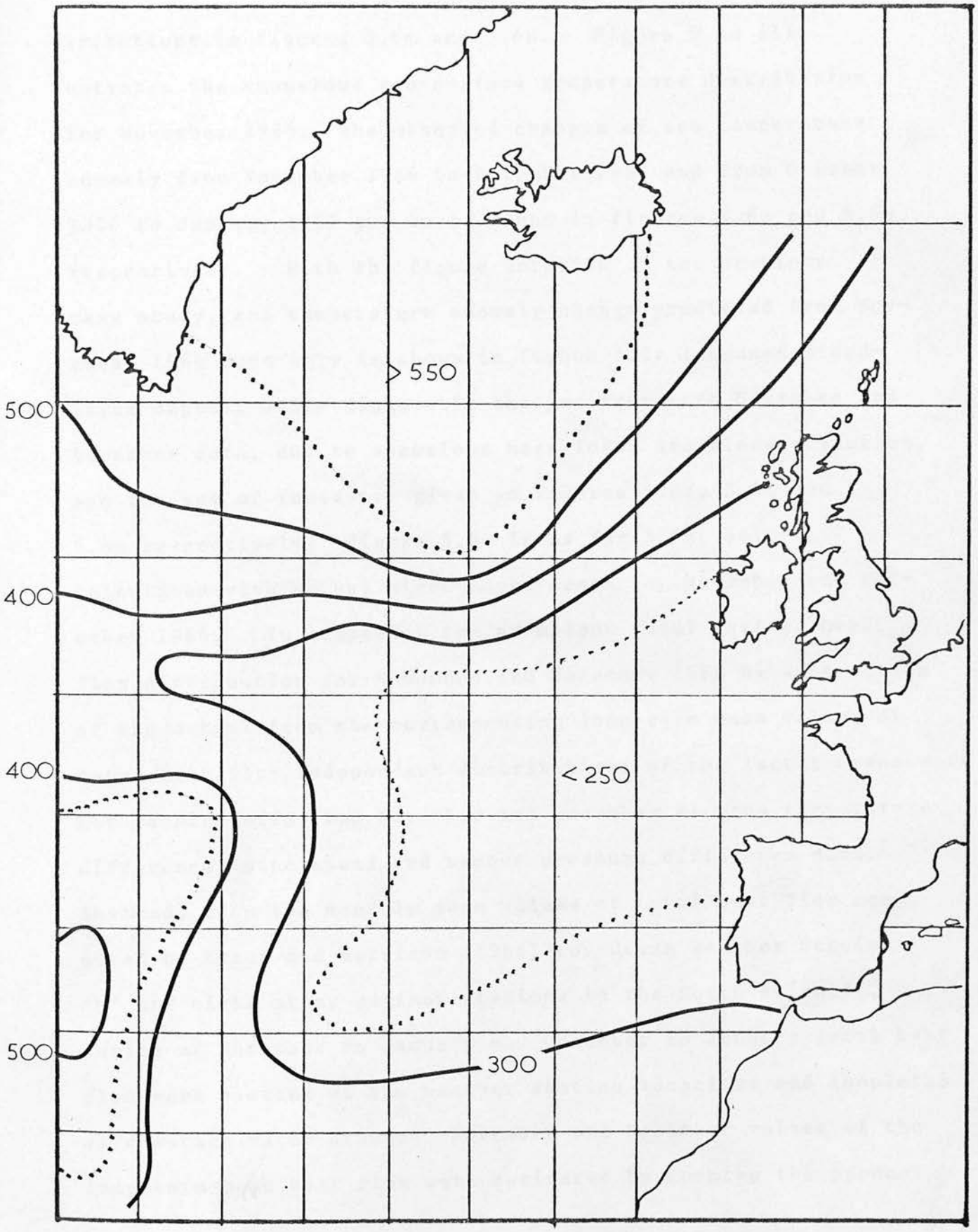

FIGURE 5.61 TOTAL SURFACE HEAT FLUX. DECEMBER 1966.

tributions in figures 5.6m and 5.6n. Figure 5.6o illustrates the anomalous sea-surface temperature distribution for November 1966; the observed changes of sea temperature anomaly from November 1966 to December 1966 and from October 1966 to January 1967 are to be found in figures 5.6p and 5.6q respectively. With the figure notation of the previous case study, sea temperature anomaly change predicted from November 1966 data only is shown in figure 5.6r (assumed mixed-layer depth), while diagnostic changes from both November and December data, due to anomalous heat loss, anomalous advection, and the sum of these are given in figures 5.6s, 5.6t and 5.6u respectively; figure 5.6v is as for 5.6u, only calculated with actual mixed-layer depth for November and December 1966. In computing the anomalous total surface heat flux distribution for November and December 1966 by subtraction of the actual from the corresponding long-term mean values of total heat flux, independent distributions of the latter means were not recalculated from November and December air-sea temperature difference, wind speed, and vapour pressure difference data. Instead, from the monthly mean values of total heat flux computed by Kraus and Morrison (1966) for Ocean Weather Station 'M' and eight other weather stations in the North Atlantic, ratios of November to January and December to January total heat flux were plotted at the weather station locations and isopleths of constant ratio drawn. November and December values of the long-term mean heat flux were estimated by forming the product

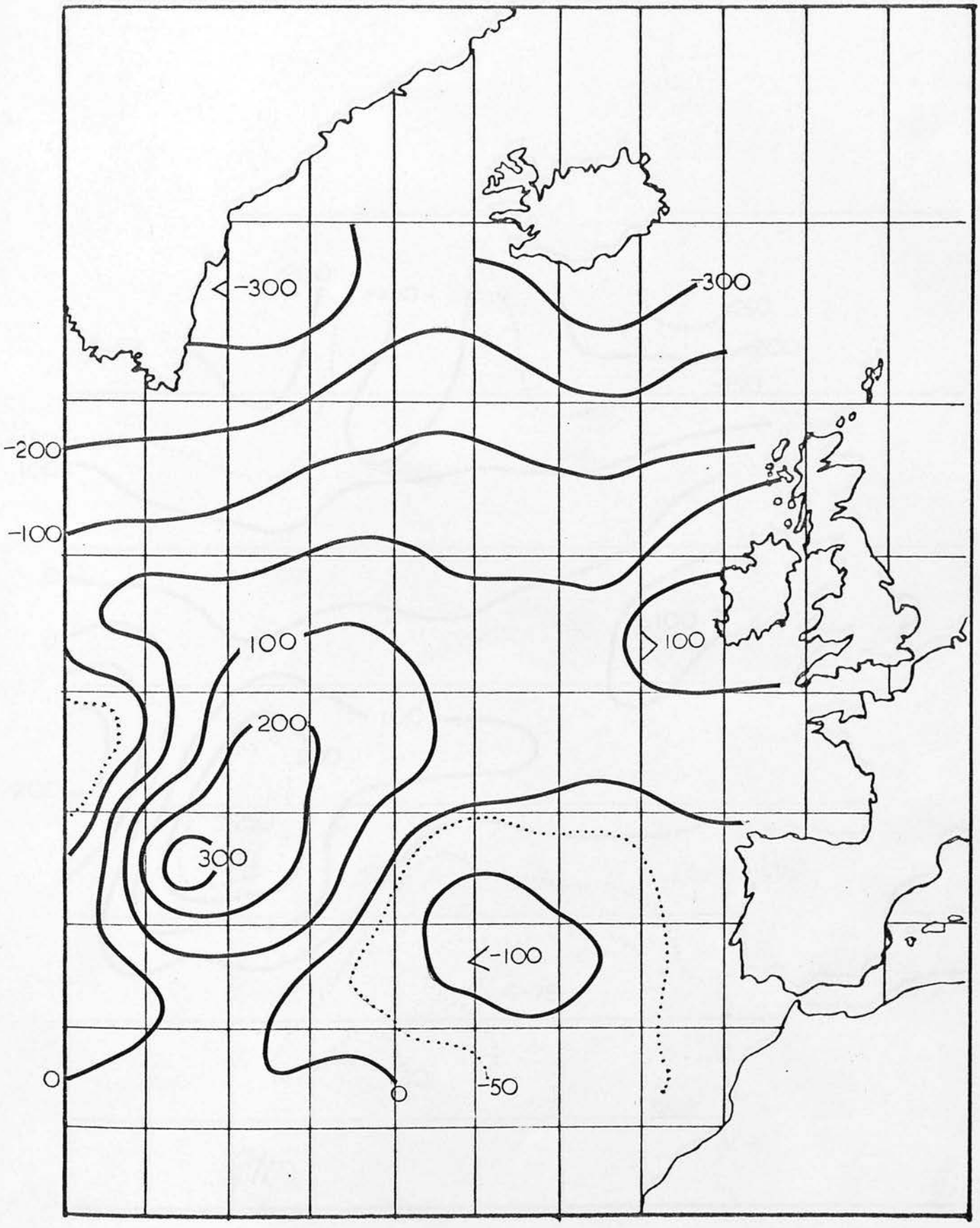

FIGURE 5.6m ANOMALOUS TOTAL SURFACE HEAT FLUX. NOVEMBER 1966

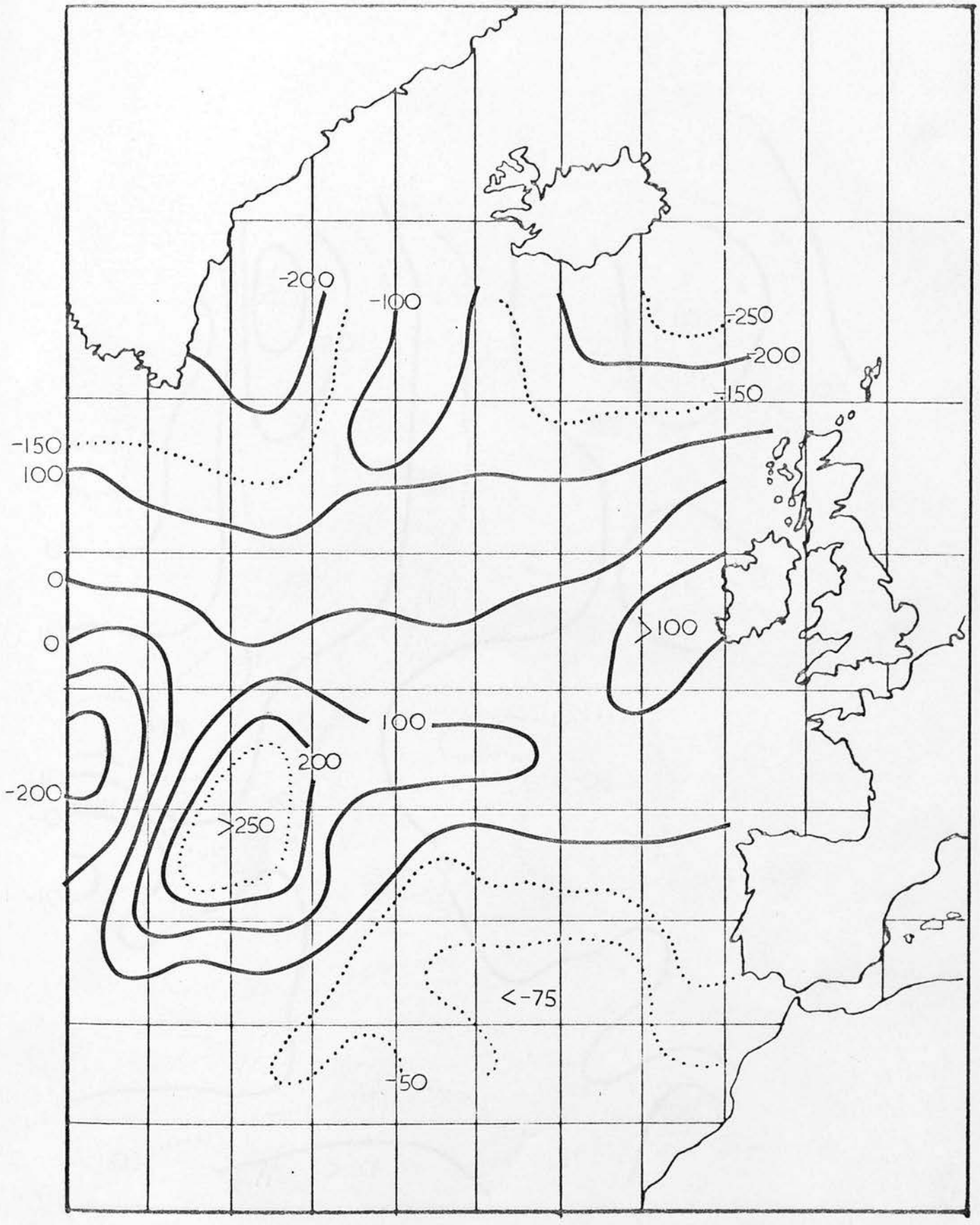

FIGURE 5.6n ANOMALOUS TOTAL SURFACE HEAT FLUX. DECEMBER 1966

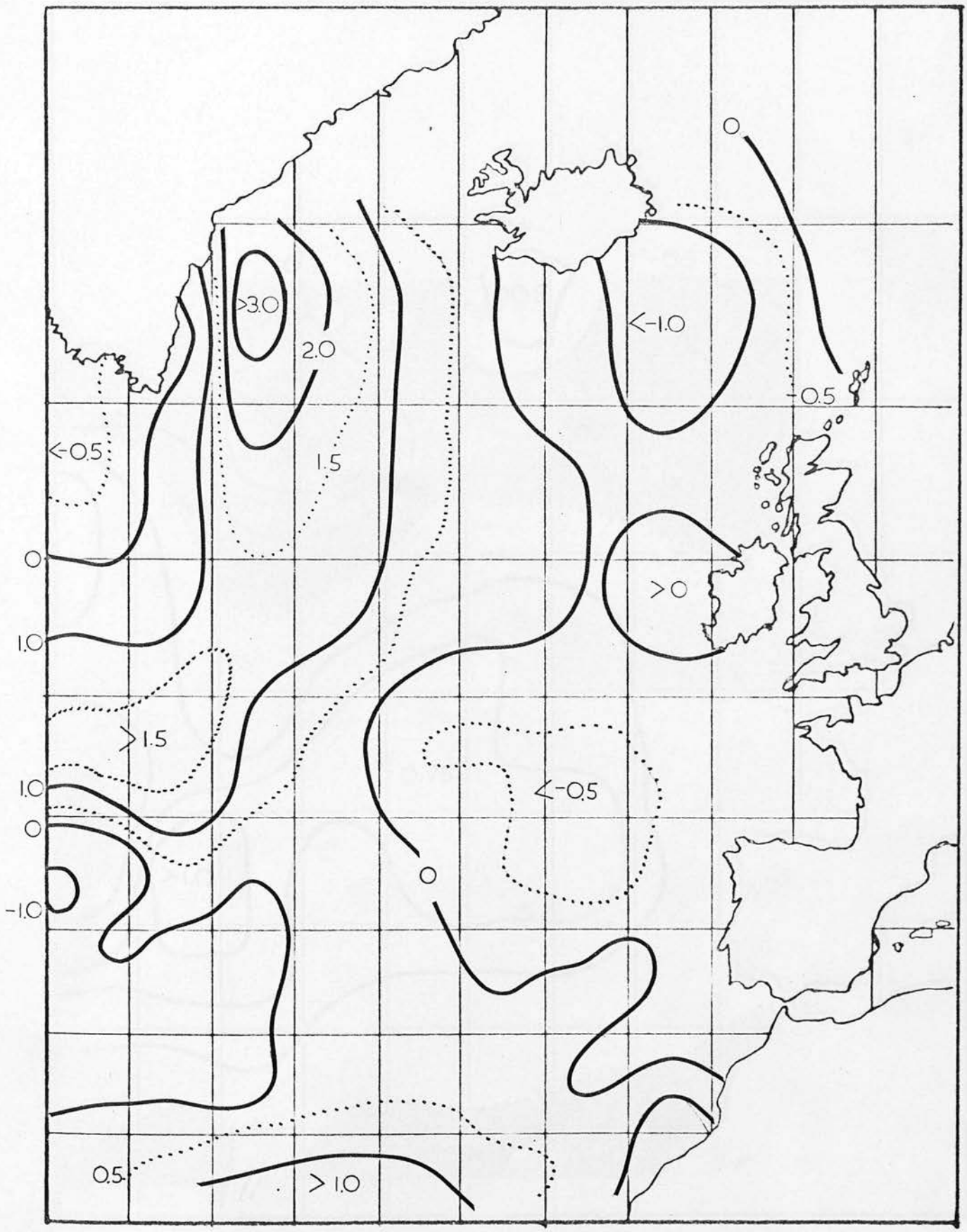

FIGURE 5.6o ANOMALOUS SEA-SURFACE TEMPERATURE DISTRIBUTION. NOVEMBER 1966.

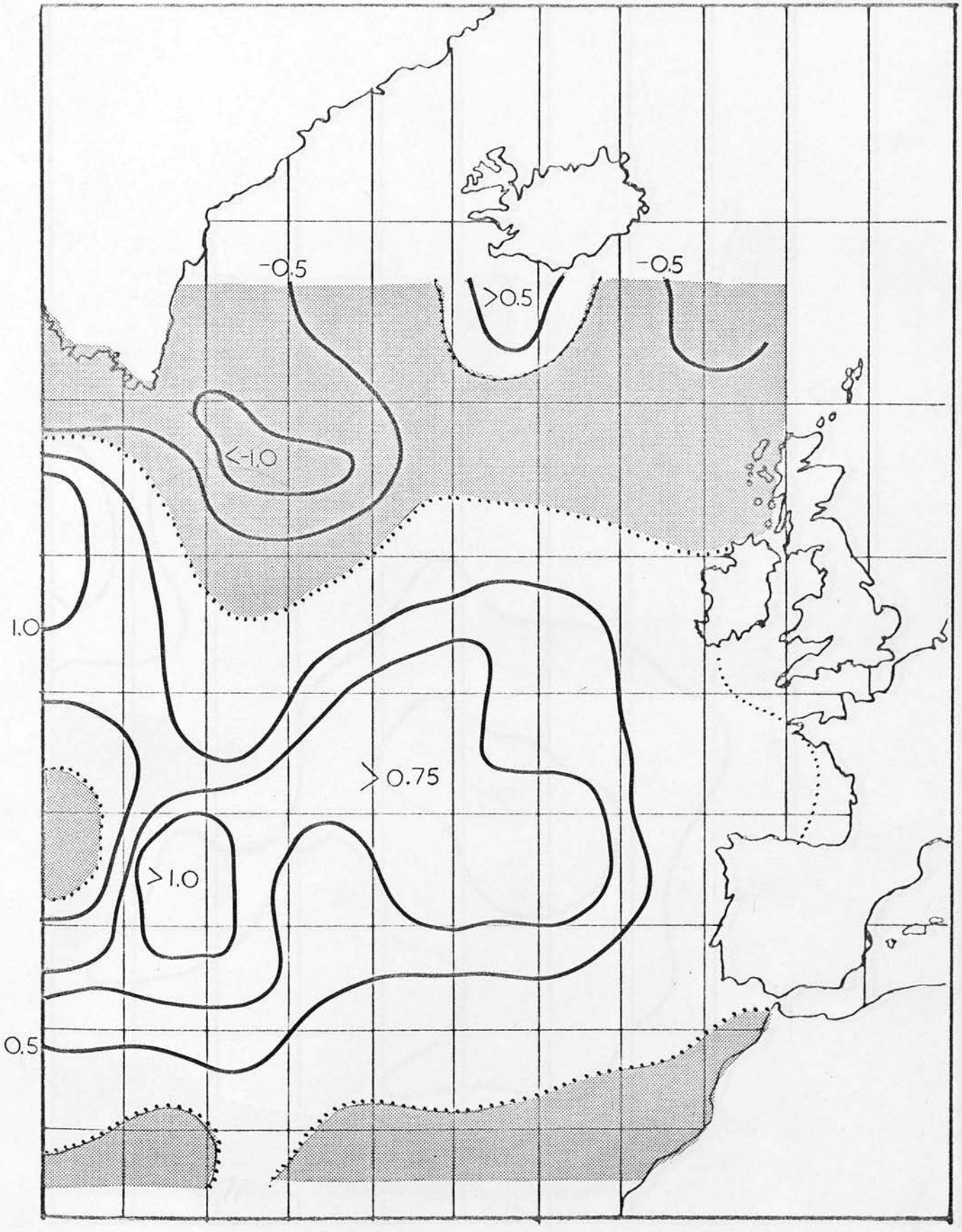

FIGURE 5.6p OBSERVED SEA-SURFACE TEMPERATURE ANOMALY CHANGE,
NOVEMBER - DECEMBER 1966.

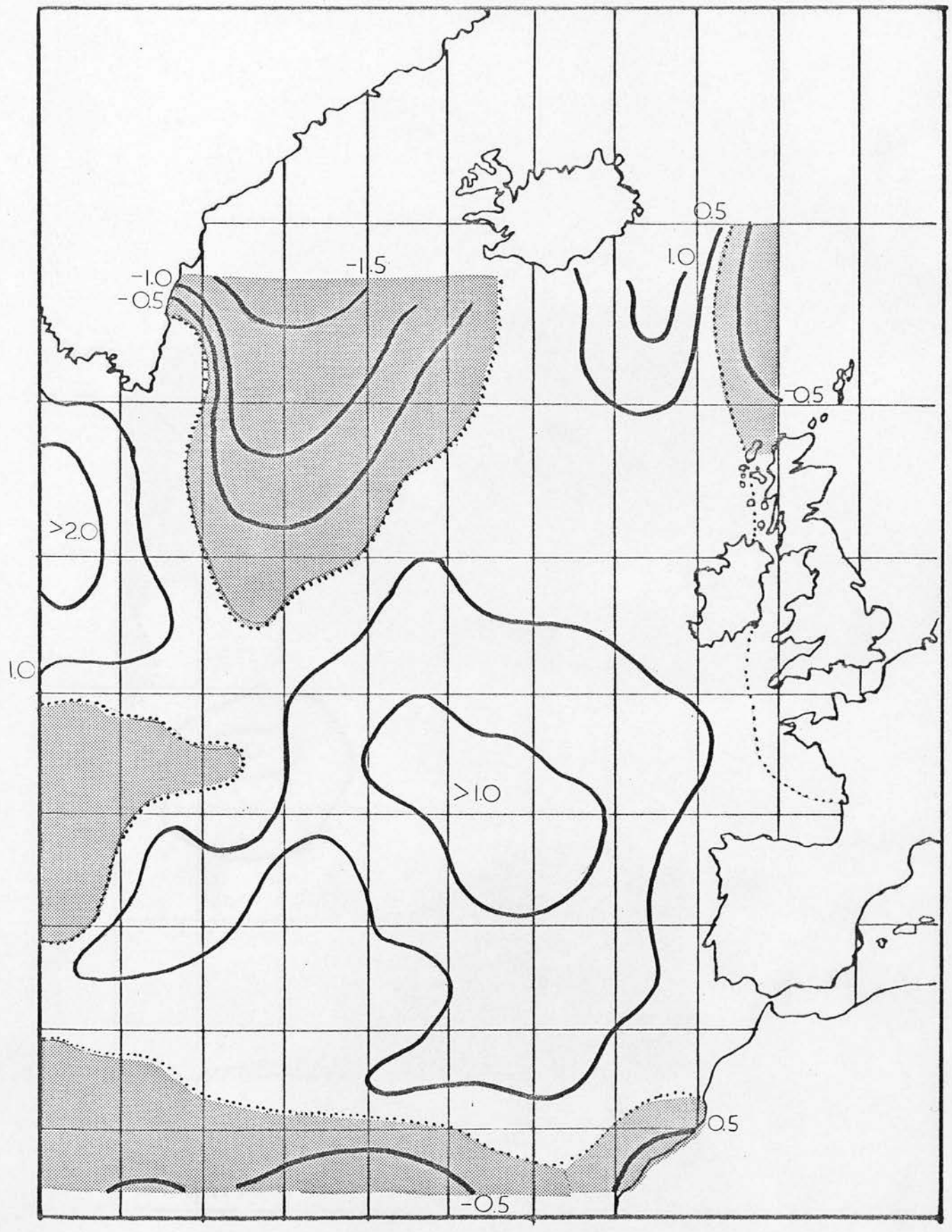

FIGURE 5.6q OBSERVED SEA-SURFACE TEMPERATURE ANOMALY CHANGE,
OCTOBER 1966 - JANUARY 1967.

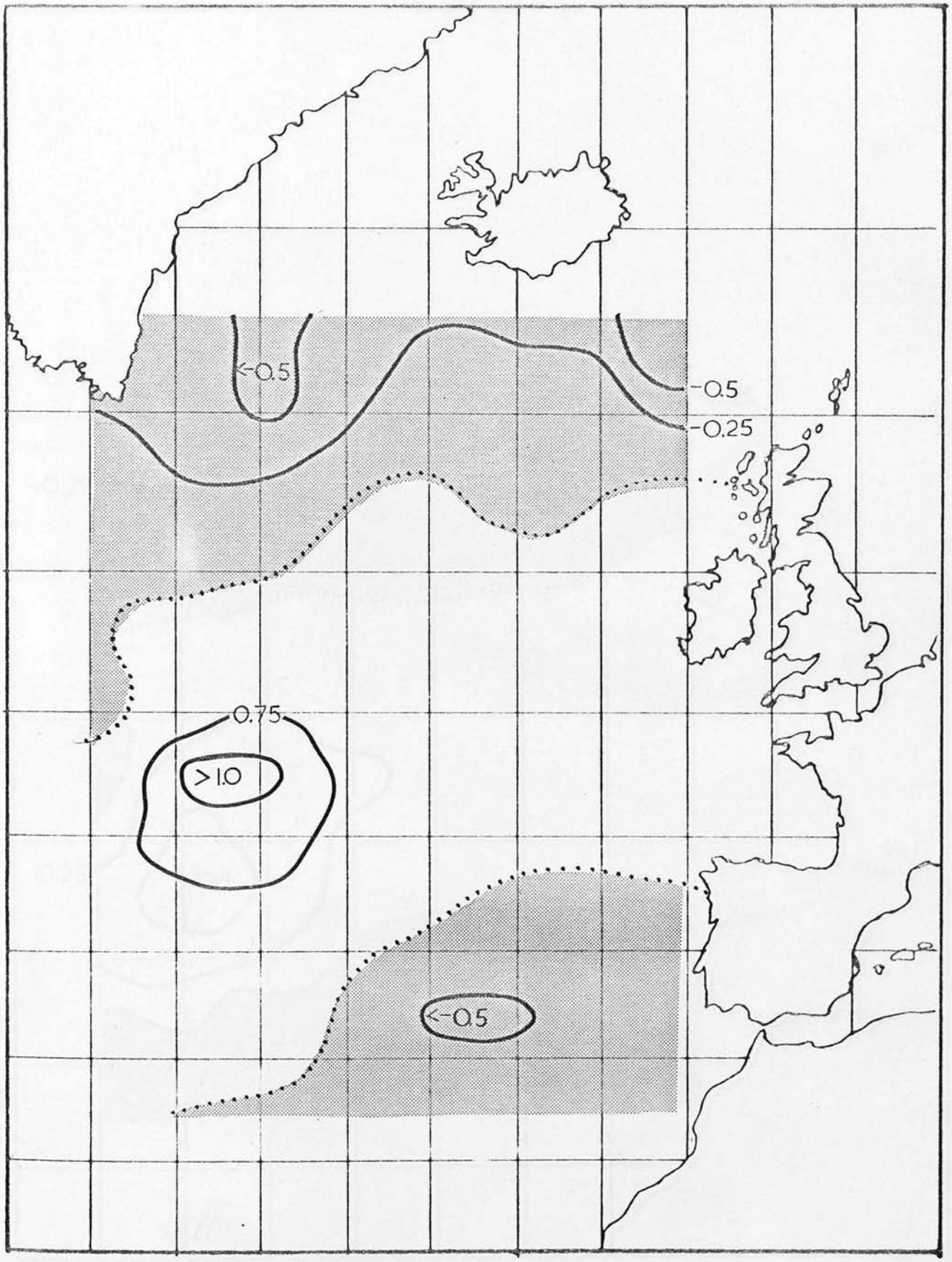

FIGURE 5.6r PREDICTED SEA TEMPERATURE ANOMALY CHANGE, NOVEMBER-DECEMBER 1966; ADVECTION PLUS HEAT LOSS CONTRIBUTIONS.

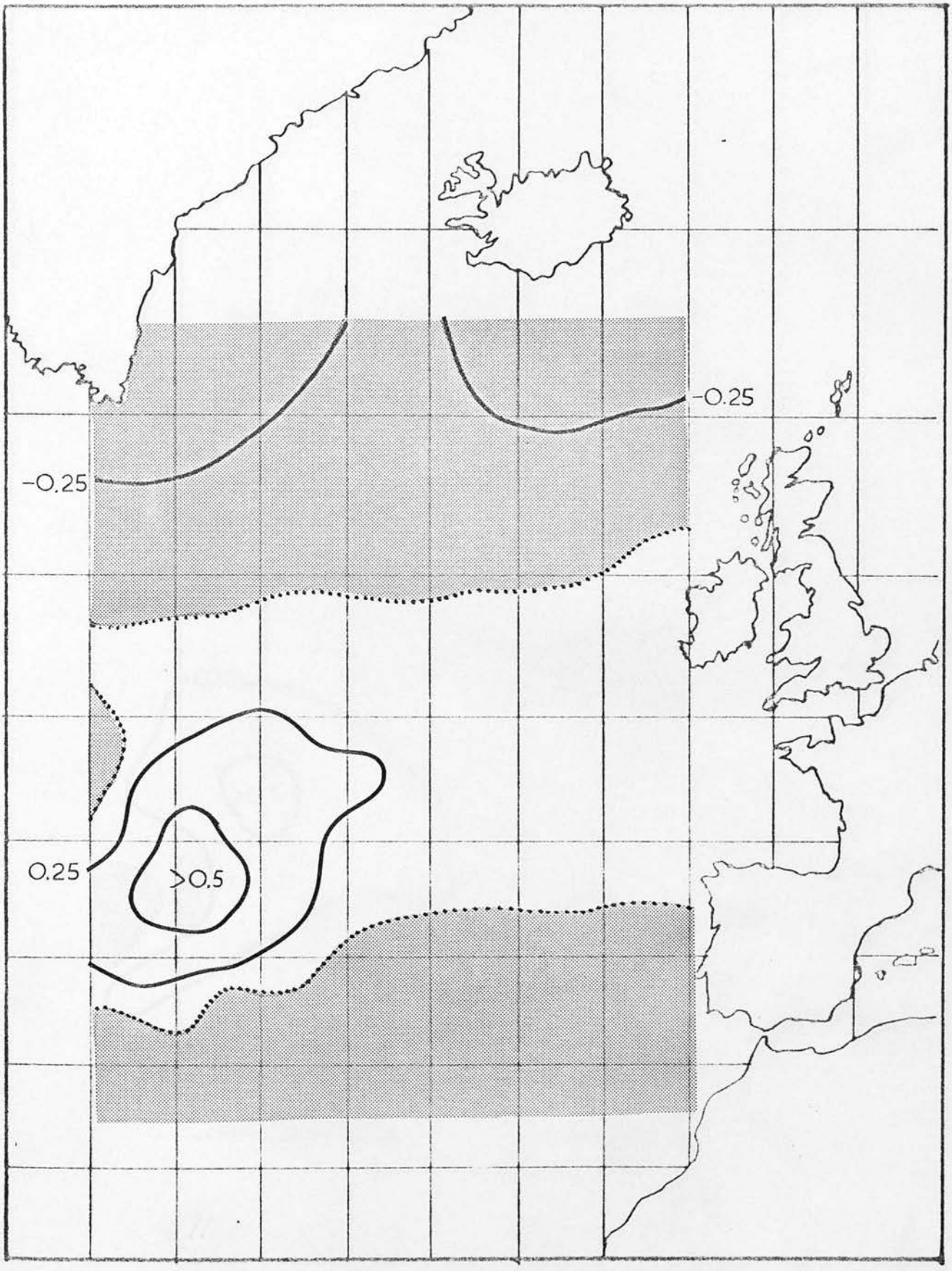

FIGURE 5.6s SEA TEMPERATURE ANOMALY CHANGE, NOVEMBER-DECEMBER 1966;
HEAT LOSS CONTRIBUTION ONLY.

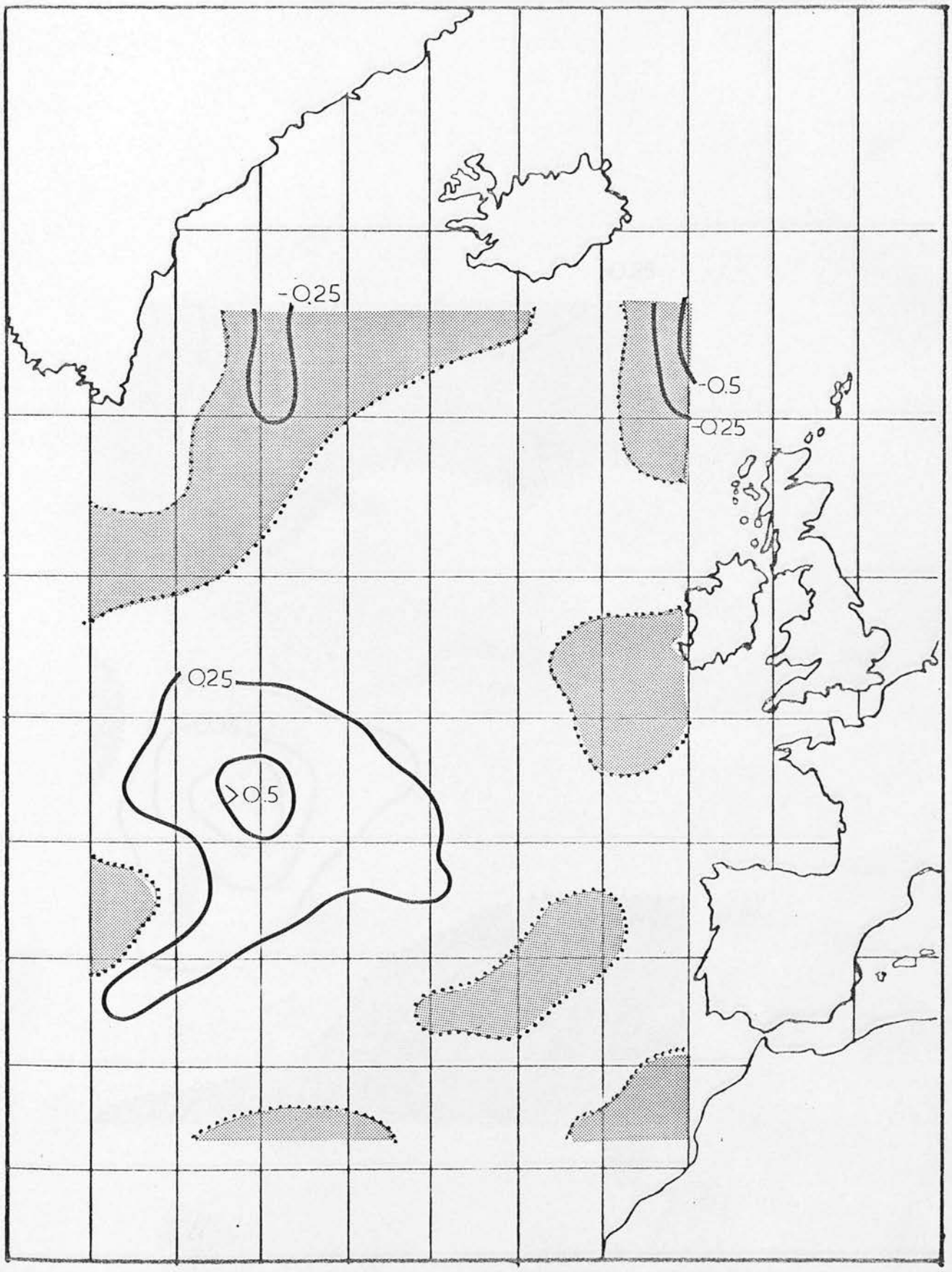

FIGURE 5.6t SEA TEMPERATURE ANOMALY CHANGE, NOVEMBER-DECEMBER 1966;
ADVECTION CONTRIBUTION ONLY.

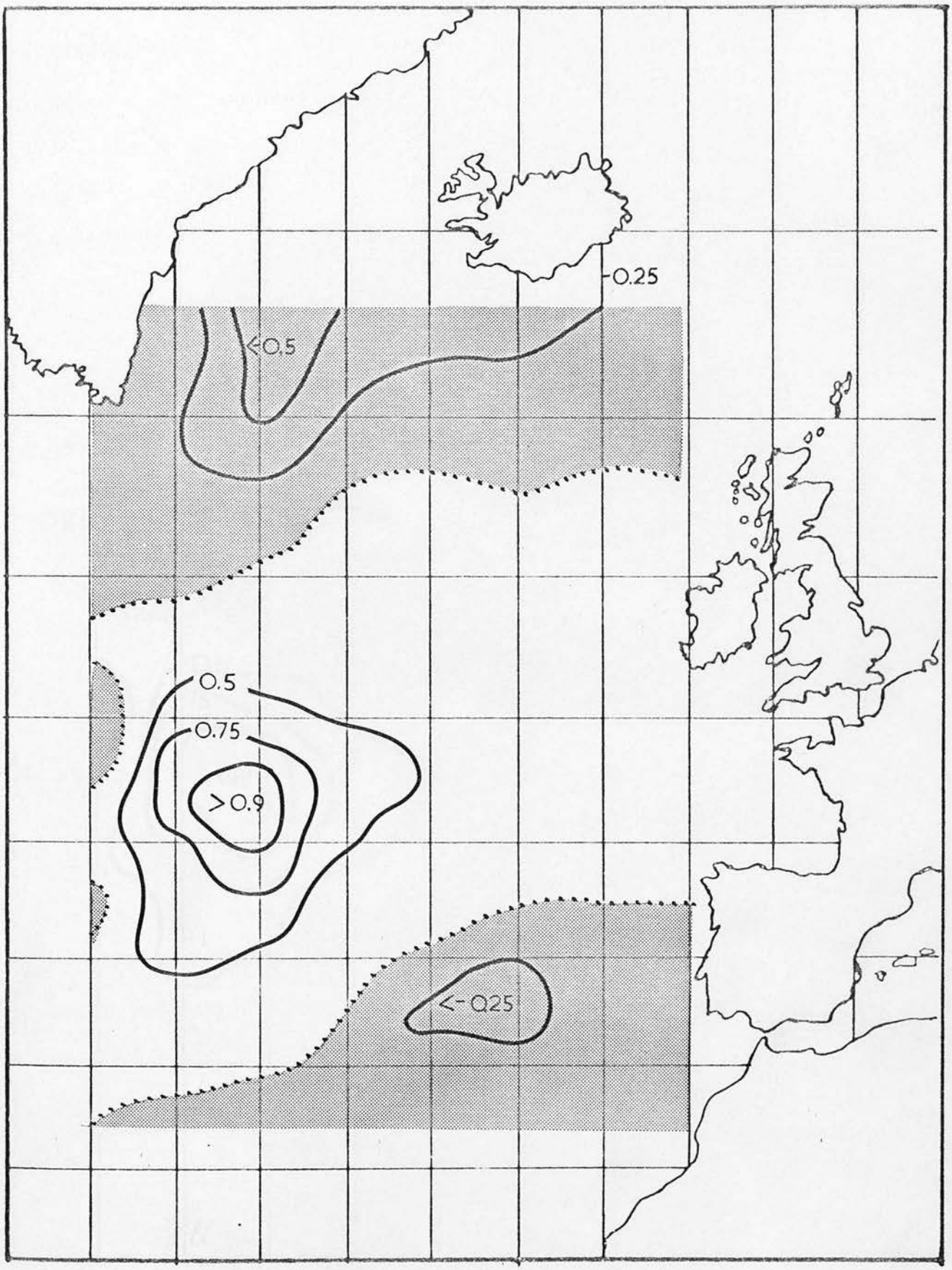

FIGURE 5.6u SEA TEMPERATURE ANOMALY CHANGE, NOVEMBER-DECEMBER 1966;
ADVECTION PLUS HEAT LOSS CONTRIBUTIONS.

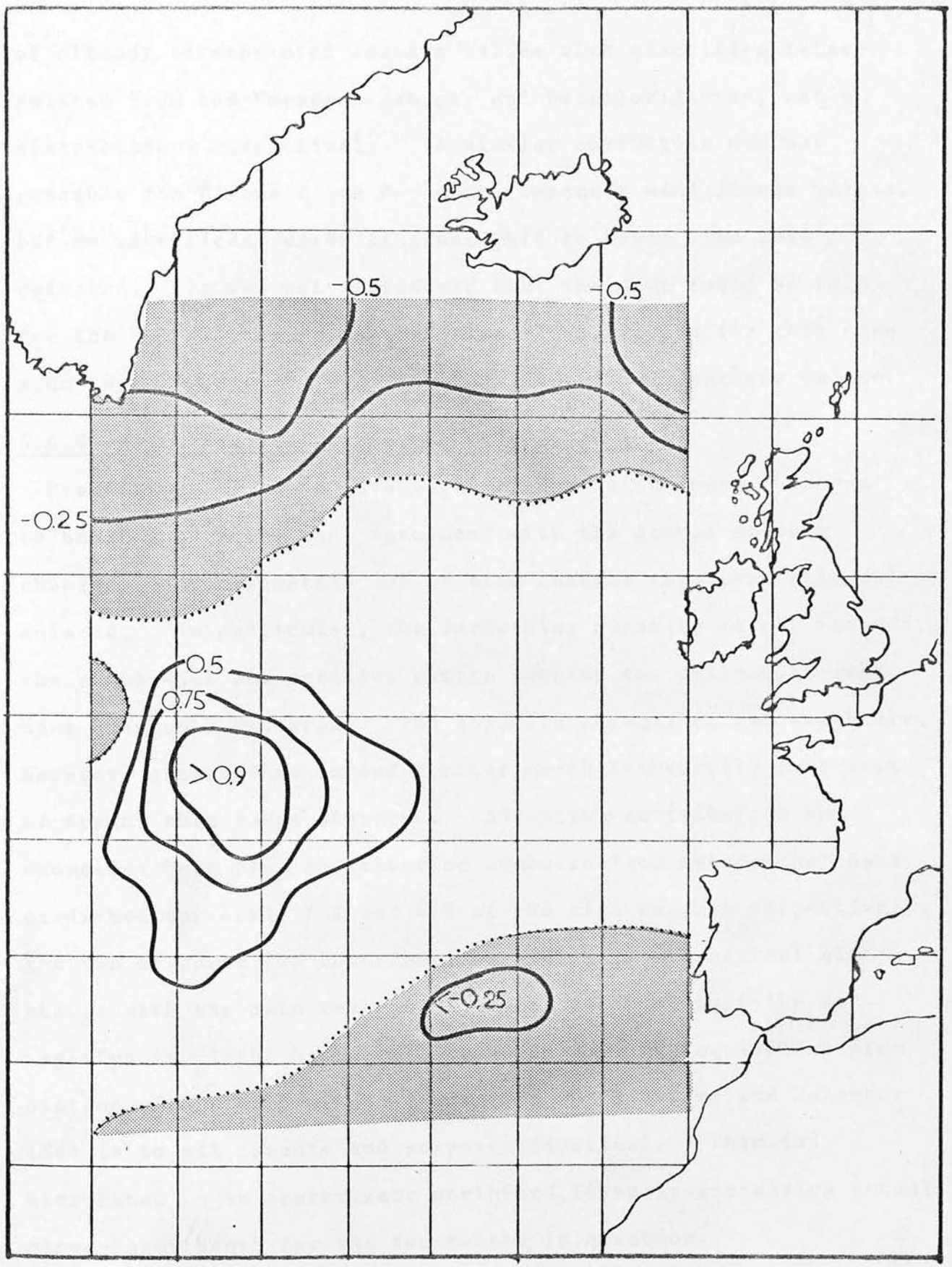

FIGURE 5.6v SEA TEMPERATURE ANOMALY CHANGE, NOVEMBER - DECEMBER 1966;
ADVECTION PLUS HEAT LOSS CONTRIBUTIONS
('REAL' MIXED-LAYER DEPTH)

of already interpolated January values with quantities interpolated from the November:January and December:January ratio distributions respectively. A similar correction was not possible for November and December component wind stress values, but no significant error is considered to arise from this omission. It was not considered that the same could be said for the heat fluxes. Assumed mixed-layer depths for this case study were reduced by 30% from the January and February values.

5.6.2 Model Results for November-December 1966.

Predictions based on November 1966 data alone were observed to be in good all-round agreement with the actual anomaly changes. Approximately 73% of sign changes were correctly calculated. In particular, the increasing negative values towards the north-east and positive centre towards the west-south-west have been well captured. The negative changes of the south are, however, observed to extend further north (especially just west of Spain) than those observed. Advective contribution and anomalous heat flux contribution computed from two months' data predicted correctly 72% and 67% of the sign changes respectively. The sum of these two contributions yielded a 76% correct sign change with the main centres and orientation of positive and negative isopleths being well reproduced. The equivalent prediction with 'real' mixed-layer depth for November and December 1966 is to all intents and purposes identical. This is attributed to an approximate northward linearly-increasing actual mixed-layer depth for the two months in question.

Figure 5.6.2a has been additionally included to show the effect of incorporating a horizontal diffusion term in the combined two month advection and heat flux prediction. Inspection of this figure, together with calculated 49% of sign changes correctly predicted, emphasises the deterioration of the prediction following inclusion of the parameterised horizontal turbulent diffusion term. Anomalous (meridional) advection produced by anomalous Sverdrup flow plus anomalous heat loss gave rise to an almost entirely negative anomaly change over the region with only local positive change in the extreme south; this distribution bears little resemblance to the observed sea temperature anomaly changes.

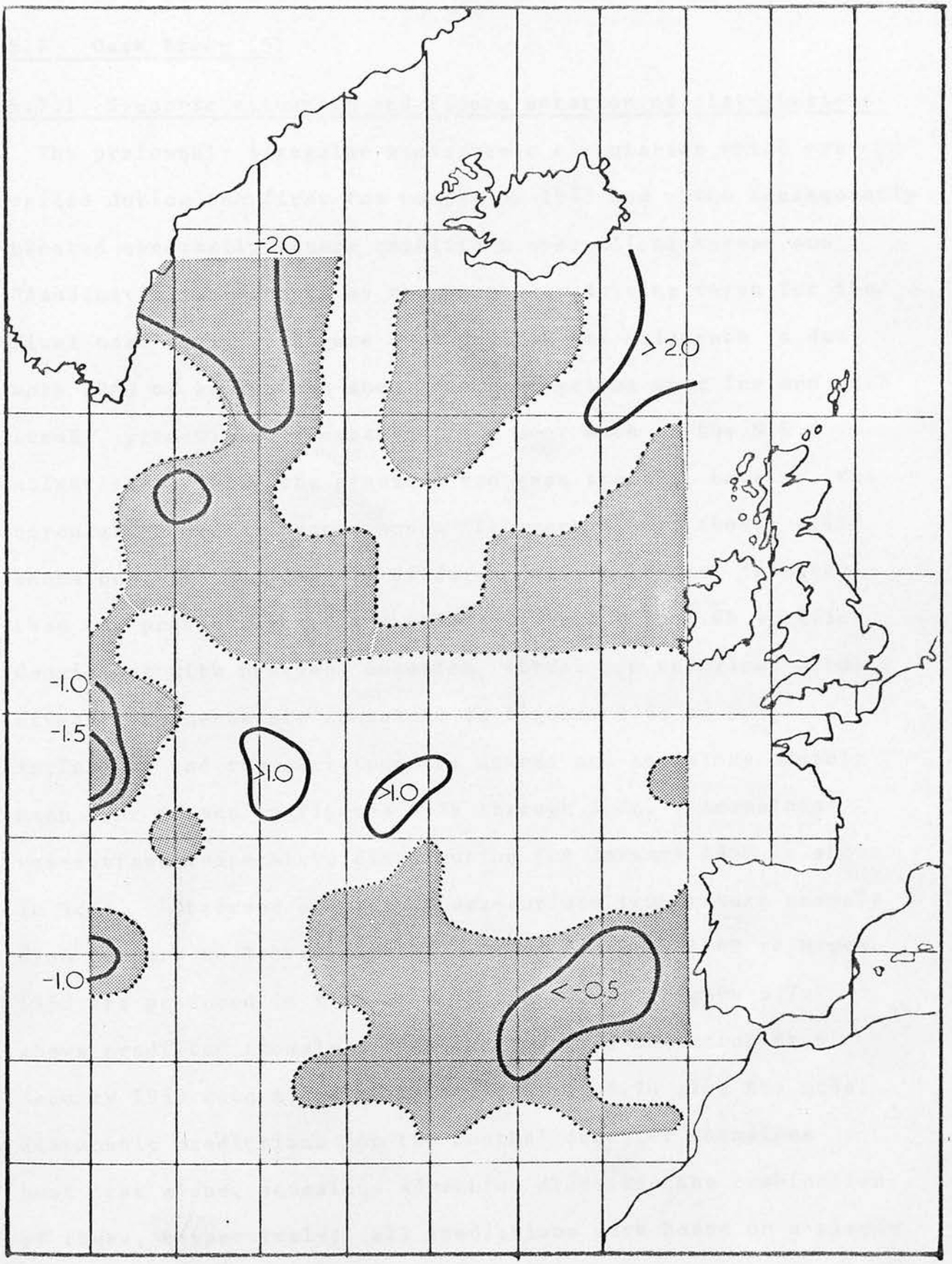

FIGURE 5.6.2a SEA TEMPERATURE ANOMALY CHANGE, NOVEMBER - DECEMBER 1966:
ADVECTION PLUS COOLING PLUS HORIZONTAL DIFFUSION CONTRIBUTIONS.

5.7 Case Study (3)

5.7.1 Synoptic situation and figure notation of distributions.

The profoundly irregular atmospheric circulation which prevailed during the first two months of 1963 and which consequently created abnormally severe conditions over all of Europe and Scandinavia, was chosen as the anomalous driving force for the final case study. Figure 5.7a reveals the existence in January 1963 of an intense anomalous anticyclone over Iceland with strong, predominantly easterly flow over much of the N.E. Atlantic. Unlike the previous two case studies, however, the circulation of the second month (February 1963), though still anomalous, is considerably different and in general 'slacker' than the previous month, as reference to figure 5.7b verifies. Consistent with previous notation, actual and anomalous wind stress components are contained in figures 5.6e to 5.7j inclusive, and the corresponding actual and anomalous monthly mean heat fluxes in figures 5.7k through 5.7n. Anomalous sea-surface temperature distribution for January 1963 is shown in 5.7o. Observed changes of sea-surface temperature anomaly from January to February 1963 and from December 1962 to March 1963 are produced in figures 5.7p and 5.7q. Figure 5.7r shows predicted anomaly change for heat and advection from January 1963 data alone while 5.7s, 5.7t, 5.7u give the model diagnostic predictions for two months' data for anomalous heat loss alone, anomalous advection alone and the combination of these, respectively; all predictions were based on a mixed-

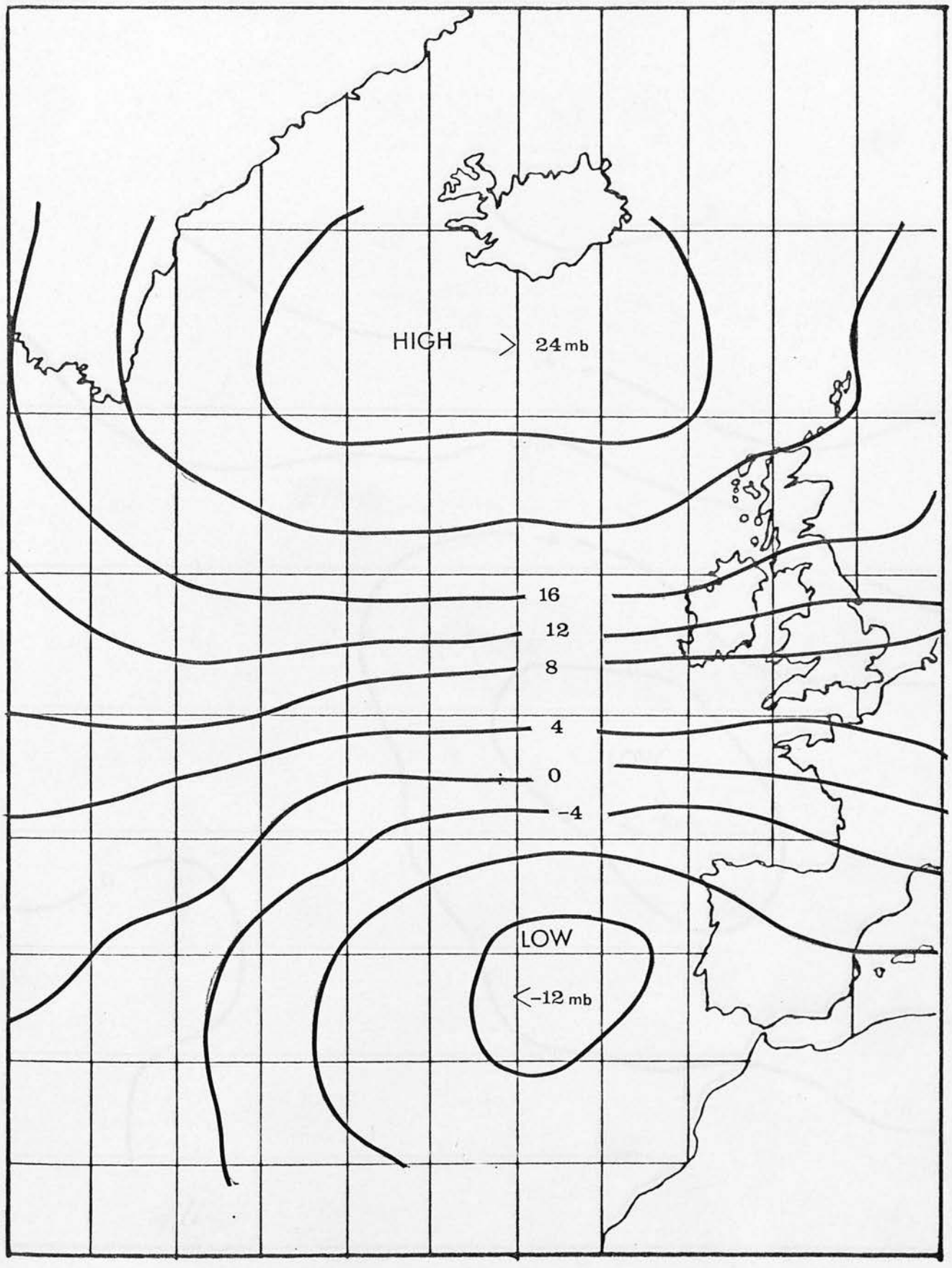

FIGURE 5.7a ANOMALOUS PRESSURE DISTRIBUTION. JANUARY 1963

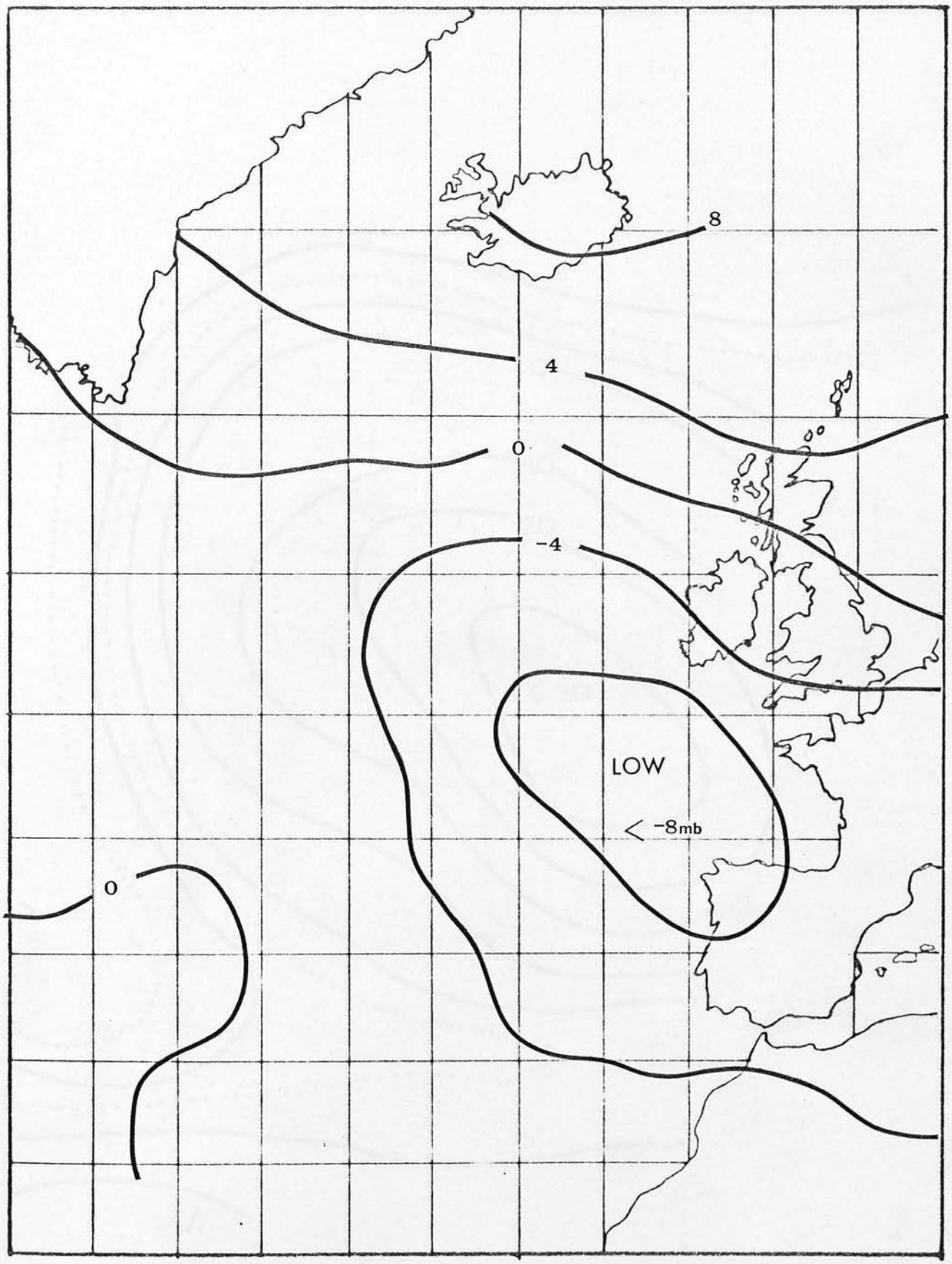

FIGURE 5.7b ANOMALOUS PRESSURE DISTRIBUTION. FEBRUARY 1963

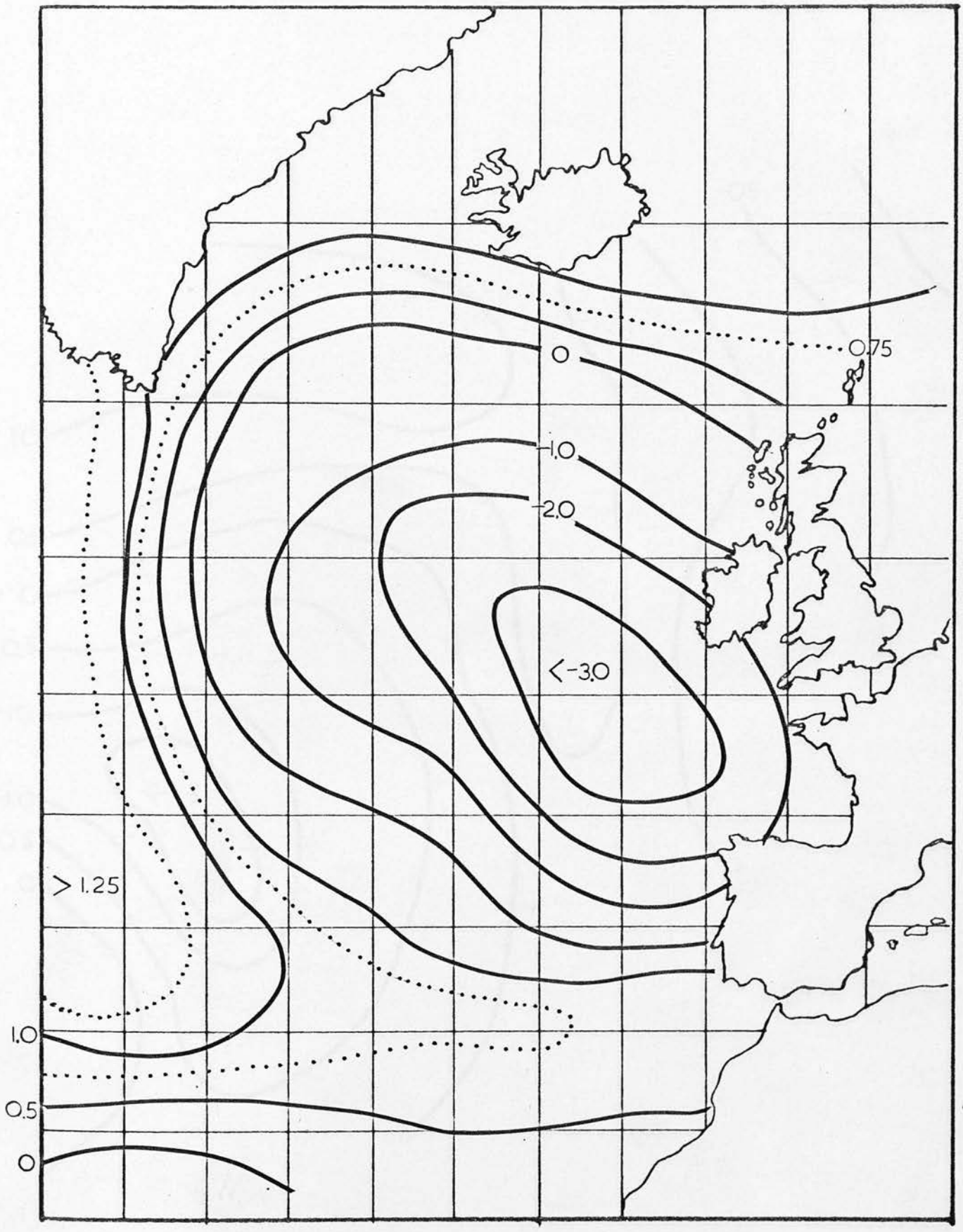

FIGURE 5.7c MEAN ZONAL CPT. WIND STRESS. JANUARY 1963

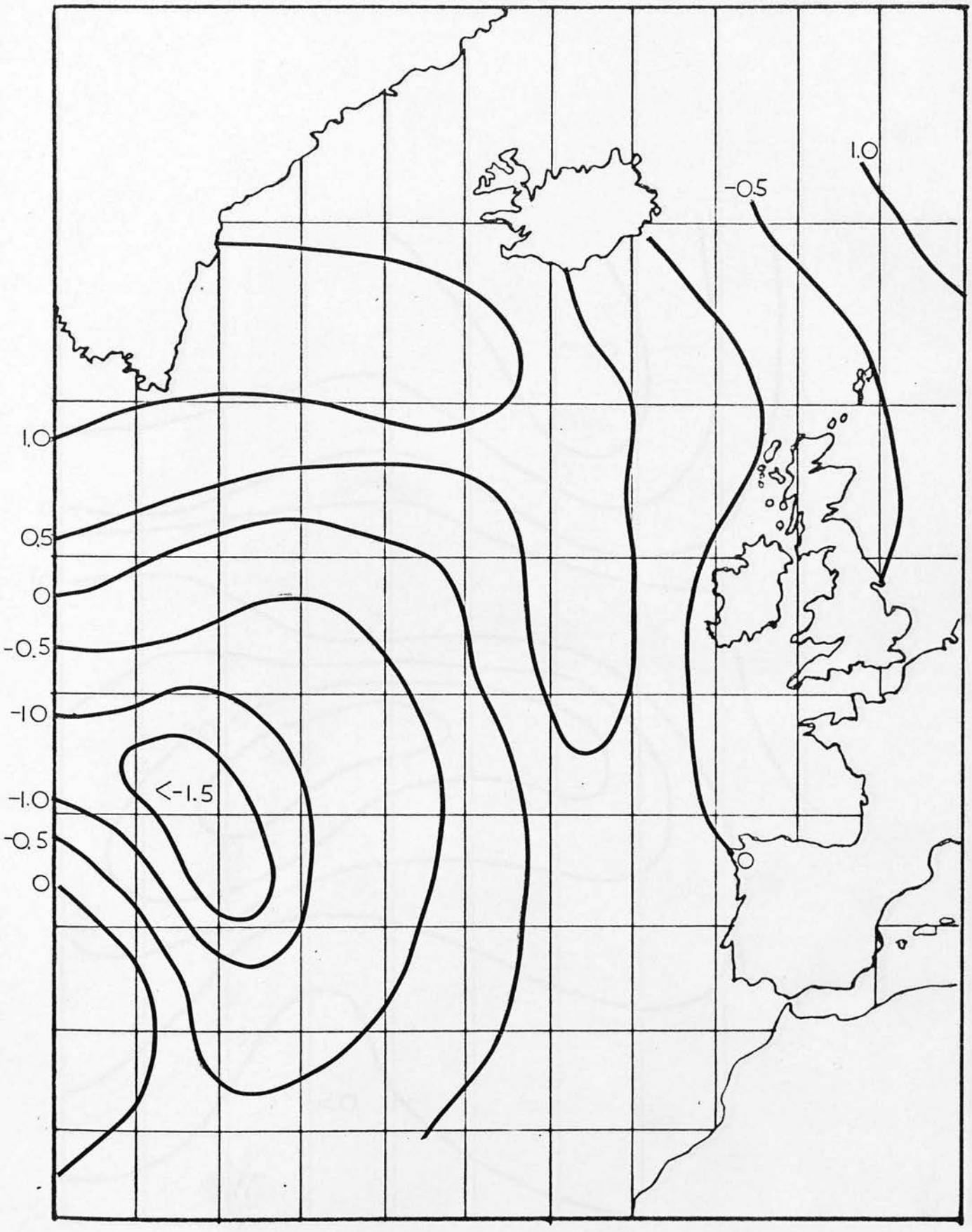

FIGURE 5.7d MEAN MERIDIONAL CPT. SURFACE WIND STRESS. JANUARY 1963.

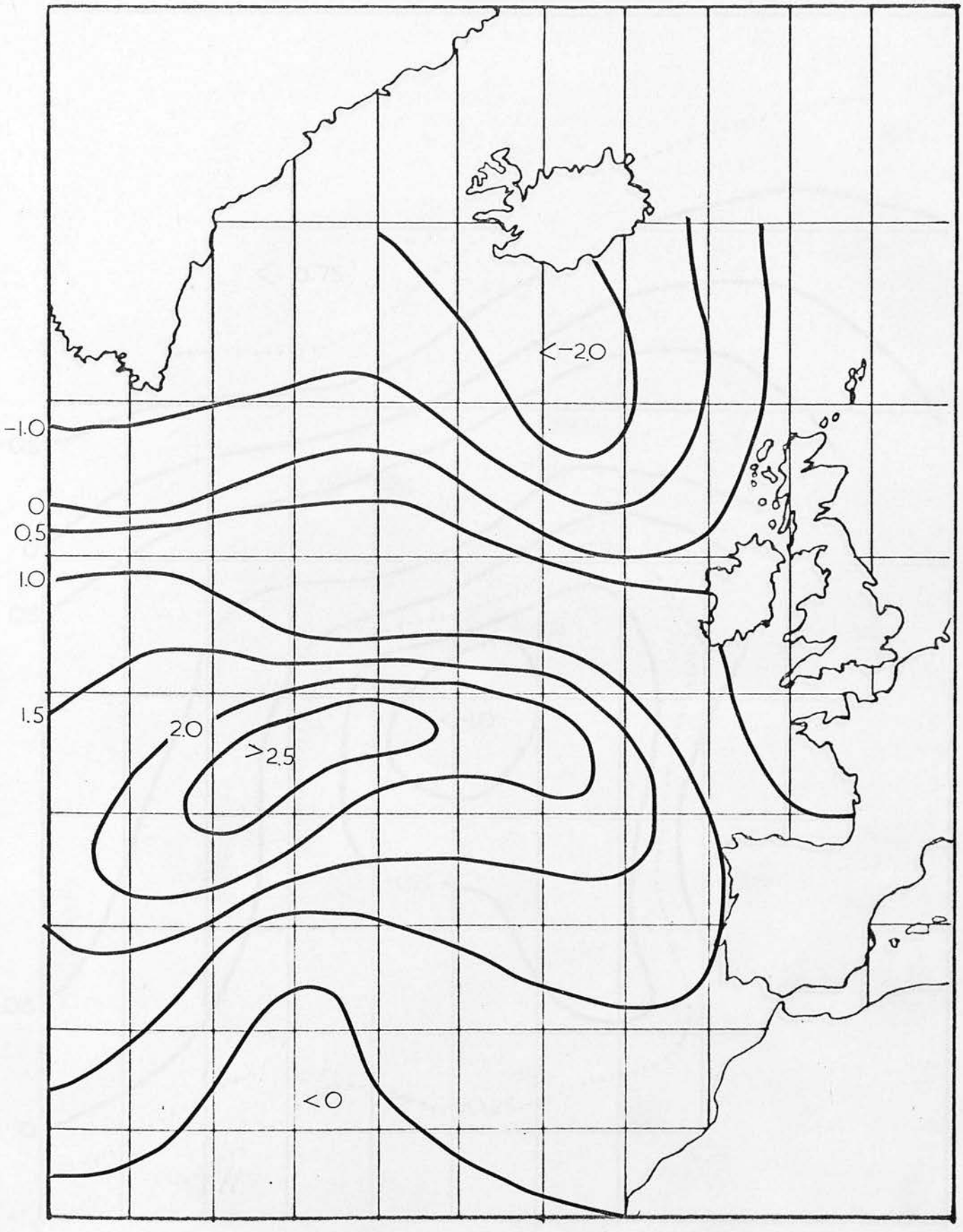

FIGURE 5.7e MEAN ZONAL CPT. WIND STRESS. FEBRUARY 1963

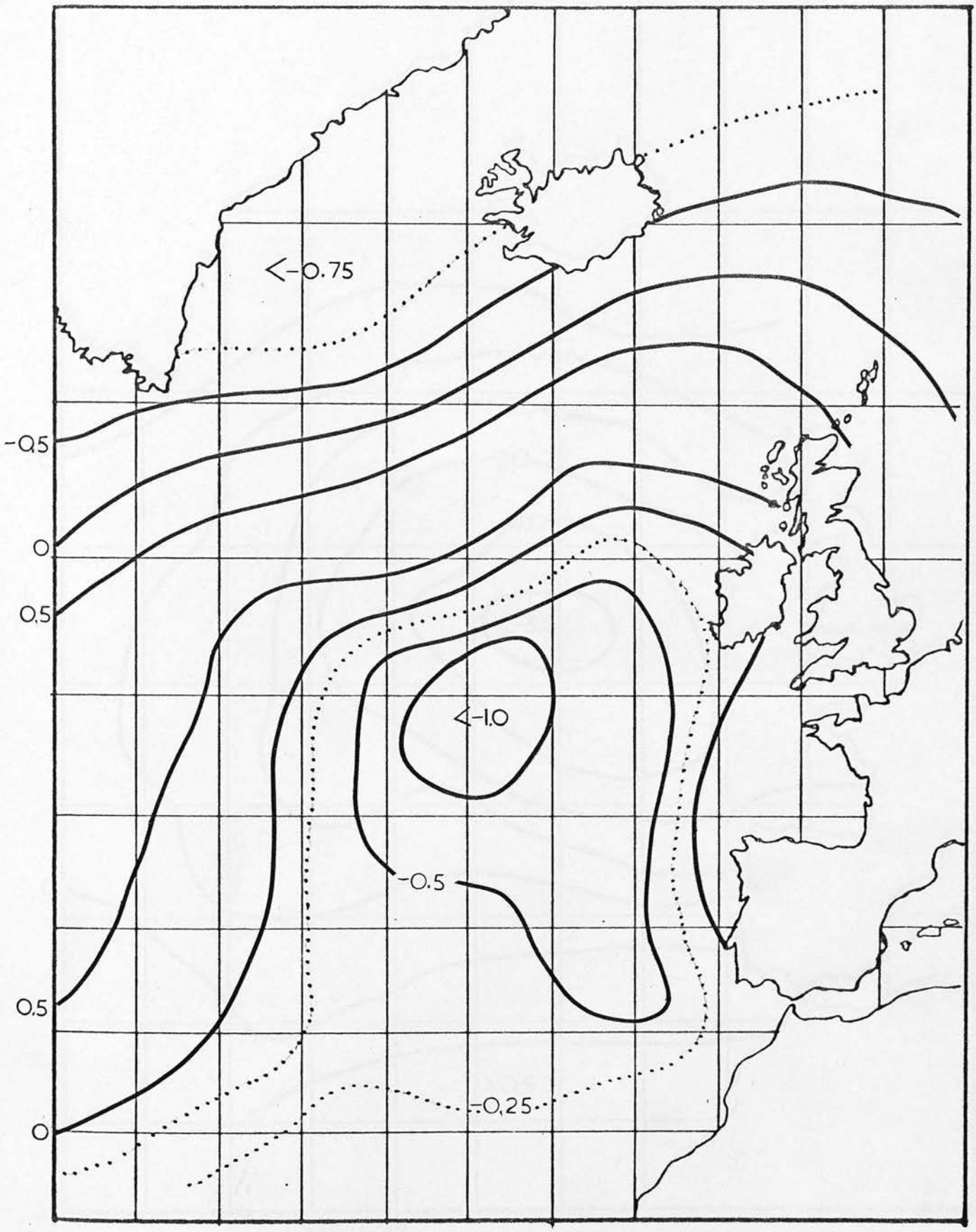

FIGURE 5.7f MEAN MERIDIONAL CPT. WIND STRESS. FEBRUARY 1963

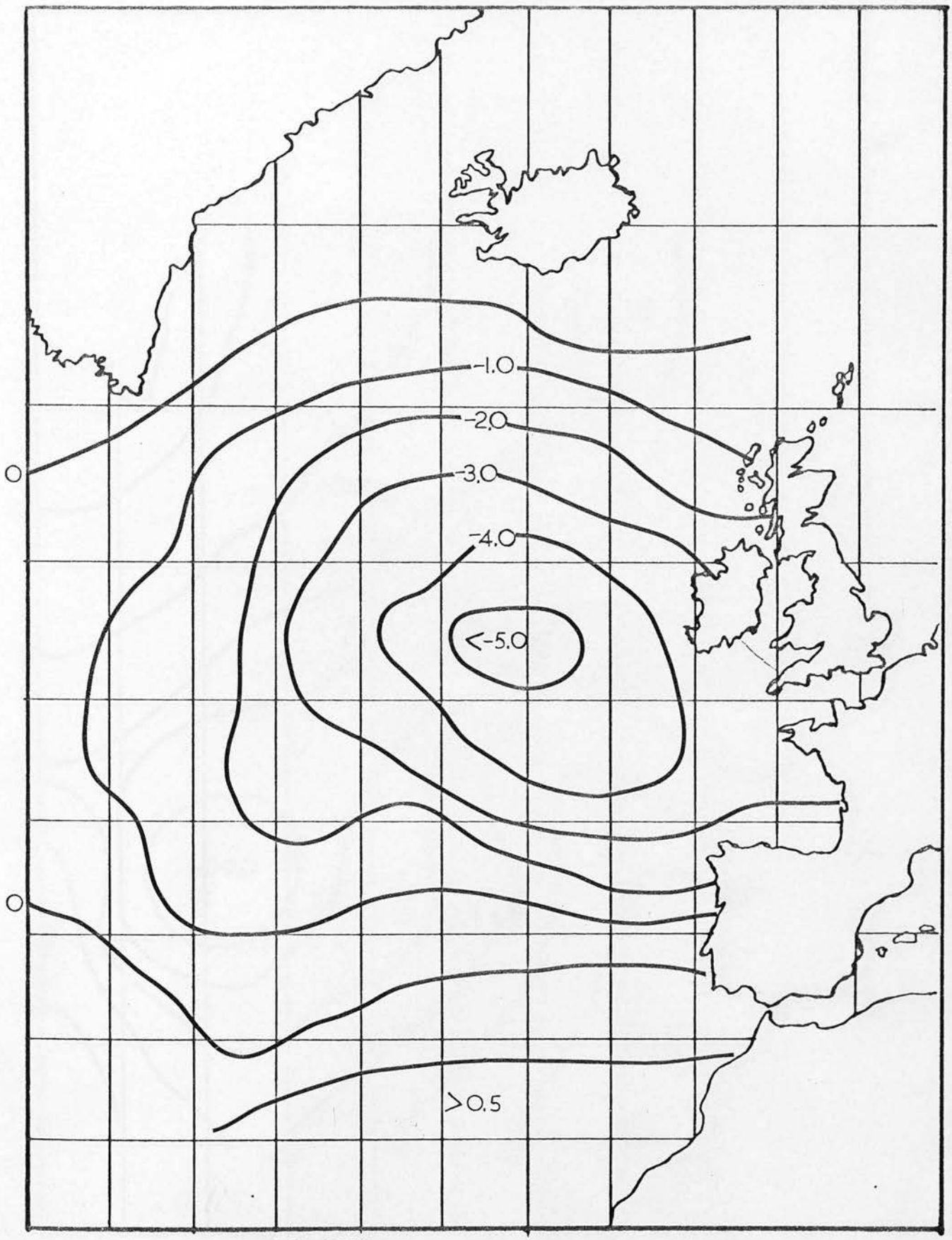

ANOMALOUS

FIGURE 5.7g ZONAL CPT. WIND STRESS. JANUARY 1963

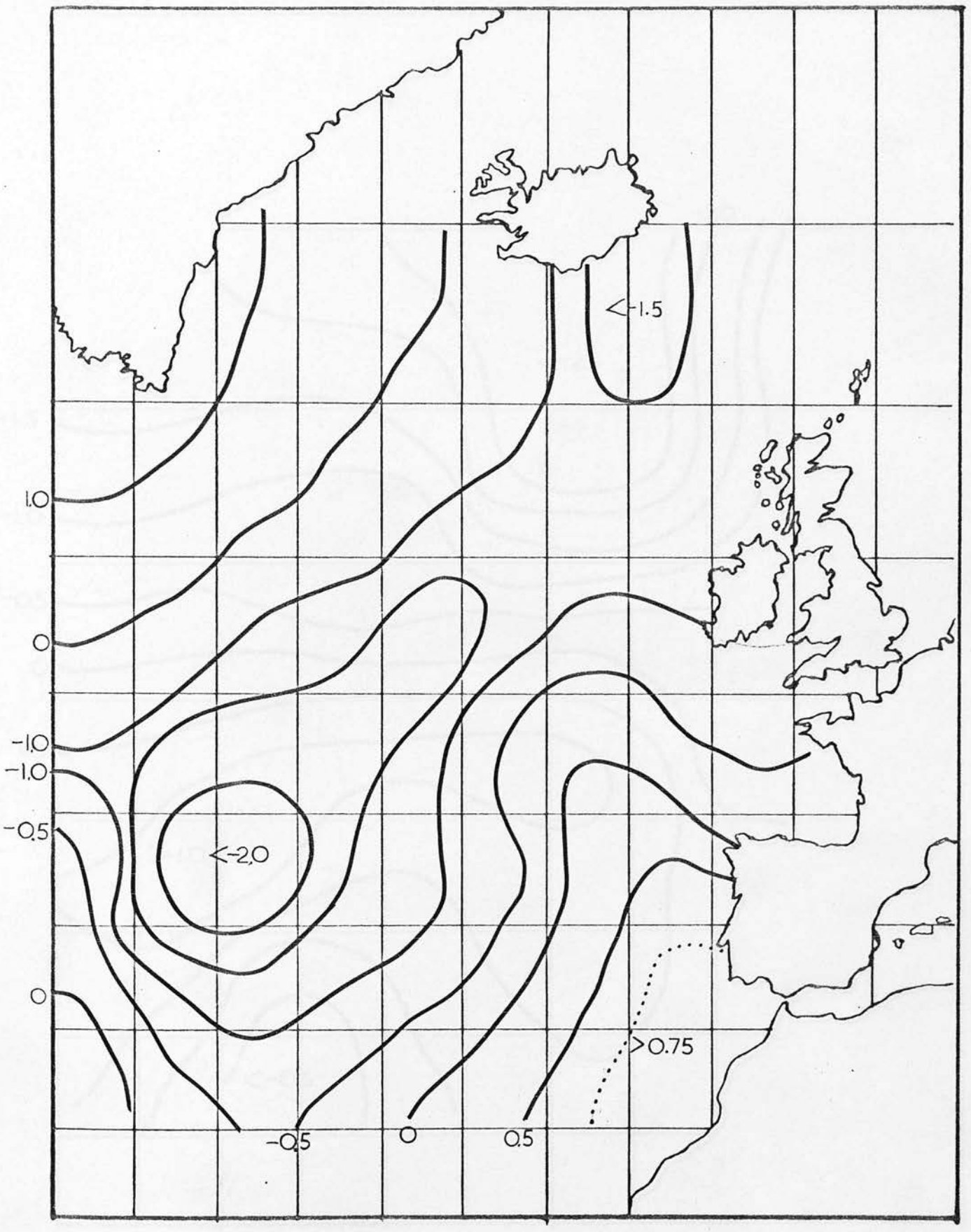

FIGURE 5.7h MERIDIONAL CPT. ANOMALOUS WIND STRESS. JANUARY 1963

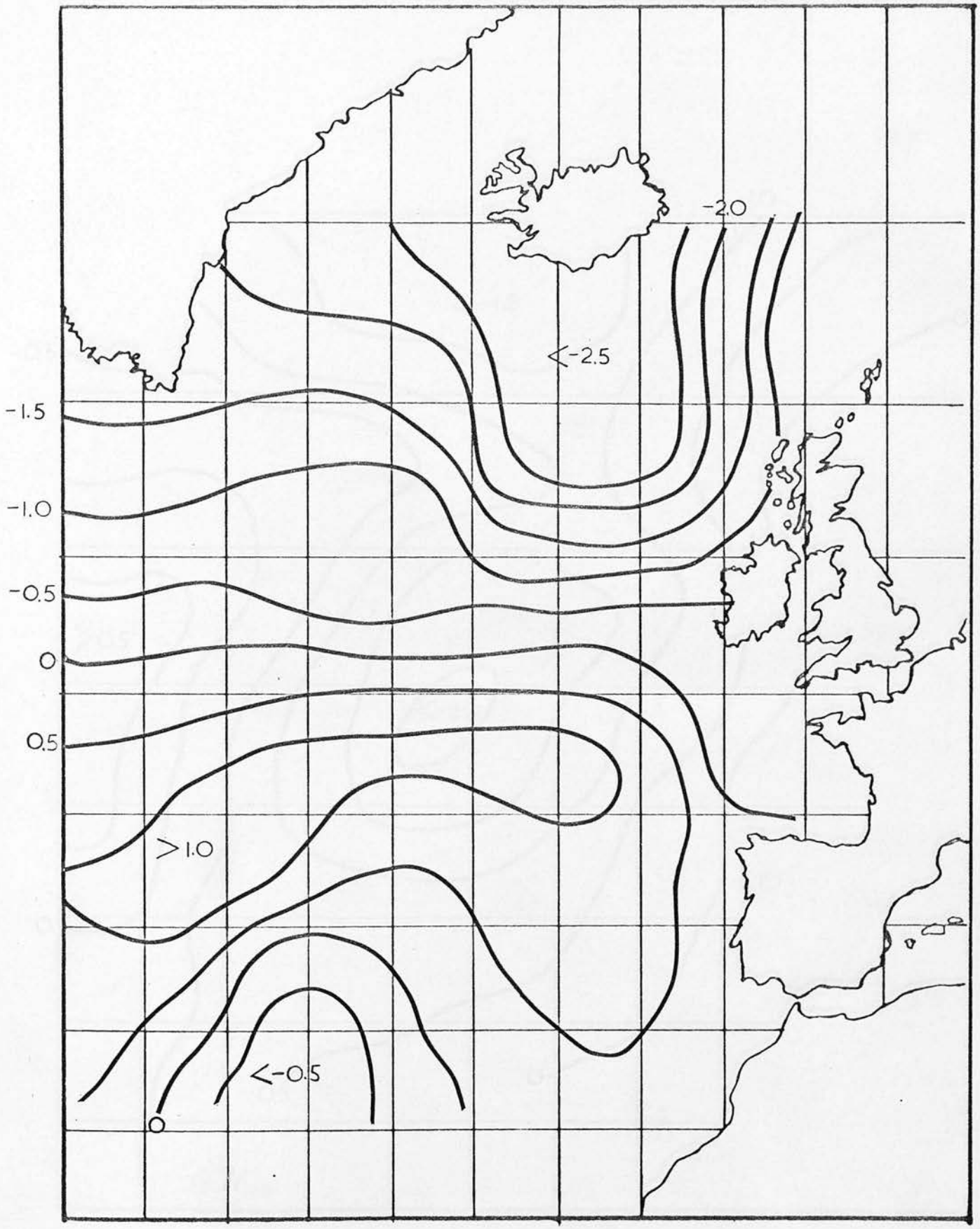

FIGURE 5.7i ZONAL CPT. ANOMALOUS WIND STRESS. FEBRUARY 1963

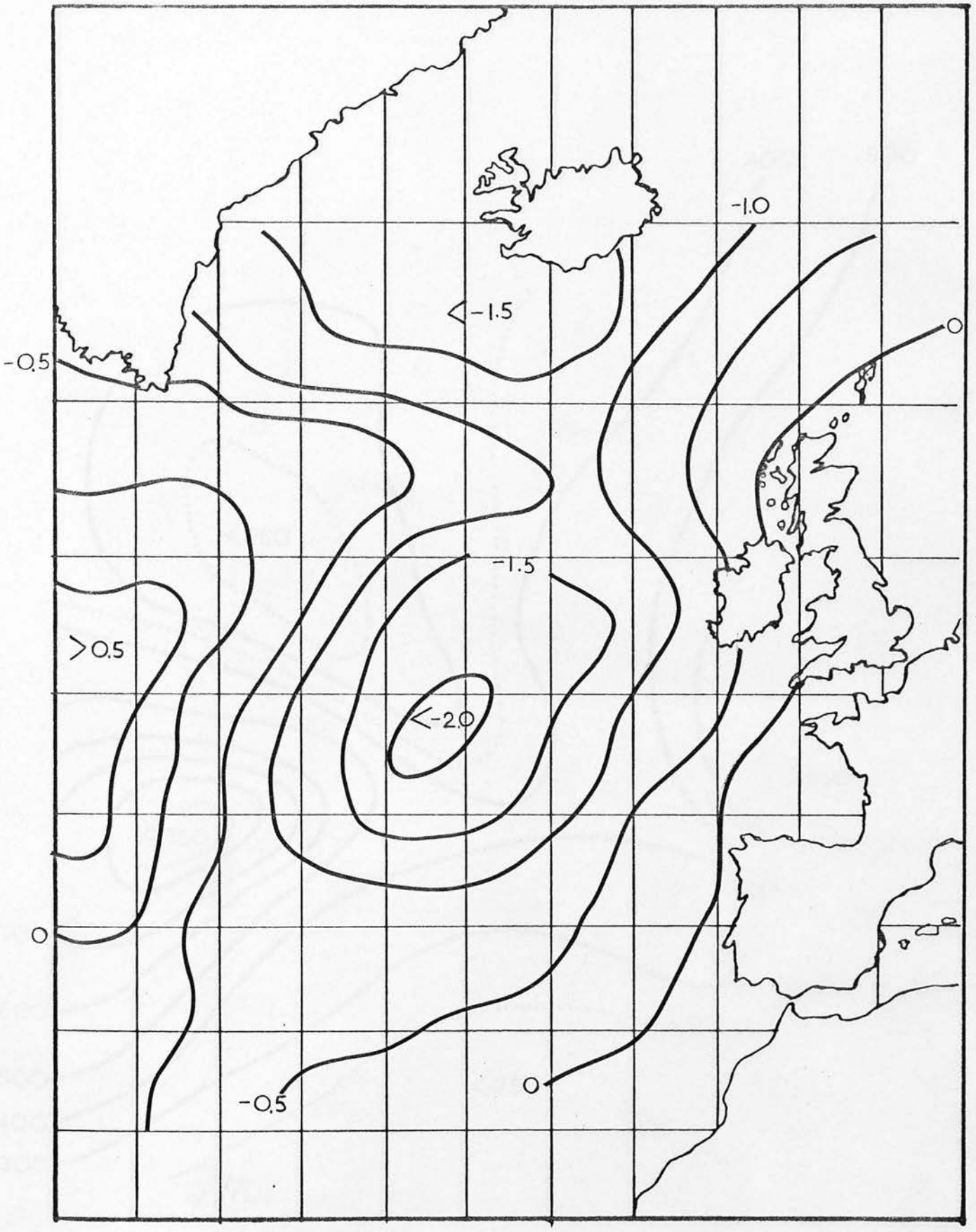

FIGURE 5.7j MERIDIONAL CPT. ANOMALOUS WIND STRESS. FEBRUARY 1963

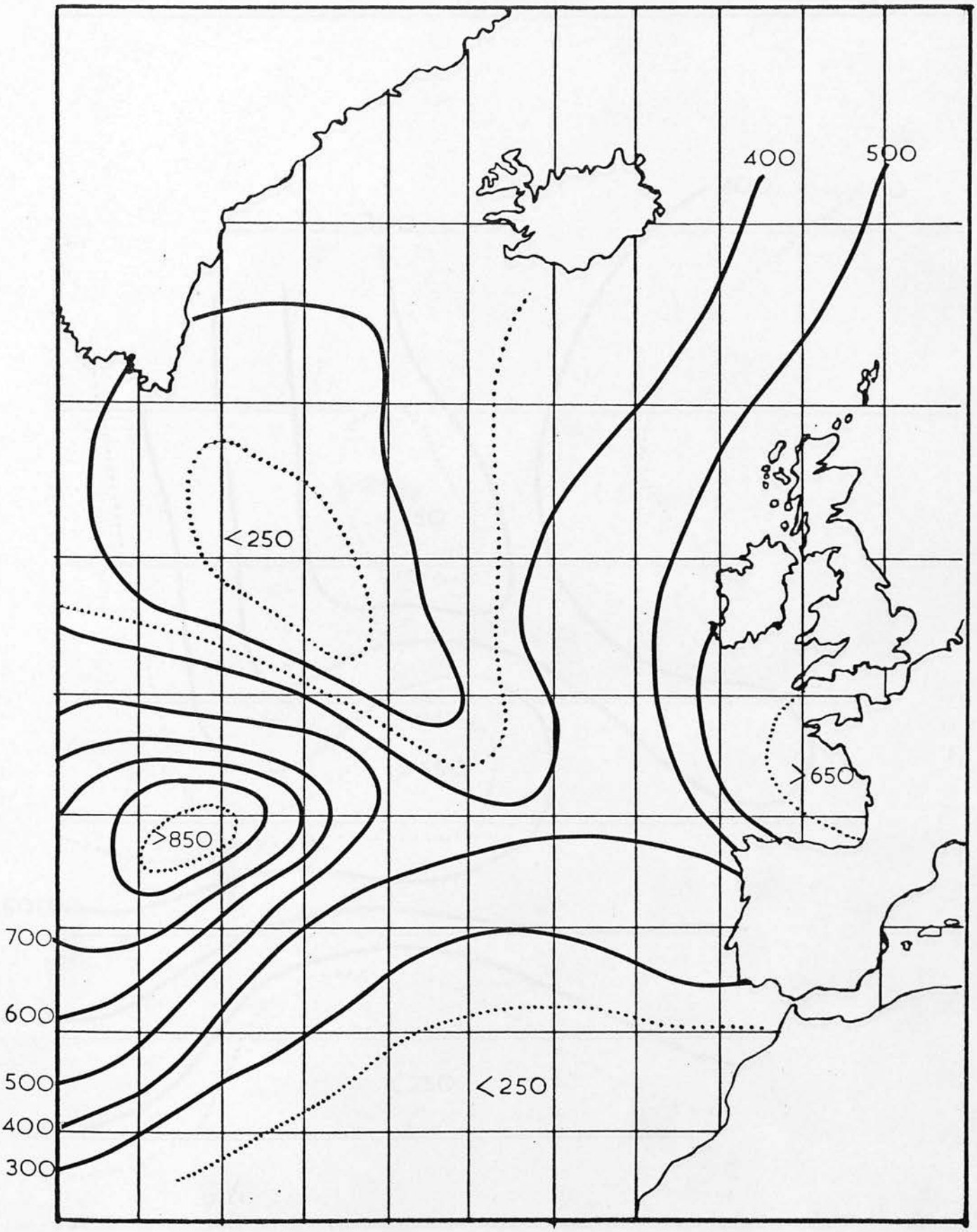

FIGURE 5.7k TOTAL SURFACE HEAT FLUX JANUARY 1963

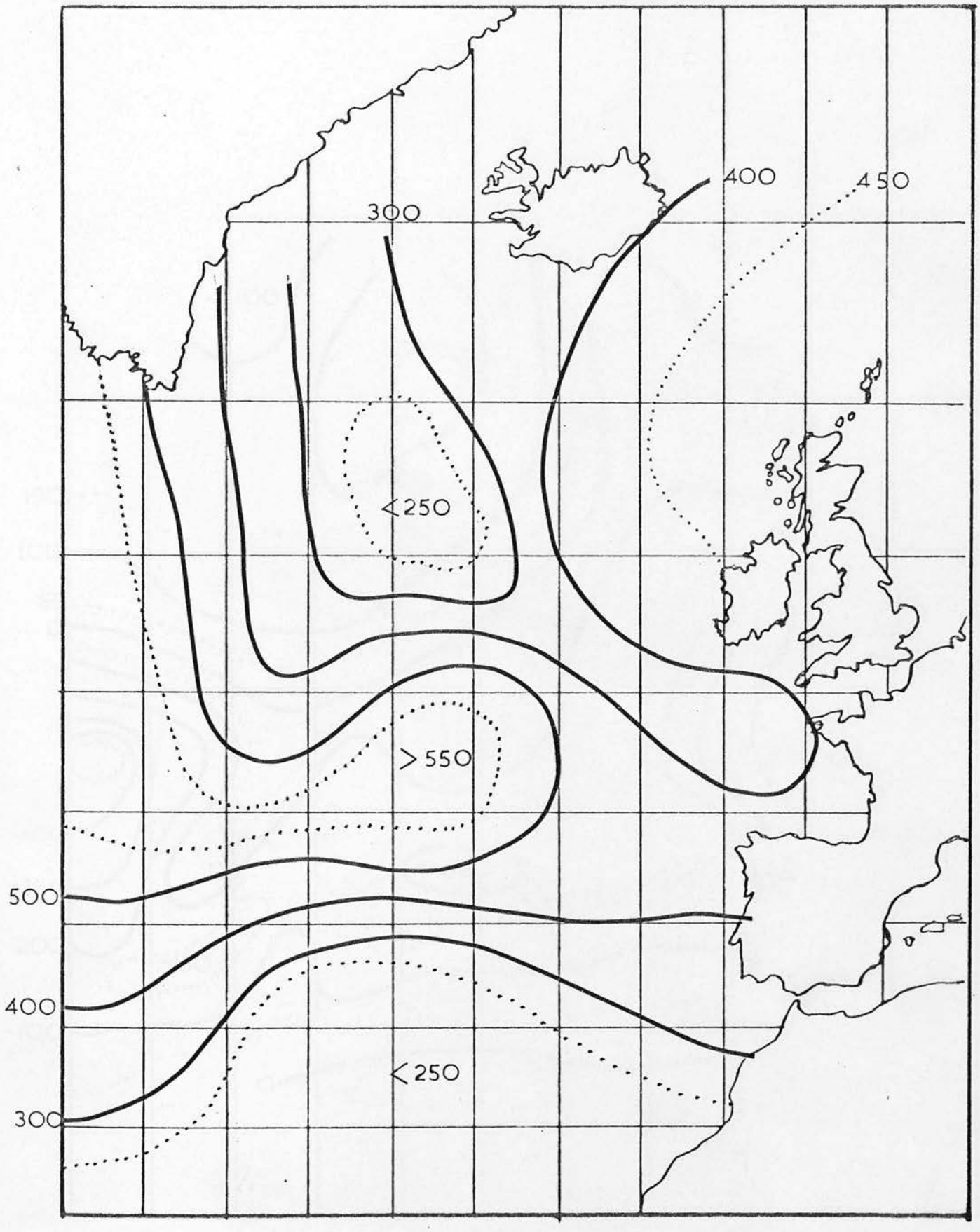

FIGURE 5.71 TOTAL SURFACE HEAT FLUX. FEBRUARY 1963

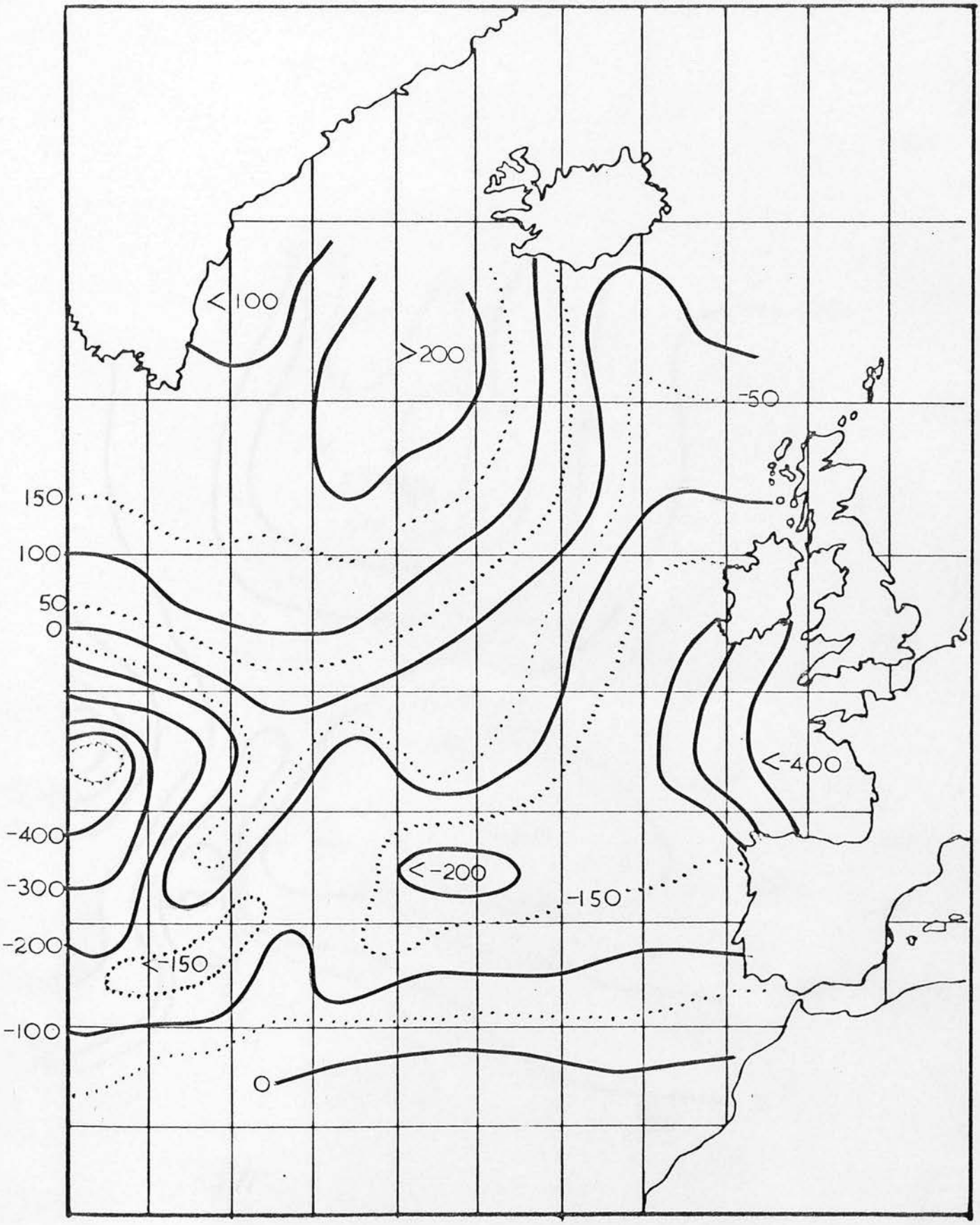

FIGURE 5.7m ANOMALOUS TOTAL SURFACE HEAT FLUX. JANUARY 1963

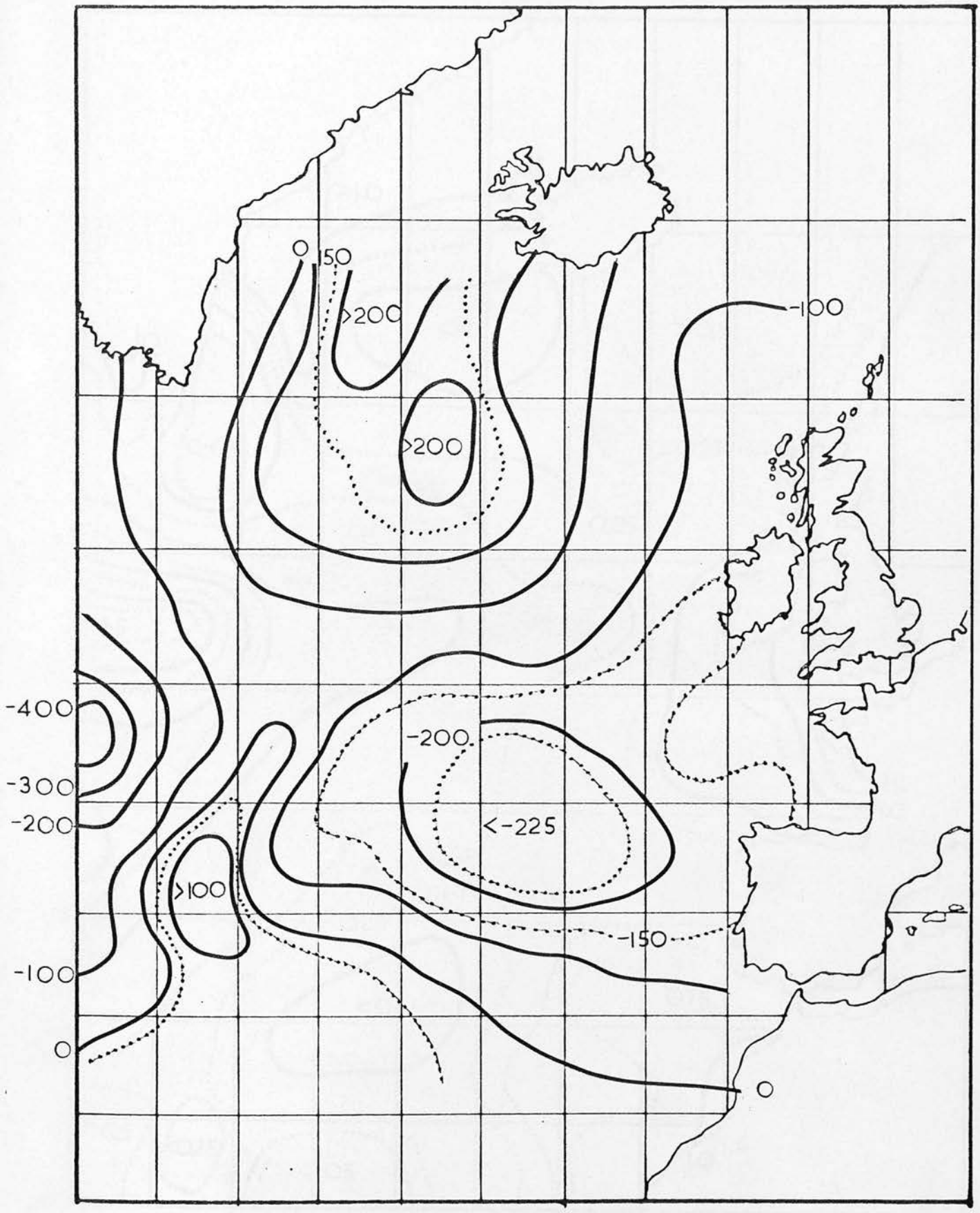

FIGURE 5.7n ANOMALOUS TOTAL SURFACE HEAT FLUX. FEBRUARY 1963

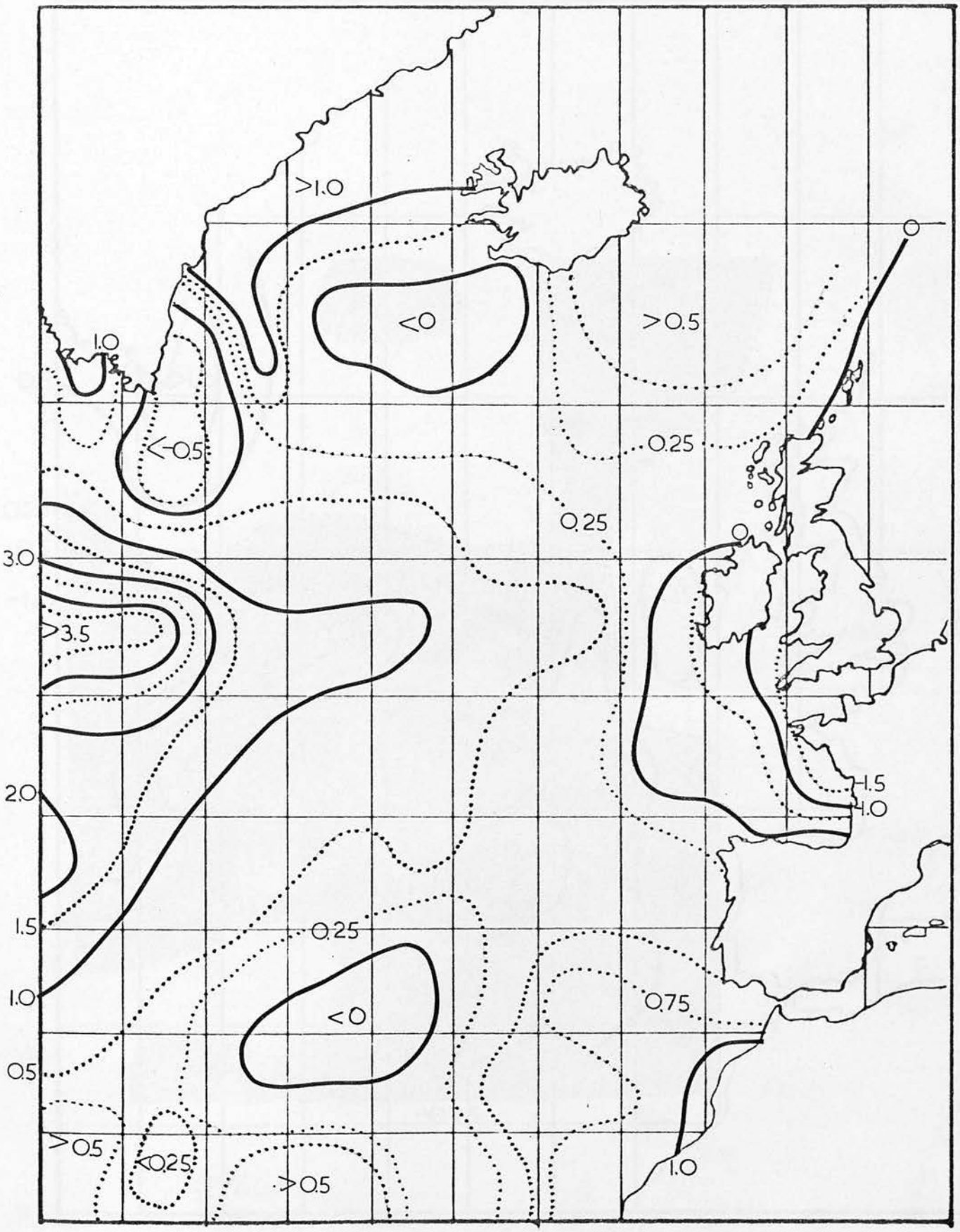

FIGURE 5.7o ANOMALOUS SEA-SURFACE TEMPERATURE DISTRIBUTION. JANUARY 1963.

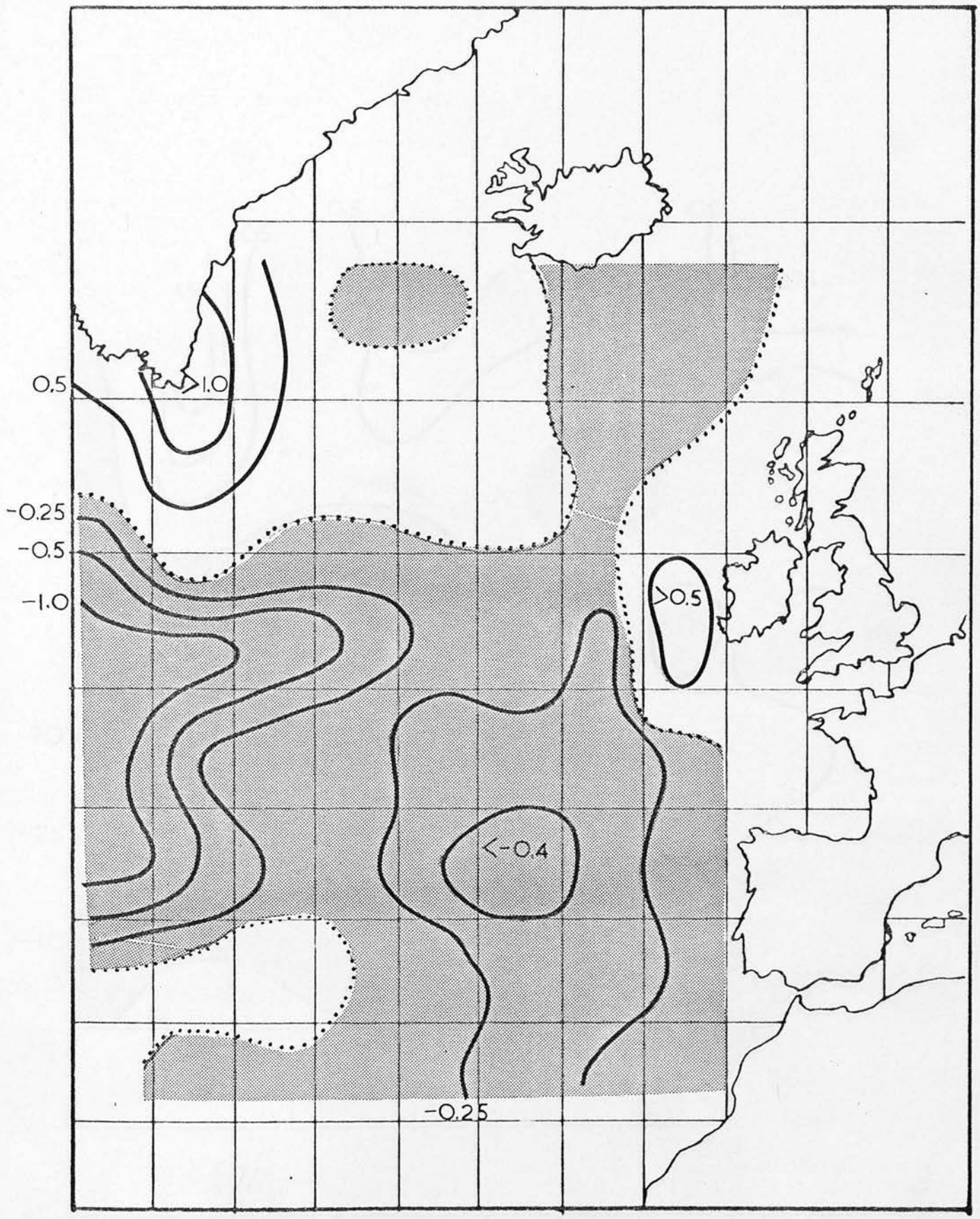

FIGURE 5.7p OBSERVED SEA-SURFACE TEMPERATURE ANOMALY CHANGE,
JANUARY-FEBRUARY 1963.

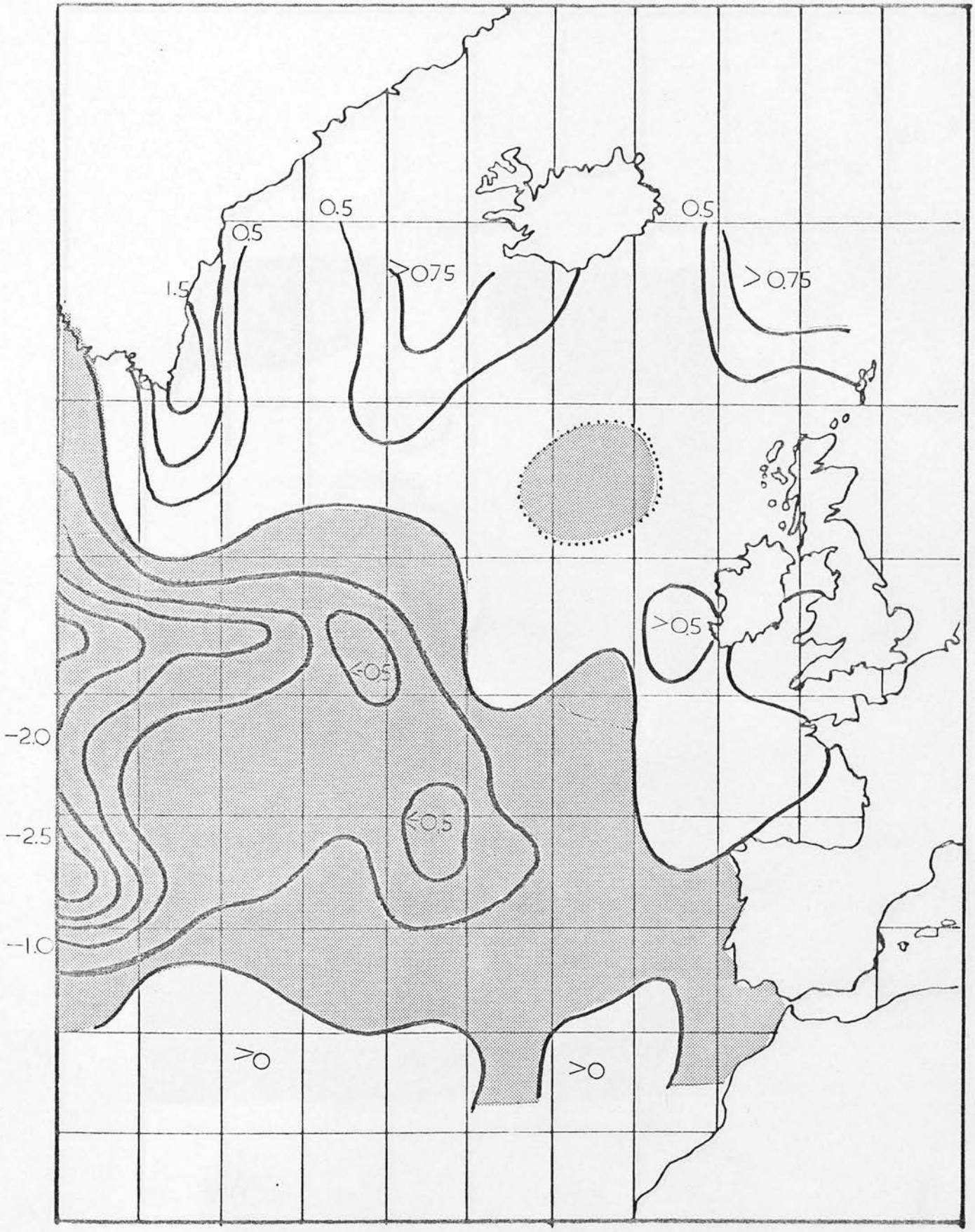

FIGURE 5.7q OBSERVED SEA-SURFACE TEMPERATURE ANOMALY CHANGE,
DECEMBER 1962 - MARCH 1963.

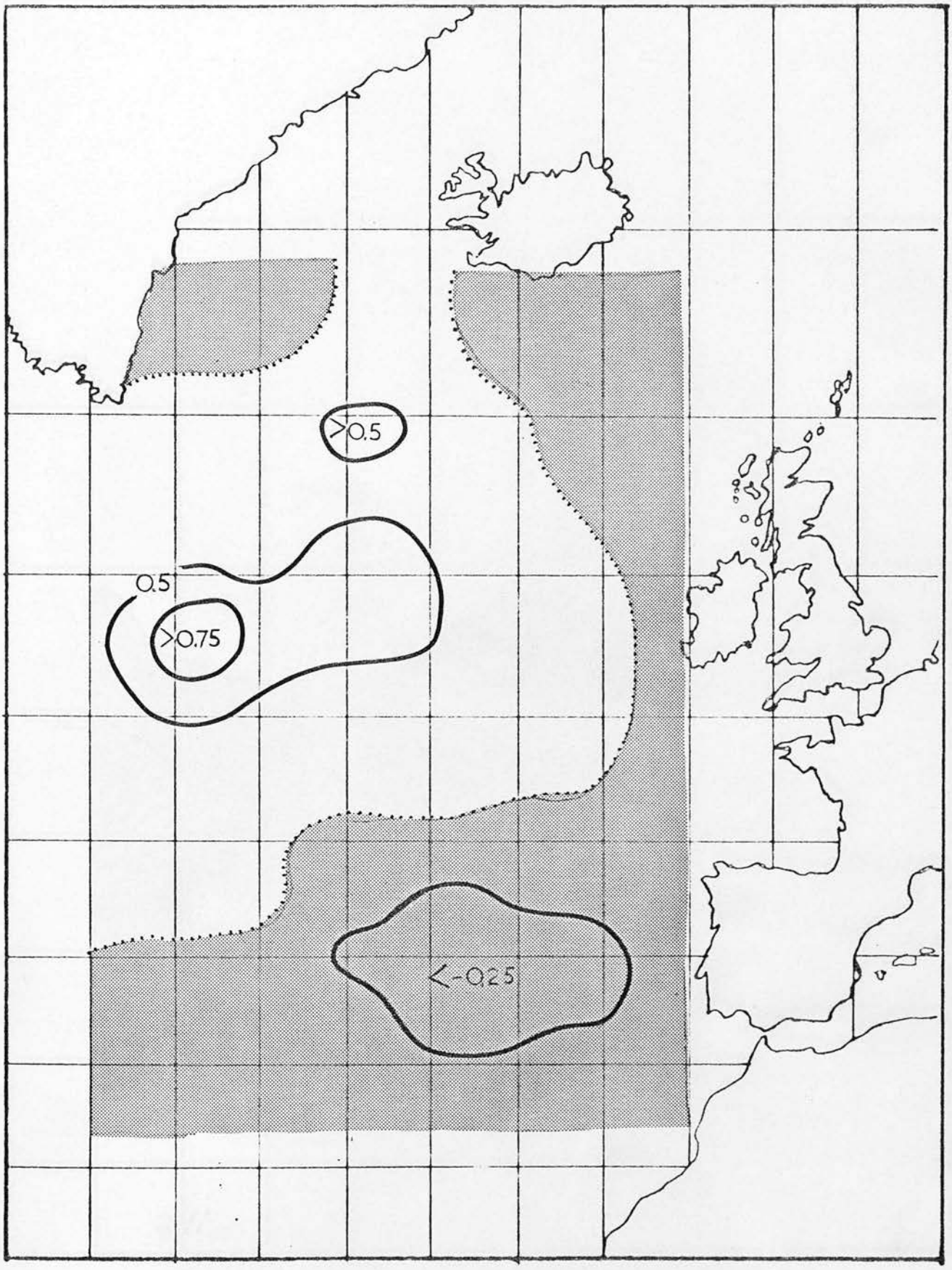

FIGURE 5.7r PREDICTED SEA TEMPERATURE ANOMALY CHANGE, JANUARY-FEBRUARY 1963; ADVECTION PLUS HEAT LOSS CONTRIBUTIONS.

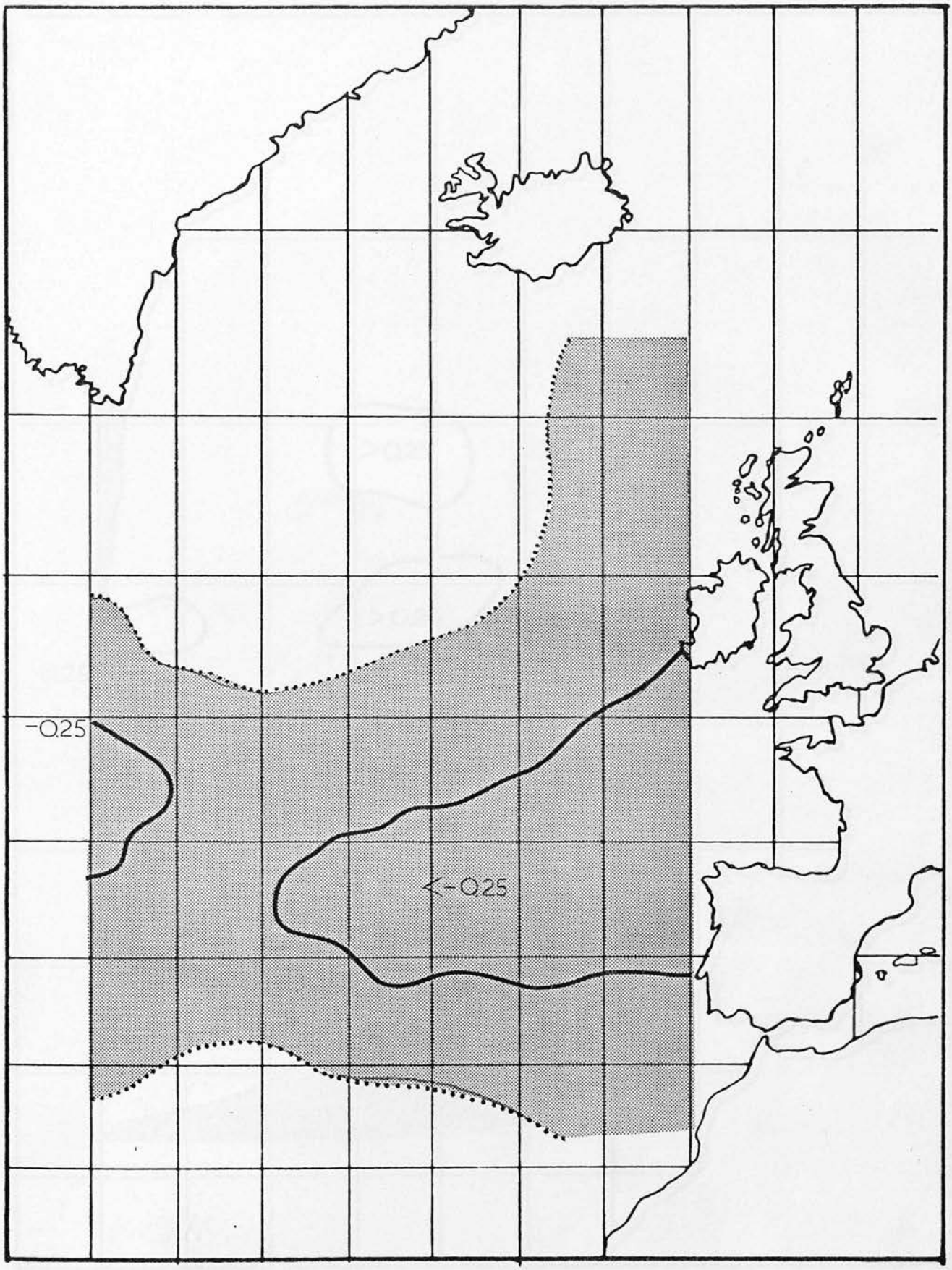

FIGURE 5.7s SEA TEMPERATURE ANOMALY CHANGE, JANUARY-FEBRUARY 1963;
HEAT LOSS CONTRIBUTION ONLY.

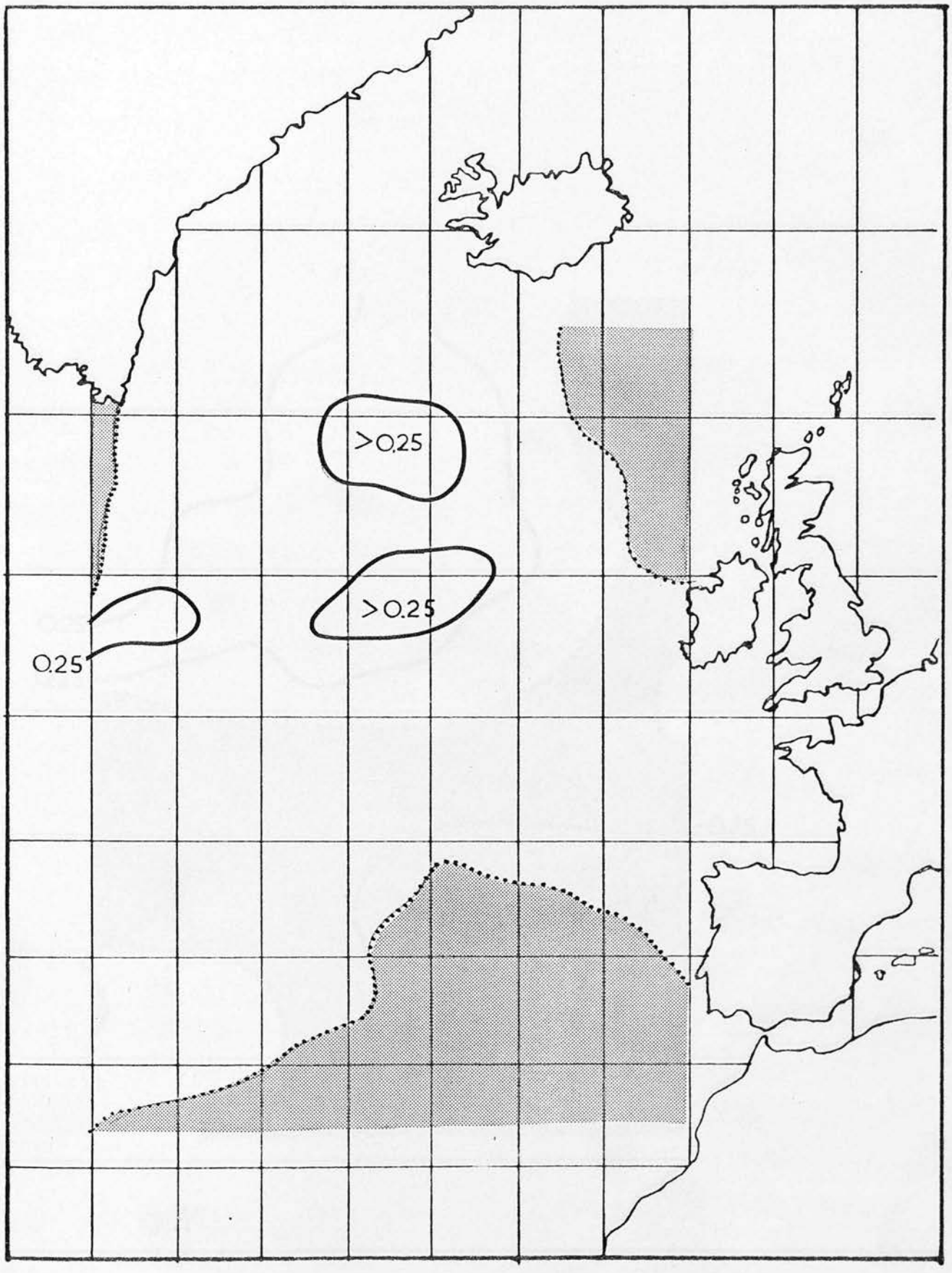

FIGURE 5.7t SEA TEMPERATURE ANOMALY CHANGE, JANUARY-FEBRUARY 1963;
ADVECTION CONTRIBUTION ONLY.

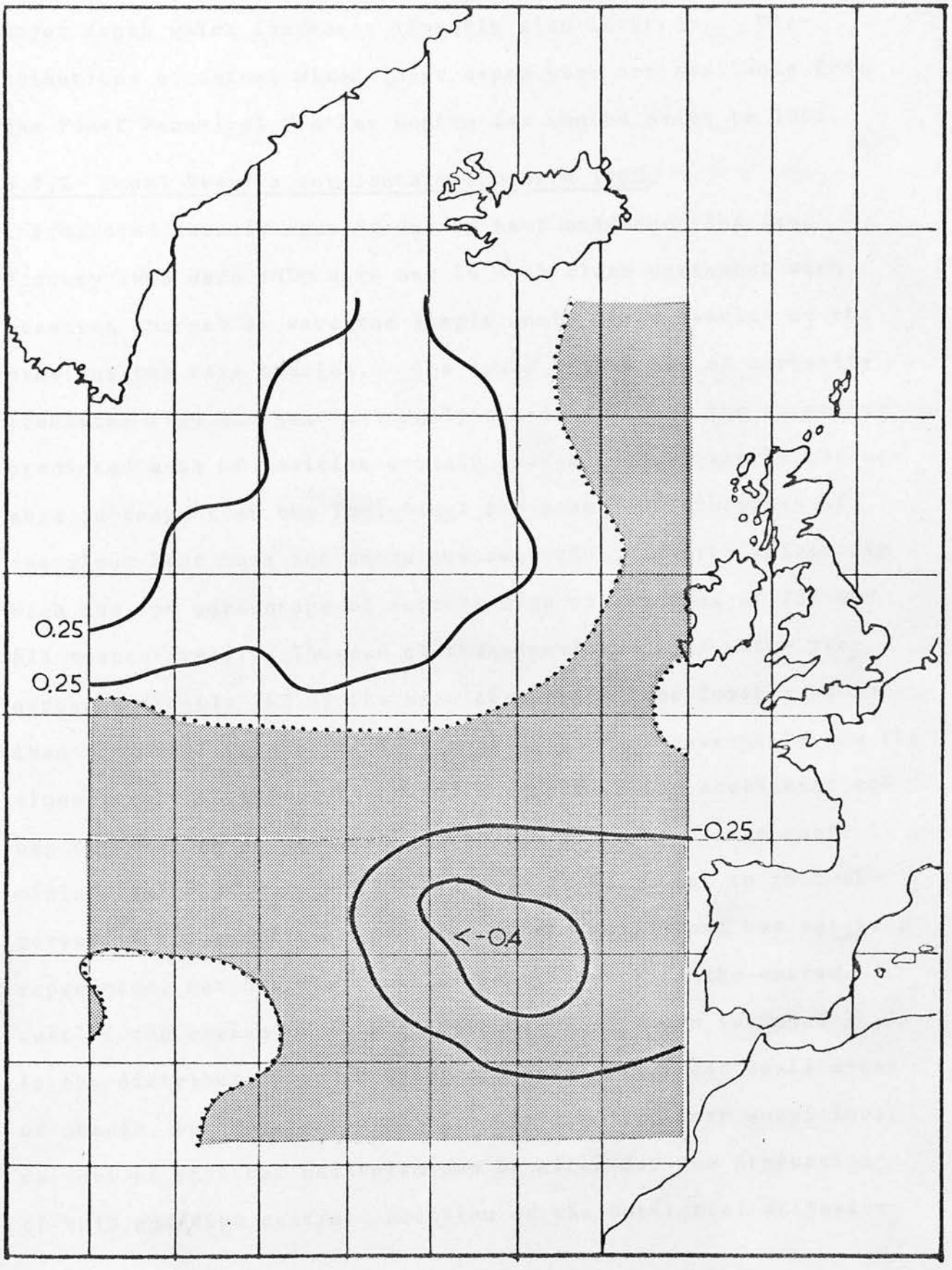

FIGURE 5.7u SEA TEMPERATURE ANOMALY CHANGE, JANUARY-FEBRUARY 1963;
ADVECTION PLUS HEAT LOSS CONTRIBUTIONS.

layer depth which increases linearly with latitude. Distributions of actual mixed-layer depth were not available from the Fleet Numerical Weather Centre for months prior to 1965.

5.7.2 Model Results for January-February 1963.

Predicted anomaly changes due to heat and advection from January 1963 data only were not in such close agreement with observed changes as were the single month based results of the previous two case studies. The lower percentage of correctly predicted sign changes is largely attributable to the extensive predicted area of positive anomaly change. Particularly noticeable in respect of the individual two-month contributions of anomalous heat loss and anomalous advection were the relatively high and low percentage of correct sign predictions of 72% and 52% respectively. The sum of these contributions which predicted correctly 76% of the sign changes is considerably better than the single month prediction of 58%. Also noteworthy are the almost exact locations of positive tongue in the south-west and negative centre in the east-south-east; the predicted central minimum value of this negative change is identical to that observed. The small negative area in the north-west has not been reproduced, nor has the small positive centre in the extreme east of the region (just off Ireland). Although included in the distribution of observed changes, both these small areas of change, but more especially the latter, are very suspicious; no obvious physical mechanism can be cited for the production of this positive centre. Addition of the horizontal diffusion

term again gave rise to several areas of positive and negative change which were not present in the observed changes distribution. Contributions due to anomalous Sverdrup advection plus anomalous heat flux contributions gave rise to a distribution of sign changes almost entirely opposite in sense to those actually observed.

5.8 Summary and Final Remarks.

Three essentially dissimilar anomalous meteorological types have been chosen for the three case studies; the circulations of January-February 1966 dominated by a deep and extensive anomalous low, and the anomalous anticyclonic conditions of November-December 1966, in particular, are entirely contrasting in nature. Whereas the circulations of January-February 1966 and November-December 1966 are quasi steady state, the same cannot be claimed for January-February 1963. In comparison with previous studies where the relative merits of particular methods are often based entirely on single case studies, it is considered justifiable to claim a higher degree of confidence in measureing the effectiveness of the present method where evaluations have been based on three case studies of different meteorological type.

Changes of the month-to-month sea-surface temperature anomaly determined from one month's data alone and including both anomalous advection and anomalous heat flux contributions exhibited reasonably good agreement with observed changes in the two cases where steady-state atmospheric conditions prevailed

for the two months, but much poorer agreement was noted in the final case of less steady-state conditions. Improvements over the single month predictions were observed in all cases when two months' data were employed. Advection contributions alone showed a varying degree of skill in predicting correctly anomaly sign changes as also did the anomalous heat loss forcing alone; the former is rated as having provided poor, fairly good and very good agreement in the three case studies in chronological order, and the latter very good, fairly good and good for the same case studies. Anomalous advection and cooling appear to have added constructively in all three case studies with a general improvement in agreement of magnitudes of centres of positive and negative change over the single parameter predictions; the same was not so apparent for the percentage of correctly predicted sign changes, where, for an especially high percentage prediction for either anomalous heat loss or anomalous advection (see case studies 1 and 3), the combination failed to improve the percentage concerned. It was occasionally observed that slight relative displacements between predicted and observed centres of anomaly change occurred. With the reminder that actual sea temperature anomaly distributions were constructed from plotted values each of which was placed at the centre of the relevant five-degree square (i.e. no account having been taken of the inevitable weighting of weather station observations within any such sub-Marsden square) whereas the same spatial discrepancy did not occur with initial plotted values of model input parameters, it is anticipated that these facts could have been partly responsible.

In no case study does inclusion of a turbulent horizontal diffusion term improve the combined heat loss and advection predictions. Anomalous advection contributions calculated from meridional Sverdrup flow produced values of sea temperature anomaly changes not only far too large, but in no way even remotely resembling the observed pattern of changes. If this meridional flow is not present, as the results would tend to imply, then in order to preserve a state of continuity within the boundary layer, it must be reasoned that with a stationary sea-surface, vertical velocities must be induced at the base of the friction layer; in this way regions previously characterised by maximum positive and minimum negative values of the meridional flow must now coincide with areas of greatest upwelling and downwelling respectively (vid. equation 4.3(7)).

No consistency in the coincidence of expected upwelling and downwelling regions with respective areas of negative and positive anomaly change was however observed.

Both the computed and observed broad-scale patterns of sea temperature anomaly change for the second case study were observed to be largely in the opposite sense to the equivalent changes of the preceding study; this is closely associated with the contrasting nature of the respective anomalous meteorological forcing types concerned. The effect of the atmospheric driving force (case study 1) in producing an intensification of the already well established pre-existing sea temperature anomaly pattern is reminiscent of a characteristic type of ocean-atmosphere interaction invoked by Namias (see

introduction); the conservative nature of this interaction was further borne out by the re-development in April of the same year of an almost identical atmospheric pressure anomaly pattern. None of the case studies revealed any evidence for a better agreement of computed values with centre difference observed values rather than with forward difference changes, a result which previous studies have tended to imply.

Application of the method to other case studies had to be ruled out both by lack of time and (especially) by the difficulty in obtaining reliable meteorological data of the type used for periods of available sea-surface temperature data. It is nevertheless claimed that the general close agreement between computed and observed results for all case studies and the superiority of each of the three over previous related investigations, support the validity of the method.

APPENDIX (i)

Neglecting advection and horizontal mixing we can write the enthalpy conservation for a deepening layer as

$$h\frac{\partial T_M}{\partial t} + (T_M - T(h+\delta))\frac{\partial h}{\partial t} = \frac{Q}{\rho C_p} \quad \ldots\ldots \quad (1)$$

where δ is some small distance below the mixed layer and Q represents total surface heat loss.

Following Pollard, Rhines and Thomson (1973) we introduce the change of variable $T = T_M - T_S$, where T_S is the initial sea-surface temperature and T_M is the temperature of the mixed layer at any instant. For no cooling and arbitrary initial stratification given by $\Lambda(z)$, equation (1) can be written as

$$\frac{\partial}{\partial t}(hT) + \frac{\partial}{\partial t}\int\int_0^h \Lambda dz dh = 0 \quad \ldots\ldots \quad (2)$$

Similarly the energy equation

$$\frac{\partial}{\partial t}\overline{P.E.} + \frac{\partial}{\partial t}\overline{K.E.} = \underline{\tau}\cdot\underline{u} \quad \ldots\ldots \quad (3)$$

(a) (b) (c)

where dissipation terms have been neglected and where term (c) of (3) represents the rate of working of the stress on the mean flow, is reduced, with the use of the time-dependent solutions for the mean flow

$$hu = \frac{-1}{f\rho}((\cos ft - 1)\tau_y + \sin ft\, \tau_x)$$

and $\quad \ldots\ldots \quad (4)$

$$hv = \frac{1}{f\rho}((\cos ft - 1)\tau_x + \sin ft\, \tau_y)$$

to:

$$\rho\alpha g\left(\frac{\partial}{\partial t}\left(\frac{1}{2}h^2T\right) + \frac{\partial}{\partial t}\int h\int_o^h \Lambda dzdh\right) - \frac{\rho}{2}(u^2 + v^2)\frac{\partial h}{\partial t} = 0 \quad \ldots\ldots (5)$$

where α = thermal coefficient of expansion of water and

g = acceleration due to gravity.

Equation (2) is integrated with respect to time to give

$$hT + \int_o\int^h \Lambda dzdh \Big|_{t_1}^{t_2} = 0 \quad \ldots\ldots (6)$$

Expanding the derivatives in equations (2) and (5) and eliminating terms in $\frac{\partial T}{\partial t}$ we obtain

$$\frac{hT}{2}\frac{\partial h}{\partial t} + \frac{\partial}{\partial t}\int h\int_o^h \Lambda dzdh - \frac{h}{2}\frac{\partial}{\partial t}\int\int_o^h \Lambda dzdh - \frac{(u^2 + v^2)}{2\alpha g}\frac{\partial h}{\partial t} = 0 \quad \ldots\ldots (7)$$

After computation of the integral terms of (7) from initial temperature-depth profile data, and expansion of all derivatives it is found that $\frac{\partial h}{\partial t}$ is common to all terms. The condition $\frac{\partial h}{\partial t} \neq 0$ then results in a predictive equation for h, e.g. with initial mixed layer depth h_1 and lapse rate Λ below, we obtain

$$h^2(h^2 - h_1^2) = \frac{4|\underline{\tau}|^2 (1 - \cos ft)}{\Lambda f^2 \rho^2 \alpha g} \quad \ldots\ldots (8)$$

The simplest initial condition of constant Λ extending to the surface follows from (8), with $h_1 = 0$,

i.e. $$h^4 = \frac{4|\underline{\tau}|^2 (1 - \cos ft)}{\Lambda f^2 \rho^2 \alpha g} \quad ;$$

clearly h is a maximum when $ft = \pi$, whence

$$h_{MAX} = \left(\frac{\tau}{\rho}\right)^{\frac{1}{2}} \left(\frac{8}{f^2 N^2}\right)^{\frac{1}{4}} \quad \ldots\ldots (9)$$

where $N^2 = \Lambda\alpha g$.

This is the same as the relationship given by Pollard, Rhines and Thomson (1973).

In this simple case equation (6) reduces to $T = -\frac{1}{2}\Lambda h$. Therefore

$$T_{MAX} = -\frac{1}{2}\Lambda\left(\frac{\tau}{\rho}\right)^{\frac{1}{2}}\left(\frac{8}{f^2N^2}\right)^{\frac{1}{4}} \quad \ldots\ldots \quad *$$

i.e. lowering of surface temperature is proportional to $\tau^{\frac{1}{2}}$, i.e. to the scalar wind speed.

APPENDIX (ii)

With reference to equation 4.2(1) and its subsequent transformation to 4.2(4), nothing has been said of the length of time integration concerned; the use of the final equation 4.3(3) with mean monthly data, however, implies a time integration of 1 month throughout. The identification of terms such as $\rho C_p \overline{\omega' T'}$ with a heat flux, and any parameterisation of such with eddy conductivity or Stanton number requires a time averaging of the order of minutes. If the shorter time period of averaging is adopted, then the representation of each mean quantity concerned, as a much longer period mean (1 month) plus a departure therefrom, followed by complete monthly averaging throughout, would give rise to, for example, in the case of the heat flux, terms such as $\overline{|\underline{W}|' \Delta T'}$; these have already been dealt with in a previous section. Similarly with the shorter period averaged mixed-layer depth written as a monthly mean plus a departure, then covariance terms of the type $\overline{h' \frac{\partial T'}{\partial t}}$ and $\overline{\Delta T' \frac{\partial h'}{\partial t}}$ may be expected to arise. In the final analysis it has been necessary to neglect such terms in comparison with monthly mean value terms.

In the computation of equation 4.3(3) values of $\underline{\bar{\bar{V}}}_{TOT}$ were obtained from isopleths which were derived from surface current data (vid. section 5.4.3). By so doing, any difference between integrated values of the long-term average current over the mixed-layer depth, to which values of $\underline{\bar{\bar{V}}}_{TOT}$ refer, and the interpolated surface value has been neglected. While the use of typical values of the mean horizontal density gradient, over the area of study, in the relevant 'Thermal Wind' equation, renders such an approximation acceptable in the case of the geostrophic

component (vid. e.g. Defant), equivalent estimations of the discrepancy due to the attenuation and shear of the drift component cannot be directly estimated, i.e. with the assumption that a mechanism other than the classical Ekman solution prevails.

REFERENCES

and

ACKNOWLEDGEMENTS

REFERENCES.

ADEM, J. 1970 'On the prediction of mean monthly ocean temperatures', Tellus, 22, pp 410-430.

ASSAF, G, GERARD,R., and GORDON, A.L. 1971 'Some mechanisms of oceanic mixing revealed in aerial photographs', Journal of Geophysical Research, 76,(5), pp 6550-6572.

BATHEN, K.H. 1971 'Heat storage and advection in the North Pacific Ocean', Ibid., 76(3), pp 676-687.

BERSON, F.A. 1962 'On the influence of variable large-scale wind systems on the heat balance in the active layer of the ocean', Technical Memorandum No. 25, National Meteorological Centre, United States Weather Bureau.

BJERKNES, V. 1962 'Synoptic survey of the interaction of sea and atmosphere in the North Atlantic', In Memory of Vilhelm Bjerknes, Universitetsforlaget, Oslo, pp 115-145.

BJERKNES, V. 1964 'Atmosphere-ocean interaction during the "Little Ice Age", (Seventeenth to Nineteenth Centuries A.D.), WMO-IUGG Symposium on Research and Development Aspects of Long-range Forecasting, Technical Note No. 66, World Meteorological Organisation, pp 77-88.

DEFANT, A. 'Physical Oceanography', Pergamon Press, 1961, pp 476 et seq.

DOBSON, F.N. 1971 'Measurements of atmospheric pressure of wind-generated sea waves', Journal of Fluid Mechanics, 48, 1, pp 91-127.

DUNCKEL, M., HASSE, L., KRUGERMEYER, D., SCHRIEVER, D. and WUCKNITZ, J. 1974 'Turbulent fluxes of momentum, heat and water vapour in the atmospheric surface layer at sea during ATEX', Boundary Layer Meteorology, 6, Nos. 1/2, pp 81-106.

FEDEROV, K.N. 1960 'Seasonal variations in ocean currents', Izv. Geophys, Ser. 1960, pp 278-287.

FILYUSHKIN, B.N. 1965 'Possibility of determining some parameters of the vertical temperature profile in the upper layer of the ocean.' Oceanology, 5, No. 6, 1965.

HAY, R.F.M. 1956 'Some aspects of variations of air and sea-surface temperature in short periods at Ocean Weather Stations 'I' and 'J' of significance to the synoptic climatologist', Met. Research Committee M.R.P. 949.

JACOBS, W.J. 1967 'Numerical semi-prediction of monthly mean sea-surface temperature', Journal of Geophysical Research, 72, pp 1681-1689.

KENYON, K.E. 1969 'Stokes drift for random gravity waves', Journal of Geophysical Research, 74(4), pp 6991-6994.

KITAIGORODSKY, S.A. 1960 'On the computation of the thickness of the wind-mixing layer in the ocean', Izv. Geophys. Ser. 1960, pp 425-431

KITAIGORODSKY, S.A. & MIROPOL'SKIY, Yu.Z. 1970 'On the theory of the open-ocean active layer', Izv. Atmospheric and Oceanic Physics, 6, No. 2, 1970, pp 178-188.

KRAUS, E.B. 1972 'Atmosphere-ocean interaction', Oxford Univ. Press, 426 pp.

KRAUS, E.B. & MORRISON, R.E. 1966 'Local interactions between the sea and the air at monthly and annual time scales', Quarterly Journal of the Royal Met. Soc., 92, pp 114-127.

LIGHTHILL, M.J. 1969 'Westerly wind-driven ocean currents', Ibid. 95, pp 675-688.

LUMB, F.E. 1964 'The influence of cloud on hourly amounts of total solar radiation at the sea surface', Ibid. 90, pp 43-56.

MOSBY, H. 'Oceanographical Tables from Weather Ship Station 'M', Universitetet I, Bergen.

NAMIAS, J. 1959 'Recent seasonal interactions between North Pacific waters and the overlying atmospheric circulation', Journal of Geophysical Research, 64, 6, pp 631-645.

NAMIAS, J. 1969 'Use of sea-surface temperature in long-range prediction', Sea Surface Temperature, Technical Note No. 103, World Meteorological Organization.

POLLARD, R.T. 1970 'Surface waves and rotation: an exact solution', Journal of Geophysical Research, 75, pp 5895-5898.

POLLARD, R.T., RHINES, P.B., & THOMSON, O.R.Y. 1973 'The deepening of the wind-mixed layer', Geophysical Fluid Dynamics, 3, pp 381-404.

RAMAGE, C.S. 1972 'Interaction between tropical cyclones and The China Seas', Weather, 27, pp 484-494.

ROLL, H.U. 1965 'Physics of the marine atmosphere', Academic Press Inc., 462 pp.

SAWYER, J.S. 1964 'Notes on the possible physical causes of long-term weather anomalies', Technical Note No. 66, World Meteorological Organization.

SHEPPARD, P.A. 1958 'Transfer across the earth's surface and through the air above', Quarterly Journal of the Royal Met. Society, 84, pp 205-224.

STOMMEL, H. 'The Gulf Stream', Cambridge Univ. Press, 1965.

ACKNOWLEDGEMENTS.

I should like to thank Dr. D.H. McIntosh for his general advice at all times and Dr. A.S. Thom for his valuable contribution to stimulating discussions on matters relating to this research. I also remain grateful to Dr. R.T. Pollard (written communication) for his useful comments and suggestions.

For their willingness at any time to participate in discussions pertaining to the present research I express my appreciation to Dr. K.J. Weston, Dr. C.N. Duncan, Mr. J.C. Curran and Mr. J.A. Blair-Fish.

My thanks are due also to the following, without whose co-operation and services this research would not have been possible: Mr. R.A. Ratcliffe and Mr. J. Weller, Meteorological Office, Bracknell; Dr. Otto, K.N.M.I., De Bilt, Netherlands; Dr. Gertrud Prahm, The German Meteorological Office, Hamburg; The Marine Research Laboratory, Edinburgh; The Hydrographic Office, Taunton, Somerset; The National Oceanographic Data Centres, Washington and Surrey.

I also wish to thank most sincerely Mrs. M. Hallissey for her dedication and efficiency in typing this entire thesis.

Lastly, I thank the Natural Environment Research Council, who, by means of a post graduate studentship, supported the research throughout.